PRISMATIC MODULAR REACTOR ANALYSIS WITH MELCOR

A Thesis

by

NI ZHEN

Submitted to the Office of Graduate Studies of
Texas A&M University
in partial fulfillment of the requirements for the degree of

MASTER OF SCIENCE

December 2008

Major Subject: Nuclear Engineering

PRISMATIC MODULAR REACTOR ANALYSIS WITH MELCOR

A Thesis

by

NI ZHEN

Submitted to the Office of Graduate Studies of
Texas A&M University
in partial fulfillment of the requirements for the degree of

MASTER OF SCIENCE

Approved by:

Chair of Committee,	Karen Vierow
Committee Members,	Pavel Tsvetkov
	Guido Kanschat
Head of Department,	Raymond Juzaitis

December 2008

Major Subject: Nuclear Engineering

ABSTRACT

Prismatic Modular Reactor Analysis with MELCOR. (December 2008)

Ni Zhen, B.En., Beijing Polytechnic University (China);

M.S., Ecole Polytechnique Feminine (France)

Chair of Advisory Committee: Dr. Karen Vierow

Hydrogen, a more sustainable source of energy, is a potential substitute for hydrocarbon fuel for power generation. The Very High Temperature gas-cooled Reactor (VHTR) concept can produce hydrogen with high efficiency and in large quantities. The US Department of Energy plans to build a VHTR as a next-generation hydrogen/electricity production plant. This reactor concept is very different from that of commercial reactors in the US. In order to acquire licensing eligibility for VHTRs, analysis tools need to be validated and applied to design and evaluate VHTRs under operation conditions and accident scenarios. In this thesis, MELCOR, a severe accident code, was used to analyze one of the VHTR designs – a prismatic core Next Generation Nuclear Plant (NGNP).

The NGNP is based on General Atomics' (GA) Gas Turbine – Modular Helium Reactor (GT-MHR) 600 MW design. According to the current literature survey, more data is available for the GT-MHR than for the NGNP. Therefore, for the purposes of extending MELCOR capabilities and code validation, a model of the GT-MHR reactor pressure vessel (RPV) was developed.

Based on the currently available data, a model of the NGNP RPV was then developed through modifying the GT-MHR RPV model. For both RPV models, coolant outlet temperature under normal operating conditions corresponds well to the data from literature.

The reactor cavity cooling systems (RCCS), which passively removes heat from the RPV wall to the outside atmosphere, was then added to this GT-MHR RPV model. With this model addition, the heat removal rate of the RCCS under normal operating conditions was calculated to correspond well to the data from references. Pressurized conduction cooldown (PCC), one of the important postulated accident scenarios for a prismatic core reactor, was simulated with the complete model.

MELCOR has been demonstrated to have the ability of modeling a prismatic core VHTR. The calculated outlet temperature and mass flow rate under normal operation correspond well to references. However, the calculation for the heat distribution in the graphite and fuel is unsatisfactory which requires MELCOR modification for the PCC simulation. For future work, a complete model of the NGNP under normal operation conditions will be developed when additional data becomes available.

DEDICATION

To my parents

ACKNOWLEDGEMENTS

I would like to thank my committee chair, Dr. Vierow, for her continuous support and help and for leading me towards my masters. Without her help, I would not be able to perform this research work.

I would like to thank my committee member Dr. Tsvetkov for helping me to enter this Master of Science program. I would like to thank my advisor, Dr. de Peretti from France, for introducing me to this outstanding graduate program at Texas A&M University.

I also would like to thank my friends and colleagues here at A&M. Thanks to my GA contact for his help on my thesis research.

Finally, I would like to thank my parents for supporting me spiritually and financially.

NOMENCLATURE

CDA	Cavity Downwards Air
CUA	Cavity Upwards Air
CV	Control Volume
CVH	MELCOR Control Volume Hydrodynamics Package
COR	MELCOR Core Package
CRFB	Control Rod Fuel Block
DCC	Depressurized Conduction Cooldown
DH	Hydraulic Diameter
FBP	Fixed Burnable Poison
FL	MELCOR Flow Path Package
FPSA	Fuel Pellet Surface Area
GA	General Atomics
GT-MHR	Gas Turbine – Modular Helium Reactor
HS	MELCOR Heat Structure Package
HTGR	High Temperature Gas-Cooled Reactor
IAEA	International Atomic Energy Agency
MP	MELCOR Material Properties Package
NCG	MELCOR Noncondensible Gas Package
NGNP	Next Generation Nuclear Plant
NRC	United States Nuclear Regulatory Commission

PBMR	Pebble Bed Modular Reactor
PCC	Pressurized Conduction Cooldown Accident
PCD	Preconceptual Design
PCS	Power Conversion System
PyC	Pyrolytic Carbon
RC	Reactor Cavity
RCCS	Reactor Cavity Cooling System
RPV	Reactor Pressure Vessel
RSC	Reserve Shutdown System Control
SCS	Shutdown Cooling System
SFB	Standard Fuel Block
SNL	Sandia National Laboratories
SS	Supporting Structure(s) in MELCOR
VHTR	Very High Temperature Reactor

TABLE OF CONTENTS

Page

Page

LIST OF FIGURES

FIGURE Page

LIST OF TABLES

TABLE Page

TABLE Page

TABLE Page

TABLE Page

1. INTRODUCTION

Hydrocarbon fuels have been used worldwide in transportation, residential, power generation and a wide range of other industrial application for decades. The demand for fossil fuel is increasing, especially in the developing world due to the population growth and the industrial development. The burning of fossil fuel results in the emission of greenhouse gases which contribute to global warming. Since fossil fuels are non-renewable resources, according to the current world consumption, fossil fuel will be depleted in about two centuries. [16] Due to the projections in demand and depletion of these natural resources, costs are increasing and causing changes in the global economy. There are also uncertainties associated with its supply.

Hydrogen has been considered as a substitute for fossil fuel for providing motive power in transportation and for electricity production. Because it produces significantly less greenhouse gas emission, it is considered a more environmentally friendly source of energy than fossil fuel. There are several processes for hydrogen production which include: steam reforming of natural gas, high-temperature electrolysis and thermochemical processes. Sulfur-Iodine cycle (S-I cycle) has been considered as one of the most promising production methods among various types of thermochemical processes. This process is more efficient than the high-temperature electrolysis, and it does not require hydrocarbon like the steam reforming process. The net reactant of S-I

This thesis follows the style of *Nuclear Materials*.

cycle is just water and its net reaction products are just hydrogen and oxygen. However, this process does require high temperature heat. This high temperature heat can be provided by the High Temperature Gas-cooled Reactors (HTGR). [14] The HTGR concept [1] provides high temperature process heat up to 950°C. This temperature can be used to produce hydrogen with high efficiency and it has been considered as one of the most promising approach for this application. The Japan Atomic Energy Agency (JAEA) has conducted research on large-scale hydrogen production using S-I cycle with their High Temperature Engineering Test Reactor (HTTR) [1]. Sandia National Laboratories (SNL) [2] and Idaho National Laboratories (INL) [3] have performed research on HTGR concept for hydrogen production application as well.

1.1 Motivation for Work

The Next Generation Nuclear Plant (NGNP) will be the demonstration of HTGR technology for producing hydrogen economically and reliably. This reactor design envisions a helium outlet temperature up to 950°C. In the Energy Policy Act of 2005 (EPAct), the United States Department of Energy plans to complete the licensing and construction of the NGNP and initiate its hydrogen production by 2021. [3]

HTGR design concept is quite different compared with the existing conventional nuclear reactor systems due to their design characteristics, requirements for material performance and fabrication process. In order to acquire licensing eligibility, The HTGR

concept needs new tools to carry out analytical studies and direct simulation to test the HTGR under different operating conditions and accident scenarios.

MELCOR code has been used to model accident progression in light water reactor systems. This code has been developed by SNL as a plant risk assessment tool for the U. S. Nuclear Regulatory Commission (NRC). A wide spectrum of accident phenomena in light water reactors are treated in MELCOR. [4] The motivation of this research is to demonstrate MELCOR's capabilities for modeling a NGNP with an outlet temperature around 950°C.

1.2 Validation of MELCOR in Modeling A Prismatic Core NGNP

It has been demonstrated that a pebble bed modular gas cooled reactor (PBMR) can be modeled by MELCOR code via an input deck. [3] This research wants to demonstrate MELCOR's capabilities in modeling a prismatic gas cooled reactor. The final core design of the NGNP will be chosen between pebble bed design and prismatic core design. The MELCOR modeling efforts want to provide assessments regarding the allowable operational characteristics for both configurations and facilitate the final decision-making and the licensing strategy development of the NGNP.

The main objectives of this thesis study are the following:

1. To develop a model representative of prismatic core GT-MHR RPV and RCCS with an outlet temperature around 850°C for assessments and analyses to provide recommendations to the design and analysis of Generation IV reactors.

2. To develop a model representative of the prismatic core NGNP with an outlet temperature around 950°C to 1000°C for assessments and analysis.
3. To perform analyses under different accident scenarios for a prismatic core reactor design.
4. To evaluate the applicability of the MELCOR code for prismatic core reactor analysis.

1.3 Technical Approach

A literature survey was performed. Data on the prismatic core design was obtained. MELCOR's existing models that need to be used to develop the input deck were identified. A model representative of the GT-MHR RPV was developed. This model was then modified and an NGNP RPV model was developed. Sensitivity studies are performed with these two models to evaluate the effects of important variables, including power factors and material properties, on key output including outlet temperature and peak fuel temperature. An RCCS model was added to the GT-MHR RPV model, and a complete model of the GT-MHR was developed. Results of these three models under reactor normal operating condition were acquired and assessed with the data from the literature. The PCC was simulated with the complete model, and the results were assessed as well. The capabilities of MELCOR for modeling a prismatic reactor and the improvements that need to be made were concluded.

1.4 Overview of Thesis

Section 2 gives a literature review on the prismatic core design and describes MELCOR's capabilities for modeling gas cooled reactors and its challenges. The GT-MHR model is described in Section 3. The NGNP RPV model is described in Section 4 with the demonstration of the passive heat removal feature of the prismatic core design. Both these two sections describe sensitivity studies. The RCCS model is described in Section 5. The PCC model is described in Section 6. Heat removal calculation of the RCCS under normal operating condition was described in Section 5, under PCC was described in Section 6. Conclusions are drawn in Section 7 and future work was defined in Section 8.

2. PRISMATIC CORE DESIGN OVERVIEW

2.1 VHTR Overview

The VHTR is one of the reactor design concepts among the Generation IV (Gen IV) nuclear energy systems. The VHTR is graphite-moderated and helium-cooled with an outlet temperature of around 1100°C. [12] This high temperature will require advancements in material and fuel design which will bring issues to cost and feasibility. [12] The current HTGR concept is similar to the VHTR concept, but it aims to achieve an outlet temperature of around 950°C. [6] The VHTRs have two types of configurations: pebble bed design and prismatic core design. In a pebble bed design, fuel materials are in the form of pebbles with the size of a tennis ball, and include the moderator. The pebbles are in an annular region in the core. In the center of the core, there is a graphite reflector column. In a prismatic core design, fuel compacts are inserted into hexagonal graphite blocks which are then inserted into a circular reactor core.

Pebble bed HTGRs which have been previously operated include the German AVR. [17] Prismatic core HTGRs which have been previously operated in the United States included Peach Bottom-1 and Fort St. Vrain. [17] There are some other prismatic core HTGRs which were constructed in Europe too, including the British Dragon and the French MARIUS IV. [17] The Chinese HTR-10 [6] is the only operating pebble bed HTGR, although the South African utility ESKOM plans to build PBMRs. [8] The

Japanese HTTR is the only operating prismatic core HTGR in the world today. [6] The core design of the US DOE's NGNP will be chosen between the pebble bed and the prismatic core designs. There are some differences between historical gas-cooled reactors and the NGNP. The outlet temperature was lower in the older designs due to lack of gas turbines in the 1970's compared with the NGNP. The NGNP also has a center graphite region which provides passive safety. This component was not included in the previous gas-cooled reactor designs.

2.2 Prismatic Core Design Overview

2.2.1 Prismatic Core

Table 2.1

Comparison of GT-MHR, NGNP and VHTR

	GT-MHR	NGNP	VHTR
Reactor power (MWt)	600	600	850
Coolant flow rate (kg/s)	320	226	NA
Active core height (m)	7.93	7.93	6
Active core effective radius (m)	2.41	2.41	3
Helium inlet temperature (°C)	491	491	800
Helium outlet temperature (°C)	850	1000	1100
Helium inlet pressure (psi)	1025	1025	1000
Core pressure drop (psi)	7.4	6.7	NA
Graphite block distance cross flats (m)	0.36	0.36	NA

Ref. [7], [2] and [12]

The reference design is the prismatic core NGNP. It is based on GA's VHTR concept submitted to the Generation IV Roadmap, which is in turn based on GA's GT-MHR design. [2] General design specifications of the NGNP are compared with those of the GT-MHR and VHTR in Table 2.1.

Figure 2.1 is a diagram of the GT-MHR/NGNP RPV. Figure 2.2 shows the cross-sectional view of the core which consists of hexagonal graphite blocks divided into three radial regions: an inner reflector region, an annular active core region and an outer reflector region. As indicated in Figure 2.1, there are also an upper reflector region on the top of the active core region and a lower reflector region beneath it. The helium inlet flows through the outer ring of the hot duct and flows upwards through the coolant channels between the inner RPV wall and the core barrel as shown in Figure 2.2. It then reaches the upper plenum volume within the upper plenum shroud where it is distributed and guided through the coolant channels which penetrate the upper reflector region, the fueled active core region and the lower reflector region and reach the core exit plenum. There are around 10,626 coolant channels in the core. The helium inlet travels all its way through the core, and then it is collected at the core exit plenum and flows out of the core through the inner section of the concentric pipe. [2]

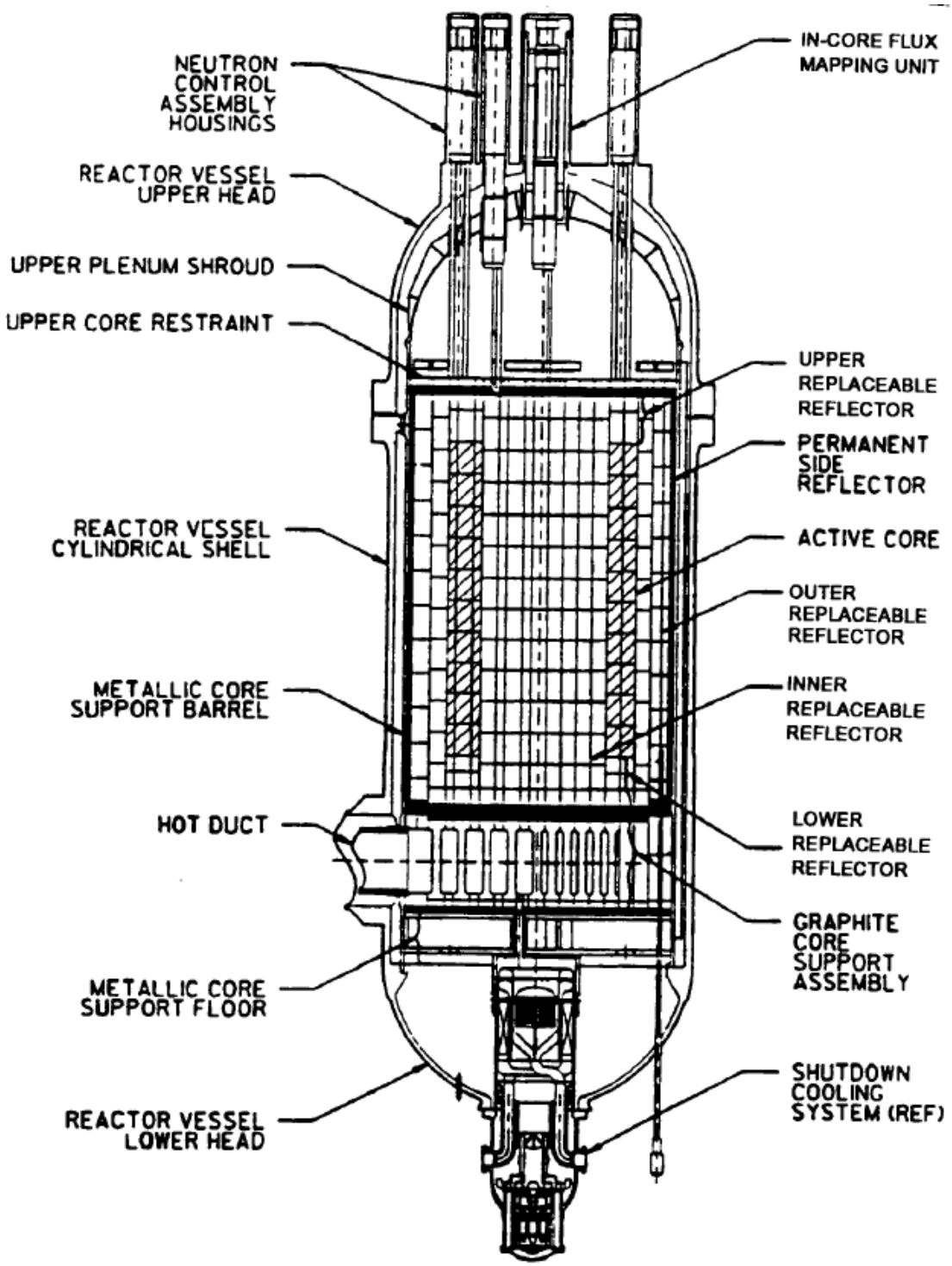

Figure 2.1. Diagram of the GT-MHR/NGNP RPV [7] [Courtesy of General Atomics]

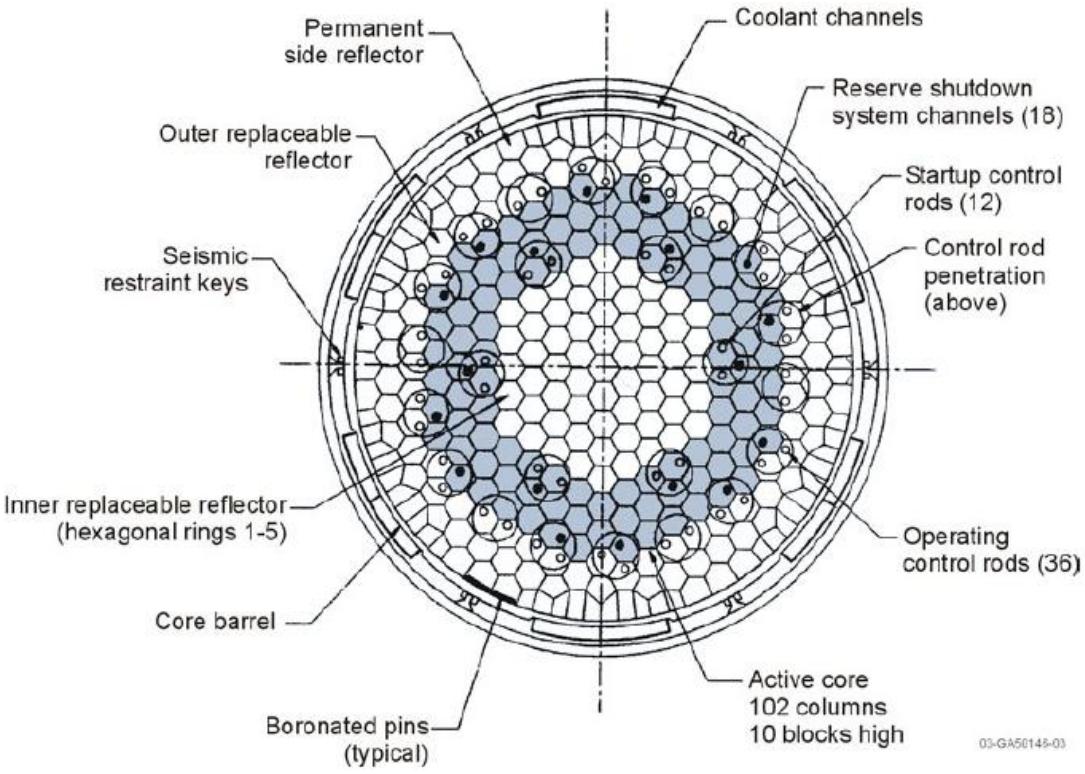

Figure 2.2. Cross Sectional View of the GT-MHR/NGNP Core [2]

2.2.2 Prismatic Core Fuel

The fuel specifics are given in Table 2.2. The fuel is low-enriched uranium oxycarbide (UCO) in a Tristructural-isotropic (TRISO) configuration as shown in Figure 2.3. TRISO fuel particle is composed of fuel kernels in the center, surrounded by four layers of particle coatings as indicated in Figure 2.4. The first layer adjacent to the kernel is a porous low density pyrolytic carbon (PyC) buffer layer, followed by a layer of high density PyC (IPyC), then a layer of silicon carbide (SiC), and a final buffer layer of high

density PyC (OPyC). Those fuel particles are then molded into compacts. The compacts are then inserted into hexagonal graphite blocks.

The TRISO configuration provides barriers to retain fission products. The fuel kernel retains a significant fraction of short-lived fission gases. The coatings are the most important barrier to the release of fission products. Experimental results have proved that TRISO particle can retain fission products up to 1600°C which corresponds to the maximum temperature of TRISO fuel under accident conditions. [22] The most important coating is SiC which serves as the primary barrier to confine fission products, particularly metallic fission products. The graphite fuel compact matrix where the particles are located can effectively confine fission products as well. [7]

Table 2.2

NGNP Fuel Particle Parameters

Parameter	Value
Kernel Composition	UCO
Kernel Diameter	350 microns
Kernel Density	> 10.5 g/cc
Buffer Thickness	100 microns
Buffer Density	~ 1 g/cc
IPyC Thickness	40 microns
IPyC Density	~ 1.9 g/cc
SiC Thickness	35 microns
SiC Density	~ 3.2 g/cc
OPyC Thickness	40 microns
OPyC Density	~ 1.9 g/c

Ref. [2]

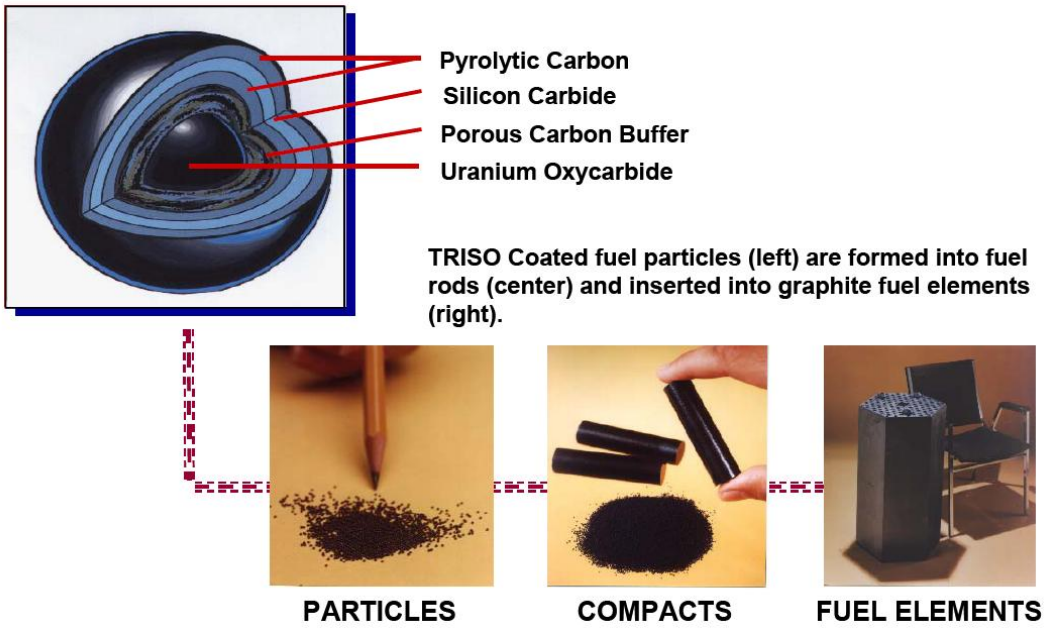

Figure 2.3. Prismatic Fuel Particles, Compacts and Elements [2]

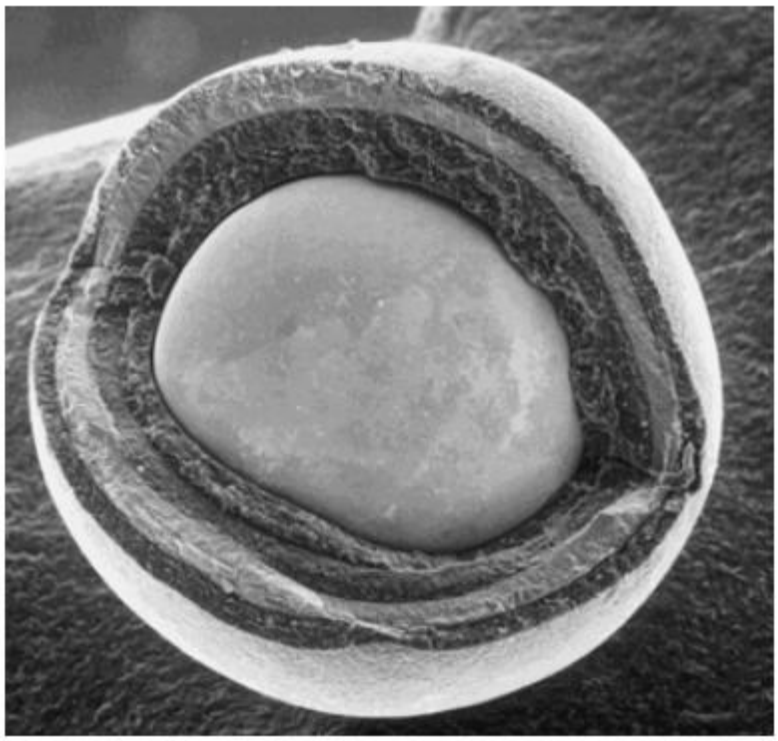

Figure 2.4. Prismatic Fuel Particles with Part of the Coatings Removed [2]

2.2.3 Reactor Control

As shown in Figure 2.2, there are 12 startup control rods and 18 reserve shutdown control rods in the active core. There are 36 operating control rods in the outer reflector region. During startup or shutdown, the startup control rods are inserted. They are fully withdrawn when the reactor is critical and fully inserted when subcritical. The operating control rods are inserted with various positions during operation and fully inserted for protection. The reserve shutdown rods are fully withdrawn during normal operation and they are inserted should the control rods become inoperable due to the failure of the neutron control assembly. [7] As shown in Figure 2.5, on the edges of the each graphite fuel block, there are 6 burnable poison rods. The control rods are annular. The reserve shutdown rods and burnable poison rods are cylindrical.

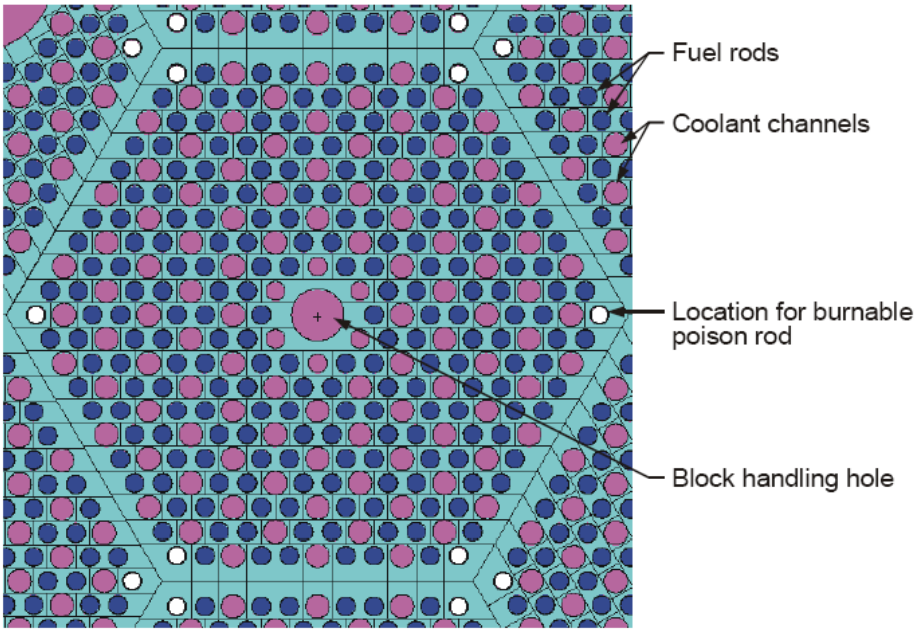

Figure 2.5. A Standard Hexagonal Fuel Block [2]

2.2.4 Safety Features

Power Conversion System (PCS) removes heat from the core under normal operation. This system includes turbine, compressor and generator unit. It provides the forced circulation of helium in the core. The PCS functions to remove decay heat by maintaining this circulation following a reactor shutdown. The Shutdown Cooling System (SCS) removes the decay heat through forced circulation when the PCS is unavailable. In the hypothetical scenario where neither the PCS nor the SCS functions after a shutdown, the decay heat would be removed by the RCCS through the natural circulation of helium inside the core and conduction radially outward from the core to the RCCS. This kind of situation is called a loss of forced cooling accident or conduction cooldown accident.

2.2.5 GT-MHR Plant Description

The primary reference for this thesis work is the GT-MHR 600 MW design. The GT-MHR plant design is composed of four modules. [7] As shown in Figure 2.6, each module is a steel vessel system including a reactor pressure vessel and a power conversion vessel. These two vessels are connected by a cross vessel in between. This steel vessel system is contained in an underground concrete containment with a diameter of 25.9 m and a height of 42.7 m. Both the reactor vessel and the power conversion vessel are made of modified 9Cr-lMo-V alloy steel. The reactor vessel is 31.2 m in

height and 8.4 m in diameter. It houses the control rod guide tubes at the top, the active core and core internals in the middle and a shutdown cooling system (SCS) at the bottom. The reactor vessel is surrounded by the RCCS.

The power conversion system is approximately 8.5 m in diameter and 35.4 m in height. [7] This vessel is composed of turbomachinery, a recuperator and water-cooled intercooler and precooler. The turbomachinery includes a turbine, an electrical generator and two compressors. As shown in Figure 2.7, the helium exits the reactor core at 850°C and 6.91 MPa. It then flows through the center duct of the cross vessel and is expanded through the turbine which directly drives the generator and one low pressure compressor and one high pressure compressor. The helium leaves the turbine at 510°C and 2.56 MPa and travels through the recuperator to preheat the gas coolant and through the precooler. Cold helium at 26°C and 2.51 MPa then enters the compressors. It is compressed to a pressure of 7.08 MPa and a temperature of 107°C. It flows through the recuperator again to be heated and then it enters the reactor vessel through the outer annulus of the hot duct centrally located within the cross vessel at 488°C and 7.00MPa. It then flows up through the risers located between the core barrel and the RPV wall. It reaches the upper plenum at the top of the reactor from which it then flows down through the reactor core. Finally, it reaches the lower plenum, flows through the inner section of the hot duct and completes the loop. [7]

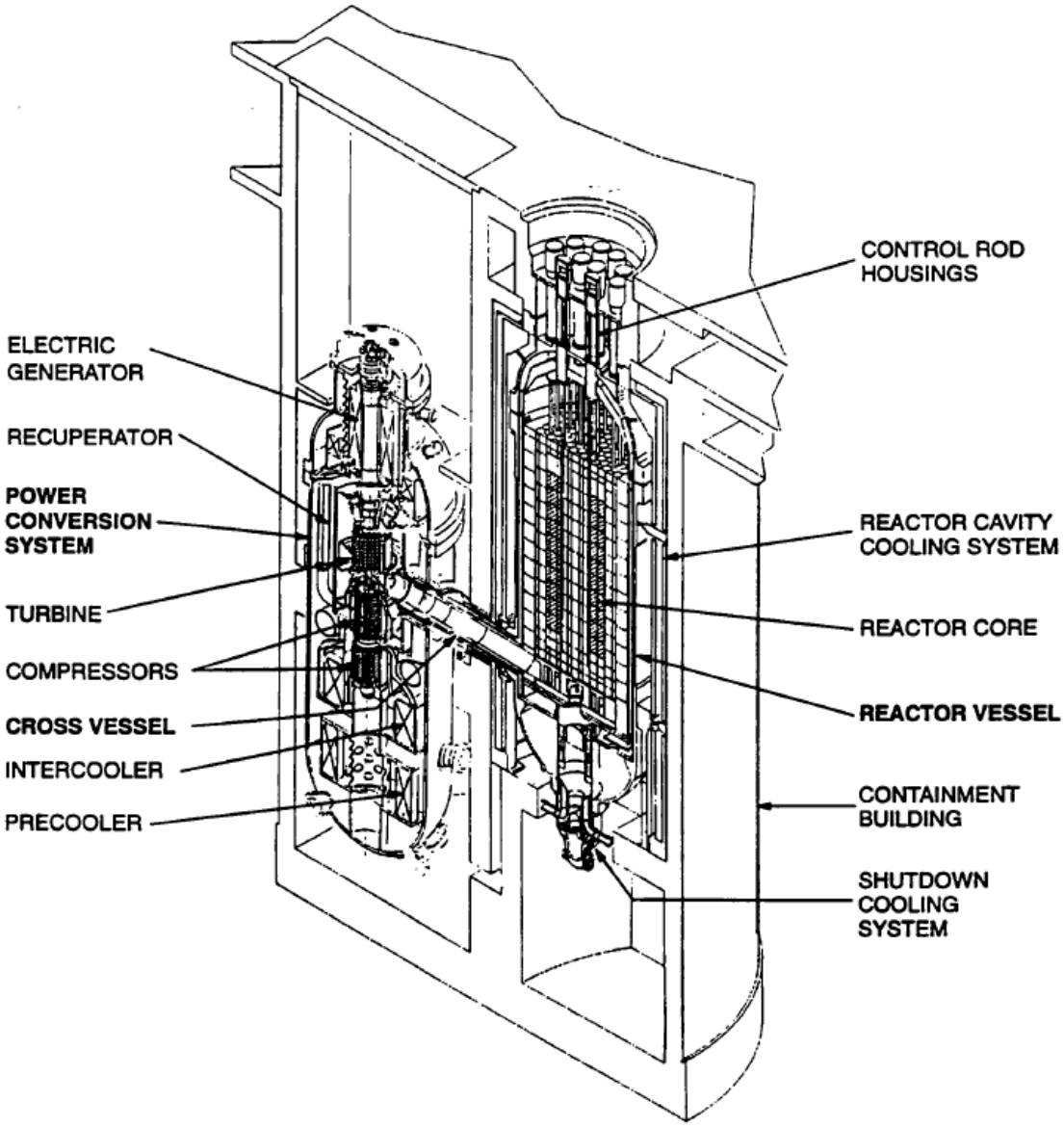

Figure 2.6. GT-MHR Module Arrangement [7] [Courtesy of General Atomics]

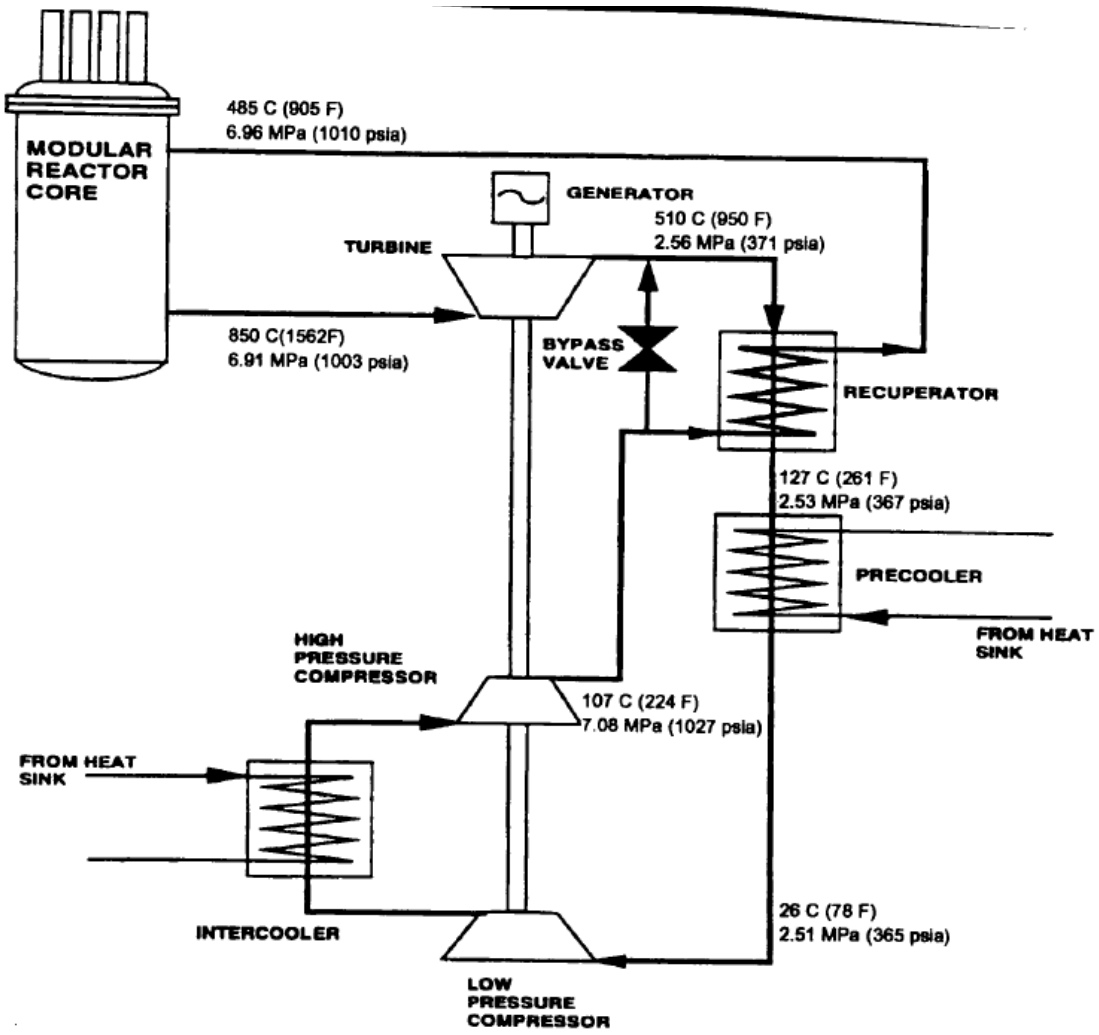

* Note flow conditions shown correspond to 600 MW(t) case

Figure 2.7. GT-MHR Process Flow Diagram [7] [Courtesy of General Atomics]

The hot duct is composed of concentric pipes where coolant enters the reactor via the annulus and it exits the reactor vessel through the central pipe. As shown in Figure 2.8, the outer diameter of the annulus of the hot duct is 90 inches (2.286m). The radius of the inner section of the hot duct for core outlet flow is not available as shown in Figure 2.9. According to John Bolin from GA, there is one insulation layer around the helium inlet, since 490°C is too hot for the cold duct wall. There is another insulation layer between the inlet and outlet since there is a temperature difference of around 360°C. The design does not intend to preheat the helium inlet. Instead, it is desirable to minimize the heat transfer between outlet helium and inlet helium and preserve the high temperature heat contained in the outlet. Currently, no data is available concerning the thickness of the above two insulation layers. [23]

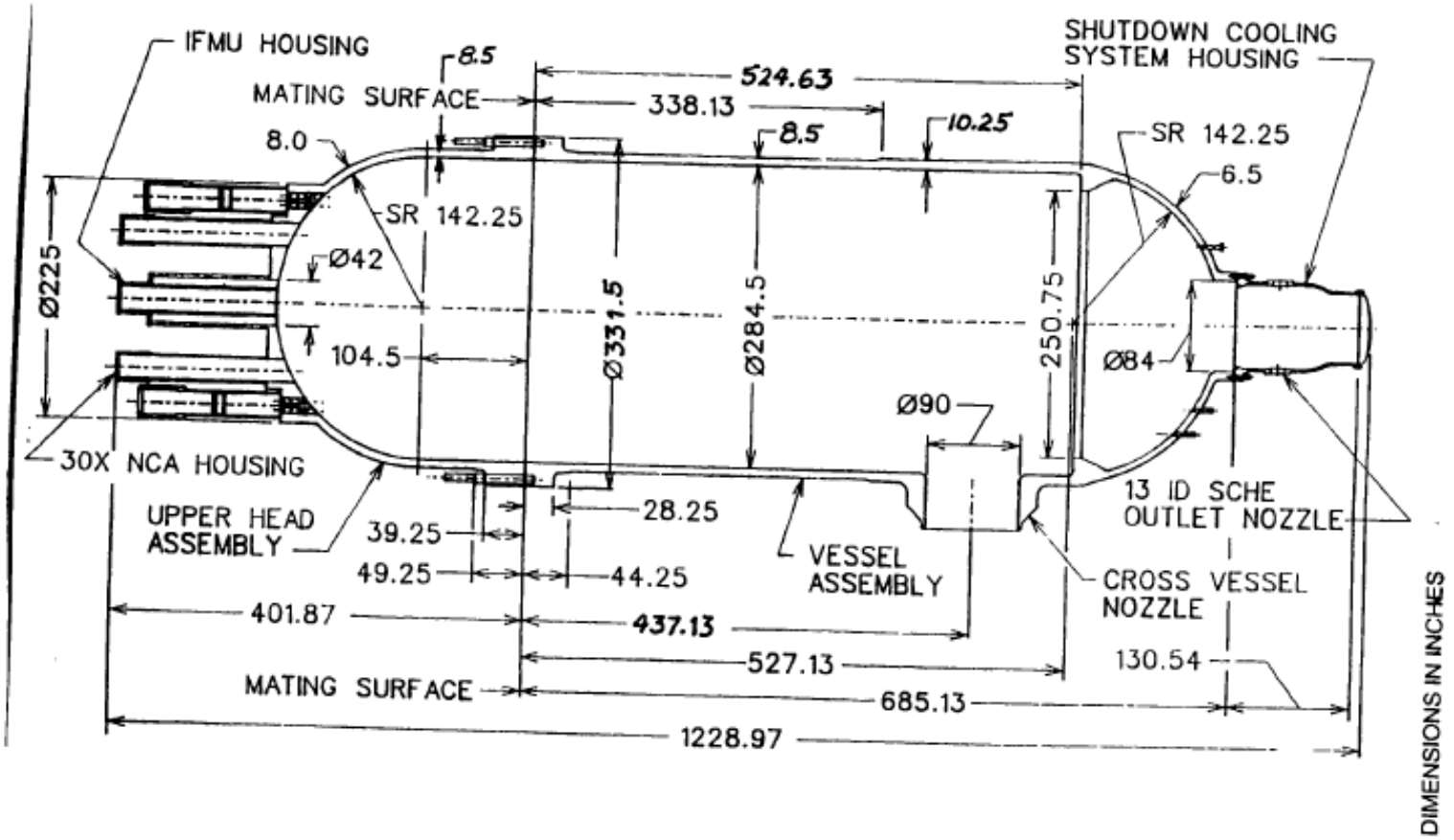

Figure 2.8. GT-MHR RPV [7] [Courtesy of General Atomics]

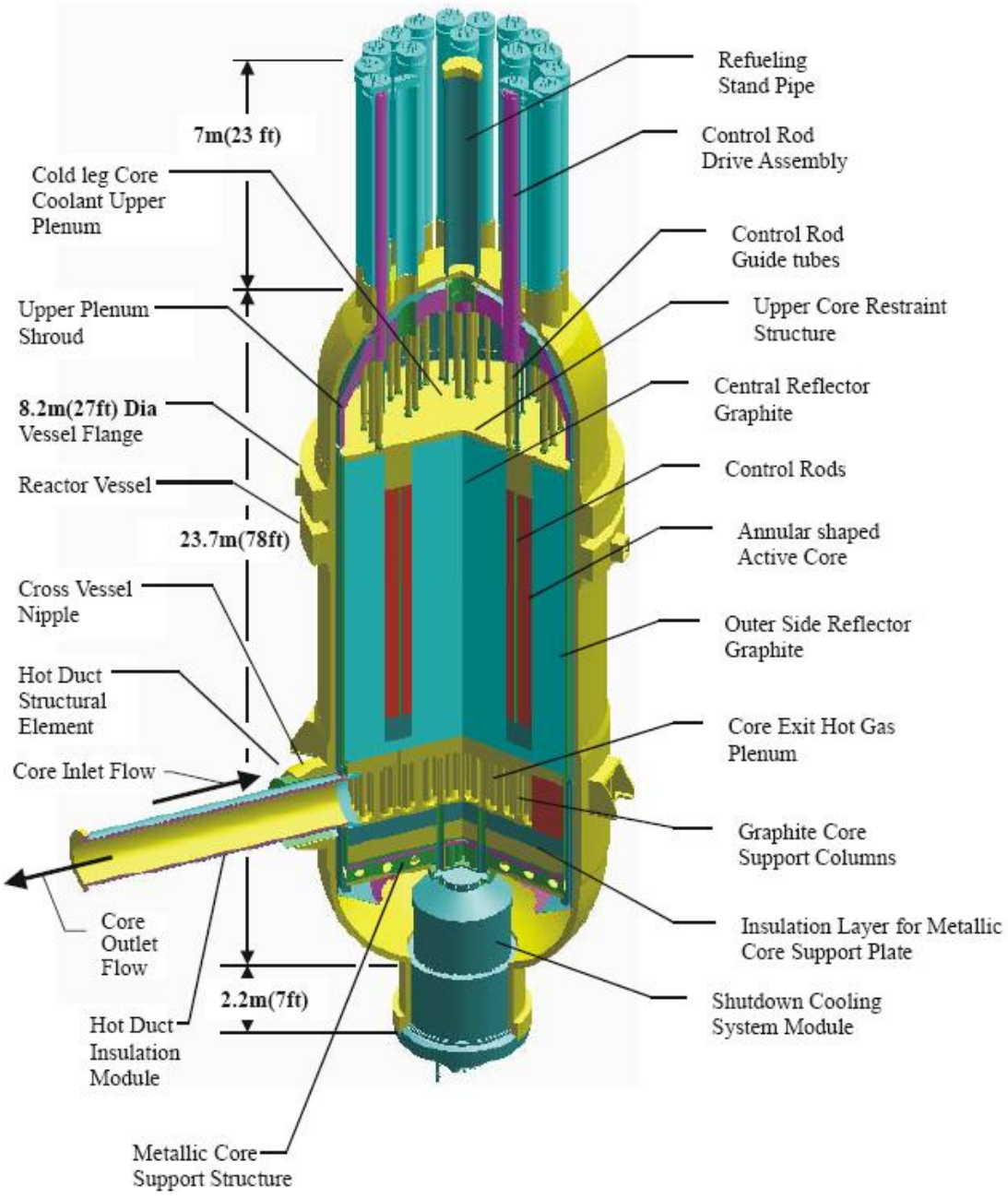

Figure 2.9. NGNP/GT-MHR RPV [2]

2.3 MELCOR's Capabilities and Challenges with Respect to the Modeling of the Prismatic Core VHTR

2.3.1 Previous Thermals-Hydraulic Code Modeling Efforts

The Graphite Reactor Severe Accident Code (GRSAC) developed by Oak Ridge National Laboratory has been designed for performing analyses of severe accidents in gas cooled reactors. Various accident scenarios for a prismatic core - GT-MHR 600 MW have been studied by this code, and results demonstrated the inherent passive safety features of this prismatic core design [14]. This code has not been updated for about 25 years and its mathematical algorithms are old. This code can not be applied for rigorous safety analysis. MELCOR is a more modern code compared with GRSAC and it uses more advanced algorithms. [5]

RELAP5-3D/ATHENA computer code developed by the INL has been used to model a prismatic core VHTR. The basic design information used to develop this model was obtained from the GT-MHR 600 MW design. Calculations have performed for the RPV, the RCCS under normal operation and some accident conditions. Then the results were benchmarked against GA's analyses and the differences were investigated [2]. The model under normal operation conditions made oversimplifications on the inlet boundary conditions and core coolant flow distribution. Those aspects will be treated more precisely in the prismatic core MELCOR model.

In Japan, thermals-hydraulic analyses have been performed for the prismatic core HTTR. The SSPHEAT code [18] has been used to calculate the heat removal capability of the vessel cooling system (VCS) of the HTTR under various operating conditions and transients, and those results were compared with the actual experimental results. The minimum heat removal rate of VCS required to maintain the fuel and structural materials within their design limits was acquired [6]. This code was developed to analyze the temperature distribution of the structures inside the reactor core. [18] MELCOR can analyze the temperature distributions of the structures both inside and outside the core.

In Russia, thermal-hydraulic codes have been used to study HTTR cores as well. The GTAS-M code [19] was applied to calculate the temperature of the core and the structures under transients. The SM-1 code was applied to compute the temperatures of the structures under transients. These two codes together with the DUPT code were used to calculate the power transferred from the RPV to the RCCS during different operating conditions [6]. The solutions of the energy equations are not included in these codes. [6] However, mass, momentum and energy equations are solved simultaneously in MELCOR and the solutions are given in the code output.

2.3.2 MELCOR's Suitability and Challenges

2.3.2.1 MELCOR Code

MELCOR code has been used to model accident progression in light water reactor systems. This code has been developed by the SNL as a plant risk assessment tool for the NRC. A wide spectrum of accident phenomena in light water reactors are treated in MELCOR. [5] It has several capabilities which are suitable for the modeling of the HTGR and VHTR. The code allows replacing light water coolant with helium. The core materials for light water reactor systems in the code can be redefined to represent the core materials used in gas-cooled reactor systems. It has been demonstrated that the pebble bed HTGR can be modeled by MELCOR via an input deck [5].

2.3.2.2 Suitability

The Control Volume – Flow Path concept allows the modeling of reactor of any geometry. The idea is to divide the reactor volumes into a number of control volumes and have them connected by flow paths. As a light water analysis tool, the original coolant is water, but it can be replaced by helium with the implementation of helium material properties. Graphite is a gas-cooled reactor material, but not a light water reactor material. MELCOR allows the user to redefine the properties of about 8 core materials, thereby various gas-cooled reactor materials can be modeled. MELCOR

allows the modeling of the components outside of the RPV. Therefore, a full core analysis of a prismatic core RPV and the RCCS can be performed which will provide the basis for accident assessments. MELCOR is a modern code which uses advanced algorithms. It can analyze the temperature distributions of the structures both inside and outside the core. Mass, momentum and energy equations are solved simultaneously in MELCOR and the solutions are given in the code output.

2.3.2.3 Challenges

MELCOR is proposed as the VHTR analysis tool but the code's capabilities must be demonstrated with respect to the simulation of a prismatic core HTGR. It is quite challenging to model a prismatic core HTGR due to its design characteristics. Cladding and supporting structures (SSs) are two distinctive core components in MELCOR. In light water reactors, each fuel rod is surrounded by a layer of metal which is the cladding. Light water coolant flows over the surface of the cladding. SSs have the ability to support the weight of other core components. In a prismatic core reactor, graphite blocks have fuel channels and coolant channels in them, so the graphite supports the weight of other core components. The graphite within the compacts serves as the cladding. A creative modeling strategy is required to separate graphite into two components in order to properly calculate the heat transfer and conduction between fuel and cladding and between cladding and coolant and to obtain sufficient SSs masses to support the weight of other core components. This modeling strategy also needs to

satisfy MELCOR input requirements in order to ensure normal code execution. Moreover, the properties of some core materials are still unknown and the selection of certain materials is still under discussion. An assessment regarding the effects of those uncertainties on the operating characteristics is necessary in order to evaluate their order of importance.

3. MODELING OF THE GT-MHR 600 MW WITHIN THE REACTOR PRESSURE VESSEL (RPV)

3.1 Model Development

The objective of this modeling effort is to develop an input deck representative of the prismatic core GT-MHR RPV with an outlet temperature of around 850°C. Values for MELCOR's input parameters were obtained based on references to the greatest extent possible. When values were not available, engineering judgment was used. All assumptions, newly defined core materials and existing MELCOR models used in prismatic core input development are described herein.

3.1.1 GT-MHR RPV

The GT-MHR reactor core consists of reflector and fuel prismatic blocks, upper and lower plena and control materials. The active core is shown as the blue region in Figure 2.2. It consists of three rings with 102 hexagonal columns in total. The inner ring has 30 columns. The middle ring and outer ring have 36 columns each. Each column is composed of 10 fuel blocks axially. The height of one block is 0.793 m. The distance across the flats of one block is 0.36 m. The structural material of fuel blocks is H-451 graphite with a density of 1740 kg/ m^3 . [7]

There are three types of fuel blocks: standard fuel blocks as shown in Figure 3.1, RSC fuel blocks which contain a channel for a RSC rod and control rod fuel blocks that have a channel for control rod. As shown in Figure 2.2, there are 12 startup control rod blocks in the inner fueled ring, 6 RSC blocks in the middle fueled ring and 12 RSC blocks in the outer fueled ring. In this figure, RSCs are represented with black solid points. In each prismatic fuel block, fuel and coolant channels run in a triangular pattern with one coolant channel per fuel rods. This pattern propagates continuously in a standard fuel block as shown in Figure 2.5. [7] The control rod fuel block and reserve shutdown fuel block differ from the standard fuel block in that they contain one channel for control material. The diameter of a control rod channel is 101.6 mm, while the RSC channel has a diameter of 95.3 mm as shown in Figure 3.2. Each one of these channels replaces 11 coolant and 24 fuel channels. The pitch of the coolant and fuel channel array is 18.8 mm. At the center of each graphite fuel block, there is a fuel handling hole with a diameter of 35.0 mm. [7] Major core design parameters are summarized in Table 3.1.

The fuel channels have a diameter of 12.7 mm while the fuel compacts have a diameter of 12.45 mm and a height of 49.3 mm. Between the fuel compact and the fuel channel, there is a radial gap of 0.125 mm. Each fuel compact is a mixture of fissile and fertile particles embedded in a graphite matrix. Both fissile and fertile fuels are fabricated into a TRISO configuration. The fuel kernel of the fissile fuel is a two-phase mixture of 19.8% enriched UO2 and UC2, usually called UCO, while natural uranium is used as the fuel kernel in the fertile fuel. [7] A standard fuel block has 210 fuel channels

while a control rod or reserve shutdown fuel block has 186 fuel channels. So there are altogether 20,700 fuel channels in the active core. [7]

Table 3.1

Core Design Parameters

Core power, MWt	600
Core columns	102
Power density, MW/m3	6.6
Hexagonal fuel block	
Flat-to-flat dimension, m	0.36
Height, m	0.793
Effective active core diameter, m	
Outer	4.83
Inner	2.96
Active core height, m	7.93
Number of fuel blocks (10 blocks per column)	
Standard	720
Control	120
Reserve shutdown	180
Number of control rods	
Inner reflector	0
Active core	12
Outer reflector	36
Number of reserve shutdown channels in active core	18

Ref. [7]

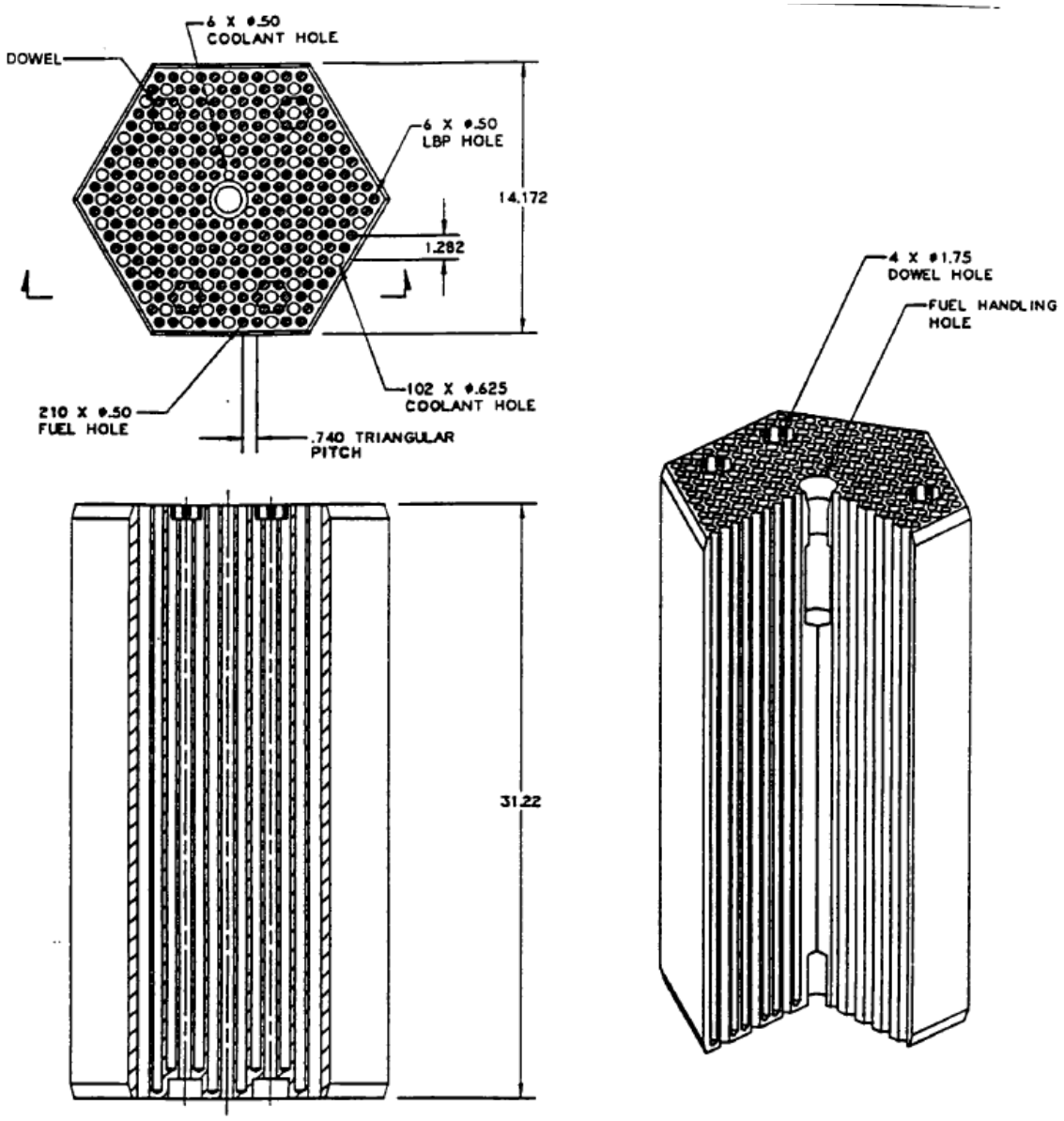

Figure 3.1. Standard Fuel Block [7] [Courtesy of General Atomics]

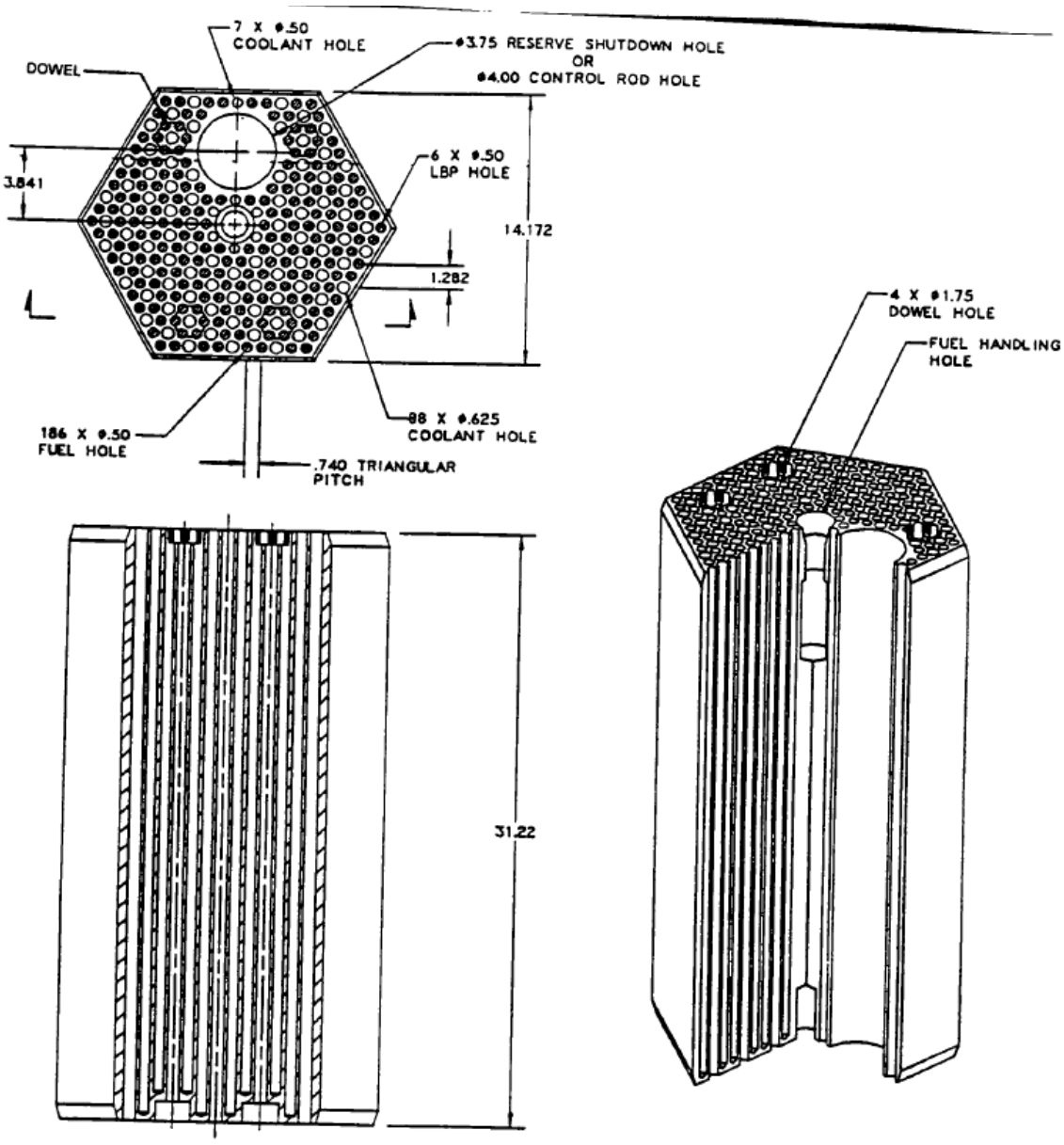

Figure 3.2. Control or Reserve Shutdown Fuel Block [7] [Courtesy of General Atomics]

There are small and large coolant channels, with diameters of 12.7 mm and 15.88 mm, respectively. A standard fuel block has 108 coolant channels while a control rod or reserve shutdown fuel block has 95 coolant channels. There are altogether 10,626 coolant channels in the active core, in which 10,014 are large channels and 612 are small channels. [1]

Each graphite fuel block contains six fixed burnable poison (FBP) rod channels with a diameter of 12.7 mm. [1] On average, one fuel block has five burnable poison rods with a diameter of 11.43 mm. [7] Those rods are composed of B4C granules dispersed in graphite compacts with a height of 51.5 mm. The characteristics of graphite fuel blocks are summarized in Table 3.2.

The hexagonal graphite reflector blocks are similar to the fuel blocks in their size, shape, handling hole and coolant channels. The upper reflector blocks on the top of the active core have the same array of coolant channels, control rod channels and RSC channels as the fuel blocks. This allows the coolant to flow into the active core and provides for the insertion of control devices into the active core. [7] The lower reflector blocks at the bottom of the active core guide the coolant from the active core to flow into the core support area. So these lower reflector blocks have the same layout of coolant channels as the fuel blocks. The control material channels stop at the top of the lower reflector blocks.

As shown in Figure 2.2, there is no control material in the inner reflector region. The outer reflector region is composed of three rings, and its inner ring contains 36 operating control rods. The middle ring consists of solid graphite blocks. The outer ring

includes the permanent side reflector blocks. Those blocks are solid too, except for two which contain boronated poison that acts a neutron absorber. There are no coolant channels in the inner or outer reflector regions.

The control rods are annular compacts with an inner diameter of 52.8 mm and an outer diameter of 82.6 mm. The control material consists of 40% wt. enriched boron (90%B10) contained in B4C granules. These granules are uniformly dispersed in a graphite matrix which forms into control rod compacts. The RSC rods consists of 40% wt. enriched natural boron in B4C granules. These granules are uniformly dispersed in a graphite matrix which forms into pellets. These pellets are cylindrical with a diameter of 14 mm. During startup or shutdown, the startup control rods are inserted. They are fully withdrawn when the reactor is critical and fully inserted when subcritical. The operating control rods are inserted with various positions during operation and fully inserted for protection. The RSC rods are fully withdrawn during normal operation and they are inserted should the control rods become inoperable due to the failure of the neutron control assembly support. [7]

As shown in Figure 2.2, there are gaps between all the hexagonal blocks. Helium not only flows through the coolant channels inside the blocks, but also flows through the bypass flow regions including the gaps, the inner section of the annular control rod compacts and the empty space contained in the control material channels. The ratio between the bypass flow to the total core flow is 20% in this reactor design. [2]

Table 3.2

Graphite Fuel Block Design Data

Distance across flats, m	
Not including gaps	0.36
Including gaps between blocks	0.361
Control rod channel diameter, mm	101.6
RSC channel diameter, mm	95.25
Coolant channels per block, large/small	
Standard block	102/6
Control and RSC block	88/7
Coolant channel diameter, mm	
Large	15.88
Small	12.7
FBP channels per block	6
FBP channel diameter, mm	12.7
FBP channel length, m	0.7815
FBP rods per block, average	5
FBP rod diameter, mm	11.43
FBP rod length, m	0.7214
Fuel channels per block, under dowels/not under dowels	
Standard block	24/186
Control and RSC block	24/162
Fuel channel diameter, mm	12.7
Fuel channel length, m	
Under dowels	0.7526
Not under dowels	0.7815
Fuel compact diameter, mm	12.45
Fuel compact length, mm	49.28

Ref. [7]

3.2 MELCOR Input Model of GT-MHR

This section explains the methodology used for calculating MELCOR input parameters and modeling strategy for thermal-hydraulics packages. Input calculation methods are listed for each package. The modeling strategy lies in simulating the thermal-hydraulics behavior in a prismatic core to the greatest extent possible using the existing MELCOR models.

3.2.1 Input Model Overview

The input model represents helium coolant flow through a prismatic core reactor, as seen in Figure. 3.3. This model is in two dimensions. Helium enters the system via control volume (CV) 190. The flow is upward through the inlet risers located between the core barrel and the RPV wall to an upper plenum volume (CV 280), where it is distributed to five radial rings. Each ring is divided into seven CVs axially. Ring 1 is the inner reflector region. Rings 2, 3, 4 are the inner most ring of the fueled region, the middle ring of the fueled region and the outermost ring of the fueled region, respectively. The outer reflector region is represented by ring 5. Among the CVs in rings 2, 3, and 4, those located at the top most level represent the upper reflector region, and those at bottom most level represent the lower reflector region. All the others are in the active fueled core region. Helium exits the core and flows into a core exit plenum (CV054), and out of the system through CV200. The thermal boundary of the reactor

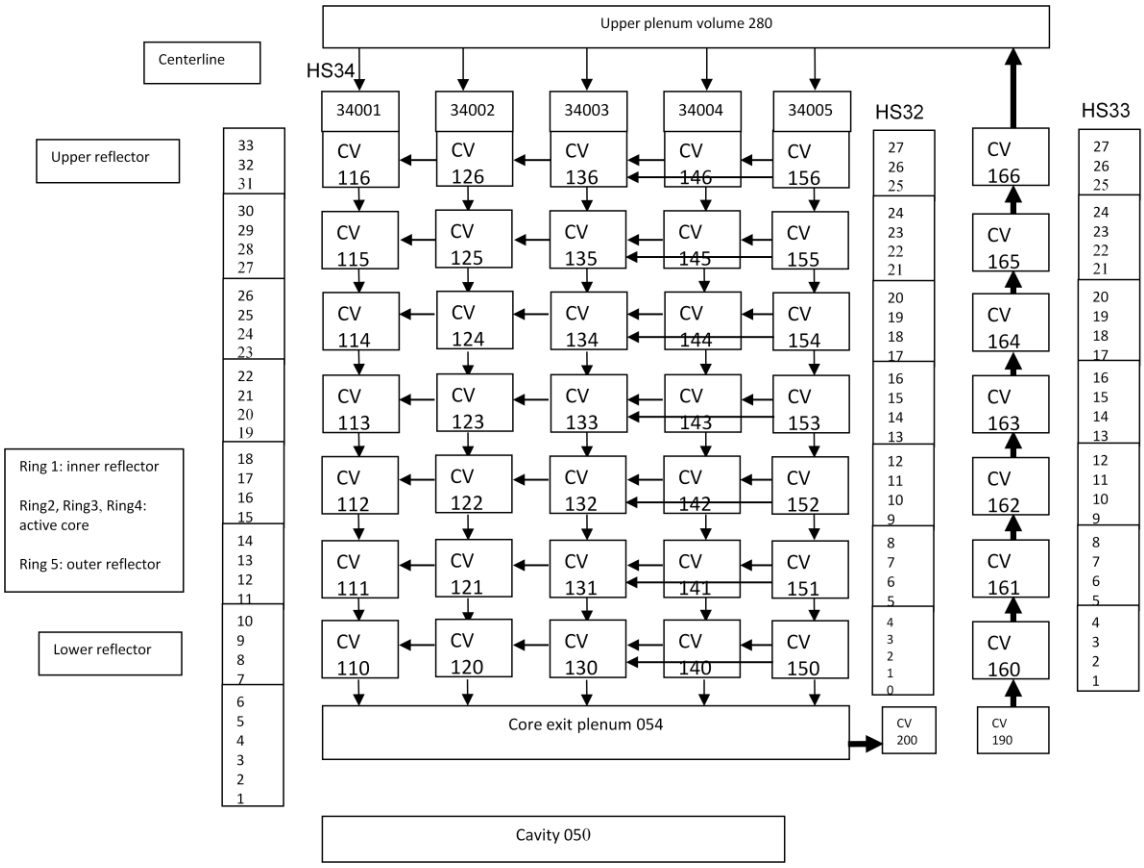

Figure 3.3. Nodalization of the GT-MHR/NGNP Input Model

core as explained in detail in 3.2.2.5 is modeled as Heat Structure (HS) 32 while HS 33 represents the RPV wall, which is also the boundary of this input model.

All the CVs in the five rings have core cells attached to them, and the levels of the core cells are given at the left hand side of Figure 3.3. Level 1 to 6 corresponds to the core exit plenum, among which levels 1 to 5 correspond to the lower plenum in the core exit plenum and level 6 corresponds to the core support plate in it. Levels 7 to 10 correspond to the lower reflector region. The lower reflector is 1.585 m high. Levels 11 to 30 correspond to the active core region. The active core has a height of 7.93 m. Levels 31 to 33 correspond to the upper reflector region. The height of the upper reflector is 1.189 m. [7] The masses of fuel, control materials, cladding, supporting components, the graphite reflectors and the heat transfer areas between different core components were modeled through the input for each core cell.

Bypass flow was also modeled. In this model, the bypass flow is in rings 1 and 5. The total flow areas in rings 2, 3 and 4 were calculated based on the data from the references. [7] This area was multiplied by 6% to obtain the flow area in the inner reflector region, and the same total flow area in rings 2, 3 and 4 was multiplied by 14% to obtain the flow area in the outer reflector region. The bypass flow area is larger in ring 5 versus ring 1, since there are operating control rods in the outer reflector region and there are no control materials in the inner reflector region. Those control rod channels are filled up with helium during the reactor operation.

Natural circulation of helium inside the RPV was also modeled through horizontal flow paths between adjacent rings. Helium flows from fueled ring to its

adjacent reflector ring through the gaps between hexagonal blocks. In the three fueled rings, helium also flows from hotter region to cooler region due to non-uniform temperature distribution through the gaps between hexagonal blocks.

This input deck is composed of the following files:

mmgen.in: this file initializes the calculation.

mmcor.in: this file advances the calculation in time.

cvh-fl-hs.gen: input file for the control volume hydrodynamics (CVH) package, the flow path (FL) package and the heat structures (HS) package.

core.gen: core package input file in which the core components are modeled.

ncg-mp.gen: input file for the noncondensible gas (NCG) package and material properties (MP) package.

3.2.1.1 EXEC Package Input

The mmgen.in file is the input file that initializes the calculation. The mmcor.in file specifies the time control of the simulation and provides the list of output files. The input model runs for 10,000 s which appears to be sufficient for the system to reach steady state under the given conditions.

3.2.1.2 CVH Package Input

The CVH and FL packages are responsible for the modeling of thermal-hydraulic behavior of coolant liquids and gases. The content in each CV and its initial condition plus its volume data are specified via the CVH input. FL package allows the calculation of the transfer of the contents between each two adjacent CVs. The CVH and FL concept treats flow calculation in a rather coarse scale due to the dimensions of the CVs. The specific turbulence models are not used in this concept.

The CVs in the lower reflector region are 1.585 m tall which is the height of this region. In the active core region, all the CVs are 1.586 m tall which corresponds to the height of two fuel blocks. The upper reflector region is 1.189 m tall and its CVs have the same height. The CVs in the above three regions are divided into five radial rings. As shown in Figure 3.3, the helium risers are modeled as a set of CVs. Each of them has the same height as those CVs in the core at the same axial location. The upper plenum volume is modeled as one CV. Its height is assumed to be 2.53 m and its radius is assumed to be the same as the outer radius of ring 5. This CV changes the direction of the helium flow from the risers and distributes it into five rings.

The core exit plenum is modeled as one CV which collects and mixes helium flows coming from the five rings. It is composed of two components: a core support plate at the top and a lower plenum at the bottom. This plate has no available design basis and its thickness is assumed to be 0.25 m. Its implementation is to ensure the normal execution of MELCOR. This plate is required to support the weight of the

reactor core. According to Figure 2.8, the diameter of the helium inlet is 90 in. which is 2.286 m. However, the diameter of the helium outlet is not available. It is assumed to be 85 in. which is 2.159 m in this input model. One further assumption is that the height of the lower plenum is the same as that of the helium outlet. By adding the height of its two components, the height of the core exit plenum is then obtained to be 2.409 m. The radius of this CV is assumed to be the same as the outer radius of ring 5.

The cavity is modeled as one large CV with the same height and elevation as the core exit plenum. The diameter is assumed to be 10 m which is larger than the outer diameter of the RPV. There is no available design basis for the cavity. Its implementation is just to satisfy MELCOR input requirements. The elevation and volume data of the upper and lower plenum CVs and cavity CV are listed in Table A.13 in Appendix A.

The initial conditions, including temperature and pressure, are given for each CV, as are the volume of the CV and the content of fluid in it. The initial temperature is the helium inlet temperature for all the CVs except for CV200. [7] The pressure for CV190 is 7.12 MPa corresponding to the helium inlet pressure entering the RPV. [2] Core upper plenum has a pressure of 7.07 MPa. [7] The active core pressure drop is 0.051 MPa. [7] As shown in Figure 3.3, from CV190 to CV166, an average pressure drop of 0.005 Mpa is assumed between each adjacent CV. A pressure drop of 0.015 is assumed between CV166 and CV280. From CV280 to CV054, between each adjacent CV, an average pressure drop of 0.006375 MPa is assumed. And the difference in pressure between CV280 and CV054 is the active core pressure drop. Between CV054

and CV200, a pressure drop of 0.005 MPa is assumed. The initial pressure in each CV is listed in Table A.1 in Appendix A.

CV190 and CV200 are time independent. Fixed boundary conditions of the RPV including temperatures and pressures were given via the input for these two CVs. The temperature of CV200 is the helium outlet temperature. The temperatures and pressures in all the other CVs are calculated over time.

As shown in Figure 2.2, all the graphite blocks in this reactor, both in the active core region and the reflector region, have a hexagonal shape with the same distance across flats except some in the side reflector region. In order to calculate the cross sectional area of each ring, the following procedures were applied:

a) The cross-sectional area of one hexagonal graphite block was obtained.
b) For ring 1, 2, 3, the number of graphite blocks in each ring times the cross-sectional area of one graphite block results in the cross-sectional area of the ring.
c) For ring 4, the same cross sectional area as ring 3 would be acquired if procedure (b) would be used. Both ring 3 and ring 4 have 36 graphite blocks. However, a different procedure was applied for ring 4. The outer radius of the active core was used to calculate the total cross sectional area of ring 1, 2, 3, 4. This value was then subtracted by the total cross sectional areas of ring 1, 2, 3, and the result is the cross sectional area of ring 4. This result is slightly bigger than the cross sectional area of ring 3 which indicates that there are gaps in the reactor. At this point, how to model the gaps with MELCOR is still unknown, so they have not been modeled in this input deck. The difference between the cross sectional area

of ring 4 and ring 3 is the area of gaps which are assumed to be the gaps in ring 1, 2, 3, 4.

d) For ring 5, no all the graphite blocks at the periphery of the side reflector region have a perfect shape, so it is not appropriate to use the procedure (b) to calculate the cross sectional area of ring 5. The total cross sectional area of ring 1, 2, 3, 4, 5 was obtained using the outer radius of ring 5. The result was then subtracted by the total cross sectional area of ring 1, 2, 3, 4 to obtain cross sectional area of ring 5.

More calculation details are found in Table A.2 - A.5 in Appendix A. The cross-sectional area of helium inlet CV is its flow area which is calculated in the next section. Once the cross-sectional area of each CV and the height of each CV were calculated, the volume of each CV was obtained as well as shown in Table A.7 - A.12 in Appendix A.

3.2.1.3 FL Package Input

Forced circulation and natural circulation of helium inside the RPV were modeled via the input for the Flow Path package. The flow path length is defined as the distance between the centers of two CVs connected by that flow path. The flow areas of the active core rings, including ring 2, 3 and 4, are obtained by multiplying the coolant channel cross-sectional area by the number of the channels in each ring. The sum of these three flow areas is the total flow area in the fueled region. The flow area in ring 1 is obtained by multiplying this total flow area by 6%. 14% times the total fueled region

flow area results in the flow area in ring 5. The total flow area of the helium inside the inlet risers is assumed to be equal to the total flow area in the fueled region. More calculation details are found in Appendix A.

Inside the core, the hydraulic diameter of the flow area in each ring is assumed to be equal to the diameter of the majority of the coolant channels. As shown in Figure 2.2, there are six helium riser channels located between the RPV wall and core barrel. In order to calculate the hydraulic diameter of these riser channels, several assumptions were made:

a) The angle between the short sides of one inlet channel is 30 degrees.
b) All the six inlet channels have the same size, so one inlet channel flow area is the total flow area divided by six.
c) The shape of an inlet channel is approximate to be that of a rectangle.

Then the hydraulic diameter was obtained by using the following formulae:

$$\frac{\pi}{12} * (R_2^2 - R_1^2) = \text{ inlet channel flow area} \tag{3.1}$$

R_1 : core barrel outer radius (m)

R_2 : core barrel outer radius plus the width of the inlet channel (m)

the width of the inlet channel (IC) = $R_2 - R_1$

$$\text{inlet channel length} = \frac{\text{inlet channel flow area}}{\text{inlet channel width}} \tag{3.2}$$

$$\text{Dh of the IC} = \frac{4 * \text{total flow area}}{2 * (\text{IC width} + \text{IC length})} \tag{3.3}$$

The calculation details are found in Table A.19 in Appendix A.

Natural circulation is modeled via horizontal flow paths between each two adjacent rings. As shown in Figure 2.2, ring 5 is not only in contact with ring 4, but also with ring 3, so there is natural circulation between ring 5 and ring 3 as well. The area of the natural circulation flow path is the cross-sectional area of the gaps between the two adjacent rings. The width of the gaps is 1 mm based on Table 3.2. The following procedures are used in order to calculate the flow areas:

a) For the flow area between ring 1 and ring 2, the hexagonal sides of ring 1 which are in contact with ring 2 are counted.
b) This number is then multiplied by the length of one side which results in the length of the gap between ring 1 and ring 2.
c) This length times the width of the gaps gives the flow area.

The same procedure is repeated for the calculation of all the other horizontal flow paths.

3.2.1.4 HS Package Input

The HS package calculates the heat conduction within each solid structures, radiation heat transfer between two solid structures and energy transfer between each structure and its adjacent CVs across boundary contacting surfaces.

Based on MELCOR's requirements, uppermost CVs and outermost CVs containing core cells need to have boundary HS attached to them as shown in Figure 3.3. Upper boundary HS is represented by HS 34. This HS has no design basis. Its height is

assumed to be 0.1 m, and its bottom corresponds to the top of the reactor core. HS 32 is the outer boundary HS. As shown in Figure 2.2, the region between the core barrel and RPV wall contains helium inlet risers and metal. The cross-sectional area of this region was obtained using the formula as the following:

$$\pi * (R_3^2 - R_1^2) = S_1 \tag{3.4}$$

R_3 : RPV wall inner radius (m)

S_1 : area of the region between the core barrel and RPV inner wall (m^2)

Then the cross-sectional area of the metal in this region was acquired by subtracting the total area of this region by the flow area of the inlet risers. This metal was added to the core barrel and they were combined together into one HS. The inner radius of this HS is the radius of ring 5 and its outer radius is calculated using the formula below:

$$R_4 = \sqrt{(S_1 + S_2 - S_3)/\pi} \tag{3.5}$$

S_2 : total cross-sectional area of ring 1, 2, 3, 4 and 5 (m^2)

S_3 : inlet riser flow area (m^2)

These two radii were used by MELCOR to calculate the cross-sectional area of the HS 32. This cross-sectional area is not part of the user input. The cross-sectional area of HS 33 was obtained using the inner and outer radii of the RPV wall. The axial length data of each HS was given in the input, then the volume of each HS was calculated by the code.

The material of all the HSs in this input model is stainless-steel-304, since the properties of the actual materials of the core barrel and the RPV wall are not available. CVs that are attached to HSs are defined as boundary CVs of the corresponding HSs by

MELCOR. Characteristic lengths of those CVs need to be specified for the input of the HSs. Those lengths are the hydraulic diameters of the flow areas in the CVs. The flow in those CVs in the upper reflector region and outer reflector region is evaluated as external flow since helium flows into the gaps between hexagonal blocks and the control material channels. Internal flow is defined for the CVs representing helium risers since helium only flows through the riser ducts. Hydraulic diameters are used by MELCOR to calculate Reynolds, Grashof, Nusselt and Sherwood numbers. The code uses different heat transfer correlations for external and internal flow. Between each HS and its boundary CV, a convective boundary condition is applied. HS 33 represents the RPV wall. It has an insulated boundary condition at its outside. The boundary surface area between each HS and its boundary CV needs to be specified in the input which is used for conduction calculation between the two. More calculation details are found in Tables A.23 - A.27 in Appendix A.

3.2.1.5 COR Package Input

The COR package is responsible for the calculation for the thermal response of the core and the lower plenum. This package also calculates the heat transfer to and from the CVH package and HS package.

In the core exit plenum, the height of the core cells in level 1 to 5 was obtained by dividing the height of the lower plenum by 5. The thickness of the core support plate is the height of the core cells at level 6. For the core cells in level 7 to 10, their height is

one fourth of that of the lower reflector. The core cells in level 11 to 30 have a height which is half of one fuel block. Core cells in level 31 to 33 belong to the upper reflector region. Those in level 31 and 32 are 0.3963 m high and those in level 33 are 0.3964 m high which add up to a total height of 1.189 which is the height of this reflector. The height of the core cells at each axial level and their elevation are listed in Table A.28 and A.29 in Appendix A. The elevation at 0.0 m corresponds to the bottommost point of the active core. The area of outer radial cell boundary which is the input variable ASCELR in MELCOR was acquired for each core cell by using the following formula:

$$ASCELR = 2\pi R * DZ \quad (3.6)$$

R: outer radius of the ring, DZ: the axial level length of the cell

The detailed calculation is listed in Table A.34 in Appendix A.

1) Modeling of Graphite

In the active core region, one part of graphite is modeled as cladding, and the other part of graphite is modeled as SSs. In order to calculate the mass of each component, the following procedures were applied:

a) The cross sectional area of each ring was obtained previously in Section 3.2.1.2.
b) In each ring, the cross sectional area of the fuel, coolant, burnable poison, control rod and reserve shutdown channels was calculated respectively.
c) Those cross sectional were then added together, the total cross sectional area of all the holes in each ring was acquired.

d) In each ring, the cross sectional area of the ring was subtracted by the total cross sectional area of all the holes, then the total cross sectional area of graphite in that ring was obtained.

e) This cross sectional area was then multiplied by the height of the core cell and the density of graphite, then the result will be the mass of graphite in that core cell.

f) In each ring, the ratio (R_c) between cross sectional areas occupied by the sum of fuel holes plus coolant holes to that of all the holes was calculated. Multiplying this ratio by the total mass of graphite of one core cell, then the result will be the mass of cladding in that core cell. The total mass of graphite was then subtracted by the mass of cladding in one core cell, then the result will be the mass of SSs in that core cell. As shown in Figure 3.1 and 3.2, there is a block handling hole at the center of each block. This hole extends down about one-third of the height of one graphite block with a diameter of 35.0 mm. It is not all the way through the reactor core like the coolant channels even though the block handling hole will be filled with helium during reactor operation. This hole is neglected in the calculation of this model.

The masses of the cladding and SSs of each fueled core cell are listed in Table A. 38 in Appendix A.

MELCOR is a light water reactor code. A prismatic core reactor is required to be defined as a pressurized water reactor (PWR) in the user's input. In a PWR, a clad is in contact with fuel pellets at its inside, and coolant at its outside. Between the clad and the

fuel pellet, there is a gas gap. MELCOR requires the intact surface area of each core component for convection and oxidation calculation. The cladding surface area (ASCL) in each core cell is obtained by using the following formula:

ASCL =axial surface areas of all the fuel channels + axial surface areas of all the coolant channels (3.7)

ASFU per ring = number of SFB per ring * total FPSA per block + number of CRFB per ring * total FPSA per block + no. of RSC fuel block per ring* total FPSA per block

ASFU per cell = ASFU per ring / 2 (3.8)

By using the formula below, the surface area of the SSs (ASSS) in each ring was acquired:

ASSS = ASCELR of the adjacent cell at its inside if there is one + ASCELR of this cell + cross sectional area of the graphite + axial surface areas of all the burnable poison rods + axial surface areas of the control rod or reserve shutdown rod channels (3.8)

The cross sectional area of the graphite in (3.8) corresponds to the cross sectional area of the ring subtracted by the cross sectional areas of the coolant holes and control rod or reserve shutdown rod holes. As shown in Table 3.2, fuel holes and burnable poison holes are not all the way through the block. Since each fuel block is split into two core cells, the ASSS of the top cell counts the cross sectional area of graphite block at the top edge while the ASSS for the bottom cell counts the bottom edge.

The graphite in the reflector region is modeled as SSs only. The following procedures were applied to determine the cross-sectional area of graphite in order to calculate SS masses:

a) For ring 1, the cross-sectional area of the ring is the cross sectional area of graphite.
b) For the lower reflector region in ring 2, 3, 4 and 5, the cross sectional area of the ring was subtracted by the cross sectional area of all the coolant holes, then the total cross sectional area of graphite in that ring was obtained.
c) For ring 5, the cross sectional area of graphite was acquired by subtracting the cross sectional area of control rod channels from the cross sectional area of the ring.

The following formula was applied in order to calculate the ASSS:

ASSS = ASCELR of the adjacent cell at its inside if there is one + ASCELR of this cell + cross sectional area of the graphite + axial surface areas of the control rod channels if there are any + axial surface areas of all the coolant channels if there are any (3.9)

2) Modeling of Fuel

According to reference [7], in the fuel compacts, there are two types of fuel particles: fissile particles and fertile particles. The fraction of each particles and the particle packing fraction of the compacts are not available. The particle packing fraction

(PF) is the volumetric fraction occupied by particles in a fuel compact. Assumptions were made based on reference [2]: a single fissile particle system with a PF of 0.289 is used in this input model. The composition of one fuel particle is listed in Table 3.3.

Table 3.3

Composition of a Fissile Fuel Particle

	Fuel *UO2*	Buffer *C*	PyC *C*	SiC *SiC*	PyC *C*
Density (g/cm3)	10.5	1	1.87	3.2	1.83
Density (g/m3)	1.05E+07	1.00E+06	1.87E+06	3.20E+06	1.83E+06
Layer dX (10-6m)	350	100	35	35	40
Outer Radius (10-6m)	175	275	310	345	385
Mass/Coated Particle (g)	2.357E-04	6.466E-05	7.045E-05	1.511E-04	1.227E-04
Mass/Fuel compact (g)	1.710E+00	4.692E-01	5.112E-01	1.096E+00	8.901E-01

Particle Volume (m^3)	2.681E-13
Fuel Particles/Fuel compact	7.256E+03
Volume of Particles/compact (m^3/compact)	1.734E-06

Ref. [7]

The volume of the particles in one compact is obtained by multiplying the volume of the compact by PF. Dividing the resulting volume by the volume of one particle gives the number of particles in one compact. In order to calculate the number of fuel compacts (FC) in each block the following formula is used:

Number of FC per block = number of fuel channels per block * height of the block / height of one FC (3.9)

Number of FC per core cell = Number of FC per block / 2 (3.10)

A simplification is made here also in the calculation of cladding surface area, since the height of the fuel channels are smaller than that of the graphite block as indicated in Table 3.2.

Table 3.4

Fuel Compact Properties

Property	Value
Radius (cm)	0.6225
Radius (m)	0.006225
Height (cm)	4.93
Height (m)	0.0493
Total compact Volume (cm3)	6.001716866
Total compact Volume (m3)	6.00172E-06
Volume of carbon in compact (m3)	4.26722E-06
Density of carbon in compact (g/cm3)	1.74
Density of carbon in compact (g/m3)	1740000
carbon Mass in compact (g)	7.424964004
Density of Total Fuel compact (g/cm3)	2.016467429
Density of Total Fuel compact (kg/m3)	2016.467429

Ref. [7] and [2]

Table 3.5

Fuel Compact Content

	UO2	C(Buffer)	C(PyC)	SiC	carbon	Total
Mass/Fuel compact (g/compact)	1.710	0.469	1.401	1.096	7.425	12.102
Mass Percentage/Fuel compact (%)	14.133	3.877	11.579	9.059	61.352	
Mass Percentage/Fuel compact (%)	0.141	0.039	0.116	0.091	0.614	

Ref. [7] and [2]

3) Modeling of Control Materials

Control materials are defined as nonsupporting structures (NSSs), including: control rod, reserve shutdown system and burnable poison rod. B4C is the control poison material in this input model due to the unavailability of the properties of the actual material used in the referenced reactor design. B4C is the default material for control poison in MELCOR with a density of 2520kg/ m^3 . The surface area and the mass of NSS were calculated for each core cell in the upper reflector, the active core and the side reflector.

4) Modeling of Power Distribution

Since the power factors for the actual reactor design are not available, those for the NGNP were used in this input model. The first set of power factors is from the point design. [2] The radial power factors are 1.1, 0.92 and 1.0 for the inner, middle and outer fueled rings respectively. The axial power factors are shown in Figure 3.4. This power distribution corresponds to a time point between the middle and end of cycle. The control rods are inserted to the middle point of the fueled core. Due to the fact that more power shifts towards the bottom of the core, this set of power peaking factors results in higher fuel temperatures. The coolant is also hottest at the bottom of the core. The axial power factors for each active core cells are obtained by hand from Figure 3.4. These values start from the top of top-most fuel block and end at the bottom of the bottom-

most one. The data corresponding to the core that is 10 blocks high is used in this input model.

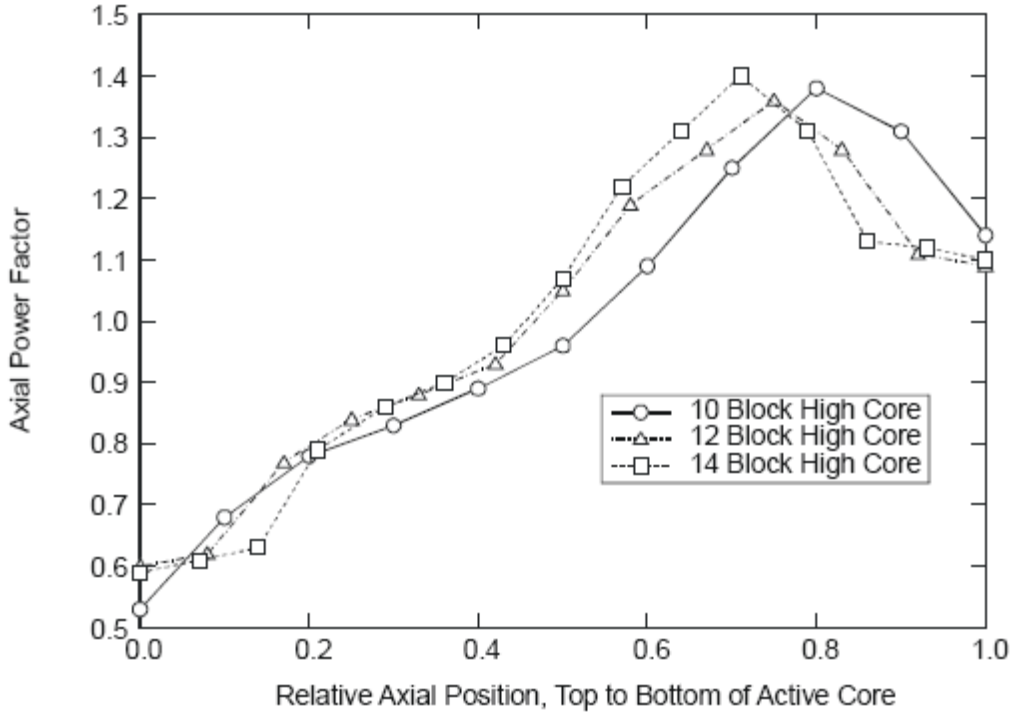

Figure 3.4. Axial Power Factors of the NGNP Point Design [2]

The second set of data is provided by Chris Ellis from GA as shown in Table 3.6. A thermal analysis code POKE is used to calculate temperatures throughout the core. The time point for the power factors corresponds to the middle of cycle with axial power peaking factors towards the bottom which should give conservative temperature values. Dr. Don Mceachern mentioned that this set of axial factors start from the bottom to the top of the core. [27] For the radial factors, there are 34 values which correspond to 34

columns since one third of the core is modeled. The order of these 34 values is assumed to start from outermost fueled ring, then the middle ring, then the innermost ring, since there are 6 values in the first 5 lines and there are 4 values in the last line as shown in Table 3.6. One third of outer or middle ring is 12 columns while one third of inner ring is 10 columns. Based on the above assumption, the radial power factors were obtained to be 1.161, 1.065 and 0.831667 for inner, middle, outer fueled ring respectively.

Table 3.6

GA Power Peaking Factors for the NGNP

POKE axial peaking (at top and bottom of each core layer, for all radial columns)

0.58 0.73 0.80 0.84 0.89 1.00 1.14 1.23 1.31 1.23 1.06

POKE radial peaking (34 columns)

0.6700	0.9900	0.5800	0.9600	0.5800	1.0000
0.5800	0.9700	0.5700	0.9900	0.9400	1.1500
0.9500	1.1900	0.9300	1.1200	0.9300	1.1400
0.9300	1.1900	0.9200	1.1500	1.2300	1.1000
1.3200	1.0800	1.2500	1.0200	1.2200	1.0600
1.3100	1.0700	1.2700	1.0100		

Ref. [25]

The point design power factors [2] are primarily applied in this model development. The GA power factors are used for sensitivity studies to gain insight on the effect of power distribution on key output. The axial power factors at the middle point of

each half fuel block were obtained as shown in Table A.42 in Appendix A since each block is cut into two core cells in this input model.

3.2.1.6 MP and NCG Package Input

The MP package models the material properties needed by various other MELCOR packages. Noncondensible gases in the CVH packages are modeled as ideal gases. The treatement of noncondensible gas as a compressible fluid has been investigated in Reference [3].

In MELCOR, the default material for cladding is zircaloy while the default material for SSs is stainless steel. The properties of these two materials have been overwritten with that of graphite in this input deck. The density of the H-451 graphite is 1740kg/m^3 based on [7], but the other properties of this graphite are not available. The properties of the POCO graphite were used instead based on reference [15]. The density of different kinds of POCO graphite ranges from 1300 to 1880 kg/m^3 , so 1740 kg/m^3 lies within this range. The thermal conductivity is obtained by hand from Figure 3.5 in which the curve corresponding to the FM-1 was used. The reason of choosing this curve is that the thermal conductivity of the graphite is fairly consistent with that of IG-110 graphite which is used in the hexagonal blocks in the HTTR reactor. [6] The specific heat values were obtained from the same reference. [15] Within the temperature range of interest, the density is assumed to be constant, the thermal conductivity decreases as the temperature increases [15] while the specific heat increases with increasing temperature

[15]. The thermal properties of graphite are listed in Table A.59 and A.60 in Appendix A.

The helium properties were taken from reference [21]. The values corresponding to 7 MPa are used in this input deck. The thermal conductivity and the specific heat of helium go up with increasing temperature while its density goes down. The properties of oxygen were overwritten with that of air which is needed for the modeling of the RCCS in Section 5. The thermal properties of helium are listed in Table A.53, A.54 and A.55 and those for oxygen are listed in Table A.56, A.57 and A.58 in Appendix A.

The properties of inconel were overwritten with that of fuel compacts. The fuel material in the compacts is UCO whose thermal properties are not available. GA has performed experiments and obtained the thermal properties of fuel compacts. However, this information is proprietary. The thermal properties of fuel pebbles of a PBMR from reference [3] are used for that of the fuel compact in this prismatic core input model. According to John Saurwien from GA, even though the compacts are made of mostly graphite, it is not appropriate to use the thermal properties of graphite for that of the compact. The fuel compact is less dense than graphite and it has a lower thermal conductivity than graphite. It is appropriate to use the thermal properties of pebbles for that of fuel compact, since they are essentially made of the same material which is homogeneous. Nonetheless, the pebbles still have a higher thermal conductivity than that of the compact. [24] The density of the compact shown in Table 3.4 is different from that of the pebbles. [3] However, in the MP input deck, in order to be consistent, all the properties of the pebbles are used, including its density.

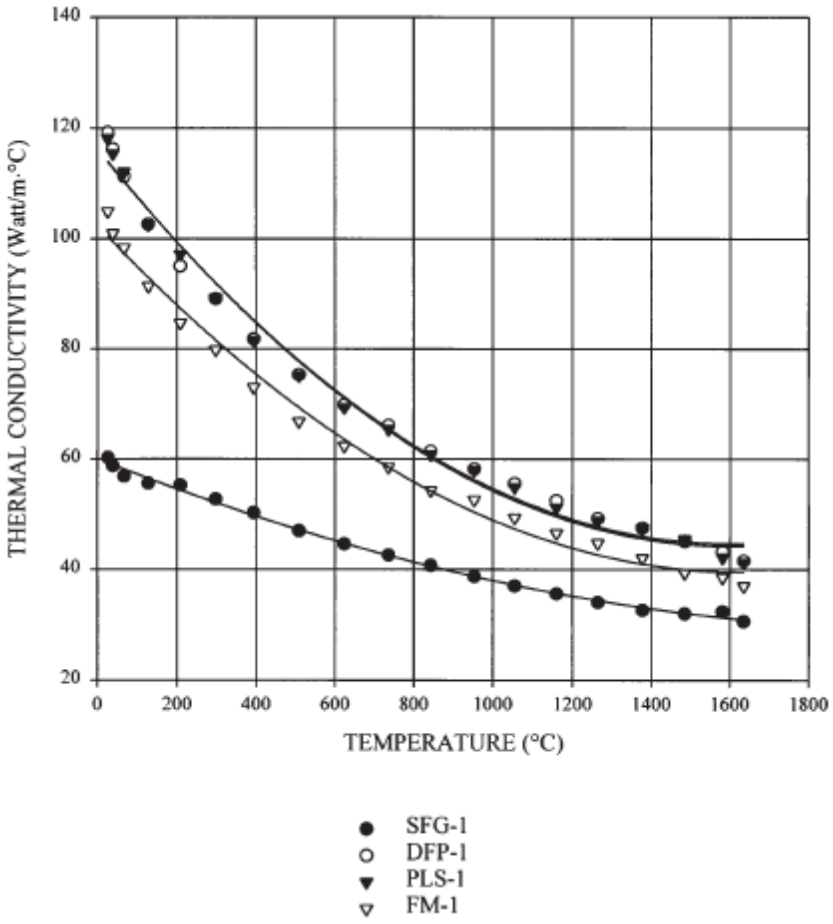

Figure 3.5. Thermal Conductivity of POCO Graphites [15]

3.3 Analysis Results

A simulation lasting 10000 s was performed to achieve near steady state condition. The total mass flow rate calculated is 319.7 kg/s as shown in Figure 3.6. The helium outlet temperature is 844°C as plotted in Figure 3.7. The peak fuel temperature is around 1514°C as indicated in Figure 3.8. The peak temperature for cladding is around

1459°C as shown in Figure 3.9 and 1060°C for SS as shown in Figure 3.10. The bypass fraction calculated is 9.5%. MELCOR is a deterministic code which does not provide uncertainties in the results. During the code execution, almost 80% of the CPU time is consumed by the COR package.

The data from the reference is shown in column 1 of Table 3.7. This data was from GA's analyses using a thermal-hydraulic code called POKE. The information regarding the uncertainties of this data is not publicly available. The fuel temperature in column corresponds to the temperature of the fuel compact instead of the fuel micro particles.

Table 3.7

GT-MHR RPV Steady State Results

	GT-MHR	MELCOR
Coolant Inlet Temperature (°C)	491	491
Average Coolant Outlet Temperature (°C)	850	844.7
Bypass Flow Fraction	0.2	0.18
Maximum Fuel Temperature (°C)	1218	1514.4
Maximum Graphite Temperature (°C)	1142	1334.3
Temperature Difference Within the Same Block (°C)	50 – 100 From GA	269.8
Maximum Coolant Outlet Temperature (°C)	1021	1044.1

Ref. [2]

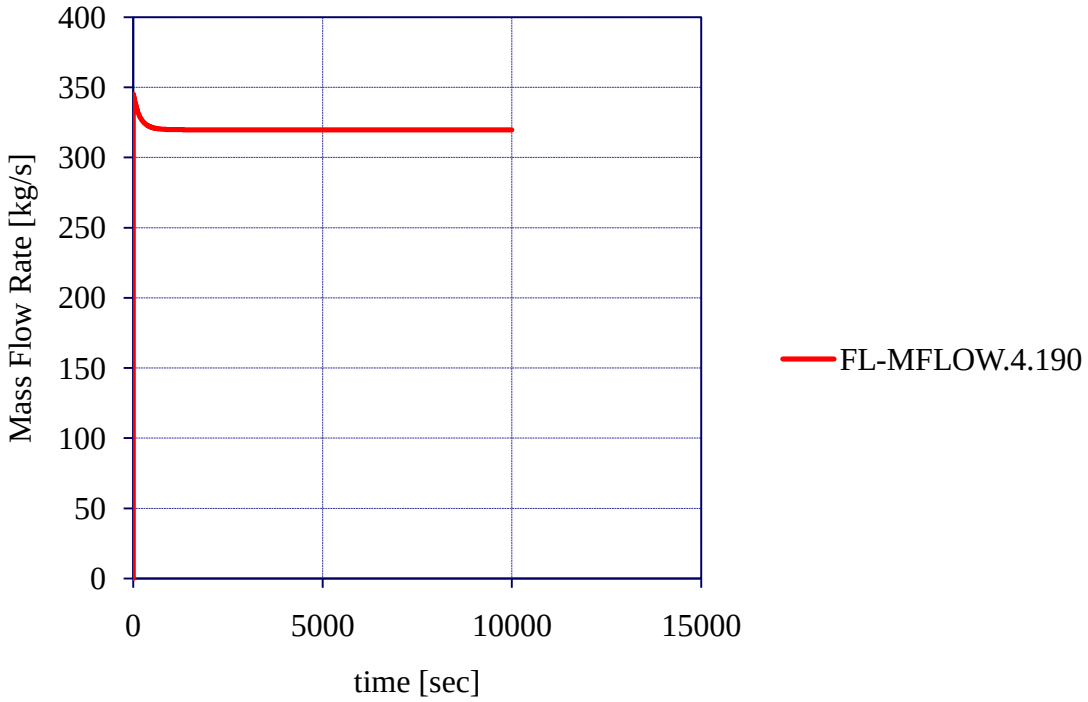

Figure 3.6. GT-MHR RPV Total Mass Flow Rate

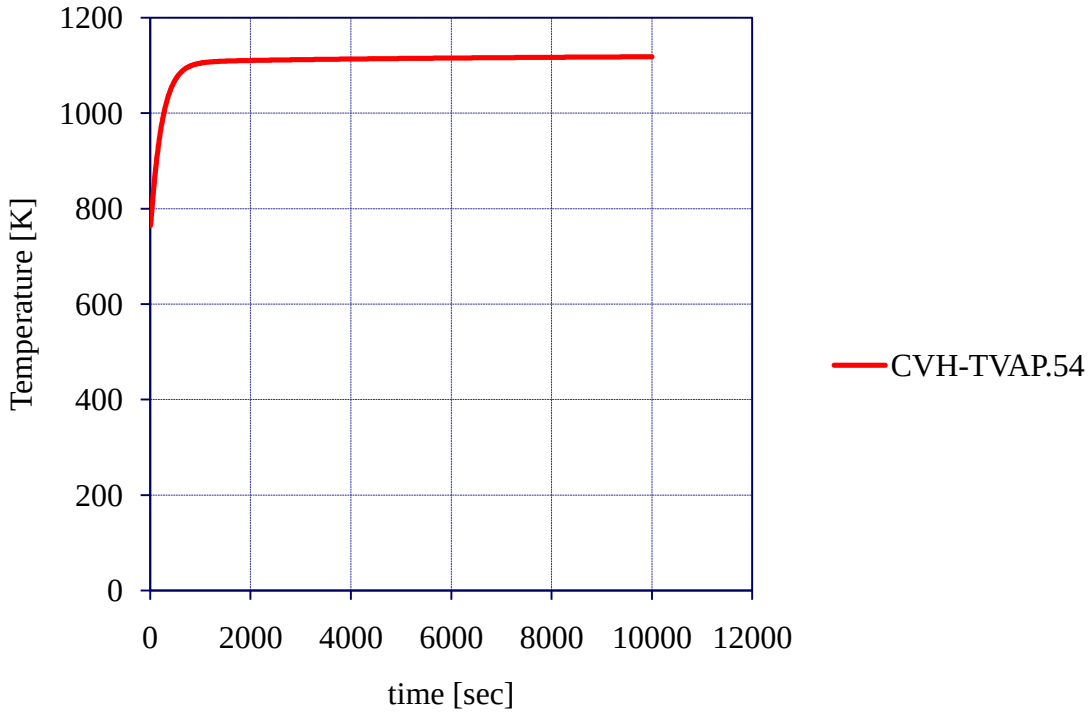

Figure 3.7. GT-MHR RPV Helium Outlet Temperature

3.4 Conclusions

MELCOR results predict mass flow rate and outlet temperature with high accuracy. The calculated bypass fraction is reasonable too. The peak fuel temperature is within design limit. According to GA, the graphite within the same block has a temperature difference ranging from 50 to 100°C. MELCOR results give a graphite

temperature difference of almost 300°C within the same block which is inconsistent with actuality.

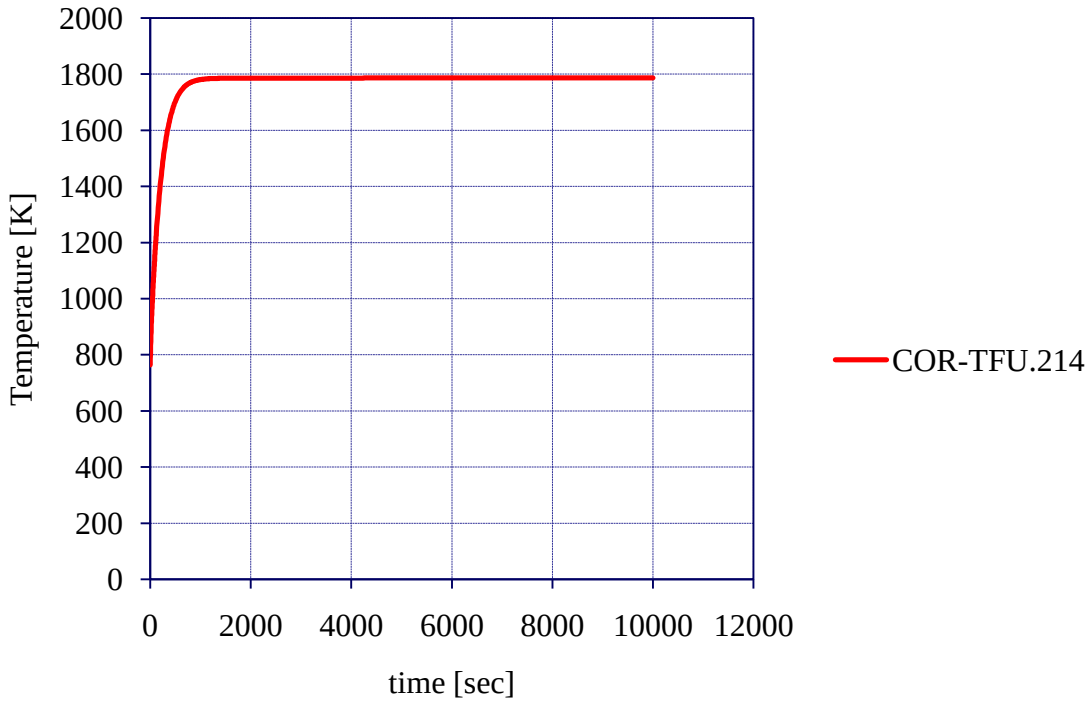

Figure 3.8. GT-MHR RPV Peak Fuel Temperature

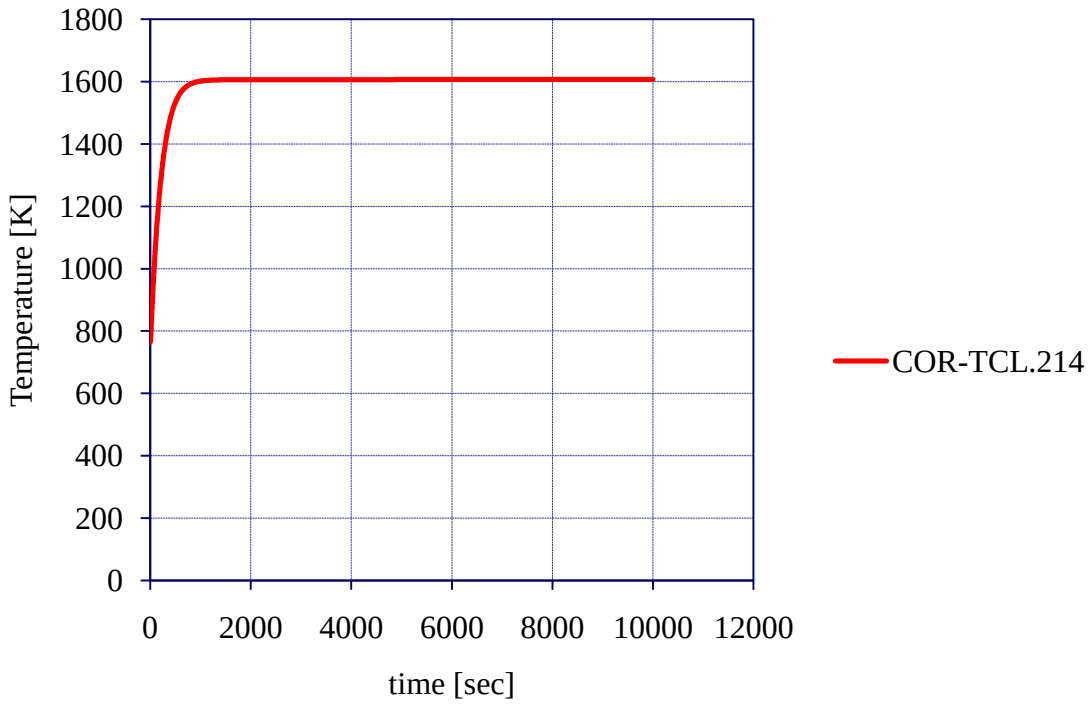

Figure 3.9. GT-MHR RPV Peak Cladding Temperature

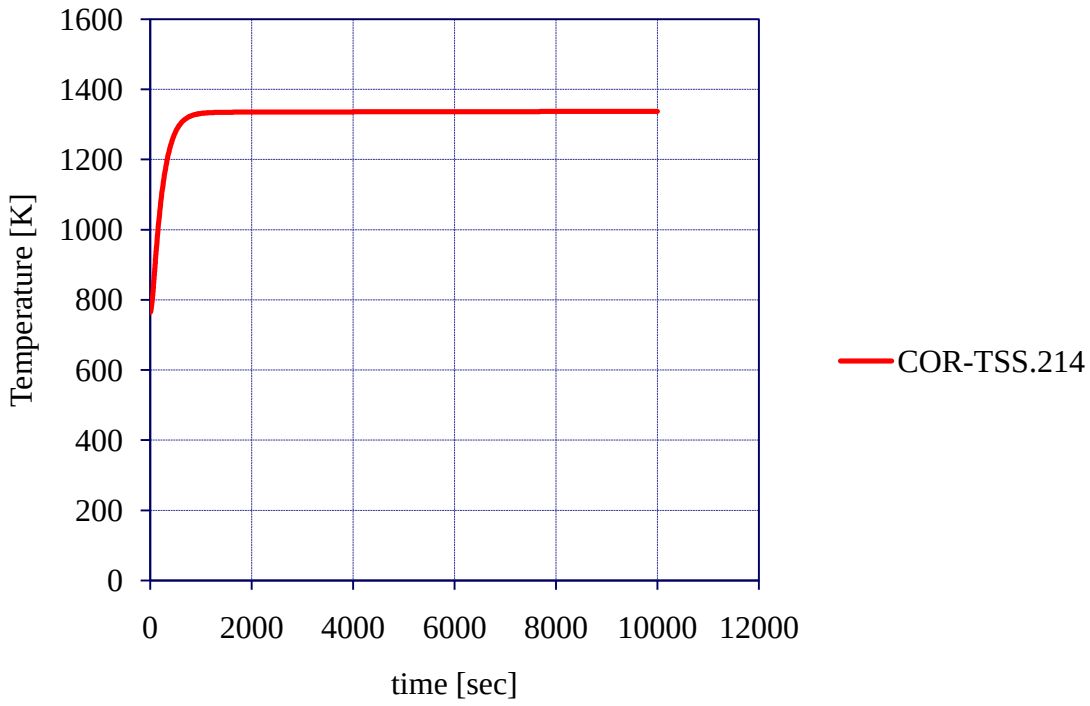

Figure 3.10. GT-MHR RPV Peak SS Temperature

4. MODELING OF THE NGNP WITHIN THE RPV

4.1 Initial Simplified Model and Results

4.1.1 Literature Survey

The prismatic core NGNP has a helium outlet temperature up to 950°C with a thermal power output ranging between 550 to 600 MW. [13] This reactor design will produce helium at an even higher efficiency versus the GT-MHR 600 MW design. General information on the NGNP prismatic core reactor was obtained from reference [2]. The prismatic core NGNP is based on GA's GT-MHR 600 MW design [2]. Data that were not available in reference [2] were estimated based on the reference [7].

Two major differences for driving the outlet temperature from 850°C to 950°C were considered in this input model, including a smaller helium forced circulation mass flow rate and a reduction in bypass fraction. The total mass flow rate of the GT-MHR 600 MW is 320 kg/s versus 226 kg/s for the NGNP. The bypass fraction is 20% for the GT-MHR while 10% for the NGNP. The NGNP also has a smaller core pressure drop as indicated in Table 2.1 which is modeled in this input deck.

GA has completed their PCD report for their recommended design for the NGNP. According to John Bolin, an expert in thermal-hydraulics from GA, reference [2] does not contain sufficient data for the NGNP. In order to have an accurate model for the NGNP, the design data from the GA PCD report needs to be used. [23] However, this

document is proprietary. Based on the current literature survey, additional data has to be obtained in order to model the NGNP. One of the major differences between the NGNP and the GT-MHR is that the helium inlet risers are located inside the side reflectors instead of the region between the core barrel and RPV wall. Reference [13] mentions this difference. However, the details of this design feature are not available.

4.1.2 Model Development

A simplified model of the prismatic core NGNP input model was developed as shown in Figure 4.1. It represents helium coolant flow over a prismatic reactor core. Helium enters the system at CV160. The flow is upward to an upper plenum volume, and then downward across an upper plenum plate, where it is distributed to three axial fuel rings divided into seven axial levels. Among these seven axial levels, the top most is an upper reflector, and the bottom most is a lower reflector. The five in between are active fuel zones. Flow exiting the core flows into a core exit plenum CV054, and out of the system at CV200.

The core content is composed of three main radial regions: an inner reflector region, an active core, and an outer reflector region. These correspond to heat structure HS 32, Rings 1, 2, 3 and HS 33, respectively.

The upper reflector is located above the active core and the outer reflector, and the lower reflector is below them. The MELCOR code does not allow the modeling of an HS adjacent to another HS. Therefore, the upper reflector region that is located above

the active core and the lower reflector region that is located beneath the active core were modeled as CVs. The upper reflector region that is located above the side reflector and the lower reflector region that is located beneath the side reflector were modeled as HSs.

A control function is implemented at the flow path connecting CV160 and CV140 which is the bottommost helium inlet CV. This function gives a helium mass flow rate of 226 kg/s. The helium inlet temperature is 491°C.

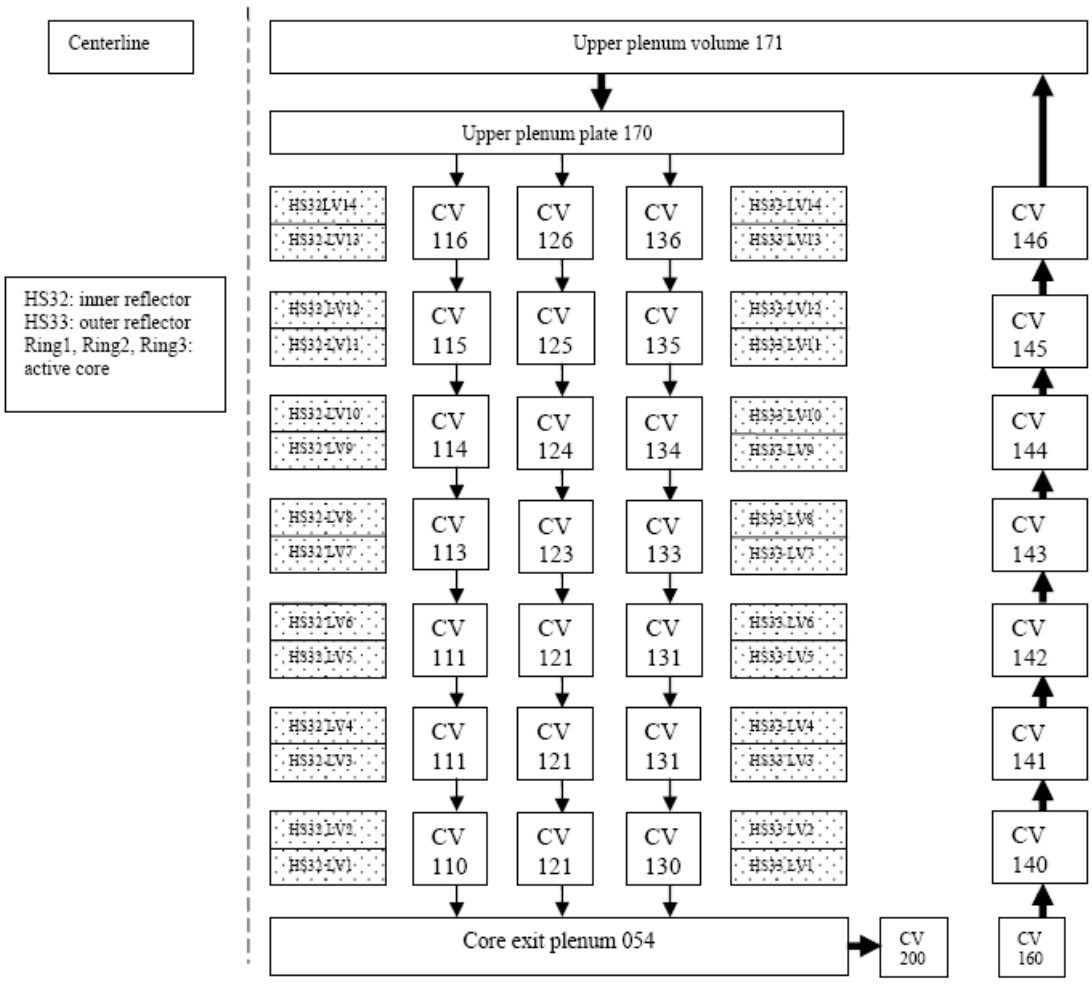

Figure 4.1. Nodalization of the Simplified NGNP Model

4.1.3 Analysis Results and Conclusions

Initial calculations demonstrate the passive heat removal capability of the inner and outer reflectors. The heat from the core region is calculated to transfer through the HSs by conduction heat transfer, as evidenced by the temperature transients throughout the inner and outer reflectors. The pressure drop in the active core and mass flow rate correspond well with the NGNP design data provided from reference [2].

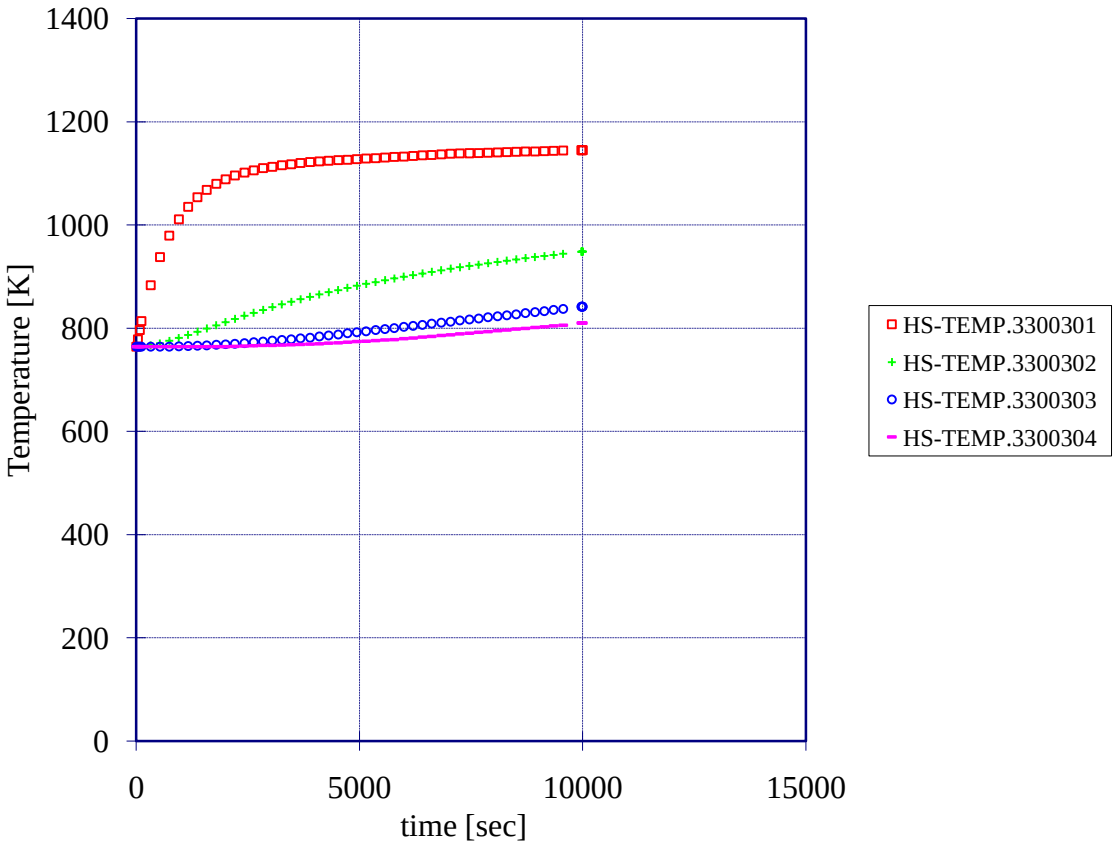

Figure 4.2. Temperature Profile in the Side Reflectors

The initial temperature in the reflector region is 491°C while the initial temperature of the coolant is 927°C. As show in Figure 4.2, the square line is the temperature profile of the innermost temperature node of the reflector region which is located next to the active core while the dash line is the temperature profile of the outermost temperature node of the reflector which is located next to the core barrel. There are altogether four temperature nodes evenly located along the radius of the outer reflector region. This figure shows the passive heat removal feature of the outer reflectors.

4.2 Detailed Model

4.2.1 Literature Survey

Bypass fraction for the NGNP is 10% for the NGNP. [2] The nodalization of the NGNP is shown in Figure 3.3. GA recommends a helium outlet temperature up to 950°C. According to Dr. Don Mceachern from GA, in the NGNP design, heat is not well transferred away from the fuel block which partially results in a high fuel temperature. A coolant outlet temperature of 1000°C will potentially result in a fuel temperature that is beyond its design limit. [26] Otherwise, it will require advancement in material and fuel design which will bring issues to cost and feasibility [12]. The reason of lowering the outlet temperature to 950°C is to maintain the fuel temperature within its design limit.

4.2.2 Model Development

The GT-MHR RPV model was modified accounting for the differences between these two designs and a model representing the NGNP RPV was developed. The bypass flow is also in ring 1 and ring 5. The total flow area in rings 2, 3 and 4 were multiplied by 3% to obtain the flow area in ring 1. The same area times 7% gives the flow area in ring 5, similar to the GT-MHR RPV model as described in section 3.2.1. The core pressure drop was also modified. The flow form loss coefficient is 2.8 for the NGNP versus 1.2 for the GT-MHR to achieve a mass flow rate of around 226 kg/s. The flow area data and the initial pressure data are listed in Table C.1 and C.2 in Appendix C.

4.2.3 Analysis Results

Table 4.1

NGNP RPV Steady State Results

	NGNP	MELCOR
Reactor Power Level (MWt)	550	550
Coolant Inlet Temperature (°C)	491	491
Average Coolant Outlet Temperature (°C)	950	944.2
Bypass Flow Fraction	0.1	0.095
Maximum Fuel Temperature (°C)	<1600	1622.1

Ref. [6]

Based on discussion with Chris Ellis from GA, the data in column 1 in the above table was obtained using a thermal-hydraulic code called POKE. [25] 1600°C is the failure criteria for the TRISO fuel which is the micro particle instead of the fuel compacts. The fuel temperature in column 2 is for compacts.

A simulation lasting 10000 s was performed to achieve near steady state condition. The total mass flow rate calculated is 226.7 kg/s as shown in Figure 4.3. The helium outlet temperature is 944°C as plotted in Figure 4.4. The peak fuel temperature is around 1618°C as indicated in Figure 4.5. The peak temperature for cladding is around 1459°C and 1160°C for SS as shown in Figures 4.6 and 4.7, respectively. The bypass fraction calculated is 9.5%.

4.2.4 Conclusions

MELCOR results predict mass flow rate and outlet temperature with high accuracy. The calculated bypass fraction is reasonable too. The peak fuel temperature overpasses the design limit of 1600°C with a difference of around 18°C. According to reference [2], when the outlet temperature is 1000°C, the corresponding peak graphite temperature is 1208°C. The peak graphite temperature calculated by MELCOR is 1459°C corresponding to an outlet temperature of around 950°C which is significantly higher than the data from the reference. According to GA, the graphite within the same block has a temperature difference ranging from 50 to 100°C. MELCOR results give a

graphite temperature difference of almost 300°C within the same block which is inconsistent with actuality.

There are uncertainties associated with the power factors in Figure 3.4. According to Don Mceachern from GA, the power factors might start from the bottom to the top instead from the top to the bottom as indicated in the figure. [27] Power factors have a significant impact on the peak fuel temperatures. A bottom peaked power profile will result in a high fuel temperature.

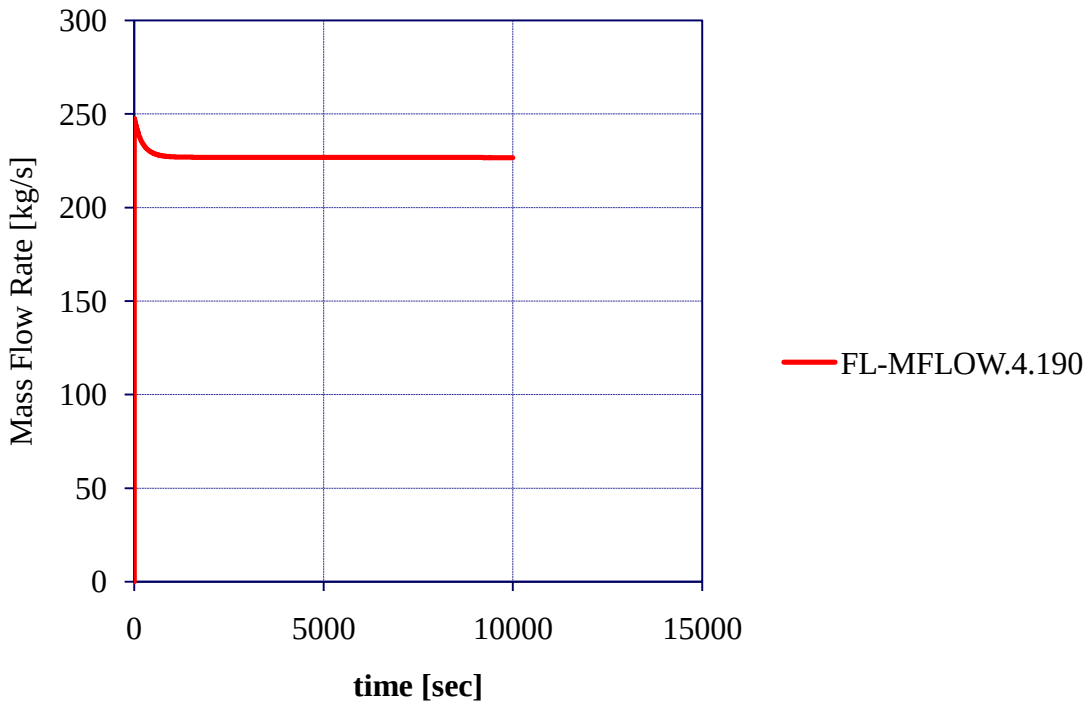

Figure 4.3. NGNP RPV Total Mass Flow Rate

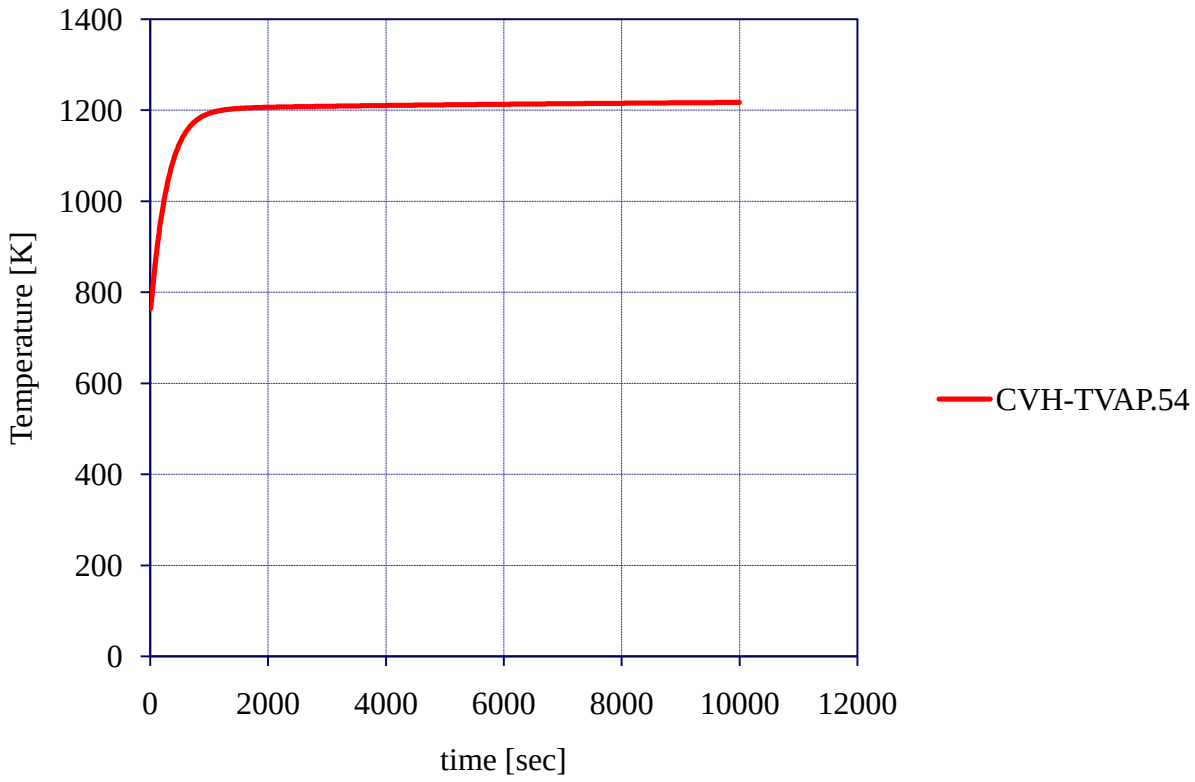

Figure 4.4. NGNP RPV Helium Outlet Temperature

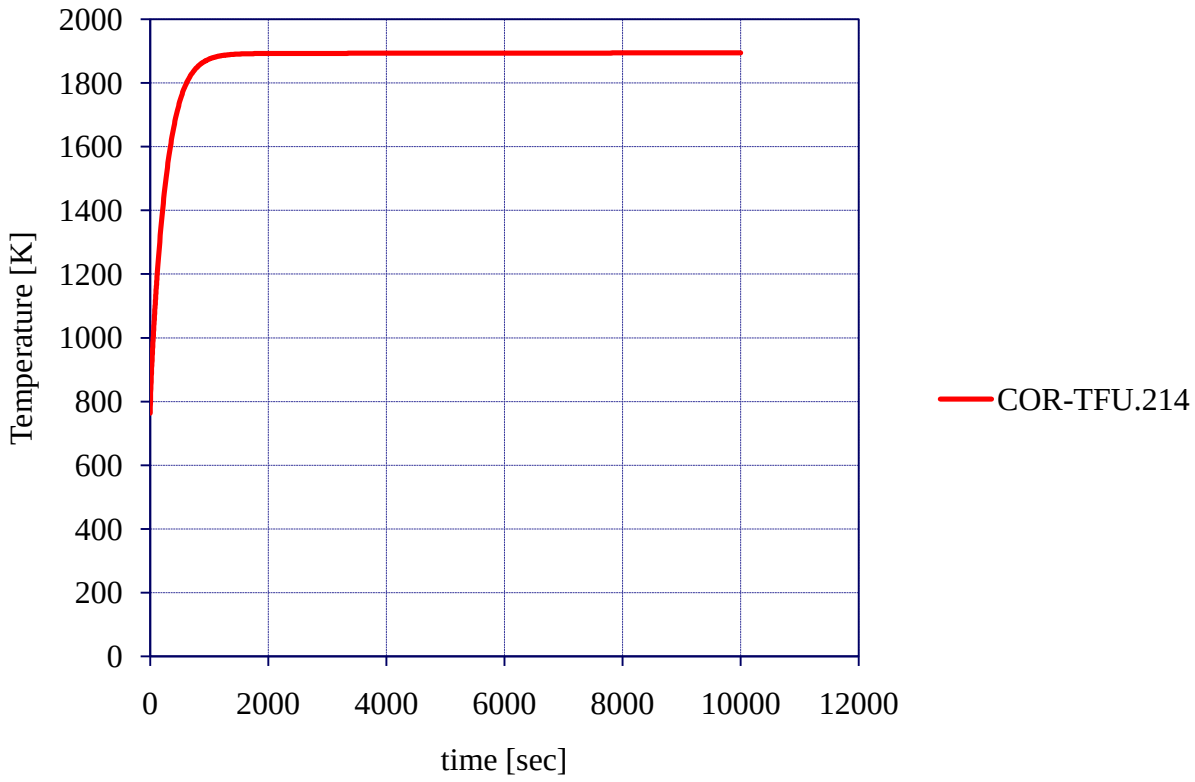

Figure 4.5. NGNP RPV Peak Fuel Temperature

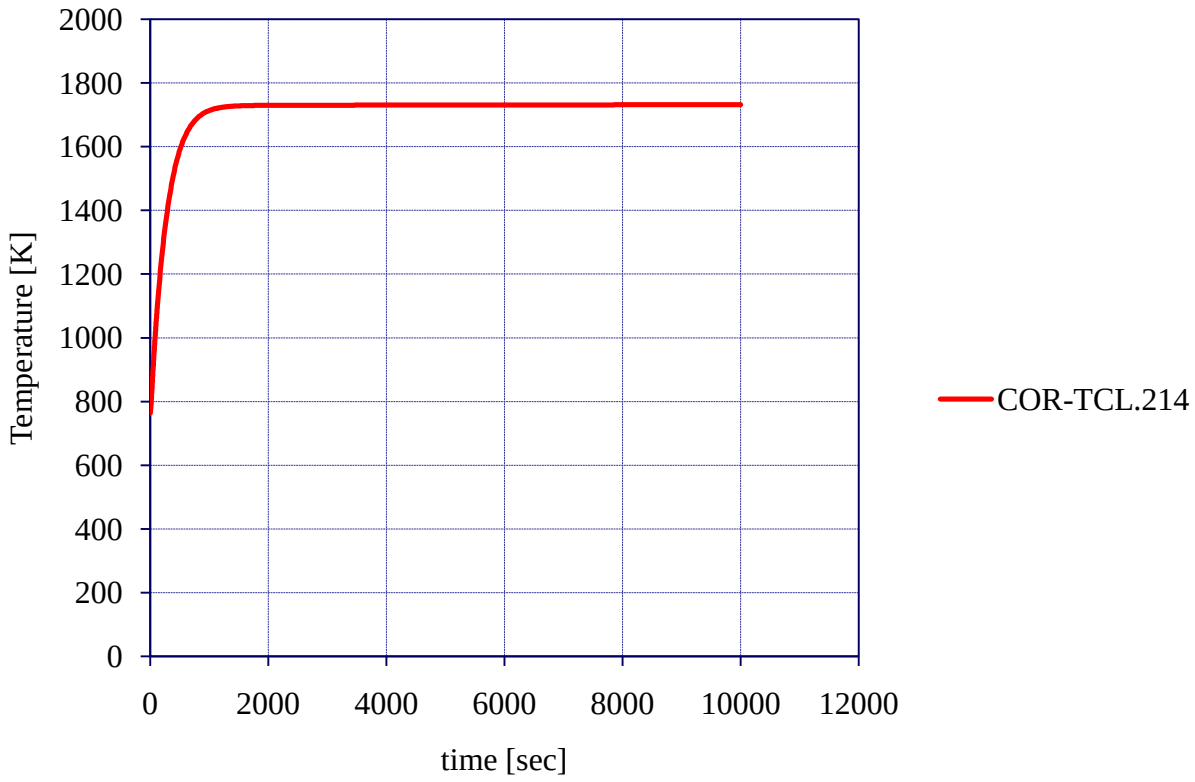

Figure 4.6. NGNP RPV Peak Cladding Temperature

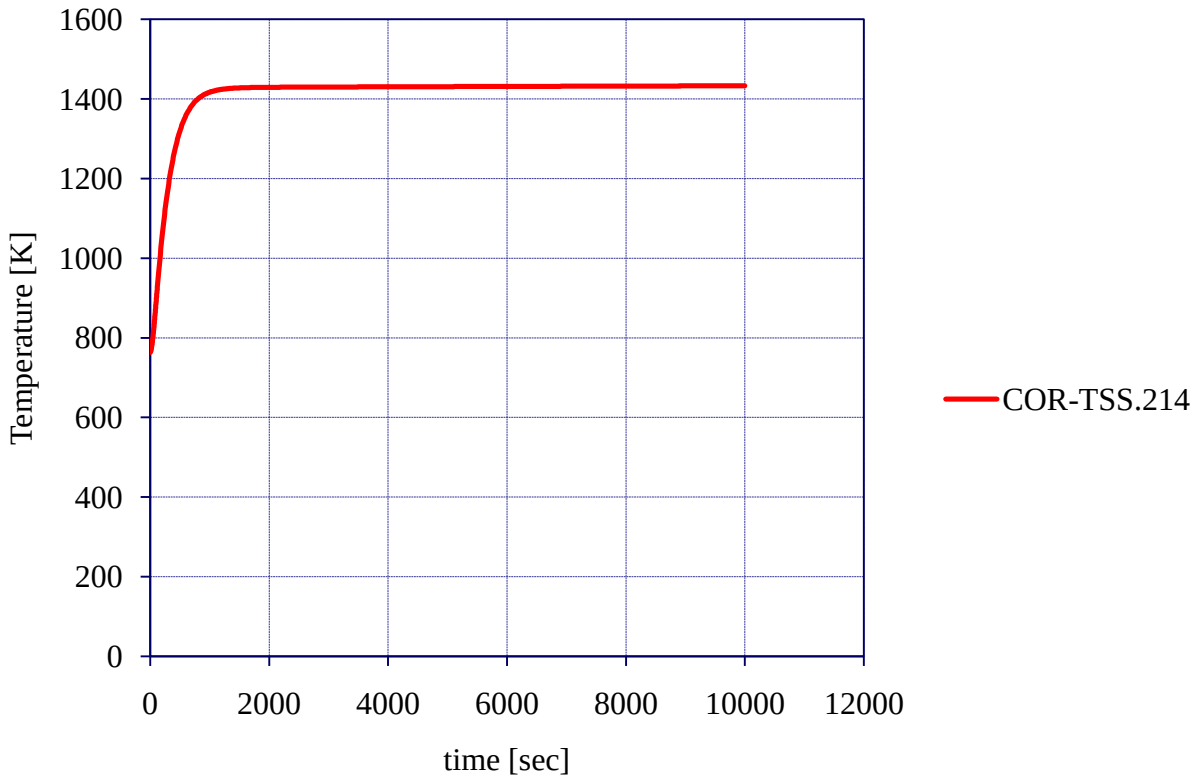

Figure 4.7. NGNP RPV Peak SS Temperature

5. MODELING OF THE RCCS

5.1 Literature Survey

The RCCS performs two safety functions. It removes core decay heat when neither the PCS nor the SCS is functioning in order to maintain the temperature of the RPV below its design limits. It separates the concrete wall of the reactor cavity (RC) from the hot RPV wall and the hot cavity air surrounding the RPV wall, thereby preventing this concrete wall from exceeding its design limits under both normal operation and accident conditions. The RCCS receives heat due to the conduction of the side reflector, the radiation of the RPV wall and the natural circulation of the hot cavity air.

The RCCS is composed of a cold downcomer and hot riser as shown in Figure 5.1. The downcomer is formed by two vertical plates 10 in. apart. The outer plate is attached to the inner cavity wall which is further away from the RPV wall versus the inner plate. Air from the outside atmosphere enters the downcomer and flows downwards due to gravity. At the bottom of the downcomer, a bottom cold plenum changes the direction of the air flow and guides it towards to the risers. The risers are closer to the RPV wall versus the downcomer. The air enters the risers, receiving heat from the RPV wall and hot cavity air, then it flows upwards inside the risers due to buoyancy forces. The air then reaches the hot plenum at the top of the risers and escapes from the RCCS and exhausts to the outside atmosphere. The hot risers are composed of

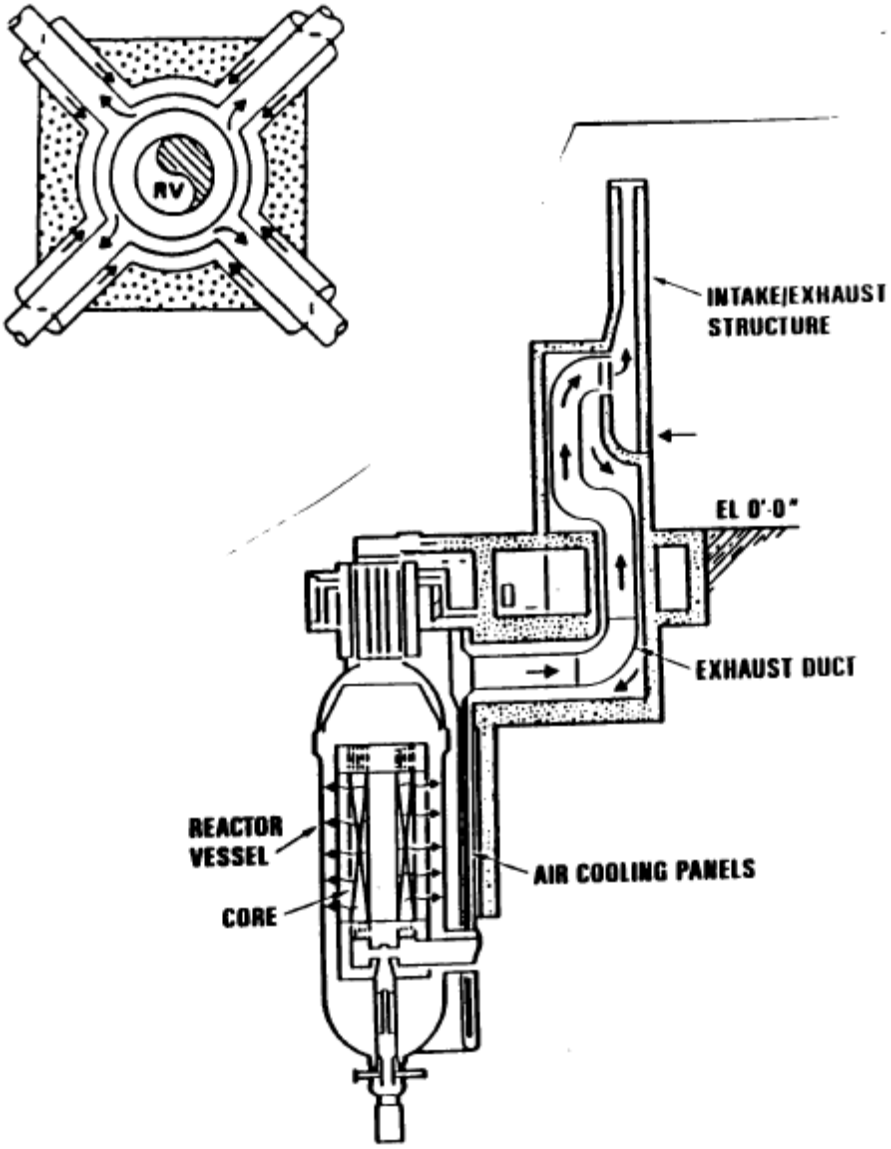

Figure 5.1. RCCS of the GT-MHR 600 MW Reactor [7] [Courtesy of General Atomics]

292 rectangular ducts with 2 in. * 10 in. external dimension and a thickness of 0.1875 in. There is a gap of 2 in. between each two ducts as shown in Figure 5.2. For each hot duct, one of its two short sides faces the RPV wall. Those ducts are vertically supported by the

bottom cold plenum and lateral supported by the downcomer through lateral support plates.

Radiation from the RPV wall reaches the front sides the risers. It also reaches the inner plate of the downcomer. A reflective insulation layer is attached to the inner plate. This layer radiates back the radiation heat from the RPV wall which has two important effect: preventing the cold air from outside atmosphere from being heated since this cold air is used in the risers to remove heat, the heat radiated back by this layer reaches the backsides of the riser ducts, thus fully utilizing all the sides of the hot ducts.

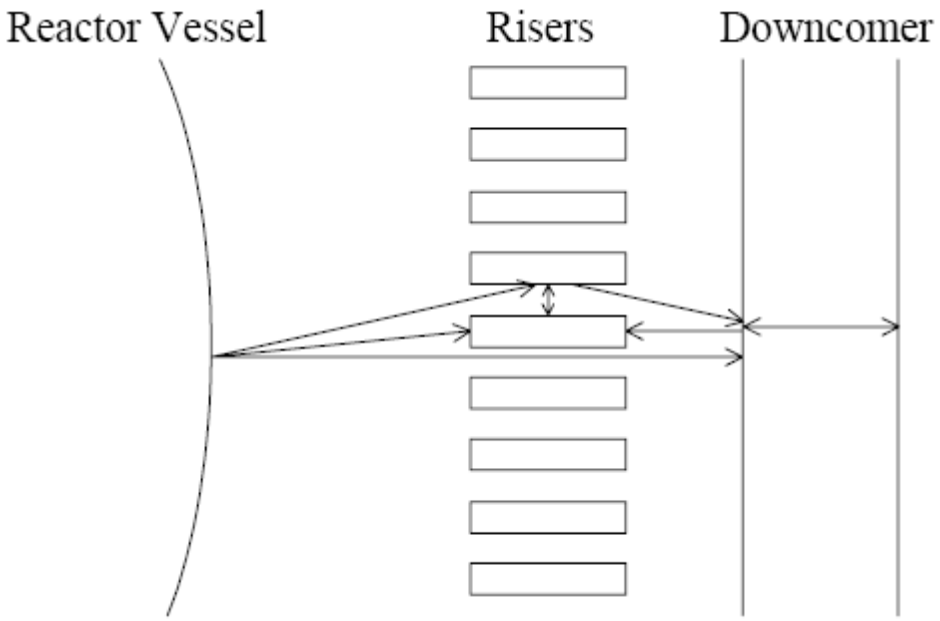

Figure 5.2. RCCS Risers and Downcomer [2]

5.2 Model Development

Some assumptions were made in order to develop this MELCOR model of the RCCS. The inner plate of the downcomer is assumed to be fully insulated and reflective. The air which enters the risers has the same temperature and pressure as the air from the outside atmosphere which excludes the necessity of modeling the downcomer.

In the actual design, the cavity air is contained between the RPV wall and the inner plate of the downcomer. This air is hotter than the air in the riser ducts in order that the riser air removes heat from the RC. There is a natural circulation in the cavity air. The cavity air closer to the RPV wall is hotter than that closer to the downcomer and further away from the RPV wall. The hotter cavity air flows upwards while the cooler cavity air flows downwards. Assumptions were made regarding the areas for the cavity upward air and the downward air. The upward air is contained between the RPV wall and the backsides of the hot ducts while the downward air is between the same backsides and the inner plate of the downcomer. The reasoning is that in order to achieve optimum heating of hot ducts by the cavity air, the short front sides and long lateral sides of hot ducts are in contact with the cavity air. The short backsides are connected to the lateral support plates which are connected to the downcomer. The heating of the downcomer by the cavity air needs to be minimized, so the backsides of the hot ducts need to be in contact with the cooler cavity air instead of the hotter one.

MELCOR does not allow the modeling of the HS connected to another HS. The following strategy was defined for the RCCS input model as show in Figure 5.3: A set of

CVs next to the RPV wall representing the cavity upwards air, a set of HSs for the three sides of the hot ducts in contact with the cavity upwards air, a set of CVs for the air inside the hot duct risers, a set of HSs for the backsides of the hot ducts, a set of CVs for the cavity downwards air, finally, a set of HSs for the lateral support plates which serves as a heat sink both in the actual design and in this input model.

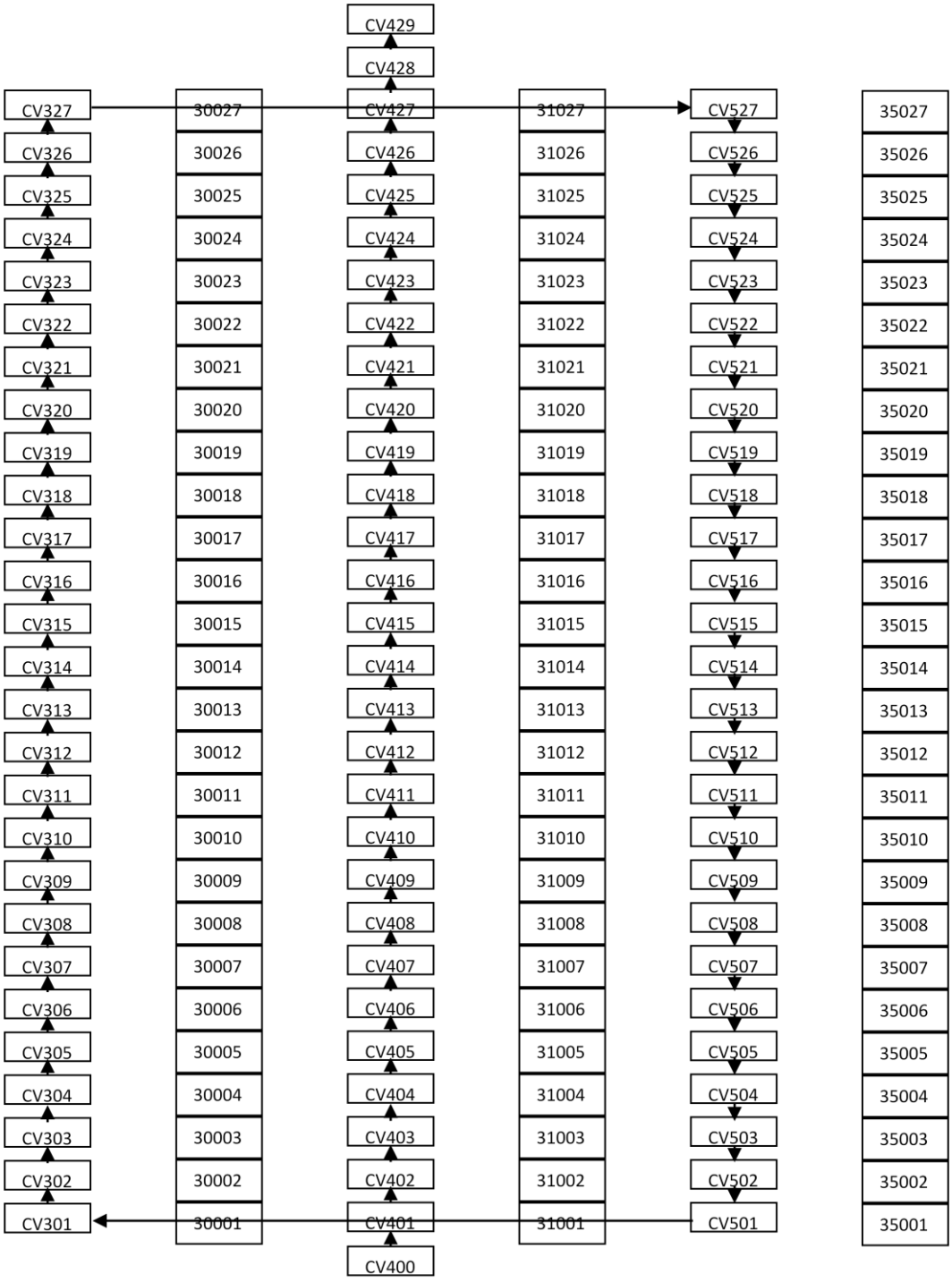

Figure 5.3. Nodalization of the RCCS Model

5.2.1 CVH and HS Packages

The inner radius of the cavity upwards air (CUA) is the outer radius of the RPV wall which is 3.82905 m. [7] In order to calculate its outer radius, the steps below were followed:

a) In order to obtain the radius of the ring of risers, the following formula was used:

$$R_5 = 2 * (292+292) * 2.54 /100 /2 / \pi \quad (5.1)$$

R_5 : the radius of the circle connecting the sides of all the risers facing the RPV wall at the surface closer to the RPV wall (m)

b) The formula below was applied in order to obtain the actual outer radius of the CUA:

$$R_6 = R_5 + (10 - 0.1875) * 2.54 /100 \quad (5.2)$$

c) The CUA cross-sectional area was calculated as the following:

$$S_c = \pi * (R_6^2 - R_7^2) - 292 * (L_1 - L_2) * L_3 \quad (5.3)$$

R_7 : RPV wall outer radius (m)

L_1 : outer length or long side of the riser ducts: 0.254 (m) = 10 in.

L_2 : thickness of the riser ducts: 0.0047625 (m) = 0.1875 in.

L_3 : outer width or short side of the riser ducts: 0.0508 (m) = 2 in.

d) Finally, the outer radius of the CUA for the MELCOR input was acquired:

$$R_8 = \sqrt{(S_c + \pi * R_7^2) / \pi} \quad (5.4)$$

CVs with a height of around 0.4 m are proved to be appropriate in this RCCS model in order that MELCOR capture the density difference between each two adjacent CVs so that it can simulate natural circulation. The difference in density is due to the difference in temperature and pressure between CVs. The CVs in the CUA has the same elevation and height data as HS 33. The volume data of each CUA CV is listed in Table D.2 in Appendix D.

The cross sectional area of CUA is assumed to be the flow area of this air. In order to calculate the hydraulic diameter of this flow area, the following steps were applied:

a) The wetted perimeter was acquired using this formula:

$$P_1 = [(L_1 - L_2) * 2 + L_3] * 292 + R_7 * \pi * 2 \quad (5.5)$$

b) Then the hydraulic diameter was obtained:

$$D_1 = S_c * 4 / P_1 \quad (5.6)$$

The inner radius of the HS 30 is the outer radius of CUA CVs. In order to calculate its outer radius (R_9), its cross sectional area was acquired using the formula below:

$$S_h = (L_1 * L_3 - L_4 * L_5) * 292 - 292 * L_2 * L_3 \quad (5.7)$$

L_4 : inner length of the riser ducts: 0.244475 (m) = 10 in. – 0.1875*2 in.

L_5 : inner width of the riser ducts: 0.041275 (m) = 2 in. – 0.1875*2 in.

Then its outer radius was obtained as the following:

$$R_9 = \sqrt{(S_h + \pi * R_8^2) / \pi} \quad (5.8)$$

The contact surface area between HS 30 and its boundary CVs are listed in Table D.5 in Appendix D. The contact area between HS 30 and CUA CVs were obtained using formula (5.9) while formula (5.10) was used to calculate the area between HS 30 and riser CVs.

$$S_a = [(L_1 - L_2) * 2 + L_3] * 292 * h \quad (5.9)$$

h: the height of each HS (m)

$$S_b = (L_4 * 2 + L_5) * 292 * h \quad (5.10)$$

For the riser CVs, its cross sectional area is given by:

$$S_r = (L_4 * L_5) * 292 \quad (5.11)$$

The volume data of each riser CV is listed in Table D.6 in Appendix D. The flow area of the riser air is the cross sectional area of the duct. The hydraulic diameter was then obtained:

$$D_2 = S_r * 4 / (L_4 * 2 + L_5 * 2) \quad (5.12)$$

The hot plenum CV428 on the top of the riser is assumed to have the same height as that of the upper plenum CV280 in the GT-MHR RPV model and the same cross sectional area as the RCCS riser CVs. At the bottom the riser CVs, there is a bottom time independent volume CV400. This CV has the pressure as the outside atmosphere and the riser inlet temperature which is 43°C as shown in Table 5.1 on page 88. At the top of the hot plenum, there is another time independent volume CV429. This CV has a temperature of 274°C corresponding to the riser outlet temperature as shown in Table 5.2 on page 89. These two time independent CVs provide fixed boundary conditions to

the riser CVs. All the CVs in this RCCS input model have an initial temperature of 43°C except for CV429.

The air in the risers moves upwards. In this model, the initial pressures of the CVs decrease as their elevation goes up. CV400 has the highest initial pressure which is also the CV with lowest elevation. In order to calculate the initial pressure of CV401, the following formula was used:

$$P = P_0 - \rho_0 * g * h \tag{5.13}$$

P : the initial pressure of CV401 (Pa)

P_0 : the initial pressure of CV400 (Pa)

ρ_0 : the initial density of the coming air which is the air from CV400 (kg/m^3) as calculated in Table A.56 in Appendix A

h: the distance between the center points of CV400 and CV401 (m)

g : 9.8 N/kg

The density of the air of CV401 is needed in order to obtain the initial pressure of CV402. Based on the same formula shown in Table A.56 in Appendix A, since CV401 and CV400 has the same temperature, the initial pressure of CV401 is given by:

$$\rho = \frac{\rho_0}{P_0} * P \tag{5.13}$$

ρ : the initial density of the air in CV401 (kg/m^3)

The same method is applied for all the CVs in this RCCS input deck.

For HS 31, its cross sectional area was acquired with formula (5.13), its inner radius with (5.14) and its outer radius with (5.15):

$$S_{ba} = L_2 * L_3 * 292 \tag{5.13}$$

$$R_{10} = \sqrt{(S_r + \pi * R_9^2)/\pi} \tag{5.14}$$

$$R_{11} = \sqrt{(S_{ba} + \pi * R_{10}^2)/\pi} \tag{5.15}$$

The lateral support plates are assumed to have the same thickness as the hot duct risers. The contact area between HS 31 and riser CVs were obtained using formula (5.16) while formula (5.17) was used to calculate the area between HS 31 and cavity downwards air (CDA) CVs. The reasoning is that the outer length of HS 31 subtracting the part connected with the plates is in direct contact with CDA CVs.

$$S_i = L_5 * 292 * h \tag{5.16}$$

$$S_b = (L_1 - L_7) * 292 * h \tag{5.17}$$

L_7: thickness of the plates: 0.0047625 (m) = 0.1875 in.

The outer diameter of the concrete is 25.9 m and its thickness is 1 m which gives a inner radius of 11.95 for the concrete. This is also the outer radius of the downcomer. The thickness of the inner plate and outer plate of the downcomer is assumed to be the same as that of the hot duct risers. Then the inner radius (R_{12}) of the downcomer was obtained with (5.18) and the length of the lateral plates (L_{10}) with (5.19):

$$R_{12} = R_{13} - L_8 * 2 - L_9 \tag{5.18}$$

R_{13}: inner radius of the concrete (m)

L_8 : thickness of the two plates of the downcomer (m)

L_9 : distance between these two plates: 25.4 (m) = 10 in.

$$L_{12} = R_{12} - R_5 - L_1 \tag{5.19}$$

The formula below was used to calculate the cross sectional area of HS 35:

$$S_L = L_7 * 292 * L_{10} \tag{5.20}$$

Then the cross sectional area of the CDA could be calculated:

$$S_{cda} = \quad \pi * (R_{12}^2 - R_{11}^2) \; - \; S_L \tag{5.21}$$

The total flow area for the air in the CDA is the cross sectional area of the CDA. Its hydraulic diameter was acquired by following the steps below:

a) The wetted perimeter was acquired using this formula:

$$P_2 = [L_{10} * 2 + L_3 - L_2] * 292 + R_{12} * \pi * 2 \tag{5.22}$$

The CDA air is in contact with both sides of each plate.

b) Then the hydraulic diameter was obtained:

$$D_2 = S_{cda} * 4 / P_2 \tag{5.23}$$

For MELCOR input, the outer radius of the lateral support plates is the inner radius of the concrete. The inner radius of this HS (R_{14}) was calculated as the following:

$$R_{14} = \quad \sqrt{(S_{cda} + \pi * R_{11}^2) / \pi} \tag{5.24}$$

Thermal radiation is modeled from HS 32 to HS 33, also from HS 33 to HS 30 and 31. The radiation can not be modeled between HS 33 to HS 35 since HS 35 has a

symmetric boundary condition. According to MELCOR requirements, HS with this condition can not have radiation from or to another HS.

5.2.2 FL Package

Horizontal FLs are used: one connecting the CUA and CDA at their bottommost CVs and another for their topmost CVs. The air goes up in the CUA. It then reaches CDA where it flows downwards. When it comes to the bottom, it reaches the CUA. It then flows upwards again.

5.3 Results under Normal Operation Condition

Table 5.1

RCCS Model Results

	[7]	MELCOR
Heat Loss to the RCCS from the RPV (MW)	3.3	3.26
Riser Air Inlet Temperature (°C)	43	43
Riser Air Outlet Temperature (°C)	274	229.0
Riser Air Flow Rate (kg/s)	14.3	17.6

The data under steady state from the reference is provided in the table below. The information regarding how this data was obtained is not available.

Table 5.2

RCCS Steady-State Performance under Normal Plant Operation

Parameter	100% Power
Reactor Vessel	
Heat loss to RCCS, kW	3300
Inside wall temperature, °C	485
Average outside wall temperature, °C	446
Maximum outside wall temperature, °C	474
Cooling Panel (Front)	
Average temperature, °C	267
Maximum temperature, °C	323
Air inlet temperature, °C	43
Air outlet temperature, °C	274
Airflow, kg/sec	14.3
Maximum velocity at exit from panel, m/sec	11.5
Structure	
Concrete surface temperature, °C	49

Ref. [7]

A steady state simuation of 36000 s was performed in order that the RCCS HS temperatures become nearly constant. The mass flow rate is 17.57 kg/s as shown in Figure 5.4. The outlet temperature of the RCCS is 229°C as shown in Figure 5.5. The heat removal rate calculated by MELCOR is 3.26 MW. The air flow in the CUA goes up while air in the CDA goes down as shown in Figure 5.6. It corresponds well with the expected natural circulation flow pattern.

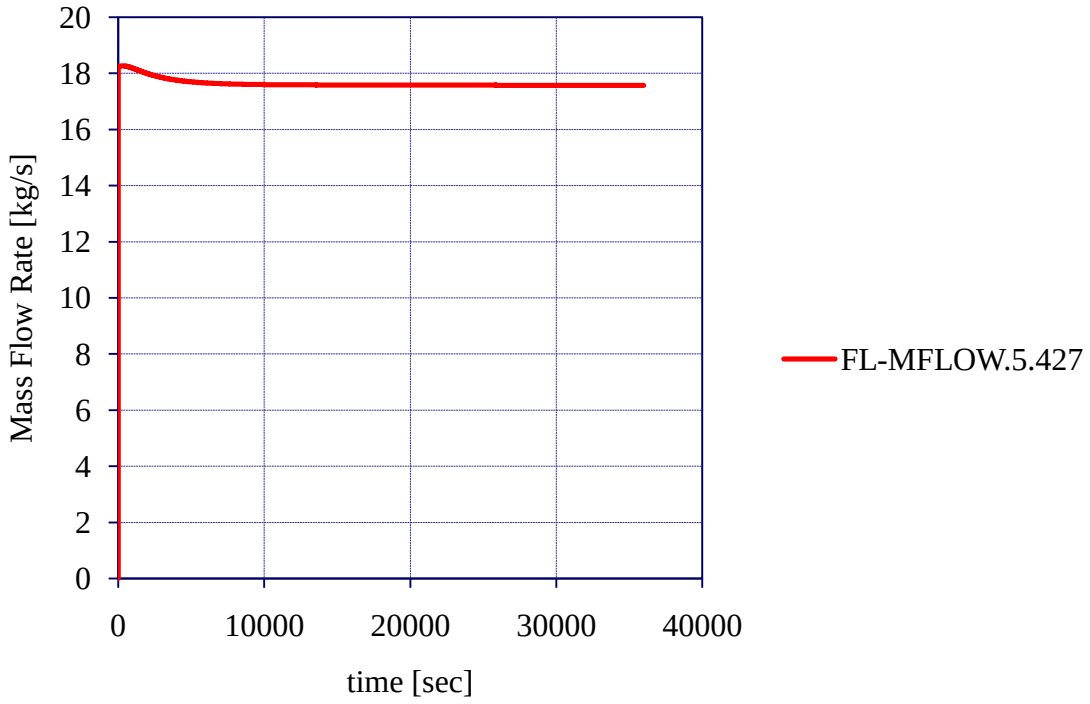

Figure 5.4 RCCS Outlet Mass Flow Rate

5.4 Conclusions

The heat removal rate calculated is 3.26 MW versus 3.3 MW from the reference. MELCOR has been demonstrated to have the capability of simulation an RCCS with accurate results. The model developer has made excellent engineering judgment and identified effective strategies.

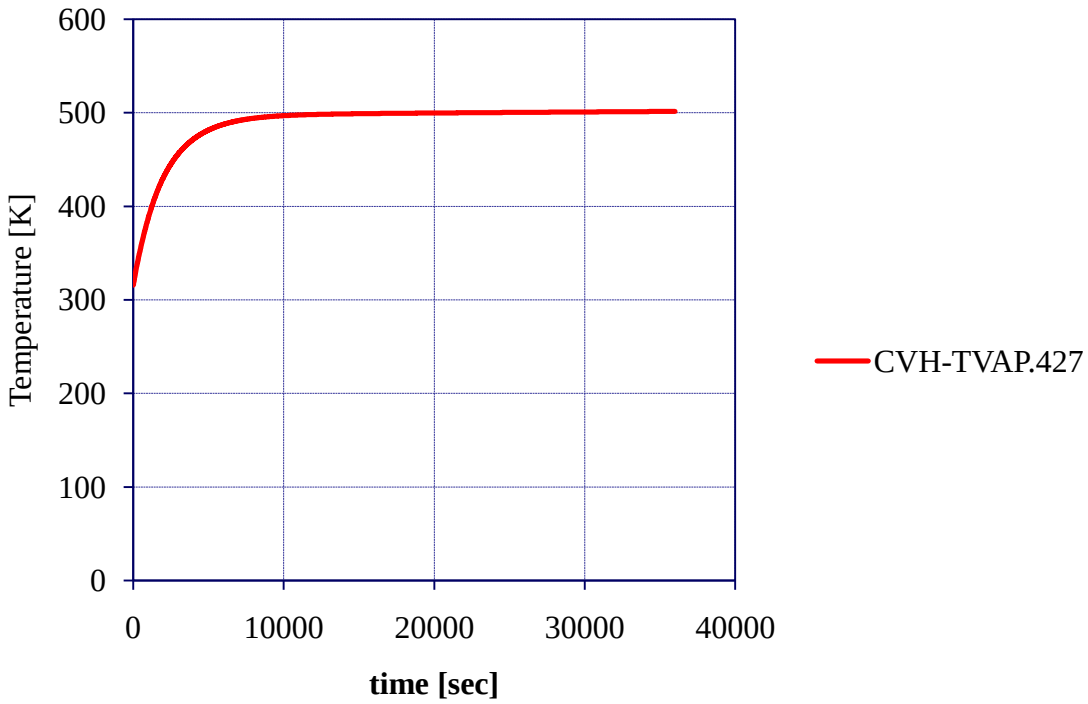

Figure 5.5 RCCS Outlet Temperature

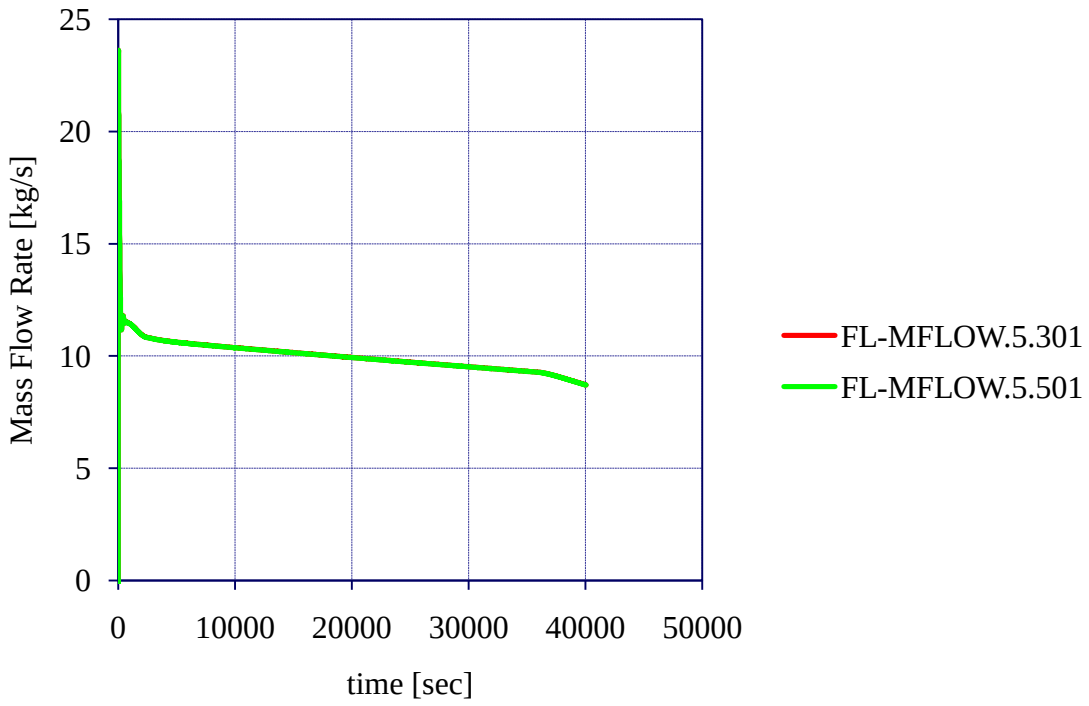

Figure 5.6 CUA and CDA Air

6. MODELING OF THE PRESSURIZED CONDUCTION COOLDOWN ACCIDENT (PCC)

6.1 Literature Survey

The PCC event is initiated by turbine trip and the SCS's failure to start. Turbine trip can be due to turbinemachine overspeed. Operating control rods are inserted to shutdown the reactor. Since the turbine is turn off, high temperature helium can not be extracted from the core, then the core will get overheated. In this case, the reactor needs to be shutdown in order to protect the core components. Both PCS and SCS fail to function. Core residual heat is removed by the RCCS. This type of hypothetical accident scenario is called the PCC or pressurized loss of forced cooling. [7]

Core residual heat includes decay heat and sensible heat stored in the graphite. This residual heat is removed by thermal radiation, natural convection and conduction from the RPV to the RCCS. [7] The decay heat profile is shown in Figure 6.1. The curve with a circle is provided by GA and is used in this MELCOR input model. Peak component temperatures under PCC are shown in Table 6.1 on page 97. Information regarding the equilibrium pressure is not available. The peak fuel temperature profile is shown in Figure 6.5 on page 101. The initial fuel temperature is 600°C which implies that time zero here is the initiation of the normal operation. The peak fuel temperature under normal operation is 1218°C [2] which means after approximately 30 hrs, the peak fuel temperature under normal operation is reached. The reactor is scrammed at around

the same time. This is the initiation of the PCC. Between 40 and 48 hrs, the peak fuel temperature under PCC is reached. The difference between the steady state and PCC fuel temperatures is 20°C. This thesis work assumes the reactor can be shutdown within 10 s.

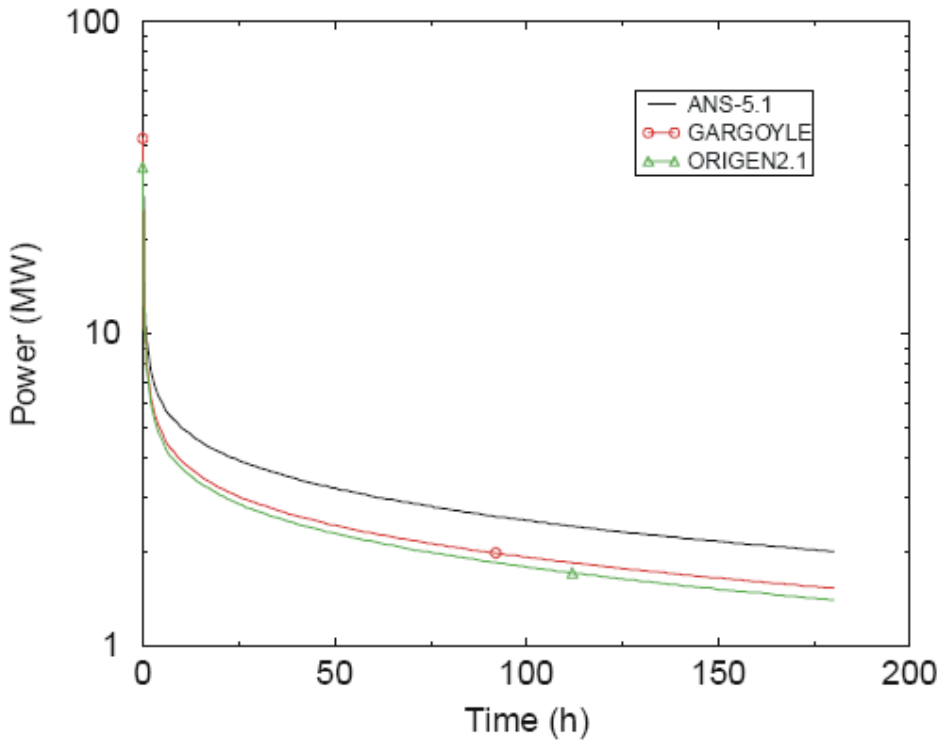

Figure 6.1. Decay Heat Profile [2]

An energy balance is applied here in order to understand Figure 6.2. After shutdown, heat generation is small since the decay power is less than 7% of the normal fission power. The heat removal is also small. Force circulation of helium is lost. The mass flow rate of helium under natural circulation is significantly smaller than that under forced circulation. Hot helium flows from the bottom to the top of the core. Based on

Table 3.9, under steady state, the difference between peak temperatures of the fuel and graphite is around 70°C and that between the fuel and helium is around 200°C. Since helium has a high temperature, the heat removal from this fuel block by helium through conduction is fairly small. The graphite also has a high temperature. The thermal conductivity of graphite with a temperature of 500°C is around 70 W/(m*K), only around 46 W/(m*K) with a temperature of 1142°C. Conduction from the fuel to graphite is proportional to the heat transfer area between the two, the temperature difference between the two and the thermal conductivity of the graphite. Since the temperature difference and graphite conductivity are both small, the heat removal from the fuel by graphite through conduction is fairly small. Another heat removal mechanism is radiation from the fuel to graphite. This heat loss is proportional to the temperature difference between the two. Since this difference is small, the radiation heat removal is also small. So for the energy balance, there is a small production term due to decay power and a small loss term due to conduction of helium and conduction and radiation from fuel to graphite. Both terms are fairly small, but since the production term is slightly bigger, the PCC peak fuel temperature is reached which is just a little higher than the peak fuel temperature under normal operation. The decay power continues to shrink over the time, and it then becomes smaller than the loss term which makes the fuel temperature finally drop. The heat removal of the RCCS does not overpass the decay power until about 2 days after the initiation of the PCC. [2] This is another mechanism which contributes to the decrease in peak fuel temperature.

As shown in Figure 6.2, 1600°C is the fuel temperature design goal. It does not include a safety margin here. In GA's DCC analyses, a safety margin of 79°C below 1600°C has been included. [7]

6.2 Modeling Approach

The reactor is assumed to be shutdown within 10 s. A decay heat will be implemented at the time when the peak fuel temperature under steady state is reached. The steady state simulation lasts for 10 hrs in the MELCOR PCC model.

Turbine is turn off. PCS fails to function as well. The compressor is contained in the PCS, so the compressor fails as well. The pressure head provided by the compressor is lost. The forced circulation of the helium coolant was driven by this pressure head. The assumptions with respect to the initial and boundary conditions for the PCC are the following:

a) The detection of turbine trip is automatic. The initiation of SCS is automatic and the detection of its failure to start is automatic. So the PCC starts right after 10 hrs.
b) When PCC starts, the inlet and outlet boundary have the equilibrium pressure of 5.03 MPa and the helium inlet temperature. These two boundaries are linked to the PCS. The whole PCS has a pressure of 5.03 Mpa and the helium inlet temperature.

Table 6.1. PCC Peak Component Temperatures

	GT-MHR	Limits
ANALYSIS CONDITIONS		
Equilibrium pressure, MPa	5.03	
Inlet temperature, °C	491	
Outlet temperatuare, °C	850	
Core power, MW	600	
MAXIMUM COMPONENT TEMPERATURES (conservative decay heat)		
Fuel, °C	1238	1600
Operating control rods, °C	966	1315
Core barrel, °C	729	760
Vessel midwall, °C	497	565
Upper core restraint, kg/sec	982	1095
Upper plenum shroud, °C	772	900

Ref. [7]

In this PCC model, one valve is implemented at the FL connecting CV190 and CV160. This valve is fully open during the first 10 hrs and fully closed afterwards. CV690 is a time independent volume with inlet boundary condition for the PCC. A FL connects CV690 to CV160. A valve is implemented on this FL. This valve is fully closed during the first 10 hrs and fully open afterwards. CV200 has the outlet boundary condition for steady state normal operation while CV700 has the condition under the PCC. Similar procedures were applied by using valves to these two CVs in this PCC model. Data points for the decay power were picked up by hand from Figure 6.1. The core power is input via a tabular function which provides fission power for the first 10

hrs and decay power thereafter. A total simulation of 20 hrs was performed with 10hrs for the PCC. More details are found in Appendix E.

6.3 Results

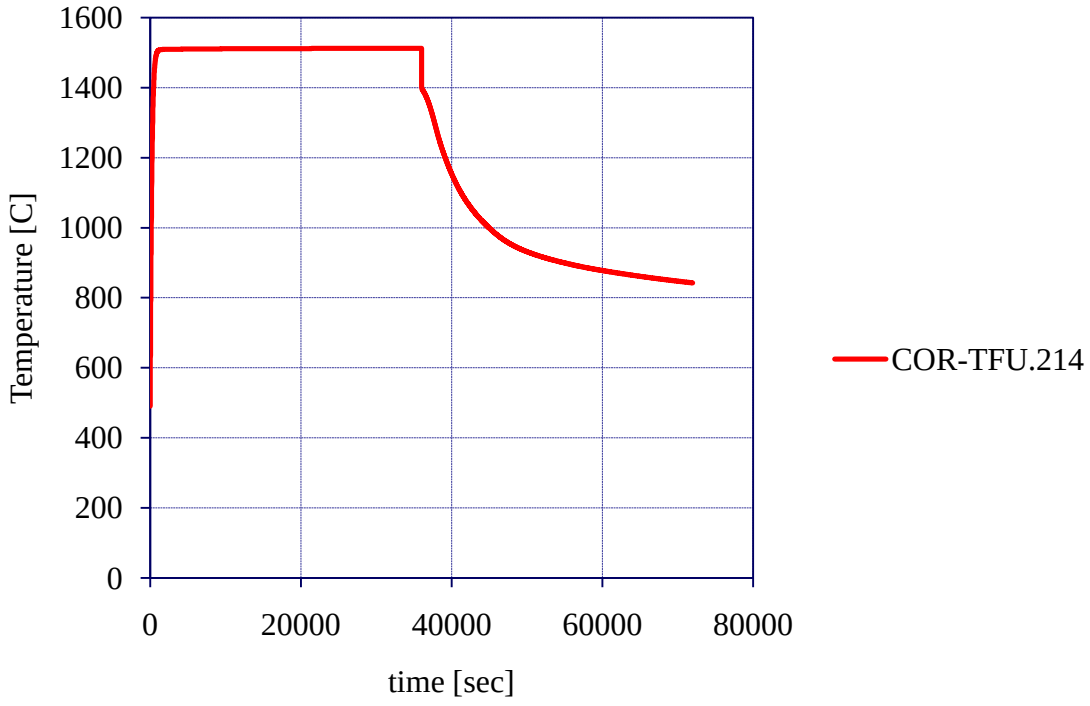

Figure 6.2. MELCOR PCC Peak Fuel Temperature

The MELCOR results show the peak fuel temperature drops significantly when PCC starts as shown in Figure 6.2. So does the peak cladding temperature. The energy balance here is inconsistent with that based on reference [7]. The calculated steady state

peak fuel temperature is about 300°C higher than the data from the reference. The peak graphite temperature which is cladding in this model is about 317°C higher. The SS in the same core cell has a temperature of 1060°C as shown in Figure 6.3. This cell is 214 which is in ring 2 at level 14. The cell next to it is 114 which is in ring 1 at the same level. This cell is in the inner reflector region. The SS temperature there is only 812°C as shown in Figure 6.4.

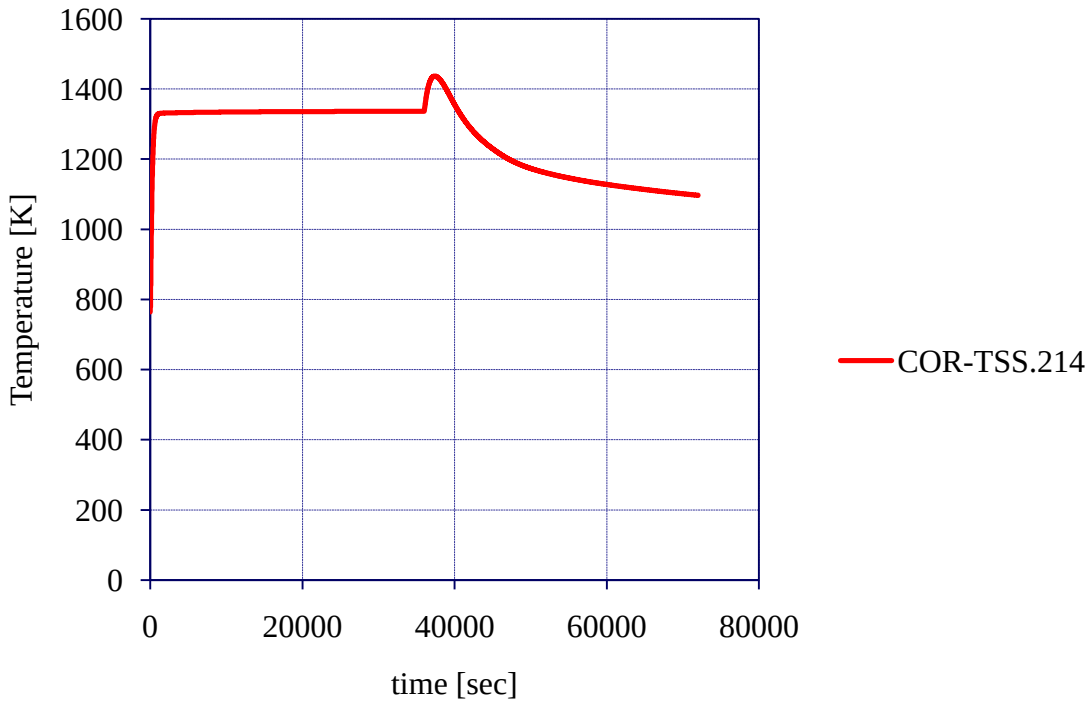

Figure 6.3. PCC Peak SS Temperatures

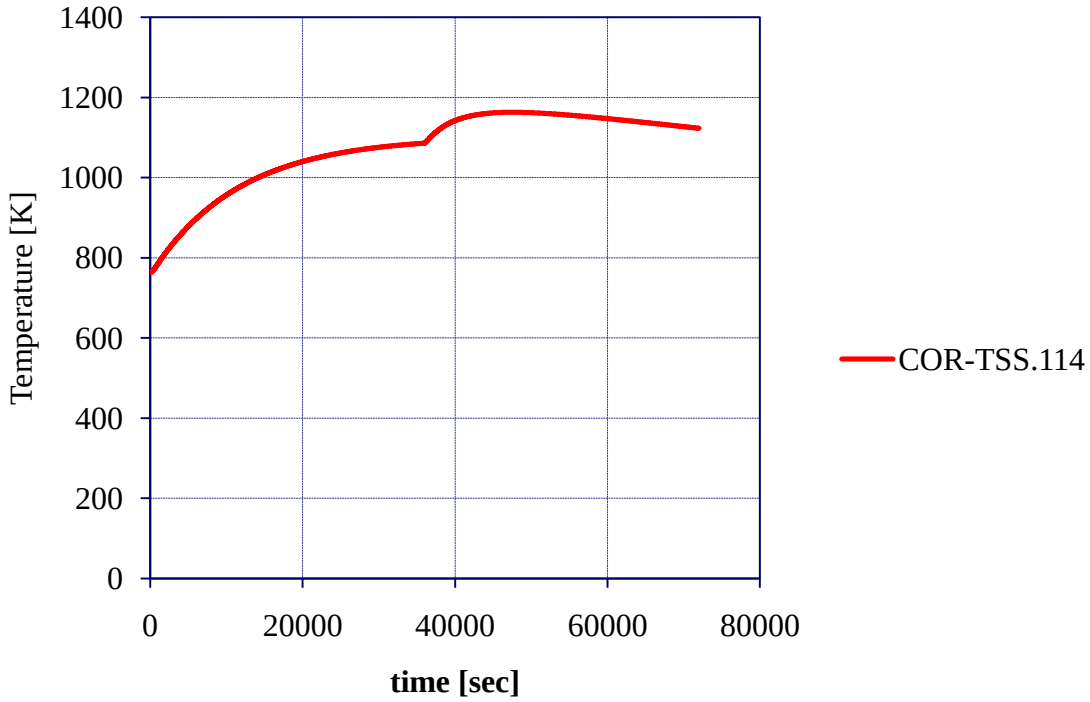

Figure 6.4. PCC Inner Reflector Temperatures

According to GA, the temperature difference between the graphite in the hottest fuel block and the graphite in the inner reflector next to that fuel block should be within 50 to 100°C which is consistent with what is implied by Figure 6.5. However, MELCOR results show a difference of more than 300°C. According to GA, the graphite in the inner reflector next to the hottest fuel block should have a temperature of around 1100°C. MELCOR results give a peak inner reflector graphite temperature of 812°C which is much lower. Cooler graphite has higher thermal conductivity versus hotter graphite. Bigger temperature difference results in bigger radiation and conduction heat removal.

The MELCOR results show a much bigger heat removal from the hottest fuel block by the inner reflector graphite. Since the heat removal is significantly bigger than the generation from decay power, fuel temperature drops.

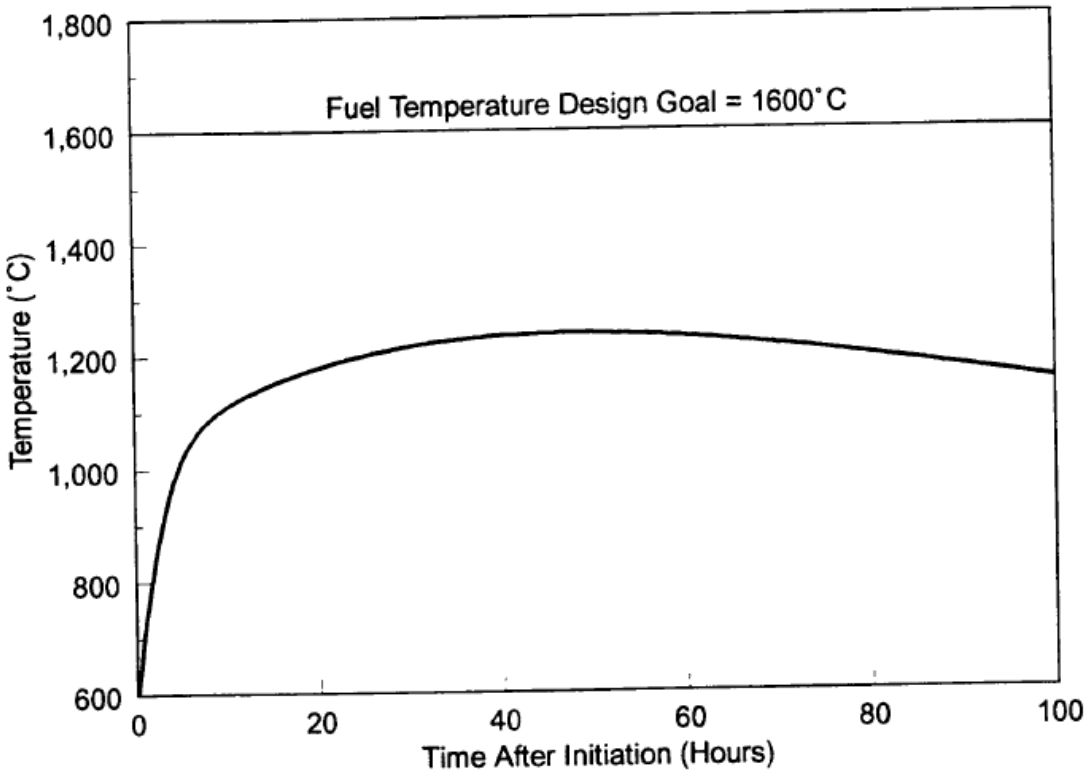

Figure 6.5. PCC Peak Fuel Temperatures [7] [Courtesy of General Atomics]

6.4 Conclusions

The results give a heat distribution in the fuel and graphite under steady state condition that is inconsistent with the data from the reference. The reflectors did not

remove enough heat since the reflectors are not hot enough, so the simulation with respect to passive heat removal features of the reflectors is not exact. This heat distribution gives inaccurate initial condition for the PCC simulation. It also causes the patterns of radiation and conduction between fuel and graphite to be incorrect.

7. CONCLUSIONS

In this thesis, MELCOR, a severe accident code, was used to analyze one of the VHTR designs – a prismatic core Next Generation Nuclear Plant (NGNP). Based on the current literature survey in which more data is available for the GT-MHR than for the NGNP, for the purposes of extending MELCOR capabilities and code validation, a model of the GT-MHR RPV was developed. Based on the currently available data, a model of the NGNP RPV was then developed through modifying the GT-MHR RPV model. The RCCS, which passively removes heat from the RPV wall to outside atmosphere, was then added to this GT-MHR RPV model. The PCC, one of the important postulated accident scenarios for a prismatic core reactor, was simulated with the complete model. In order to validate the code, the analysis results can be compared against the limited data from Fort St. Vrain and the HTTR.

MELCOR results show excellent precision in predicting coolant outlet temperatures, peak coolant outlet temperature inside the core and coolant mass flow rates. The calculated heat removal rate of the RCCS under steady state has very high accuracy too. Both the GT-MHR RPV and the complete GT-MHR model achieve a peak fuel temperature within the design limit. For the NGNP RPV model, the peak fuel temperature can be maintained below 1600°C with a coolant outlet temperature up to 900°C.

The MELCOR results give a peak fuel temperature that is much higher than the data from the references. For the NGNP RPV model, with an outlet temperature of

950°C, the peak fuel temperature surpasses the design limit. Within the same fuel block, the results give a temperature difference between SS and cladding of almost 300°C which is inconsistent with reality, since SS and cladding is the same graphite block in the actual design. The calculated peak temperatures of inner and lower reflectors are lower than the data from the reference. The simulated heat distribution in the fuel and graphite under steady state condition is inconsistent with the data from the reference. This heat distribution gives inaccurate initial condition for the PCC simulation and causes the patterns of radiation and conduction heat transfer between fuel and graphite under the PCC to be incorrect.

The physics in prismatic core reactor are different than in a light water reactor. Heat transfer mechanisms are the same but MELCOR's capabilities to predict radiative heat transfer through helium should be confirmed. MELCOR's treatment of emissivities and other radiative properties of helium should be verified. MELCOR needs other models including graphite oxidation. The PCC was chosen in this thesis work instead of the DCC for demonstration analysis, in part, because MELCOR does not have a graphite oxidation model. In the DCC event, ambient air comes into the RPV. Oxygen can interact with high temperature graphite.

MELCOR has been demonstrated to have the ability of modeling a prismatic core VHTR. The calculated outlet temperature and mass flow rate under normal operation correspond well to references. However, the calculation for the heat distribution in the graphite and fuel is unsatisfactory which requires MELCOR modification for the PCC simulation. Partition of graphite into cladding and SS needs to

be avoided. Specific components for graphite block need to incorporate in the MELCOR code.

8. FUTURE WORK

8.1 Modeling of the NGNP when Additional Data Becomes Available

According to Section 3 and 4 of this thesis, the flow form loss coefficient is 1.2 for the GT-MHR while 2.8 for the NGNP. This implies the flow condition in the NGNP will be more complicated. Based on references, the helium inlet is located in the permanent side reflector for the NGNP [13]. Design modifications are made in order to reduce bypass fraction. This means the flow condition could have more complexities. Advanced materials will be used[2]. When the data regarding the coolant flow distribution and material properties becomes available, a detailed NGNP model will be developed.

8.2 Modeling of Gaps between Graphite Blocks

Helium flows through the gaps between blocks which further cool down the fuel blocks. GA has performed experiments and calculated the effective thermal conductivity of blocks accounting the presence of the gaps. This information is proprietary right now. When this data becomes publicly available, gaps can be more accurately modeled.

8.3 Modeling of Natural Circulation inside the Active Core

According to the GA radial power factors as shown in Table 3.8, each fuel block has different power peaking factors. Under normal operation conditions, the natural circulation of helium is due to the temperature difference which causes a density difference. In the current MELCOR model, one single radial power factor is applied for each fueled ring which means each ring is isothermal. The natural circulation is modeled through the horizontal flow paths between two adjacent rings. The actual natural circulation pattern is more complicated than what was simulated in the MELCOR model. A more detailed natural circulation model can be developed accounting the fact that each fuel block has a distinct power factors. Also, the actual reflector region is not isothermal. According to GA, the inner reflector block next to the hottest fuel block has a temperature fairly close to the graphite in that block. However, graphite in the region away from the active core is much cooler. This will have an impact on the natural circulation flow pattern.

8.4 Investigation of the Overheating of the Fuel

In the actual MELCOR calculation, heat generated in the fuel is partially removed by the cladding. Some heat is taken away by SS from the cladding and some is taken away by the coolant. This is inconsistent with reality. In the actual design, graphite in each fuel block is one single component which is in direct contact with both fuel and

coolant. The MELCOR results did not show correct prediction for graphite temperatures. The partition of graphite between cladding and SS needs to be avoided in order to correctly model graphite in a prismatic core.

8.5 Modeling of the DCC Accident for the GT-MHR 600 MW Reactor

More modeling effort is orientated towards DCC versus PCC according to the literature. Based on reference [7], the peak component temperatures under DCC conditions are significantly higher than for the PCC conditions. DCC raises more safety concerns since the heat distribution in the core under this condition is more uneven compared with the PCC conditions. A MELCOR model of DCC for the GT-MHR will be developed. With respect to this model, the heat distribution in the fuel and graphite under steady state will needed to be accurately simulated in order to provide correct initial conditions and boundary conditions for the DCC. Those conditions are crucial for both PCC and DCC simulations since they will have a major impact on heat redistribution inside the core when postulated accidents start.

REFERENCES

[1] G.D. Delcul, B.B. Spencer, C.W. Forsberg, E.D. Collins, W.S. Rickman, TRISO-Coated Fuel Processing to Support High-Temperature Gas-Cooled Reactors, Oak Ridge National Laboratories, Oak Ridge, TN, 2002, p. 9.

[2] P. E. Macdonald, J. W. Sterbentz, H. D. Gougar, NGNP Point Design–Results of the Initial Neutronics and Thermal-Hydraulic Assessments, Idaho National Engineering and Environmental Laboratory, Idaho Falls, ID, 2003, p. 73.

[3] K. Hogan, Pebble Bed Modular Reactor Analysis with MELCOR, M.S. Thesis, Purdue University, 2006.

[4] Gas-Cooled Reactor Associates, Evaluation of the Gas Turbine Modular Helium Reactor, San Diego, CA, 1994.

[5] R.O. Gauntt, R.K. Cole, C.M. Erickson, R.G. Gido, R.D. Gasser, S.B. Rodriguez, M.F. Young, MELCOR Computer Code Manuals, NUREG/CR-6119, vols. 1 and 2, rev. 2, Sandia National Laboratories, Albuquerque, NM, 2005.

[6] International Atomic Energy Agency, Evaluation of High Temperature Gas Cooled Reactor Performance: Benchmark Analysis Related to Initial Testing of the HTTR and HTR-10, IAEA, Vienna, Austria, 2003.

[7] General Atomics, Gas Turbine-Modular Helium Reactor (GT-MHR) Conceptual Design Description Report, General Atomics, San Diego, CA, GA Project NO. 7658, 1996.

[8] F. Reitsma, G. Strydom, J.B.M. De Haas, K. Ivanov, B. Tyobeka, R. Mphahlele, T. J. Downar, V. Seker, H.D. Gougar, D.F. Da Cruz and U.E. Sikik, Nucl. Eng. and Design, 236 (2006) 657–668.

[9] W.C. Reynolds, Thermodynamic Properties in SI: Graphs, Tables, and Computational Equations for Forty Substances, Dept. of Mechanical Engineering, Stanford University, Stanford, CA, 1979.

[10] F. Reitsma, G. Strydom, J.B.M. De Haas, K. Ivanov, B. Tyobeka, R. Mphahlele, T. J. Downar, V. Seker, H.D. Gougar and D.F. Da Cruz, Conference on High Temperature Reactors, Paper C17, Beijing, China, 2004.

[11] A. Terada, J. Iwatsuki, et al., Nucl. Sci. and Tech., 44 no. 3 (2007) 477–482.

[12] E. J. Parma, P. S. Pickard, A. J. Suo-Anttila, Very High Efficiency Reactor (VHER) Concepts for Electrical Power Generation and Hydrogen Production, Sandia National Laboratories, Albuquerque, NM, 2003.

[13] Idaho National Laboratory, Next Generation Nuclear Plant Pre-conceptual Design Report, Idaho National Laboratory, Next Generation Nuclear Plant Project, Idaho Falls, ID, 2007.

[14] S. Ball, Sensitivity Studies of Modular High-Temperature Gas-Cooled Reactor (MHTGR) Postulated Accidents, Oak Ridge National Laboratory, P.O. Box 2008, Oak Ridge, TN, 2004.

[15] Poco Graphite, Inc., Properties and Characteristics of Graphite, for the Semiconductor Industry, POCO Graphite, Inc., Decatur, TX, 2001.

[16] National Academy of Engineering, The Hydrogen Economy: Opportunities, Costs, Barriers and R&D Needs, Committee on Alternatives and Strategies for Future Hydrogen Production and Use, National Research Council, National Academy of Engineering, Washington, DC, 2004.

[17] W. K. Terry, J. K. Jewell, and J. Blair Briggs, T. A. Taiwo*, W. S. Park* and H. S. Khalil*, Preliminary Assessment of Existing Experimental Data for Validation of Reactor Physics Codes and Data for NGNP Design and Analysis, Idaho National Engineering and Environmental Laboratory, Bechtel BWXT Idaho, LLC, *Nuclear Engineering Division, Argonne National Laboratory, Argonne, IL, 2004.

[18] A. Saikusa, Y. Tachibana, and K. Kunitomi, Benchmark Problems for Rise-to-power Test of High Temperature Engineering Test Reactor in IAEA Coordinated Research Program, (Part II. Evaluation of Performance of Vessel Cooling System), Japan Atomic Energy Research Institute (JAERI), Oarai, Japan, 2000.

[19] N. Kuzavkov, S. Shepelyev, V. Afanasyev and O. Nikanorov, Benchmark Problem on the VCS Heat Removal (HTTRVC), Presented at Third RCM of CRP on Evaluation of HTGR Performance, Oarai, March 2001.

[20] H. Al-Kaabi, Severe Accident Analysis Methods for Pebble Bed Modular Reactors, M.S. Thesis, Purdue University, 2007.

[21] V. D. Arp, R. D. Mccarty, Thermophysical Properties of Helium-4 from 0.8 to 1500 K with Pressures to 2000 Mpa, National Institute of Standards and Technology, Boulder, CO, 1989.

[22] K. Minato, et. al., Nucl. Mater. 224 (1995) 85-92.

[23] J. Bolin, Meeting with Ni Zhen at GA, San Diego, CA, March 13, 2008.

[24] J. Saurwien, Meeting with Ni Zhen at GA, San Diego, March 13, 2008.

[25] C. Ellis, Meeting with Ni Zhen at GA, San Diego, March 13, 2008.

[26] D. Mceachern, Meeting with Ni Zhen at GA, San Diego, March 13, 2008.

[27] D. Mceachern, Meeting with Ni Zhen at GA, San Diego, Sept. 19, 2008.

APPENDIX A: DETAILED GT-MHR 600 MW RPV MODEL

A.1 Documentation

A.1.1 mmgen.in

CARD	WORD	VALUE	BASIS
TITLE		‘bldwn’	title of calculation
JOBID		‘bldwn’	job identifier
DIAGF		‘bldwng.dia’	filename for diagnostic output
OUTPUTF		‘bldwng.out’	filename for output listing file
RESTARTF		‘bldwn.rst’	filename for restart file
TSTART		0.0	default value of initial start time
DTTIME		1.0	default value of initial time step
R*I*F			files to be read containing MELCOR and MELGEN input: cvh-fl-hs-new.gen core-new-2.gen ncg-mp-new.gen

A.1.2 mmcor.in

CARD	WORD	VALUE	BASIS
TITLE		‘bldwn’	title of calculation
JOBID		‘bldwn’	job identifier
DIAGF		‘bldwn.dia’	filename for diagnostic output MESSAGEF
		‘bldwn.mes’	filename for diagnostic output

OUTPUTF		‘bldwn.out’	filename for output listing file
PLOTF		‘bldwn.ptf’	filename for plot file
RESTARTF		‘bldwn.rst’	filename for restart file
STOPF		‘bldwn.stp’	filename for stop file
TIME3	TIME	0.0	use the data on this card at the start of the calculation
	DTMAX	0.5	typical value for maximum timestep
	DTMIN	1.0e-4	typical value for minimum timestep
	DTEDT	600.0	long edit frequency since the information is not often needed
	DTPLT	2.0	used to verify model behavior during the beginning of the calculation
	DTRST	200.0	ensure restarts for the calculation are written
TIME4	TIME	120.0	use the data on this card after 120.0 s
	DTMAX	0.5	see TIME3
	DTMIN	1.0e-4	see TIME3
	DTEDT	3600.0	see TIME3
	DTPLT	10.0	reduce plot frequency
	DTRST	200.0	see TIME3
CYMESF	NCYEDD	500	number of cycles between messages written to the terminal
	NCYEDP	1	number of cycles between messages written to OUTPUTFILE
SOFTDTMIN	UNDERRUN_FRACTION	1.0e-4	
	NUMBER_OF_OCCURRENCES	500	
TEND	TEND	10000.0	end of calculation time
CPULIM	CPULIM	400000.0	maximum number of CPU seconds allowed for this execution

CPULEFT	CPULEF	30.0	desired minimum number of CPU seconds left at the end of the calculation
RESTART	NREST	-1	restart from last cycle

A.1.3 cvh package

CARD	WORD	VALUE	BASIS
CVTYPEnn	CVTYPE	CORCVH UPV CEHGP SRC SNK cavity	user defined CV type names
CVnnn00	CVNAME	varies	user defined control volume name
	ICVTHR	2	control volume thermodynamics switch; the nonequilibrium option is recommended in general
	ICVFF	varies	control volume flow flag; this flag is currently unused
	ICVTYP	varies	type of control volume; by default the name associated with control type nn is TYPEnn
CVnnn01	IPFSW	0	pool, fog allowed; default value
	ICVACT	0	active, with state advanced by integrating the conservation equations; default value
CvnnnA0	ITYPTH	3	type of thermodynamic input; separate pool

			and atmosphere input; default value
CvnnnA1	MLFR.4	1.0	mass fraction of material 4, helium; all mass in CVH is helium
	TATM	764.0	initial temperature of helium in CV nnn; reactor inlet temperature. In Table 11, p.70 [2]
	PVOL	Table A.1	CV pressure
	PH2O	0.0	partial pressure of water vapor in atmosphere; no water vapor
CVnnnBk	—	See BASIS	altitude-hydrodynamic volume pairs; control volumes with a large length chosen to prevent the CFL limit 115ccurring in any volume; excel worksheet “control volumes” and “lower & upper plenum & cavity”

Table A.1

Initial Control Volume Pressure

Control volme	Pressure (Mpa)
190	7.12
160	7.115
161	7.11
162	7.105
163	7.1
164	7.095
165	7.09
166	7.085
280	7.07
1n6	7.063625
1n5	7.05725
1n4	7.050875
1n3	7.0445
1n2	7.038125
1n1	7.03175
1n0	7.025375
054	7.019
200	7.014

Table A.2

Number of Graphite Blocks per Ring

Ring	Number of graphite blocks
01	61
02	30
03	36
04	36
05	NA

Table A.3

One Hexagonal Graphite Block

		Basis
Distance across flats (m) (d)	0.36 [7]	
Cross-sectional area (m2) (S)	0.112236892	$S = \frac{\sqrt{3}}{2} * d^2$
Equivalent diameter (m) (de)	0.378027049	$de = 2 * \sqrt{\frac{S}{\pi}}$
Equivalent radius (m)	0.189013524	

Table A.4

Total Cross Sectional Areas

		Basis
Outer diameter of ring 4 (m)	4.8393 [2]	d_{core}
Total cross sectional area of ring 1, 2, 3, 4 (m2)	18.393	$\frac{\pi * d_{core}^2}{4}$
Outer diameter of ring 5 (m)	6.6504 [2]	d
Total cross sectional area of ring 1, 2, 3, 4, 5 (m2)	34.736	$\frac{\pi * d^2}{4}$

Table A.5

Total Cross Sectional Area of the Radial Ring ii

Ring	Inner radius (m)	Outer radius (m)	cross-sectional area (m2)
01	0	1.476	6.846
02	1.476	1.80307	3.367
03	1.80307	2.13007	4.041
04	2.13007	2.41965	4.139
05	2.41965	3.3252	16.343

Table A.6

CVH Elevation Data

elevation (m)	CVs
-3.994	CV054, CV050
-3.5622	
-3.1304	
-2.6986	
-2.2668	
-1.835	
-1.585	
-1.585	CV110, 120, 130, 140, 150, 160
-1.18875	
-0.7925	
-0.39625	
0	
0	CV111, 121, 131, 141, 151, 161
0.3965	
0.793	
1.1895	
1.586	
1.586	CV112, 122, 132, 142, 152, 162
1.9825	
2.379	
2.7755	
3.172	
3.172	CV113, 123, 133, 143, 153, 163
3.5685	
3.965	
4.3615	
4.758	
4.758	CV114, 124, 134, 144, 154, 164
5.1545	
5.551	
5.9475	
6.344	
6.344	CV115, 125, 135, 145, 155, 165
6.7405	
7.137	
7.5335	
7.93	
7.93	CV116, 126, 136, 146, 156, 166
8.3263	
8.7226	
9.119	
9.119	CV280
9.219	
9.624	
10.029	
10.434	
10.839	
11.244	
11.649	

Table A.7

Altitude-Hydrodynamic Volume Pairs, Ring 1 CVs

CV	elevation (m)	cross sectional area of the ring (m2)	volume (m3)
110	-1.585	6.846	0.000
	-1.18875	6.846	2.713
	-0.7925	6.846	5.426
	-0.39625	6.846	8.139
	0	6.846	10.852
111	0	6.846	0.000
	0.3965	6.846	2.715
	0.793	6.846	5.429
	1.1895	6.846	8.144
	1.586	6.846	10.858
116	7.93	6.846	0.000
	8.3263	6.846	2.713
	8.7226	6.846	5.426
	9.119	6.846	8.140

Substituting the elevation data of CV 1n1 with those of CV 1n2 and using the same volume data, the altitude-hydrodynamic volume pairs of CV 1n2 are obtained. The same process is used for CV 1n3, CV 1n4 and CV 1n5.

N = 1, 2, 3, 4, 5, and 6

Table A.8

Altitude-Hydrodynamic Volume Pairs, Ring 2 CVs

CV	elevation (m)	cross sectional area of the ring (m2)	volume (m3)
120	-1.585	3.367	0
	-1.18875	3.367	1.334
	-0.7925	3.367	2.668
	-0.39625	3.367	4.003
	0	3.367	5.337
121	0	3.367	0.000
	0.3965	3.367	1.335
	0.793	3.367	2.670
	1.1895	3.367	4.005
	1.586	3.367	5.340
126	7.93	3.367	0.000
	8.3263	3.367	1.334
	8.7226	3.367	2.669
	9.119	3.367	4.003

Table A.9

Altitude-Hydrodynamic Volume Pairs, Ring 3 CVs

CV	elevation (m)	cross sectional area of the ring (m2)	volume (m3)
130	-1.585	4.041	0
	-1.18875	4.041	1.601
	-0.7925	4.041	3.202
	-0.39625	4.041	4.803
	0	4.041	6.404
131	0	4.041	0
	0.3965	4.041	1.602
	0.793	4.041	3.204
	1.1895	4.041	4.806
	1.586	4.041	6.408
136	7.93	4.041	0.000
	8.3263	4.041	1.601
	8.7226	4.041	3.203
	9.119	4.041	4.804

Table A.10

Altitude-Hydrodynamic Volume Pairs, Ring 4 CVs

CV	elevation (m)	cross sectional area of the ring (m2)	volume (m3)
140	-1.585	4.139	0
	-1.18875	4.139	1.640
	-0.7925	4.139	3.280
	-0.39625	4.139	4.920
	0	4.139	6.560
141	0	4.139	0
	0.3965	4.139	1.641
	0.793	4.139	3.282
	1.1895	4.139	4.923
	1.586	4.139	6.564
146	7.93	4.139	0.000
	8.3263	4.139	1.640
	8.7226	4.139	3.281
	9.119	4.139	4.921

Table A.11

Altitude-Hydrodynamic Volume Pairs, Ring 5 CVs

CV	elevation (m)	cross sectional area of the ring (m2)	volume (m3)
150	-1.585	16.343	0
	-1.18875	16.343	6.476
	-0.7925	16.343	12.952
	-0.39625	16.343	19.428
	0	16.343	25.904
151	0	16.343	0
	0.3965	16.343	6.480
	0.793	16.343	12.960
	1.1895	16.343	19.440
	1.586	16.343	25.921
156	7.93	16.343	0.000
	8.3263	16.343	6.477
	8.7226	16.343	12.954
	9.119	16.343	19.432

Table A.12

Altitude-Hydrodynamic Volume Pairs, Inlet CVs

CV	elevation (m)	cross sectional area of the ring (m2)	volume (m3)
160	-1.585	2.059	0
	-1.18875	2.059	0.815772056
	-0.7925	2.059	1.631544111
	-0.39625	2.059	2.447316167
	0	2.059	3.263088222
161	0	2.059	0
	0.3965	2.059	0.816286738
	0.793	2.059	1.632573476
	1.1895	2.059	2.448860215
	1.586	2.059	3.265146953
166	7.93	2.059	0.000
	8.3263	2.059	0.815874992
	8.7226	2.059	1.631749984
	9.119	2.059	2.447830849

Table A.13

Altitude-Hydrodynamic Volume Pairs, Upper and Lower Plenums and Cavity

CV	elevation (m)	cross sectional area of the ring (m2)	volume (m3)
280	9.119	34.736	0
	9.219	34.736	3.474
	9.624	34.736	17.542
	10.029	34.736	31.610
	10.434	34.736	45.678
	10.839	34.736	59.747
	11.244	34.736	73.815
	11.649	34.736	87.883
54	-3.994	34.736	0
	-3.5622	34.736	14.999
	-3.1304	34.736	29.998
	-2.6986	34.736	44.998
	-2.2668	34.736	59.997
	-1.835	34.736	74.996
	-1.585	34.736	83.680
50	-3.994	314.159	0
	-3.5622	314.159	135.654
	-3.1304	314.159	271.308
	-2.6986	314.159	406.962
	-2.2668	314.159	542.616
	-1.835	314.159	678.270
	-1.585	314.159	756.810

A.1.4 core-fl.gen

CARD	WORD	VALUE	BASIS
FLnnn00	FLNAME	Table A.14 and Table A.20	
			User defined flow path name
	KCVFM	Table A.14 and Table A.20	
			From control volume number
	KCVTO	Table A.14 and Table A.20	

			To control volume number
	ZFM	Table A.14 and Table A.21	
			Altitude of from junction; for a vertical flow path, altitude where control volumes meet; for a horizontal flow path, altitude at the center of the control volumes
	ZTO		Altitude of to junction; equal to ZFM
FLnnn01	FLARA	Table A.17, Table A.19 and Table A.22	
			Flow path area
	FLLEN	Table A.14 and Table A.22	
			Flow path length; distance between the centers of connected control volumes
	FLOPO	1.0	Fraction of flow path open
FLnnn02	KFLGFL	0	for vertical flow path; 3 for horizontal flow path
	KACTFL	0	active flow path; default value
	IBUBF	0	From junction bubble rise model switch; no bubble rise physics; default value
	IBUBT	0	To junction bubble rise model switch; no bubble rise physics; default value
FLnnnS1	SAREA	see FLARA	segment flow area; 1 segment used per flow path
	SLEN	see FLLEN	segment length
	SHYD	Table A.18, Table A.19 and Table A.22	
			segment hydraulic diameter; the conventional definition is given by 4 times

			the flow area divided by the wetted perimeter; for a ring, Dh = 2(Ro – Ri)
FLnnn03	FRICFO	1.2	Forward loss coefficient
	FRICRO	1.2	Reverse loss coefficient

The same values for FRICFO and FRICRO are used for all the flow paths in order to achieve a total mass flow rate of around 320 kg/s.

	CDCHKF	1.0	default value; Choked flow forward discharge coefficient
	CDCHKR	1.0	default value; Choked flow reverse discharge coefficient

Table A.14:

Flow Path Data

Flow path	Name	From	To	Elev. (m)	Length (m)
1n7	CoreRingF80-Tn6	280	1n6	9.119	1.8595
1n6	CoreRingFn6-Tn5	1n6	1n5	7.93	1.3875
1n5	CoreRingFn5-Tn4	1n5	1n4	6.344	1.586
1n4	CoreRingFn4-Tn3	1n4	1n3	4.758	1.586
1n3	CoreRingFn3-Tn2	1n3	1n2	3.172	1.586
1n2	CoreRingFn2-Tn1	1n2	1n1	1.586	1.586
1n1	CoreRingFn1-Tn0	1n1	1n0	0.0	1.5855
1n0	CoreRingFn0-T54	1n0	54	-1.585	1.997

n: ring 1, 2, 3, 4 and 5

Table A.15

Number of Coolant Channels

Ring	number (d=0.01588m)	number (d=0.0127m)	total number
02	2892	192	3084
03	3588	222	3810
04	3504	228	3732
Total			10626

Table A.16

Flow Area per Block

Block type	total flow area per block (m2)
Standard fuel block	0.02096
Control rod fuel block	0.01832
Reserve shutdown fuel block	0.01832

Table A.17

Flow Area per Ring

Ring	flow path area (m2)
01	0.123523844
02	0.597103701
03	0.738751896
04	0.722875143
05	0.288222304

Table A.18

Hydraulic Diameter in Each Ring

Ring	Hydraulic diameter (m)
01	0.01588
02	0.01588
03	0.01588
04	0.01588
05	0.01588

Table A.19

Helium Inlet Risers

Total flow area (m2)	2.05873074
Inlet channel flow area (m2)	0.34312179
Inlet channel width (m)	0.187
Inlet channel length (m)	1.830
Hydraulic diameter of the inlet channel (m)	0.340

Table A.20

Horizontal Flow Paths

Flow path	Name	From	To
21n	CoreRingF2n-T1n	12n	11n
22n	CoreRingF3n-T2n	13n	12n
23n	CoreRingF4n-T3n	14n	13n
24n	CoreRingF5n-T4n	15n	14n
25n	CoreRingF5n-T3n	15n	13n

n: 0, 1, 2, 3, 4, 5, 6, the last digit of each CV number

Table A.21

Horizontal Flow Path Elevation

From	To	elevation (m)
1n6	1(n-1)6	8.5245
156	136	8.5245
1n5	1(n-1)5	7.137
155	135	7.137
1n4	1(n-1)4	5.551
154	134	5.551
1n3	1(n-1)3	3.965
153	133	3.965
1n2	1(n-1)2	2.379
152	132	2.379
1n1	1(n-1)1	0.793
151	131	0.793
1n0	1(n-1)0	-0.7925
150	130	-0.7925

n: 2,3,4,5

Table A.22

Horizontal Flow Path Lengths and Areas

	Flow path length (m)	flow path area (m2)	hydraulic diameter (m)
Ring 2 to 1	0.9015	0.01372	0.002
Ring 3 to 2	0.3269	0.01621	0.002
Ring 4 to 3	0.3083	0.01496	0.002
Ring 5 to 4	0.5976	0.01746	0.002
Ring 5 to 3	0.7611	0.001247	0.002

A.1.5 core-hs.gen

Input for HS 34001, 34002, 34003, 34004, 34005

CARD	WORD	VALUE	BASIS
HSCCCCC000	NP	2	Number of temperature nodes
	IGEOM	1	rectangular geometry
	ISS	-1	a steadystate initialization calculation is not performed and the initial temperature distribution is input on the HSCCCCC8XX records
HSCCCCC001	HSNAME	Table A.23	Name of heat structure
HSCCCCC002	HSALT	9.119	elevation of the “left-most” (lowest) point of heat structure; top of the upper reflector region
	ALPHA	0.0	horizontal surface with lefthand side on the bottom
HSCCCCC100	NODLOC	-1	temp. node location data on HSCCCCC1NN records
	IFRMAT	1	each pair of data on each of these records is interpreted as the location of a temperature node and the number of this node
	XI	0.0	left (inside) boundary location;

			positioned to the origin
HSCCCCC102	XVALUE	0.1	location of temperature node
	NXVALU	2	temperature node at location XVALUE
HSCCCCC201	MATNAM		material used in mesh interval MSHNUM; design information not found; 'STAIN-LESS STEEL 304' used
	MSHNUM	1	mesh interval number

These records are required if either MCDLOC on Record HSCCCCC200 is negative or Record HSCCCCC200 is omitted.

HSCCCCC300	ISRC	0	no internal power source
HSCCCCC400	IBCL	1	a convective boundary condition applied to left boundary
	IBVL	Table A.24	boundary volume attached to left boundary
	IFLOWL	'EXT'	evaluated as an external flow
	CPFPL	0.9	critical pool fraction for pool; no pool present
	CPFAL	0.9	critical pool fraction for atmosphere; no pool present
HSCCCCC401	EMISWL	0.8	wall emissivity of left surface; p.661, Table 4 of [8]
	RMODL		utilize 'equiv-band' radiation model

	PATHL	0.25	radiation path length for the left surface; unknown value
HSCCCCC500	ASURFL	Table A.23	boundary surface area; equivalent to ASCELA for respective ring
	CLNL	Table A.18	boundary surface characteristic length; hydraulic diameter of boundary CV
	BNDZL	Table A.23	radial length of boundary surface
HSCCCCC600	IBCL	0	insulated boundary condition applied to the right surface
	IBVL	-1	no CV associated with the right surface
HSCCCCC800	NTDLOC	-1	If negative, the initial temperature distribution for Heat Structure CCCCC must be entered on the HSCCCCC8NN records.
HSCCCCC8NN	TEMPIN	764.0	Initial temperature
	NODNUM	1 or 2	Temperature node number; there are two temperature nodes in each heat structure

Table A.23

Upper Boundary Heat Structure Data

Heat Structure	Name	Area (m2)	Length (m)	Basis
34001	UPPER_BOUNDARY_RING1	6.846450	1.4762	R_1
34002	UPPER_BOUNDARY_RING2	3.367107	0.3268	$R_2 - R_1$
34003	UPPER_BOUNDARY_RING3	4.040528	0.3270	$R_3 - R_2$
34004	UPPER_BOUNDARY_RING4	4.139016	0.2896	$R_4 - R_3$
34005	UPPER_BOUNDARY_RING5	16.34335	0.9056	$R_5 - R_4$

R_1, R_2, R_3, R_4 and R_5: radius of ring 1, 2, 3, 4 and 5, respectively

Table A.24

Boundary CVHs of the Upper Boundary HSs

Ring	Heat Structure	Boundary CVH
01	34001	116
02	34002	126
03	34003	136
04	34004	146
05	34005	156

Input for all other heat structures

HSCCCCC000	NP	2	Number of temperature nodes
	IGEOM	2	cylindrical geometry
	ISS	-1	a steadystate initialization calculation is not performed and the initial temperature distribution is

			input on the HSCCCCC8XX records
HSCCCCC001	HSNAME	varies	name of heat structure
HSCCCCC002	HSALT	Table A.25	elevation of the “inner-most” and the lowest point of heat structure; core barrel HS and RPV wall HS have the same elevation data
	ALPHA	1.0	vertical surface
HSCCCCC004	IOPTL	Table A.25	Use fluid temperature calculated by COR package dT/dz model for core cell IOPTL for boundary fluid temperature on the left-hand side.
	IOPTR	0	default value
HSCCCCC100	NODLOC	-1	temp. node location data on HSCCCCC1NN records
	IFRMAT	1	each pair of data on each of these records is interpreted as the location of a temperature node and the number of this node
	XI	3.3252	for core barrel HS; 3.61315 for RPV HS left (inside) boundary location; positioned to the origin
HSCCCCC101	XVALUE		3.4014 for core barrel HS outer radius; 3.82905 for RPV HS outer

			radius; location of temperature node
	NXVALU	2	temperature node at location XVALUE
HSCCCCC200	MCDLOC	-1	If negative, the material composition data for Heat Structure CCCCC must be entered on the HSCCCCC2NN records.
HSCCCCC400	IBCL	1	a convective boundary condition applied to left boundary
	IBVL	Table A.25 and Table A.27	boundary volume attached to left boundary
	IFLOWL	‘EXT’ or ‘INT’	evaluated as an external flow for CVs in ring 5; evaluated as an internal flow for CVs in helium inlet
	CPFPL	0.9	critical pool fraction for pool; no pool present
	CPFAL	0.9	critical pool fraction for atmosphere; no pool present
HSCCCCC500	ASURFL		area of inside boundary surface; ASURFL = 2πRoDZ
	CLNL	Table A.18 and Table A.19	boundary surface characteristic length; hydraulic diameter of the boundary CV

	BNDZL		axial length of boundary surface
HSCCCCC600	IBCL	1	a convective boundary condition applied to right boundary
	IBVL	Table A.25	boundary volume attached to right boundary
	IFLOWL	‘EXT’ or ‘INT’	evaluated as an external or internal flow
	CPFPL	0.9	critical pool fraction for pool; no pool present
	CPFAL	0.9	critical pool fraction for atmosphere; no pool present
HSCCCCC700	ASURFL		area of outside boundary surface; ASURFL = 2πRoDZ
	CLNL	Table A.19	boundary surface characteristic length; hydraulic diameter of the boundary CV
	BNDZL		axial length of boundary surface; equal to the characteristic length of the boundary surface

Table A.25

Radial Boundary Heat Structure Data

HS	HSALT(m)	IOPTL	IBVL(inner)	CLNL(m)	IBVL(outer)
32000	-1.835	506	54	0.25	0
32001	-1.585	507	150	0.39625	160
32002	-1.18875	508	150	0.39625	160
32003	-0.7925	509	150	0.39625	160
32004	-0.39625	510	150	0.39625	160
32005	0.0	511	151	0.3965	161
32006	0.3965	512	151	0.3965	161
32007	0.793	513	151	0.3965	161
32008	1.1895	514	151	0.3965	161
32009	1.586	515	152	0.3965	162
32010	1.9825	516	152	0.3965	162
32011	2.379	517	152	0.3965	162
32012	2.7755	518	152	0.3965	162
32013	3.172	519	153	0.3965	163
32014	3.5685	520	153	0.3965	163
32015	3.965	521	153	0.3965	163
32016	4.3615	522	153	0.3965	163
32017	4.758	523	154	0.3965	164
32018	5.1545	524	154	0.3965	164
32019	5.551	525	154	0.3965	164
32020	5.9475	526	154	0.3965	164
32021	6.344	527	155	0.3965	165
32022	6.7405	528	155	0.3965	165
32023	7.137	529	155	0.3965	165
32024	7.5335	530	155	0.3965	165
32025	7.93	531	156	0.3963	166
32026	8.3263	532	156	0.3963	166
32027	8.7226	533	156	0.3964	166

HS 33 has the same elevation (HSALT) and axial length data (CLNL) as HS 32.

Table A.26

Heat Structure 32 Data

HS	ASURFL (inner)	ASURFL (outer)
32000	5.2232	
32001 to 32004	8.2788	8.7670
32005 to 32024	8.2840	8.7725
32025 to 32026	8.2798	8.7681
32027	8.2819	8.7703

Table A.27

Heat Structure 33 Data

HS	IBVL (inner)	ASURFL (inner)
33001 to 33004	160	8.9957
33005 to 33008	161	9.0014
33009 to 33012	162	9.0014
33013 to 33016	163	9.0014
33017 to 33020	164	9.0014
33021 to 33024	165	9.0014
33025 to 33026	166	8.9968
33027	166	8.9991

A.1.6 core.gen

CARD	WORD	VALUE	BASIS
COREDV01	ITEMP	1	print temperature variables to output file
	IMASS	1	print mass variables to output file
	IVOL	1	print volume variables to output file
	IASUR	1	print surface area variables to output file
	IPMV	1	print component mass and volume fraction variables to output file
	IPOW	1	print decay heat and fission power variables to output file
COR00000	NRAD	5	radial rings; three rings in the active core region; ring 1 for the inner reflector region; ring 5 for the outer reflector region; based on [2] Page no. 30, Figure 14
	NAXL	33	axial levels of the upper reflector region, the active core, the lower reflector region and the core exit plenum; 20 active core levels; 6 levels in the core exit plenum; 4 levels in the lower reflector; 3 levels in the upper reflector based on Fig. 2 in [2], the RELAP model on page no. 73 of [2] and Fig. 5-14 in [4]
	NTLP	6	axial levels in the core exit plenum; based on Fig. 5-14 in [3]; level 1 to level 5 are the lower plenum; level 6 is the core support plate

	NCVOL	36	number of CVH fluid volumes in the upper reflector region, the active core, the lower reflector region, the inner reflector region, the outer reflector region and the core exit plenum
	NLH	3	lower head temperature nodes; based on the assumption that the thickness of the lower head is equal to the thickness of reactor vessel which is 0.2159m; the vessel thickness is given by the RELAP model on page no. 73 of [2]
	NLHTA	5	Number of segments in noncylindrical (flat or hemispherical) portion of lower head. Suggested by MELGEN diagnostic message
	NPNTOT	0	no lower head penetration

The lower head in this reactor is the bottom of the reactor vessel.

COR00001	RFUEL	0.006225	outer radius of the fuel pellets in the fuel rods; page no. 59 of [2]
	RCLAD	0.189013524	outer radius of the fuel rod cladding; the distance across flats of a graphite fuel block is 0.36m; for the radius of the cladding, please refer to the work sheet “ring cross sectional area” in the work book “graphite fuel block” and look for equivalent radius of the graphite block
	DRGAP	0.000125	thickness of the gas gap between fuel pellets and cladding; diameter of the fuel

			hole: 0.0127m; [1] Fig. 2.6. Page no. 8; radius of the fuel hole: 0.00635m: gap = 0.00635m – 0.006225m
	PITCH	0.0188	center-to-center spacing of the fuel rods, [1] Fig. 2.6. Page no. 9;
	DXCAN	0.0	thickness of the canister wall; there is no canister in this reactor
	DXSS	0.0	thickness of other structure; there is no other structure in this reactor
COR00001A	RCOR	3.3252	Outer radius for COR package in active core region; diameter of the outer reflector: 6.6504, [2] Page no. 73 which is the diameter of ring 5 – the outermost ring in my model; 6.6504/2 = 3.3252 which is the radius
	RVLH	3.61315	Radius of curvature of inside of lower head; The value is unused for a flat head; I use the value of RPV inner radius, [2] Page no. 73; RPV inner diameter = 7.2263 m, 7.2263/2 = 3.61315 which is the radius
	RVESS	3.3252	Radius of inside of vessel cylinder; I use the radius of the outer reflector; in my model, I've a straight cylindrical lower head; value for RVESS and value for ILHTRN are interrelated.
	ILHTYP	1	Reactor lower-head type; 1 indicates that lower head is flat.
	ILHTRN	1	Reactor lower head transition type; 1

			indicates that transition is at RVESS, as in typical PWR.
	DZRV	0.2159	Thickness of cylindrical vessel wall; the thickness of reactor vessel, [2] Page no. 73
	DZLH	0.2159	Thickness of lower head inside the transition radius specified by ILHTRN
COR00001B	HLST	-1.835	Elevation of PWR bottom plate.
	HCSP	-1.835	Elevation of core support plate
COR00002	IRTYP	PWR	reactor type
	MCRP	B4C	control rod poison material
COR00003	FCNCL	1.0	a value must be entered for PWRs but is not used
	FSSCN	0.0	Radiative exchange factor for radiation from an other structure
	FCELR	0.9	Radiative exchange factor for radiation radially outward from the cell boundary to the next adjacent cell
	FCELA	0.1	Radiative exchange factor for radiation axially upward from the cell boundary to the next adjacent cell.

The sum of FCELR and FCELA should not be greater than 1, otherwise an error message will be generated by MELGEN.

	FLPUP	0.0	Radiative exchange factor for radiation from the liquid pool to the core components.

COR00004	NTPCOR	0	‘In’ Transfer Process number; For convenience, a value of 0, indicating no TP, may be used for calculations that will not fail the lower head and eject debris.
	ICFFIS	-10	Fission power control function number; the control function number for the steady state core fission power in my model is 10

If ICFFIS is 0 or omitted, no fission power is calculated.

If |ICFFIS| is less than 100, fission power is distributed over all core cells (not lower plenum cells) on a per fuel mass basis. Decay heat is automatically added to the fission power to obtain total core power, so the user input value should not include the contribution from fission product decay.

	ICFGAP	0	Fuel-cladding gap conductance control function number. If it is 0 or omitted, no additional gap resistance is calculated.

If a positive value is entered, the conductance is added serially to the gap gas conduction for all cells with fuel rods, in parallel to the gap radiation.

COR00012	HDBH2O	100.0	default value; Heat transfer coefficient from in-vessel falling debris to pool.
	PPFAIL	2.0e7	default value; Differential pressure between lower plenum volume and reactor cavity volume that will fail the lower head.
	IAXSUP	6	Axial level number of core cells containing the core support plate.
	VFALL	1.0	default value; velocity of falling debris.
COR00006	IEUMOD	0	Materials interactions model switch is inactive

	IHSDT	0	HS boundary condition option switch; dT/dz boundary condition option is required for core radial boundary structures input on record CORZjj02
	IDTDZ	0	dT/dz inlet specification option switch; dT/dz inlet flow and temperature from default hydrodynamic calculation in CVH/FL.
	IOLDOS	0	OS option switch; Input may not contain specification of OS. Structures must be modeled using SS and NS.
	ICORCV	0	CVH volume consistency switch; Consistency between fluid volumes in CVH and in COR, meaning that the volume in COR may not exceed that in CVH, is required.

CF01000	CFNAME	COREPOW	
	CFTYPE	EQUALS	
	NCFARG	1	
	CFSCAL	0.0	
	CFADCN	600.0e6	fission power is 600 MW

CFn…n00 – Control Function Definition Record

CF01010	ARSCAL	1.0
	ARADCN	0.0
	CHARG	TIME

CFn…nkk – Control Function Arguments

CORZjj01	Z	Table A.28	elevation of lower boundary axial level
	DZ	Table A.29	axial length of level from lower boundary to upper boundary
	PORIN	0.111	unused
	PORDP	0.0	porosity of particulate debris for all cells in axial level jj; not used in this calculation since there is no particulate debris in this reactor.
CORZjj02	IHSA	Table A.30	Boundary heat structure number for this axial level, or 0 for levels below HLST. A unique heat structure must be specified for each axial level above HLST.
CORZjj03	FZPOW	Table A.31	Relative power density in this level; Axial Power Density Profile
CORRii03	FRPOW	Table A.32	Relative power density in this ring
CORRii00	RINGR	Table A.5	Radial Ring Outer Radius
CORRii02	IHSR	Table A.23	Upper-boundary heat structure number for this radial ring
CORijj01	IREFN	Table A.33	reference cell for settings not input for cell ijj
	ICVHC	Table A.33	channel control volume adjacent to cell ijj
	ICVHB		bypass control volume adjacent to this cell; default value: ICVHC = ICVHB

Core support plate:

CORi06SS	ISSMOD	PLATEG	default value, SS in a cell will be treated as a grid-supported plate.
	THICK	0.25	thickness of core support plate, assumed
	SPACE	0.2000	Spacing of supporting beams, *x*.
	AKMG	10e-20	Coefficient *KG*.
CORi06KSS	XMSSSS		Mass of steel in the cell supporting structure component.
	XMSSZR		no Zircaloy in cells
	XMSSSX		no steel oxide in cells
	XMSSZX		no zirconium dioxide in cells

i= 1,2,3,4,5 – ring no.

CORi0606	ASFU	0.0	fuel surface area
	ASCL	0.0	cladding surface area
	ASOS	0.0	“other structure” surface area
	ASCN	0.0	total canister inside surface area
	ASSS	Table A.34	supporting structure surface area
	ASNS	0.0	nonsupporting structure surface area
CORijj03	TFU	764.0	initial temp. of uranium dioxide in cell ijj; reactor inlet temp. [2] Page no. 73
	TCL	764.0	initial temp. of cladding in cell ijj; reactor inlet temp.
	TOS	764.0	there is no other structure in this reactor core; coolant channel are not considered as other structures

	TCN	764.0	initial temp. of canister (CN) in cell ijj; reactor inlet temp.; ignored for PWR calculations; no canister in this reactor core
	TCB	764.0	initial temp. of canister (CB) in cell ijj; reactor inlet temp.; ignored for PWR calculations
	TPD	0.0	initial temp. of particulate debris in cell ijj; no particulate debris in this reactor
	TSS	764.0	initial temp. of supporting structures in cell ijj; reactor inlet temp.
	TNS	764.0	initial temp. of "nonsupporting structures" incell ijj; reactor inlet temp.
	TPB	0.0	initial temp. of particulate debris in the bypass in cell ijj
CORijj04	DHYCL	0.378027049	cladding equivalent outside diameter;
	DHYOS	1.0	"other structure" equivalent diameter; not utilized in this calculation
	DHYPD	1.0	particulate debris equivalent diame ter; not utilized in this calculation
	DHYCNC	1.0	Canister inside equivalent diameter; ignored for this calculation
	DHYCNB	1.0	Canister outside equivalent diameter; ignored for this calculation
	DHYSS	0.378027049	Supporting structure equivalent diameter; in my model, part of the graphite is modeled as cladding and the other part is modeled as supporting structure; I use the same equivalent diameter for both cladding and

			supporting structure in the core region; but for the core support plate, I use the diameter of each ring
	DHYNS	Table A.35	equivalent diameter of NSSs

Since the diameters of control rod and reserve shutdown system are much bigger than that of burnable poison rod, so the diameter of control rod or reserve shutdown system for NSS equivalent diameter.

	DHYPB	1.0	default value; particulate debris equivalent diameter in the bypass of a BWR; not utilized in this calculation
CORijj06	ASFU	Table A.41	fuel surface area
	ASCL	Table A.41	cladding surface area
	ASOS	0.0	“other structure” surface area
	ASCN	0.0	total canister inside surface area
	ASSS	Table A.42	supporting structure surface area
	ASNS	Table A.43	nonsupporting structure surface area
CORijjKSS	XMSSSS	Table A.44, 45, 46, 47 and 48	Mass of steel in the cell supporting structure component
	XMSSZR		no zircaloy in cells
	XMSSSX		no steel oxide in cells
	XMSSZX		no zircaloy dioxide in cells
CORijjKFU	XMFUUO		mass of UO2 in the cell fuel component; UCO is actually used in this reactor; since the properties of UCO are not available, the

			properties of UO2 is used instead; 1.0e-6 is used to activate the use of power profiles
	XMFUHT	0.0	no electric heating element in the cell fuel component
	XMFUXM	Table A.50	Mass of additional fuel material (as defined on the CORXFUMAT record) in the cell fuel component
CORijjSS	ISSMOD	PLATEG	default value, SS in a cell will be treated as a grid-supported plate.
	ISSFAI	TSFAIL	Failure model
	TSSFAI	1700.0	Failure temperature for the TSFAIL model; without setting this criterion, supporting structure will have over temperature failure when they reach the default failure temperature of 1273.15 K; I use the melting temperature of stainless steel in my model as the failure temperature
jj=>7			
CORijjKNS	XMNSSS	0.0	no steel in the cell NSS component
	XMNSCP	Table A.51	mass of control poison
	XMNSZR	0.0	no Zircaloy associated in the cell NSS component
	XMNSSX	0.0	no steel oxide associated in the cell NSS component
	XMNSZX	0.0	no ZrO2 associated in the cell NSS component

CORijjKCL	XMCLZR	Table A.47	Mass of Zircaloy in the cell cladding component
	XMCLIN		no Inconel associated with the cell cladding component
	XMCLZX		no ZrO2 in the cell cladding component
CORijj05	ASCELR	Table A.52	area of outer radial cell boundary of cell ijj; ASCELR = 2πRoDZ
	AFLOWC	Table A.17	channel flow area of cell
	AFLOWB	0.0	bypass flow area of cell in a BWR; for a PWR, AFLOWB will simply be added to AFLOWC.
CORLHDii	IS		Segment number; 5 segments correspond to 5 rings respectively; there're 10 segments altogether
	TLH	764.0	initial temp. of lower head node in Ring ii;
	RADLH	Table A.5	outer radius of lower head Ring ii
	ICVCAV	050	reactor cavity control volume number; only input for ii=01
CORXFUMAT	XFUMAT		INC
CORMATx	CORMAT		Permitted values are 'UO2', 'ZR', 'ZRO2', 'SS', and 'SSOX'.
	MATNAM		Permitted values include but not limited to: 'URANIUM-DIOXIDE', 'STAINLESS-STEEL', 'ZIRCALOY'; I recommend to write the input values in the above fashion,

		otherwise an error message from MELGEN will be generated.
CORCLMAT	CLMAT	Zircaloy is the cladding

Materials recognized by the COR package: (Zircaloy, ZrO2, stainless steel, SS Oxide, Control Poison, Inconel, UO2 and heating material)

Table A.28

Elevation of Lower Boundary Axial Level of COR Cells

Level	Elevation (m)	Basis
01	- 3.994	the height of the core exit hot gas plenum is 2.159 m, assumed; 2.159/5 = 0.4318 m which is the height of level 1 to level 5
02	- 3.5622	
03	- 3.1304	
04	- 2.6986	
05	- 2.2668	
06	-1.835	
07	-1.585	
08	-1.18875	
09	-0.7925	
10	-0.39625	
11	0.0	corresponding to the bottom-most point of the active core
12	0.3965	corresponding to half of the block height which is 0.793 m
13	0.793	
14	1.1895	
15	1.586	
16	1.9825	
17	2.379	
18	2.7755	
19	3.172	
20	3.5685	
21	3.965	
22	4.3615	
23	4.758	
24	5.1545	
25	5.551	
26	5.9475	
27	6.344	
28	6.7405	
29	7.137	
30	7.5335	
31	7.93	
32	8.3263	
33	8.7226	

Table A.29

Axial Length of Each Level from Lower Boundary to Upper Boundary

Level	Cell length (m)
01	0.4318
02	0.4318
03	0.4318
04	0.4318
05	0.4318
06	0.25
07	0.39625
08	0.39625
09	0.39625
10	0.39625
11	0.3965
12	0.3965
13	0.3965
14	0.3965
15	0.3965
16	0.3965
17	0.3965
18	0.3965
19	0.3965
20	0.3965
21	0.3965
22	0.3965
23	0.3965
24	0.3965
25	0.3965
26	0.3965
27	0.3965
28	0.3965
29	0.3965
30	0.3965
31	0.3963
32	0.3963
33	0.3964

Table A.30

Radial Boundary Heat Structure

Level	Heat Structure
01	0
02	0
03	0
04	0
05	0
06	32000
07	32001
08	32002
09	32003
10	32004
11	32005
12	32006
13	32007
14	32008
15	32009
16	32010
17	32011
18	32012
19	32013
20	32014
21	32015
22	32016
23	32017
24	32018
25	32019
26	32020
27	32021
28	32022
29	32023
30	32024
31	32025
32	32026
33	32027

Table A.31

Axial Power Factors for the NGNP

	Point design values	GA values
CORZ1103	1.1734	0.6175
CORZ1203	1.2578	0.6925
CORZ1303	1.3164	0.7475
CORZ1403	1.3492	0.7825
CORZ1503	1.3336	0.81
CORZ1603	1.2696	0.83
CORZ1703	1.1985	0.8525
CORZ1803	1.1203	0.8775
CORZ1903	1.0492	0.9175
CORZ2003	0.9852	0.9725
CORZ2103	0.9359	1.035
CORZ2203	0.9013	1.105
CORZ2303	0.86925	1.1625
CORZ2403	0.83975	1.2075
CORZ2503	0.8125	1.25
CORZ2603	0.7875	1.29
CORZ2703	0.75	1.29
CORZ2803	0.7	1.25
CORZ2903	0.63905	1.1875
CORZ3003	0.56715	1.1025

Ref. [2] and [25]

Table A.32

Radial Power Factors for the NGNP

	Point design values	GA values
CORR0203	1.1	1.161
CORR0303	0.92	1.065
CORR0403	1.0	0.832

Ref. [2] and [25]

Table A.33

Cell Reference and Fluid Boundary Volumes

Reference cell	Description	Adjacent CV	Cells using reference
i01	core exit plenum	054	i02,i03, i04, i05
i06	core support plate	054	
i07	lower reflector	1i0	i08, i09, i10
i11	active core level	1i1	i12, i13, i14
i15	active core level	1i2	i16, i17, i18
i19	active core level	1i3	i20
i21	active core level	1i3	i22
i23	active core level	1i4	i24, i25, i26
i27	active core level	1i5	i28, i29, i30
i31	upper reflector	1i6	i32
i33	upper reflector	1i6	

i= 1,2,3,4,5 – ring no.

Table A.34

Core Support Plate ASSS

cell	cell height (m)	cell boundary area (m2)	ASSS (m2)
106	0.25	2.3189	2.3189
206	0.25	2.8323	5.1511
306	0.25	3.3459	6.1782
406	0.25	3.8008	7.1467
506	0.25	5.2232	9.0240

Table A.35

Nonsupporting Structure Equivalent Diameter

Block type	nonsupporting structure equivalent diameter
control rod fuel block	0.1016m [2] Page no. 34
reserve shutdown system block	0.09525m [2] Page no. 34
block without control materials	1.0

Table A.36

Standard Fuel Block Axial Surface Areas

	Number	Diameter (m)	Axial surface area (m2)
Fuel holes	210	0.0127	3.3221
Fuel pellet	210	0.01245	3.2567
Coolant channel	102	0.01588	2.0176
	6	0.0127	0.0949
All coolant channels			2.1126
Burnable poison rod channel	6	0.0127	0.0949

Table A.37

Control Rod Fuel Block Axial Surface Areas

	Number	Diameter (m)	Axial surface area (m2)
Fuel holes	186	0.0127	2.94245
Fuel pellet	186	0.01245	2.88453
coolant channel	93	0.01588	1.83961
	6	0.0127	0.09492
all coolant channels			1.93453
control rod channel	1	0.1016	0.12656
burnable poison rod channel	6	0.0127	0.09492

Table A.38

Reserve Shutdown Rod Fuel Block Axial Surface Areas

	Number	Diameter (m)	Axial surface area (m2)
Fuel holes	186	0.0127	2.942454271
Fuel pellet	186	0.01245	2.884531943
coolant channel	93	0.01588	1.839613142
	6	0.0127	0.09491788
all coolant channels			1.934531022
reserve shutdown channel	1	0.09525	0.11864735
burnable poison rod channel	6	0.0127	0.09491788

Table A.39

Burnable Poison Rods in One Fuel Block

Level	Number per block	Diameter (m)	surface area (m2)	volume (m3)
LV21-LV30	5	0.01143	0.07118841	0.00020342
LV31-LV32				0.00020332
LV33				0.00020337

Table A.40

One Control Rod

Level	outer diameter (m)	Axial surface area (m2)	volume (m3)
LV21-LV30	0.0826	0.168659854	0.001256516
LV31-LV32	inner diameter (m)	cross-sectional area (m2)	0.001255882
LV33	0.0528	0.003169019	0.001256199

Table A.41

ASFU and ASCL for Core Cell Level 11 to 30

	ring 2	ring 3	ring 4	ring 5
standard fuel block	18	30	24	
control rod fuel block	12			36
RSC fuel block		6	12	
ASFU - Fuel surface area (m2)	93.2355	115.0091	112.7759	
fuel hole surface area (m2)	95.1077	117.3185	115.0405	
coolant channel surface area (m2)	61.2404	74.9839	73.9158	
FBP channel surface area (m2)	2.8475	3.4170	3.4170	
control rod channel surface area (m2)	1.5187			4.5561
RSC channel surface area (m2)		0.7119	1.4238	
ASCL - Cladding surface area (m2)	156.3481	192.3024	188.9562	

Table A.42

ASSS – Supporting Structure Surface Area

	ring 1	ring 2	ring 3	ring 4	ring 5
ASSS (m2) LV11-LV30	10.5242	15.2086	17.1865	19.5061	34.9196
ASSS (m2) LV7-LV10	10.5219	72.1364	88.0308	88.6128	30.6464
ASSS (m2) LV31-LV32	10.5223	73.5657	88.7103	89.9611	34.9101
ASSS (m2) LV33	10.5233	73.5836	88.7317	89.9826	34.9148

Table A.43

ASNS – Nonsupporting Structure Surface Area

	ring 2	ring 3	ring 4	ring 5
standard fuel block	18	30	24	
control rod fuel block	12			36
RSC fuel block		6	12	
FBP rod surface area	2.1357	2.5628	2.5628	
control rod surface area	2.0239			6.0718
RSC channel surface area (m2)		0.0000	0.0000	
ASNS (m2) LV11-LV20	2.1357	2.5628	2.5628	0.0000
ASNS (m2) LV21-LV30	4.1596	2.5628	2.5628	6.0718
ASNS (m2) LV31-LV32	2.0229	0.0000	0.0000	6.0687
ASNS (m2) LV33	2.0234	0.0000	0.0000	6.0702

Table A.44

Core Support Plate Graphite Masses

Cell	area (m2)	graphite mass (kg)	supporting structure mass (kg)
106	6.846450432	2978.205938	2978.205938
206	3.36710677	1464.691445	1464.691445
306	4.040528124	1757.629734	1757.629734
406	4.139016417	1800.472141	1800.472141
506	16.34334698	7109.355936	7109.355936

Table A.45

Core Exit Plenum Graphite Masses

Cell	area (m2)	graphite mass (kg)	supporting structure mass (kg)
101	6.846450432	5143.957296	5143.957296
201	3.36710677	2529.815064	2529.815064
301	4.040528124	3035.778076	3035.778076
401	4.139016417	3109.775483	3109.775483
501	16.34334698	12279.27957	12279.27957

Table A.46

Lower Reflector Graphite Masses

Cell	area (m2)	graphite mass (kg)	supporting structure mass (kg)
107	6.846450432	4720.456412	4720.456412
207	2.770003069	1909.847866	1909.847866
307	3.301776228	2276.492165	2276.492165
407	3.416141274	2355.344005	2355.344005
507	16.34334698	11268.32916	11268.32916

Table A.47

Active Core, Inner and Outer Reflector Graphite Masses

Cell	area (m2)	total mass (kg)	cladding mass (kg)	supporting structure mass (kg)
111	6.846450432	4723.434617		4723.434617
211	1.888332055	1302.779168	1196.981901	105.7972672
311	2.292224915	1581.428891	1518.005733	63.42315792
411	2.382077987	1643.419424	1537.843012	105.5764125
511	16.05148319	11074.07877		11074.07877

Table A.48

Upper Reflector Graphite Masses

Cell	area (m2)	heigh (m)	total mass (kg)	supporting structure mass (kg)
131	6.846450432	0.3963	4721.052053	4721.052053
231	2.672715233	0.3963	1843.002861	1843.002861
331	3.259022785	0.3963	2247.29827	2247.29827
431	3.330634387	0.3963	2296.678909	2296.678909
531	16.05148347	0.3963	11068.49305	11068.49305
133	6.846450432	0.3964	4722.243335	4722.243335
233	2.672715233	0.3964	1843.467914	1843.467914
333	3.259022785	0.3964	2247.86534	2247.86534
433	3.330634387	0.3964	2297.25844	2297.25844
533	16.05148347	0.3964	11071.286	11071.286

Table A.49

Number of Fuel Compacts per Block

Standard fuel block	3378
Control rod fuel block	2992
Reserve system shutdown fuel block	2992

Table A.50

Fuel Compact Masses

	ring 2	ring 3	ring 4
Number of fuel compacts per ring	96704	119288	116972
Mass of fuel rods per ring (kg)	1170.340	1443.653	1415.621
Mass of fuel rods per cell (kg)	585.170	721.826	707.810

Table A.51

NS Masses

	ring 2	ring 3	ring 4	ring 5
total no. of fuel block	30	36	36	
standard fuel block	18	30	24	
control rod block	12			36
RSC fuel block		6	12	
NS volume (m3) LV11-LV20	0.0061	0.0073	0.0073	0.0000
NS masses (kg) LV11-LV20	15.3786	18.4543	18.4543	0.0000
NS volume (m3) LV21-LV30	0.0212	0.0073	0.0073	0.0452
NS masses (kg) LV21-LV30	53.3757	18.4543	18.4543	113.9911
NS volume (m3) LV31-LV32	0.0151	0.0000	0.0000	0.0452
NS masses (kg) LV31-LV32	37.9779	0.0000	0.0000	113.9336
NS volume (m3) LV33	0.0151	0.0000	0.0000	0.0452
NS masses (kg) LV33	37.9875	0.0000	0.0000	113.9624

Table A.52

Area of Outer Radial Cell Boundary of Cell ijj

Cell	Outer radius (m)	Height (m)	Area (m2)
101	1.476	0.4318	4.005164002
201	1.80307	0.4318	4.891883242
301	2.13007	0.4318	5.77906058
401	2.41965	0.4318	6.564702608
501	3.3252	0.4318	9.021531673
106	1.476	0.25	2.318876796
206	1.80307	0.25	2.832262183
306	2.13007	0.25	3.345912795
406	2.41965	0.25	3.800777332
506	3.3252	0.25	5.223211946
107	1.476	0.39625	3.675419722
207	1.80307	0.39625	4.489135559
307	2.13007	0.39625	5.30327178
407	2.41965	0.39625	6.024232071
507	3.3252	0.39625	8.278790934
111	1.476	0.39625	3.677738598
211	1.80307	0.3965	4.491967822
311	2.13007	0.3965	5.306617693
411	2.41965	0.3965	6.028032849
511	3.3252	0.3965	8.284014146
131	1.476	0.3963	3.675883497
231	1.80307	0.3963	4.489702012
331	2.13007	0.3963	5.303940963
431	2.41965	0.3963	6.024992227
531	3.3252	0.3963	8.279835577
133	1.476	0.3964	3.676811048
233	1.80307	0.3964	4.490834917
333	2.13007	0.3964	5.305279328
433	2.41965	0.3964	6.026512538
533	3.3252	0.3964	8.281924861

A.1.7 ncg-mp.gen

CARD	WORD	VALUE	BASIS
NCG000	MP NAME	HE	define noncondensible gas
	MP VALUE	4	assign to material 4
NCG001	MP NAME	O2	define noncondensible gas
	MP VALUE	5	assign to material 5
NCG002	MP NAME	N2	define noncondensible gas
	MP VALUE	6	assign to material 6
NCG003	MP NAME	CO2	define noncondensible gas
	MP VALUE	7	assign to material 7
NCG004	MP NAME	CH4	define noncondensible gas
	MP VALUE	8	assign to material 8
NCG005	MP NAME	H2	define noncondensible gas
	MP VALUE	9	assign to material 9
NCG006	MP NAME	CO	define noncondensible gas
	MP VALUE	10	assign to material 10

MPMAT00100	MATNAM	HELIUM	define helium as material 001
MPMAT00101	PROP	RHO	define density vs. temperature
	ITBPRP	1	tabular function for RHO

MPMAT00102	PROP	CPS	define specific heat vs temperature
	ITBPRP	2	tabular function for CPS
MPMAT00103	PROP	THC	define thermal conductivity vs temperature
	ITBPRP	3	tabular function for THC
TF001	Table A.53		at 7 MPa, from [21]
TF002	Table A.54		at 7 MPa, from [21]
TF003	Table A.55		at 7 MPa, from [21]
MPMAT00200	MATNAM		’OXYGEN’; define oxygen as material 002; I redefine the properties of oxygen with that of outside air, since the reactor cavity cooling system contains outside air in it
MPMAT00201	PROP	RHO	define density vs. temperature
	ITBPRP	4	tabular function for RHO
MPMAT00202	PROP	CPS	define specific heat vs temperature
	ITBPRP	5	tabular function for CPS
MPMAT00203	PROP	THC	define thermal conductivity vs temperature
	ITBPRP	6	tabular function for THC

TF004	Table A.56	at 0.1 MPa, calculated based on from [5] Vol. 2, page no. 581/776
TF005	Table A.57	at 0.1 MPa, from [9]
TF006	Table A.58	at 0.1 MPa, from [5] Vol. 2, page no. 551/776

MPMAT00300	MATNAM		‘INC’; redefine the properties of inconel as those of homogeneous fuel rods using material 003
MPMAT00301	PROP	ENH	enthalpy vs temperature
	ITBPRP	100	tabular function for ENH
MPMAT00302	PROP	TMP	temperature vs enthalpy
	ITBPRP	101	tabular function for TMP
MPMAT00303	PROP	CPS	specific heat vs temperature
	ITBPRP	102	tabular function for CPS
MPMAT00304	PROP	THC	thermal conductivity vs temperature
	ITBPRP	103	tabular function for THC
MPMAT00305	PROP	RHO	density vs temperature
	ITBPRP	104	tabular function for RHO
MPMAT00350	PROP	DEN	constant density

	ITBPRP	1831.9	density of homogeous fuel compacts
MPMAT00351	PROP	MLT	melting temperature
	ITBPRP	2900.0	mimimum of MLT-UO2 and MLT-GRAPHITE, which is MLT-UO2; [5] p.530/776 Vol. 2
MPMAT00352	PROP	LHF	latent heat of fusion
	ITBPRP	1.0E3	unused in calculation

TF100			enthalpy as a function of temperature; calculated using the definition of enthalpy used in MELCOR, h = Cp (T − 300K); p.MP-RM-11 of [5]
TF101			inverse of TF100
TF102			specific heat assumed to be constant, 1725.0 W/m K; based on p.661, Table 4 of [10]
TF103			thermal conductivity assumed to be constant, 20.0 J/kg K; based on p.661, Table 4 of [10]
TF104			density assumed to be constant; see DEN
MPMAT00400	MATNAM		’ ZIRCALOY’; redefine the

		properties of ZIRCALOY as those of graphite block using material 004

Properties redefined for Zircaloy calculated using methods similar to those used for Inconel

MPMAT00500	MATNAM	’ STAINLESS-STEEL’; redefine the properties of STAINLESS-STEEL as those of graphite block using material 005

Table A.53

Helium: Density vs. Temperature

Temperature (K)	Density (kg/m3)
700.0	4.757
800.0	4.169
900.0	3.711
1000.0	3.343
1100.0	3.042
1200.0	2.79
1300.0	2.577
1400.0	2.394
1500.0	2.235

Table A.54

Helium: Specific Heat vs. Temperature

Temperature (K)	Specific heat (J/kg K)
700.0	5188.0
800.0	5189.0
900.0	5189.0
1000.0	5190.0
1100.0	5190.0
1200.0	5190.0
1300.0	5191.0
1400.0	5191.0
1500.0	5191.0

Table A.55

Helium: Thermal Conductivity vs. Temperature

Temperature (K)	Thermal conductivity (W/m K)
700.0	0.2847
800.0	0.3121
900.0	0.3385
1000.0	0.364
1100.0	0.3888
1200.0	0.413
1300.0	0.4365
1400.0	0.4596
1500.0	0.4821

Table A.56

Oxygen: Density vs. Temperature

Temperature (K)	Density (kg/m3)
200.00	1.764995923
316.00	1.117086027
400.00	0.882497961
600.00	0.588331974
800.00	0.441248981
1000.00	0.352999185

[5]: page no. 581/776

Molecular weight (kg/mol)	0.028966
Pressure (Pa)	101325
Universal gas constant (J/mol*k)	8.31441
Compressibility	1.0

Rho = MW * Pres / (R * T * CPRS)

Table A.57

Oxygen: Specific Heat vs. Temperature

Temperature (K)	Specific heat (J/kg K)
300.00	1007.0
1000.00	1141.0
1500.00	1230.0

Table A.58

Oxygen: Thermal Conductivity vs. Temperature

Temperature (K)	Thermal conductivity (W/m K)
255.370	0.0227081
310.926	0.0270005
366.482	0.0311544
422.038	0.0360006
477.594	0.0399815
533.150	0.0425777
588.706	0.0458662

Table A.59

Graphite: Specific Heat vs. Temperature

Temperature (K)	Specific heat (J/kg K)
750.0	1599.4
800.0	1645.4
850.0	1683.1
900.0	1712.4
950.0	1737.5
1000.0	1762.6
1100.0	1808.7
1200.0	1854.7
1300.0	1892.4
1400.0	1925.9
1500.0	1959.4
1600.0	1984.5

Table A.60

Graphite: Thermal Conductivity vs. Temperature

Temperature (K)	Thermal conductivity (W/m K)
673.0	75.6
773.0	70.0
800.0	69.6
900.0	64.0
1000.0	59.3
1100.0	55.4
1200.0	52.0
1300.0	49.1
1400.0	46.6
1500.0	44.3
1600.0	42.3

A.6 src snk.gen

CARD	WORD	VALUE	BASIS
FL19000	FLNAME	SOURCEtoINLET	
	KCVFM	190	from time-independent source
	VCVTO	160	to helium upriser
	ZFM	-2.9145	center elevation of the source
	ZTO	-0.7925	center elevation of the bottom most CVH in the helium upriser
FL19001	FLARA	2.0587	based on the total flow area in the active core

	FLLEN	2.122	distance between centers of control volumes
	FLOPO	1.0	flow path is open
FL19002	KFLGFL	0	normal vertical flow path
	KACTFL	0	active flow path
	IBUBF	0	no bubble rise physics
	IBUBT	0	no bubble rise physics
FL190S1	SAREA	2.0587	see FLARA
	SLEN	2.122	see FLLEN
	SHYD	0.344	hydraulic diameter of helium upriser
FL190T1	NTFLAG	2	use control function number NFUN to define velocity versus time
	NFUN	200	control function number
FL20000	FLNAME		OUTLETToSINK
	KCVFM	054	from lower plenum
	VCVTO	200	to time-independent sink
	ZFM	-2.9145	center altitude of lower plenum
	ZTO	-2.9145	see ZFM
FL20001	FLARA	3.661	flow area of outlet
	FLLEN	3.3633	distance between centers of control volumes
	FLOPO	1.0	flow path is open
FL20002	KFLGFL	3	normal horizontal flow path

	KACTFL	0	active flow path
	IBUBF	0	no bubble rise physics
	IBUBT	0	no bubble rise physics
FL200S1	SAREA	3.661	see FLARA
	SLEN	3.3633	see FLLEN
	SHYD	2.159	hydraulic diameter of helium outlet
CV19000	CVNAME	SOURCE	control volume name
	ICVTHR	2	use nonequilibrium thermodynamics; recommended option
	ICVFF	0	not used
	ICVTYP	4	CV type SRC
CV19001	IPFSW	0	pool, fog allowed; default value
	ICVACT	-1	time-independent
CV190A0	ITYPTH	3	type of thermodynamic input; separate pool and atmosphere input; default value
CV190A1	MLFR.4	1.0	mass fraction of material 4, helium; all mass in CVH is helium
	TATM	764.0	initial temp. of helium in CV nnn; reactor inlet temp.
	PVOL	7.12e6	time-independent pressure at reactor inlet
	PH20	0.0	partial pressure of water vapor in atmosphere; no water vapor atmosphere
CV190B0	-3.994	0.0	user-defined volume table

CV190B1	-1.835	0.775208605	
CV20000	CVNAME	SINK	control volume name
	ICVTHR	2	use nonequilibrium thermodynamics; recommended option
	ICVFF	0	not used
	ICVTYP	5	CV type SNK
CV20001	IPFSW	0	pool, fog allowed; default value
	ICVACT	-1	time-independent
CV200A0	ITYPTH	3	type of thermodynamic input; separate pool and atmosphere input; default value
CV200A1	MLFR.4	1.0	mass fraction of material 4, helium; all mass in CVH is helium
	TATM	1123.0	in Table 11, p.70 [2]
	PVOL	7.014e6	time-independent pressure at reactor outlet
	PH20	0.0	partial pressure of water vapor in atmosphere; no water vapor atmosphere
CV200B0	-3.994	0.0	user-defined volume table
CV200B1	-1.835	0.278965269	

A.2 Input decks

A.2.1 mmgen.in

```
* sample MELGEN input file for blowdown test case *
*
TITLE     'bldwn'
JOBID     'bldwn'

*MELGEN output files
DIAGF     'bldwng.dia'
OUTPUTF   'bldwng.out'
RESTARTF  'bldwn.rst'

*Initialize problem
TSTART       0.0
DTTIME       1.0

*MELGEN input files

R*I*F      'cvh-fl-hs-new.gen'
R*I*F      'core-new-2.gen'
R*I*F      'ncg-mp-new.gen'
.
```

A.2.2 mmcor.in

```
* sample MELCOR input file for blowdown test case *
TITLE     'bldwn'
```

```
JOBID     'bldwn'

*MELCOR output files
DIAGF     'bldwn.dia'
MESSAGEF  'bldwn.mes'
OUTPUTF   'bldwn.out'
PLOTF     'bldwn.ptf'
RESTARTF  'bldwn.rst'
STOPF     'bldwn.stp'

*Time-step definitions
*          TIME    DTMAX   DTMIN    DTEDT   DTPLT   DTRST
TIME3       0.0     0.5    1.0e-4    600.0    2.0    200.0
TIME4     120.0     0.5    1.0e-4   3600.0   10.0    200.0

CYMESF     500     1
SOFTDTMIN  1.0e-4  500

*SOFTDTMIN  1.0e-5  500

*Problem time constraints
TEND       10000.
CPULIM     100000.
CPULEFT    30.
RESTART    -1
.
```

A.2.3 cvh-fl-hs-new.gen

```
*CV type definitions
CVTYPE01 CORCVH
CVTYPE02 upv
CVTYPE03 cehgp
CVTYPE04 SRC
CVTYPE05 SNK
CVTYPE06 cavity

*upper plenum volume
CV28000 upv 2 0 2
CV28001 0 0
CV280A0 3
CV280A1 MLFR.4 1.0 TATM 764.0 PVOL 7.07e6 PH2O 0.0
CV280B0 9.119 0.0
CV280B1 9.219 3.473644813
CV280B2 9.624 17.54190631
CV280B3 10.029 31.6101678
CV280B4 10.434 45.67842929
CV280B5 10.839 59.74669078
CV280B6 11.244 73.81495228
CV280B7 11.649 87.88321377

*core exit hot gas plenum
CV05400   cehgp 2 0 3
CV05401   0 0
CV054A0   3
CV054A1   MLFR.4 1.0 TATM 764.0 PVOL 7.019e6 PH2O 0.0
CV054B0   -3.994   0.0
CV054B1   -3.5622  14.9992
```

```
CV054B2   -3.1304  29.9984
CV054B3   -2.6986  44.99759
CV054B4   -2.2668  59.99679
CV054B5   -1.835   74.99599
CV054B6   -1.585   83.68010355

*cavity
CV05000   cavity 2 0 6
CV05001   0 0
CV050A0   3
CV050A1   MLFR.4 1.0 TATM 764.0 PVOL 7.019e6 PH2O 0.0
CV050B0   -3.994   0.0
CV050B1   -3.5622  135.6539708
CV050B2   -3.1304  271.3079416
CV050B3   -2.6986  406.9619123
CV050B4   -2.2668  542.6158831
CV050B5   -1.835   678.2698539
CV050B6   -1.585   756.8096702

**********
* CVH cells for the core
**********
*Ring 1
CV11000   COR110  2  0  1
CV11001   0  0
CV110A0   3
CV110A1   MLFR.4  1.0  TATM  764.0  PVOL  7.025375e6  PH2O  0.0
CV110B0   -1.585   0.0
CV110B1   -1.18875  2.712905984
```

```
CV110B2   -0.7925  5.425811967
CV110B3   -0.39625  8.138717951
CV110B4   0.0  10.85162393

CV11100   COR111  2  0  1
CV11101   0  0
CV111A0   3
CV111A1   MLFR.4  1.0  TATM  764.0  PVOL  7.03175e6  PH2O  0.0
CV111B0   0.0   0.0
CV111B1   0.3965   2.714617596
CV111B2   0.793    5.429235193
CV111B3   1.1895   8.143852789
CV111B4   1.586    10.85847039

CV11200   COR112  2  0  1
CV11201   0  0
CV112A0   3
CV112A1   MLFR.4  1.0  TATM  764.0  PVOL  7.038125e6  PH2O  0.0
CV112B0   1.586   0.0
CV112B1   1.9825  2.714617596
CV112B2   2.379   5.429235193
CV112B3   2.7755  8.143852789
CV112B4   3.172   10.85847039

CV11300   COR113  2  0  1
CV11301   0  0
CV113A0   3
CV113A1   MLFR.4  1.0  TATM  764.0  PVOL  7.0445e6  PH2O  0.0
CV113B0   3.172    0.0
```

```
CV113B1   3.5685   2.714617596
CV113B2   3.965    5.429235193
CV113B3   4.3615   8.143852789
CV113B4   4.758    10.85847039

CV11400   COR114  2  0  1
CV11401   0  0
CV114A0   3
CV114A1   MLFR.4  1.0  TATM  764.0  PVOL  7.050875e6  PH2O  0.0
CV114B0   4.758   0.0
CV114B1   5.1545  2.714617596
CV114B2   5.551   5.429235193
CV114B3   5.9475  8.143852789
CV114B4   6.344   10.85847039

CV11500   COR115  2  0  1
CV11501   0  0
CV115A0   3
CV115A1   MLFR.4  1.0  TATM  764.0  PVOL  7.05725e6  PH2O  0.0
CV115B0   6.344   0.0
CV115B1   6.7405  2.714617596
CV115B2   7.137   5.429235193
CV115B3   7.5335  8.143852789
CV115B4   7.93    10.85847039

CV11600   COR116  2  0  1
CV11601   0  0
CV116A0   3
CV116A1   MLFR.4  1.0  TATM  764.0  PVOL  7.063625e6  PH2O  0.0
```

CV116B0 7.93 0.0

CV116B1 8.3263 2.713248306

CV116B2 8.7226 5.426496612

CV116B3 9.119 8.140429564

*Ring 2

CV12000 COR120 2 0 1

CV12001 0 0

CV120A0 3

CV120A1 MLFR.4 1.0 TATM 764.0 PVOL 7.025375e6 PH2O 0.0

CV120B0 -1.585 0.0

CV120B1 -1.18875 1.334216058

CV120B2 -0.7925 2.668432115

CV120B3 -0.39625 4.002648173

CV120B4 0.0 5.33686423

CV12100 COR121 2 0 1

CV12101 0 0

CV121A0 3

CV121A1 MLFR.4 1.0 TATM 764.0 PVOL 7.03175e6 PH2O 0.0

CV121B0 0.0 0.0

CV121B1 0.3965 1.335057834

CV121B2 0.793 2.670115669

CV121B3 1.1895 4.005173503

CV121B4 1.586 5.340231337

CV12200 COR122 2 0 1

CV12201 0 0

CV122A0 3

CV122A1 MLFR.4 1.0 TATM 764.0 PVOL 7.038125e6 PH2O 0.0
CV122B0 1.586 0.0
CV122B1 1.9825 1.335057834
CV122B2 2.379 2.670115669
CV122B3 2.7755 4.005173503
CV122B4 3.172 5.340231337

CV12300 COR123 2 0 1
CV12301 0 0
CV123A0 3
CV123A1 MLFR.4 1.0 TATM 764.0 PVOL 7.0445e6 PH2O 0.0
CV123B0 3.172 0.0
CV123B1 3.5685 1.335057834
CV123B2 3.965 2.670115669
CV123B3 4.3615 4.005173503
CV123B4 4.758 5.340231337

CV12400 COR124 2 0 1
CV12401 0 0
CV124A0 3
CV124A1 MLFR.4 1.0 TATM 764.0 PVOL 7.050875e6 PH2O 0.0
CV124B0 4.758 0.0
CV124B1 5.1545 1.335057834
CV124B2 5.551 2.670115669
CV124B3 5.9475 4.005173503
CV124B4 6.344 5.340231337

CV12500 COR125 2 0 1
CV12501 0 0

```
CV125A0   3
CV125A1   MLFR.4  1.0  TATM  764.0  PVOL  7.05725e6  PH2O  0.0
CV125B0   6.344   0.0
CV125B1   6.7405  1.335057834
CV125B2   7.137   2.670115669
CV125B3   7.5335  4.005173503
CV125B4   7.93    5.340231337

CV12600   COR126  2  0  1
CV12601   0  0
CV126A0   3
CV126A1   MLFR.4  1.0  TATM  764.0  PVOL  7.063625e6  PH2O  0.0
CV126B0   7.93   0.0
CV126B1   8.3263  1.334384413
CV126B2   8.7226  2.668768826
CV126B3   9.119  4.00348995

*Ring 3
CV13000   COR130  2  0  1
CV13001   0  0
CV130A0   3
CV130A1   MLFR.4  1.0  TATM  764.0  PVOL  7.025375e6  PH2O  0.0
CV130B0   -1.585   0.0
CV130B1   -1.18875   1.601059269
CV130B2   -0.7925  3.202118538
CV130B3   -0.39625  4.803177807
CV130B4   0.0  6.404237077

CV13100   COR131  2  0  1
```

```
CV13101   0  0
CV131A0   3
CV131A1   MLFR.4  1.0  TATM  764.0  PVOL  7.03175e6  PH2O  0.0
CV131B0   0.0   0.0
CV131B1   0.3965  1.602069401
CV131B2   0.793   3.204138802
CV131B3   1.1895  4.806208203
CV131B4   1.586   6.408277605

CV13200   COR132  2  0  1
CV13201   0  0
CV132A0   3
CV132A1   MLFR.4  1.0  TATM  764.0  PVOL  7.038125e6  PH2O  0.0
CV132B0   1.586   0.0
CV132B1   1.9825  1.602069401
CV132B2   2.379   3.204138802
CV132B3   2.7755  4.806208203
CV132B4   3.172   6.408277605

CV13300   COR133  2  0  1
CV13301   0  0
CV133A0   3
CV133A1   MLFR.4  1.0  TATM  764.0  PVOL  7.0445e6  PH2O  0.0
CV133B0   3.172   0.0
CV133B1   3.5685  1.602069401
CV133B2   3.965   3.204138802
CV133B3   4.3615  4.806208203
CV133B4   4.758   6.408277605
```

CV13400 COR134 2 0 1

CV13401 0 0

CV134A0 3

CV134A1 MLFR.4 1.0 TATM 764.0 PVOL 7.050875e6 PH2O 0.0

CV134B0 4.758 0.0

CV134B1 5.1545 1.602069401

CV134B2 5.551 3.204138802

CV134B3 5.9475 4.806208203

CV134B4 6.344 6.408277605

CV13500 COR135 2 0 1

CV13501 0 0

CV135A0 3

CV135A1 MLFR.4 1.0 TATM 764.0 PVOL 7.05725e6 PH2O 0.0

CV135B0 6.344 0.0

CV135B1 6.7405 1.602069401

CV135B2 7.137 3.204138802

CV135B3 7.5335 4.806208203

CV135B4 7.93 6.408277605

CV13600 COR136 2 0 1

CV13601 0 0

CV136A0 3

CV136A1 MLFR.4 1.0 TATM 764.0 PVOL 7.063625e6 PH2O 0.0

CV136B0 7.93 0.0

CV136B1 8.3263 1.601261296

CV136B2 8.7226 3.202522591

CV136B3 9.119 4.804187939

```
*Ring 4
CV14000   COR140  2  0  1
CV14001   0  0
CV140A0   3
CV140A1   MLFR.4  1.0  TATM  764.0  PVOL  7.025375e6  PH2O  0.0
CV140B0   -1.585   0.0
CV140B1   -1.18875  1.640085256
CV140B2   -0.7925  3.280170511
CV140B3   -0.39625  4.920255767
CV140B4   0.0  6.560341023

CV14100   COR141  2  0  1
CV14101   0  0
CV141A0   3
CV141A1   MLFR.4  1.0  TATM  764.0  PVOL  7.03175e6  PH2O  0.0
CV141B0   0.0   0.0
CV141B1   0.3965  1.64112001
CV141B2   0.793   3.282240019
CV141B3   1.1895  4.923360029
CV141B4   1.586   6.564480039

CV14200   COR142  2  0  1
CV14201   0  0
CV142A0   3
CV142A1   MLFR.4  1.0  TATM  764.0  PVOL  7.038125e6  PH2O  0.0
CV142B0   1.586   0.0
CV142B1   1.9825  1.64112001
CV142B2   2.379   3.282240019
CV142B3   2.7755  4.923360029
```

```
CV142B4   3.172   6.564480039

CV14300   COR143  2  0  1
CV14301   0  0
CV143A0   3
CV143A1   MLFR.4  1.0  TATM  764.0  PVOL  7.0445e6  PH2O  0.0
CV143B0   3.172   0.0
CV143B1   3.5685  1.64112001
CV143B2   3.965   3.282240019
CV143B3   4.3615  4.923360029
CV143B4   4.758   6.564480039

CV14400   COR144  2  0  1
CV14401   0  0
CV144A0   3
CV144A1   MLFR.4  1.0  TATM  764.0  PVOL  7.050875e6  PH2O  0.0
CV144B0   4.758   0.0
CV144B1   5.1545  1.64112001
CV144B2   5.551   3.282240019
CV144B3   5.9475  4.923360029
CV144B4   6.344   6.564480039

CV14500   COR145  2  0  1
CV14501   0  0
CV145A0   3
CV145A1   MLFR.4  1.0  TATM  764.0  PVOL  7.05725e6  PH2O  0.0
CV145B0   6.344   0.0
CV145B1   6.7405  1.64112001
CV145B2   7.137   3.282240019
```

CV145B3 7.5335 4.923360029
CV145B4 7.93 6.564480039

CV14600 COR146 2 0 1
CV14601 0 0
CV146A0 3
CV146A1 MLFR.4 1.0 TATM 764.0 PVOL 7.063625e6 PH2O 0.0
CV146B0 7.93 0.0
CV146B1 8.3263 1.640292206
CV146B2 8.7226 3.280584413
CV146B3 9.119 4.921290521

*Ring 5
CV15000 COR150 2 0 1
CV15001 0 0
CV150A0 3
CV150A1 MLFR.4 1.0 TATM 764.0 PVOL 7.025375e6 PH2O 0.0
CV150B0 -1.585 0.0
CV150B1 -1.18875 6.476051131
CV150B2 -0.7925 12.95210226
CV150B3 -0.39625 19.42815339
CV150B4 0.0 25.90420452

CV15100 COR151 2 0 1
CV15101 0 0
CV151A0 3
CV151A1 MLFR.4 1.0 TATM 764.0 PVOL 7.03175e6 PH2O 0.0
CV151B0 0.0 0.0
CV151B1 0.3965 6.480136968

```
CV151B2   0.793   12.96027394
CV151B3   1.1895  19.4404109
CV151B4   1.586   25.92054787

CV15200   COR152  2  0  1
CV15201   0  0
CV152A0   3
CV152A1   MLFR.4  1.0  TATM  764.0  PVOL  7.038125e6  PH2O  0.0
CV152B0   1.586   0.0
CV152B1   1.9825  6.480136968
CV152B2   2.379   12.96027394
CV152B3   2.7755  19.4404109
CV152B4   3.172   25.92054787

CV15300   COR153  2  0  1
CV15301   0  0
CV153A0   3
CV153A1   MLFR.4  1.0  TATM  764.0  PVOL  7.0445e6  PH2O  0.0
CV153B0   3.172   0.0
CV153B1   3.5685  6.480136968
CV153B2   3.965   12.96027394
CV153B3   4.3615  19.4404109
CV153B4   4.758   25.92054787

CV15400   COR154  2  0  1
CV15401   0  0
CV154A0   3
CV154A1   MLFR.4  1.0  TATM  764.0  PVOL  7.050875e6  PH2O  0.0
CV154B0   4.758   0.0
```

```
CV154B1   5.1545  6.480136968
CV154B2   5.551   12.96027394
CV154B3   5.9475  19.4404109
CV154B4   6.344   25.92054787

CV15500   COR155  2  0  1
CV15501   0  0
CV155A0   3
CV155A1   MLFR.4  1.0  TATM  764.0  PVOL  7.05725e6  PH2O  0.0
CV155B0   6.344   0.0
CV155B1   6.7405  6.480136968
CV155B2   7.137   12.96027394
CV155B3   7.5335  19.4404109
CV155B4   7.93    25.92054787

CV15600   COR156  2  0  1
CV15601   0  0
CV156A0   3
CV156A1   MLFR.4  1.0  TATM  764.0  PVOL  7.063625e6  PH2O  0.0
CV156B0   7.93   0.0
CV156B1   8.3263  6.476868298
CV156B2   8.7226  12.9537366
CV156B3   9.119  19.43223923

**********
* CVH cells for the helium inlet
**********
CV16000   inlet160  2  0  1
CV16001   0  0
```

CV160A0 3
CV160A1 MLFR.4 1.0 TATM 764.0 PVOL 7.115e6 PH2O 0.0
CV160B0 -1.585 0.0
CV160B1 -1.18875 0.815772056
CV160B2 -0.7925 1.631544111
CV160B3 -0.39625 2.447316167
CV160B4 0.0 3.263088222

CV16100 inlet161 2 0 1
CV16101 0 0
CV161A0 3
CV161A1 MLFR.4 1.0 TATM 764.0 PVOL 7.11e6 PH2O 0.0
CV161B0 0.0 0.0
CV161B1 0.3965 0.816286738
CV161B2 0.793 1.632573476
CV161B3 1.1895 2.448860215
CV161B4 1.586 3.265146953

CV16200 inlet162 2 0 1
CV16201 0 0
CV162A0 3
CV162A1 MLFR.4 1.0 TATM 764.0 PVOL 7.105e6 PH2O 0.0
CV162B0 1.586 0.0
CV162B1 1.9825 0.816286738
CV162B2 2.379 1.632573476
CV162B3 2.7755 2.448860215
CV162B4 3.172 3.265146953

CV16300 inlet163 2 0 1

```
CV16301   0  0
CV163A0   3
CV163A1   MLFR.4  1.0  TATM  764.0  PVOL  7.1e6  PH2O  0.0
CV163B0   3.172   0.0
CV163B1   3.5685  0.816286738
CV163B2   3.965   1.632573476
CV163B3   4.3615  2.448860215
CV163B4   4.758   3.265146953

CV16400   inlet164  2  0  1
CV16401   0  0
CV164A0   3
CV164A1   MLFR.4  1.0  TATM  764.0  PVOL  7.095e6  PH2O  0.0
CV164B0   4.758   0.0
CV164B1   5.1545  0.816286738
CV164B2   5.551   1.632573476
CV164B3   5.9475  2.448860215
CV164B4   6.344   3.265146953

CV16500   inlet165  2  0  1
CV16501   0  0
CV165A0   3
CV165A1   MLFR.4  1.0  TATM  764.0  PVOL  7.09e6  PH2O  0.0
CV165B0   6.344   0.0
CV165B1   6.7405  0.816286738
CV165B2   7.137   1.632573476
CV165B3   7.5335  2.448860215
CV165B4   7.93    3.265146953
```

CV16600 inlet166 2 0 1

CV16601 0 0

CV166A0 3

CV166A1 MLFR.4 1.0 TATM 764.0 PVOL 7.085e6 PH2O 0.0

CV166B0 7.93 0.0

CV166B1 8.3263 0.815874992

CV166B2 8.7226 1.631749984

CV166B3 9.119 2.447830849

****

* Axial downward core flowpaths

****

*Ring 1

FL11700 CoreRingF80-T16 280 116 9.119 9.119

FL11701 0.123523844 1.8595 1.0

FL11702 0 0 0 0

FL117S1 0.123523844 1.8595 0.01588

FL11600 CoreRingF16-T15 116 115 7.93 7.93

FL11601 0.123523844 1.3875 1.0

FL11602 0 0 0 0

FL116S1 0.123523844 1.3875 0.01588

FL11500 CoreRingF15-T14 115 114 6.344 6.344

FL11501 0.123523844 1.586 1.0

FL11502 0 0 0 0

FL115S1 0.123523844 1.586 0.01588

FL11400 CoreRingF14-T13 114 113 4.758 4.758

FL11401 0.123523844 1.586 1.0

FL11402 0 0 0 0

FL114S1 0.123523844 1.586 0.01588

FL11300 CoreRingF13-T12 113 112 3.172 3.172

FL11301 0.123523844 1.586 1.0

FL11302 0 0 0 0

FL113S1 0.123523844 1.586 0.01588

FL11200 CoreRingF12-T11 112 111 1.586 1.586

FL11201 0.123523844 1.586 1.0

FL11202 0 0 0 0

FL112S1 0.123523844 1.586 0.01588

FL11100 CoreRingF11-T10 111 110 0.0 0.0

FL11101 0.123523844 1.5855 1.0

FL11102 0 0 0 0

FL111S1 0.123523844 1.5855 0.01588

FL11000 CoreRingF10-T54 110 54 -1.585 -1.585

FL11001 0.123523844 1.997 1.0

FL11002 0 0 0 0

FL110S1 0.123523844 1.997 0.01588

*Ring 2

FL12700 CoreRingF80-T26 280 126 9.119 9.119

FL12701 0.597103701 1.8595 1.0

FL12702 0 0 0 0

FL127S1 0.597103701 1.8595 0.01588

FL12600 CoreRingF26-T25 126 125 7.93 7.93

FL12601 0.597103701 1.3875 1.0

FL12602 0 0 0 0

FL126S1 0.597103701 1.3875 0.01588

FL12500 CoreRingF25-T24 125 124 6.344 6.344

FL12501 0.597103701 1.586 1.0

FL12502 0 0 0 0

FL125S1 0.597103701 1.586 0.01588

FL12400 CoreRingF24-T23 124 123 4.758 4.758

FL12401 0.597103701 1.586 1.0

FL12402 0 0 0 0

FL124S1 0.597103701 1.586 0.01588

FL12300 CoreRingF23-T22 123 122 3.172 3.172

FL12301 0.597103701 1.586 1.0

FL12302 0 0 0 0

FL123S1 0.597103701 1.586 0.01588

FL12200 CoreRingF22-T21 122 121 1.586 1.586

FL12201 0.597103701 1.586 1.0

FL12202 0 0 0 0

FL122S1 0.597103701 1.586 0.01588

FL12100 CoreRingF21-T20 121 120 0.0 0.0

FL12101 0.597103701 1.5855 1.0

FL12102 0 0 0 0

FL121S1 0.597103701 1.5855 0.01588

FL12000 CoreRingF20-T54 120 54 -1.585 -1.585
FL12001 0.597103701 1.997 1.0
FL12002 0 0 0 0
FL120S1 0.597103701 1.997 0.01588

*Ring 3
FL13700 CoreRingF80-T36 280 136 9.119 9.119
FL13701 0.738751896 1.8595 1.0
FL13702 0 0 0 0
FL137S1 0.738751896 1.8595 0.01588

FL13600 CoreRingF36-T35 136 135 7.93 7.93
FL13601 0.738751896 1.3875 1.0
FL13602 0 0 0 0
FL136S1 0.738751896 1.3875 0.01588

FL13500 CoreRingF35-T34 135 134 6.344 6.344
FL13501 0.738751896 1.586 1.0
FL13502 0 0 0 0
FL135S1 0.738751896 1.586 0.01588

FL13400 CoreRingF34-T33 134 133 4.758 4.758
FL13401 0.738751896 1.586 1.0
FL13402 0 0 0 0
FL134S1 0.738751896 1.586 0.01588

FL13300 CoreRingF33-T32 133 132 3.172 3.172

FL13301 0.738751896 1.586 1.0

FL13302 0 0 0 0

FL133S1 0.738751896 1.586 0.01588

FL13200 CoreRingF32-T31 132 131 1.586 1.586

FL13201 0.738751896 1.586 1.0

FL13202 0 0 0 0

FL132S1 0.738751896 1.586 0.01588

FL13100 CoreRingF31-T30 131 130 0.0 0.0

FL13101 0.738751896 1.5855 1.0

FL13102 0 0 0 0

FL131S1 0.738751896 1.5855 0.01588

FL13000 CoreRingF30-T54 130 54 -1.585 -1.585

FL13001 0.738751896 1.997 1.0

FL13002 0 0 0 0

FL130S1 0.738751896 1.997 0.01588

*Ring 4

FL14700 CoreRingF80-T46 280 146 9.119 9.119

FL14701 0.722875143 1.8595 1.0

FL14702 0 0 0 0

FL147S1 0.722875143 1.8595 0.01588

FL14600 CoreRingF46-T45 146 145 7.93 7.93

FL14601 0.722875143 1.3875 1.0

FL14602 0 0 0 0

FL146S1 0.722875143 1.3875 0.01588

FL14500 CoreRingF45-T44 145 144 6.344 6.344

FL14501 0.722875143 1.586 1.0

FL14502 0 0 0 0

FL145S1 0.722875143 1.586 0.01588

FL14400 CoreRingF44-T43 144 143 4.758 4.758

FL14401 0.722875143 1.586 1.0

FL14402 0 0 0 0

FL144S1 0.722875143 1.586 0.01588

FL14300 CoreRingF43-T42 143 142 3.172 3.172

FL14301 0.722875143 1.586 1.0

FL14302 0 0 0 0

FL143S1 0.722875143 1.586 0.01588

FL14200 CoreRingF42-T41 142 141 1.586 1.586

FL14201 0.722875143 1.586 1.0

FL14202 0 0 0 0

FL142S1 0.722875143 1.586 0.01588

FL14100 CoreRingF41-T40 141 140 0.0 0.0

FL14101 0.722875143 1.5855 1.0

FL14102 0 0 0 0

FL141S1 0.722875143 1.5855 0.01588

FL14000 CoreRingF40-T54 140 54 -1.585 -1.585

FL14001 0.722875143 1.997 1.0

FL14002 0 0 0 0

FL140S1 0.722875143 1.997 0.01588

*Ring 5
FL15700 CoreRingF80-T56 280 156 9.119 9.119
FL15701 0.288222304 1.8595 1.0
FL15702 0 0 0 0
FL157S1 0.288222304 1.8595 0.01588

FL15600 CoreRingF56-T55 156 155 7.93 7.93
FL15601 0.288222304 1.3875 1.0
FL15602 0 0 0 0
FL156S1 0.288222304 1.3875 0.01588

FL15500 CoreRingF55-T54 155 154 6.344 6.344
FL15501 0.288222304 1.586 1.0
FL15502 0 0 0 0
FL155S1 0.288222304 1.586 0.01588

FL15400 CoreRingF54-T53 154 153 4.758 4.758
FL15401 0.288222304 1.586 1.0
FL15402 0 0 0 0
FL154S1 0.288222304 1.586 0.01588

FL15300 CoreRingF53-T52 153 152 3.172 3.172
FL15301 0.288222304 1.586 1.0
FL15302 0 0 0 0
FL153S1 0.288222304 1.586 0.01588

FL15200 CoreRingF52-T51 152 151 1.586 1.586

FL15201 0.288222304 1.586 1.0

FL15202 0 0 0 0

FL152S1 0.288222304 1.586 0.01588

FL15100 CoreRingF51-T50 151 150 0.0 0.0

FL15101 0.288222304 1.5855 1.0

FL15102 0 0 0 0

FL151S1 0.288222304 1.5855 0.01588

FL15000 CoreRingF50-T54 150 54 -1.585 -1.585

FL15001 0.288222304 1.997 1.0

FL15002 0 0 0 0

FL150S1 0.288222304 1.997 0.01588

*Form loss coefficient

FL11703 1.2 1.2 1.0 1.0

FL11603 1.2 1.2 1.0 1.0

FL11503 1.2 1.2 1.0 1.0

FL11403 1.2 1.2 1.0 1.0

FL11303 1.2 1.2 1.0 1.0

FL11203 1.2 1.2 1.0 1.0

FL11103 1.2 1.2 1.0 1.0

FL11003 1.2 1.2 1.0 1.0

FL12703 1.2 1.2 1.0 1.0

FL12603 1.2 1.2 1.0 1.0

FL12503 1.2 1.2 1.0 1.0

FL12403 1.2 1.2 1.0 1.0

FL12303 1.2 1.2 1.0 1.0

FL12203 1.2 1.2 1.0 1.0
FL12103 1.2 1.2 1.0 1.0
FL12003 1.2 1.2 1.0 1.0

FL13703 1.2 1.2 1.0 1.0
FL13603 1.2 1.2 1.0 1.0
FL13503 1.2 1.2 1.0 1.0
FL13403 1.2 1.2 1.0 1.0
FL13303 1.2 1.2 1.0 1.0
FL13203 1.2 1.2 1.0 1.0
FL13103 1.2 1.2 1.0 1.0
FL13003 1.2 1.2 1.0 1.0

FL14703 1.2 1.2 1.0 1.0
FL14603 1.2 1.2 1.0 1.0
FL14503 1.2 1.2 1.0 1.0
FL14403 1.2 1.2 1.0 1.0
FL14303 1.2 1.2 1.0 1.0
FL14203 1.2 1.2 1.0 1.0
FL14103 1.2 1.2 1.0 1.0
FL14003 1.2 1.2 1.0 1.0

FL15703 1.2 1.2 1.0 1.0
FL15603 1.2 1.2 1.0 1.0
FL15503 1.2 1.2 1.0 1.0
FL15403 1.2 1.2 1.0 1.0
FL15303 1.2 1.2 1.0 1.0
FL15203 1.2 1.2 1.0 1.0
FL15103 1.2 1.2 1.0 1.0

FL15003 1.2 1.2 1.0 1.0

FL16703 1.2 1.2 1.0 1.0
FL16603 1.2 1.2 1.0 1.0
FL16503 1.2 1.2 1.0 1.0
FL16403 1.2 1.2 1.0 1.0
FL16303 1.2 1.2 1.0 1.0
FL16203 1.2 1.2 1.0 1.0
FL16103 1.2 1.2 1.0 1.0

****
* Radial core flowpaths
****
*no. 6
FL21600 CoreRingF26-T16 126 116 8.5245 8.5245
FL21601 0.013717842 0.90153705 1.0
FL21602 3 0 0 0
FL216S1 0.013717842 0.90153705 0.002

FL22600 CoreRingF36-T26 136 126 8.5245 8.5245
FL22601 0.016211996 0.326915712 1.0
FL22602 3 0 0 0
FL226S1 0.016211996 0.326915712 0.002

FL23600 CoreRingF46-T36 146 136 8.5245 8.5245
FL23601 0.014964919 0.308287947 1.0
FL23602 3 0 0 0
FL236S1 0.014964919 0.308287947 0.002

FL24600 CoreRingF56-T46 156 146 8.5245 8.5245

FL24601 0.017459072 0.597562879 1.0

FL24602 3 0 0 0

FL246S1 0.017459072 0.597562879 0.002

FL25600 CoreRingF56-T36 156 136 8.5245 8.5245

FL25601 0.001247077 0.761062947 1.0

FL25602 3 0 0 0

FL256S1 0.001247077 0.761062947 0.002

*no. 5

FL21500 CoreRingF25-T15 125 115 7.137 7.137

FL21501 0.013717842 0.90153705 1.0

FL21502 3 0 0 0

FL215S1 0.013717842 0.90153705 0.002

FL22500 CoreRingF35-T25 135 125 7.137 7.137

FL22501 0.016211996 0.326915712 1.0

FL22502 3 0 0 0

FL225S1 0.016211996 0.326915712 0.002

FL23500 CoreRingF45-T35 145 135 7.137 7.137

FL23501 0.014964919 0.308287947 1.0

FL23502 3 0 0 0

FL235S1 0.014964919 0.308287947 0.002

FL24500 CoreRingF55-T45 155 145 7.137 7.137

FL24501 0.017459072 0.597562879 1.0

FL24502 3 0 0 0

FL245S1 0.017459072 0.597562879 0.002

FL25500 CoreRingF55-T35 155 135 7.137 7.137
FL25501 0.001247077 0.761062947 1.0
FL25502 3 0 0 0
FL255S1 0.001247077 0.761062947 0.002

*no. 4
FL21400 CoreRingF24-T14 124 114 5.551 5.551
FL21401 0.013717842 0.90153705 1.0
FL21402 3 0 0 0
FL214S1 0.013717842 0.90153705 0.002

FL22400 CoreRingF34-T24 134 124 5.551 5.551
FL22401 0.016211996 0.326915712 1.0
FL22402 3 0 0 0
FL224S1 0.016211996 0.326915712 0.002

FL23400 CoreRingF44-T34 144 134 5.551 5.551
FL23401 0.014964919 0.308287947 1.0
FL23402 3 0 0 0
FL234S1 0.014964919 0.308287947 0.002

FL24400 CoreRingF54-T44 154 144 5.551 5.551
FL24401 0.017459072 0.597562879 1.0
FL24402 3 0 0 0
FL244S1 0.017459072 0.597562879 0.002

FL25400 CoreRingF54-T34 154 134 5.551 5.551

FL25401 0.001247077 0.761062947 1.0

FL25402 3 0 0 0

FL254S1 0.001247077 0.761062947 0.002

*no. 3

FL21300 CoreRingF23-T13 123 113 3.965 3.965

FL21301 0.013717842 0.90153705 1.0

FL21302 3 0 0 0

FL213S1 0.013717842 0.90153705 0.002

FL22300 CoreRingF33-T23 133 123 3.965 3.965

FL22301 0.016211996 0.326915712 1.0

FL22302 3 0 0 0

FL223S1 0.016211996 0.326915712 0.002

FL23300 CoreRingF43-T33 143 133 3.965 3.965

FL23301 0.014964919 0.308287947 1.0

FL23302 3 0 0 0

FL233S1 0.014964919 0.308287947 0.002

FL24300 CoreRingF53-T43 153 143 3.965 3.965

FL24301 0.017459072 0.597562879 1.0

FL24302 3 0 0 0

FL243S1 0.017459072 0.597562879 0.002

FL25300 CoreRingF53-T33 153 133 3.965 3.965

FL25301 0.001247077 0.761062947 1.0

FL25302 3 0 0 0

FL253S1 0.001247077 0.761062947 0.002

*no. 2
FL21200 CoreRingF22-T12 122 112 2.379 2.379
FL21201 0.013717842 0.90153705 1.0
FL21202 3 0 0 0
FL212S1 0.013717842 0.90153705 0.002

FL22200 CoreRingF32-T22 132 122 2.379 2.379
FL22201 0.016211996 0.326915712 1.0
FL22202 3 0 0 0
FL222S1 0.016211996 0.326915712 0.002

FL23200 CoreRingF42-T32 142 132 2.379 2.379
FL23201 0.014964919 0.308287947 1.0
FL23202 3 0 0 0
FL232S1 0.014964919 0.308287947 0.002

FL24200 CoreRingF52-T42 152 142 2.379 2.379
FL24201 0.017459072 0.597562879 1.0
FL24202 3 0 0 0
FL242S1 0.017459072 0.597562879 0.002

FL25200 CoreRingF52-T32 152 132 2.379 2.379
FL25201 0.001247077 0.761062947 1.0
FL25202 3 0 0 0
FL252S1 0.001247077 0.761062947 0.002

*no. 1
FL21100 CoreRingF21-T11 121 111 0.793 0.793

FL21101 0.013717842 0.90153705 1.0

FL21102 3 0 0 0

FL211S1 0.013717842 0.90153705 0.002

FL22100 CoreRingF31-T21 131 121 0.793 0.793

FL22101 0.016211996 0.326915712 1.0

FL22102 3 0 0 0

FL221S1 0.016211996 0.326915712 0.002

FL23100 CoreRingF41-T31 141 131 0.793 0.793

FL23101 0.014964919 0.308287947 1.0

FL23102 3 0 0 0

FL231S1 0.014964919 0.308287947 0.002

FL24100 CoreRingF51-T41 151 141 0.793 0.793

FL24101 0.017459072 0.597562879 1.0

FL24102 3 0 0 0

FL241S1 0.017459072 0.597562879 0.002

FL25100 CoreRingF51-T31 151 131 0.793 0.793

FL25101 0.001247077 0.761062947 1.0

FL25102 3 0 0 0

FL251S1 0.001247077 0.761062947 0.002

*no. 0

FL21000 CoreRingF20-T10 120 110 -0.7925 -0.7925

FL21001 0.013717842 0.90153705 1.0

FL21002 3 0 0 0

FL210S1 0.013717842 0.90153705 0.002

FL22000 CoreRingF30-T20 130 120 -0.7925 -0.7925

FL22001 0.016211996 0.326915712 1.0

FL22002 3 0 0 0

FL220S1 0.016211996 0.326915712 0.002

FL23000 CoreRingF40-T30 140 130 -0.7925 -0.7925

FL23001 0.014964919 0.308287947 1.0

FL23002 3 0 0 0

FL230S1 0.014964919 0.308287947 0.002

FL24000 CoreRingF50-T40 150 140 -0.7925 -0.7925

FL24001 0.017459072 0.597562879 1.0

FL24002 3 0 0 0

FL240S1 0.017459072 0.597562879 0.002

FL25000 CoreRingF50-T30 150 130 -0.7925 -0.7925

FL25001 0.001247077 0.761062947 1.0

FL25002 3 0 0 0

FL250S1 0.001247077 0.761062947 0.002

*Form loss coefficient

FL21603 1.2 1.2 1.0 1.0

FL21503 1.2 1.2 1.0 1.0

FL21403 1.2 1.2 1.0 1.0

FL21303 1.2 1.2 1.0 1.0

FL21203 1.2 1.2 1.0 1.0

FL21103 1.2 1.2 1.0 1.0

FL21003 1.2 1.2 1.0 1.0

FL22603 1.2 1.2 1.0 1.0
FL22503 1.2 1.2 1.0 1.0
FL22403 1.2 1.2 1.0 1.0
FL22303 1.2 1.2 1.0 1.0
FL22203 1.2 1.2 1.0 1.0
FL22103 1.2 1.2 1.0 1.0
FL22003 1.2 1.2 1.0 1.0

FL23603 1.2 1.2 1.0 1.0
FL23503 1.2 1.2 1.0 1.0
FL23403 1.2 1.2 1.0 1.0
FL23303 1.2 1.2 1.0 1.0
FL23203 1.2 1.2 1.0 1.0
FL23103 1.2 1.2 1.0 1.0
FL23003 1.2 1.2 1.0 1.0

FL24603 1.2 1.2 1.0 1.0
FL24503 1.2 1.2 1.0 1.0
FL24403 1.2 1.2 1.0 1.0
FL24303 1.2 1.2 1.0 1.0
FL24203 1.2 1.2 1.0 1.0
FL24103 1.2 1.2 1.0 1.0
FL24003 1.2 1.2 1.0 1.0

FL25603 1.2 1.2 1.0 1.0
FL25503 1.2 1.2 1.0 1.0
FL25403 1.2 1.2 1.0 1.0
FL25303 1.2 1.2 1.0 1.0

FL25203 1.2 1.2 1.0 1.0

FL25103 1.2 1.2 1.0 1.0

FL25003 1.2 1.2 1.0 1.0

****

* Axial upward core flowpaths

****

FL16100 InletF60-T61 160 161 0.0 0.0

FL16101 2.05873074 1.5855 1.0

FL16102 0 0 0 0

FL161S1 2.05873074 1.5855 0.340

FL16200 InletF61-T62 161 162 1.586 1.586

FL16201 2.05873074 1.586 1.0

FL16202 0 0 0 0

FL162S1 2.05873074 1.586 0.340

FL16300 InletF62-T63 162 163 3.172 3.172

FL16301 2.05873074 1.586 1.0

FL16302 0 0 0 0

FL163S1 2.05873074 1.586 0.340

FL16400 InletF63-T64 163 164 4.758 4.758

FL16401 2.05873074 1.586 1.0

FL16402 0 0 0 0

FL164S1 2.05873074 1.586 0.340

FL16500 InletF64-T65 164 165 6.344 6.344

FL16501 2.05873074 1.586 1.0

FL16502 0 0 0 0
FL165S1 2.05873074 1.586 0.340

FL16600 InletF65-T66 165 166 7.93 7.93
FL16601 2.05873074 1.3875 1.0
FL16602 0 0 0 0
FL166S1 2.05873074 1.3875 0.340

FL16700 InletF66-T80 166 280 9.119 9.119
FL16701 2.05873074 1.8595 1.0
FL16702 0 0 0 0
FL167S1 2.05873074 1.8595 0.340

****
* Upper boundary heat structures
****

*Ring 1
HS34001000 2 1 -1
HS34001001 UPPER_BOUNDARY_RING1
HS34001002 9.119 0.0
HS34001100 -1 1 0.0
HS34001102 0.1 2
HS34001201 stainless-steel-304 1
HS34001300 0
HS34001400 1 116 'EXT' .9 .9
HS34001401 0.8 'equiv-band' 0.25
HS34001500 6.846450432 0.01588 1.4762
HS34001600 0 -1

HS34001800 -1
HS34001801 764.0 1
HS34001802 764.0 2

*Ring 2
HS34002000 2 1 -1
HS34002001 UPPER_BOUNDARY_RING2
HS34002002 9.119 0.0
HS34002100 -1 1 0.0
HS34002102 0.1 2
HS34002201 stainless-steel-304 1
HS34002300 0
HS34002400 1 126 'EXT' .9 .9
HS34002401 0.8 'equiv-band' 0.25
HS34002500 3.36710677 0.01588 0.3268
HS34002600 0 -1
HS34002800 -1
HS34002801 764.0 1
HS34002802 764.0 2

*Ring 3
HS34003000 2 1 -1
HS34003001 UPPER_BOUNDARY_RING3
HS34003002 9.119 0.0
HS34003100 -1 1 0.0
HS34003102 0.1 2
HS34003201 stainless-steel-304 1
HS34003300 0
HS34003400 1 136 'EXT' .9 .9

HS34003401 0.8 'equiv-band' 0.25
HS34003500 4.040528124 0.01588 0.3270
HS34003600 0 -1
HS34003800 -1
HS34003801 764.0 1
HS34003802 764.0 2

*Ring 4
HS34004000 2 1 -1
HS34004001 UPPER_BOUNDARY_RING4
HS34004002 9.119 0.0
HS34004100 -1 1 0.0
HS34004102 0.1 2
HS34004201 stainless-steel-304 1
HS34004300 0
HS34004400 1 146 'EXT' .9 .9
HS34004401 0.8 'equiv-band' 0.25
HS34004500 4.139016417 0.01588 0.2896
HS34004600 0 -1
HS34004800 -1
HS34004801 764.0 1
HS34004802 764.0 2

*Ring 5
HS34005000 2 1 -1
HS34005001 UPPER_BOUNDARY_RING5
HS34005002 9.119 0.0
HS34005100 -1 1 0.0
HS34005102 0.1 2

```
HS34005201 stainless-steel-304 1
HS34005300 0
HS34005400 1  156  'EXT'  .9  .9
HS34005401 0.8 'equiv-band' 0.25
HS34005500 16.34334698 0.01588 0.9056
HS34005600 0 -1
HS34005800 -1
HS34005801  764.0  1
HS34005802  764.0  2

**********
* Core barrel heat
* structures
**********
*level 0
HS32000000  2  2  -1
HS32000001  cb_LVL_0
HS32000002  -1.835  1.0
HS32000004  506  0
HS32000100  -1  1  3.3252
HS32000101  3.5213  2
HS32000200  -1  * index for material
HS32000201  stainless-steel-304  1
HS32000300  0
HS32000400  1  54  'EXT'  0.9  0.9
HS32000500  5.223211946  0.01588  0.25
HS32000600  0 -1
HS32000800  -1
HS32000801  764.0  1
```

```
HS32000802  764.0  2

*level 1
HS32001000  2  2  -1
HS32001001  cb_LVL_1
HS32001002  -1.585  1.0
HS32001004  507  0
HS32001100  -1  1  3.3252
HS32001101  3.5213  2
HS32001200  -1  * index for material
HS32001201  stainless-steel-304  1
HS32001300  0
HS32001400  1  150  'EXT'  0.9  0.9
HS32001500  8.278790934  0.01588  0.39625
HS32001600  1  160  'INT'  0.9  0.9
HS32001700  8.7670   0.340  0.39625
HS32001800  -1
HS32001801  764.0  1
HS32001802  764.0  2

*level 2
HS32002000  2  2  -1
HS32002001  cb_LVL_2
HS32002002  -1.18875  1.0
HS32002004  508  0
HS32002100  -1  1  3.3252
HS32002101  3.5213  2
HS32002200  -1  * index for material
HS32002201  stainless-steel-304  1
```

```
HS32002300  0
HS32002400  1  150  'EXT'  0.9  0.9
HS32002500  8.278790934  0.01588  0.39625
HS32002600  1  160  'INT'  0.9  0.9
HS32002700  8.7670   0.340  0.39625
HS32002800  -1
HS32002801  764.0  1
HS32002802  764.0  2

*level 3
HS32003000  2  2  -1
HS32003001  cb_LVL_3
HS32003002  -0.7925  1.0
HS32003004  509  0
HS32003100  -1  1  3.3252
HS32003101  3.5213  2
HS32003200  -1  * index for material
HS32003201  stainless-steel-304  1
HS32003300  0
HS32003400  1  150  'EXT'  0.9  0.9
HS32003500  8.278790934  0.01588  0.39625
HS32003600  1  160  'INT'  0.9  0.9
HS32003700  8.7670   0.340  0.39625
HS32003800  -1
HS32003801  764.0  1
HS32003802  764.0  2

*level 4
HS32004000  2  2  -1
```

```
HS32004001  cb_LVL_4
HS32004002  -0.39625  1.0
HS32004004  510  0
HS32004100  -1  1  3.3252
HS32004101  3.5213  2
HS32004200  -1  * index for material
HS32004201  stainless-steel-304  1
HS32004300  0
HS32004400  1  150  'EXT'  0.9  0.9
HS32004500  8.278790934  0.01588  0.39625
HS32004600  1  160  'INT'  0.9  0.9
HS32004700  8.7670   0.340  0.39625
HS32004800  -1
HS32004801  764.0  1
HS32004802  764.0  2

*level 5
HS32005000  2  2  -1
HS32005001  cb_LVL_5
HS32005002  0.0  1.0
HS32005004  511  0
HS32005100  -1  1  3.3252
HS32005101  3.5213  2
HS32005200  -1  * index for material
HS32005201  stainless-steel-304  1
HS32005300  0
HS32005400  1  151  'EXT'  0.9  0.9
HS32005500  8.284014146  0.01588  0.3965
HS32005600  1  161  'INT'  0.9  0.9
```

```
HS32005700  8.7725   0.340  0.3965
HS32005800  -1
HS32005801  764.0  1
HS32005802  764.0  2

*level 6
HS32006000  2  2  -1
HS32006001  cb_LVL_6
HS32006002  0.3965  1.0
HS32006004  512  0
HS32006100  -1  1  3.3252
HS32006101  3.5213  2
HS32006200  -1  * index for material
HS32006201  stainless-steel-304  1
HS32006300  0
HS32006400  1  151  'EXT'  0.9  0.9
HS32006500  8.284014146  0.01588  0.3965
HS32006600  1  161  'INT'  0.9  0.9
HS32006700  8.7725   0.340  0.3965
HS32006800  -1
HS32006801  764.0  1
HS32006802  764.0  2

*level 7
HS32007000  2  2  -1
HS32007001  cb_LVL_7
HS32007002  0.793  1.0
HS32007004  513  0
HS32007100  -1  1  3.3252
```

```
HS32007101  3.5213  2
HS32007200  -1  * index for material
HS32007201  stainless-steel-304  1
HS32007300  0
HS32007400  1  151  'EXT'  0.9  0.9
HS32007500  8.284014146  0.01588  0.3965
HS32007600  1  161  'INT'  0.9  0.9
HS32007700  8.7725   0.340  0.3965
HS32007800  -1
HS32007801  764.0  1
HS32007802  764.0  2

*level 8
HS32008000  2  2  -1
HS32008001  cb_LVL_8
HS32008002  1.1895  1.0
HS32008004  514  0
HS32008100  -1  1  3.3252
HS32008101  3.5213  2
HS32008200  -1  * index for material
HS32008201  stainless-steel-304  1
HS32008300  0
HS32008400  1  151  'EXT'  0.9  0.9
HS32008500  8.284014146  0.01588  0.3965
HS32008600  1  161  'INT'  0.9  0.9
HS32008700  8.7725   0.340  0.3965
HS32008800  -1
HS32008801  764.0  1
HS32008802  764.0  2
```

```
*level 9
HS32009000  2  2  -1
HS32009001  cb_LVL_9
HS32009002  1.586  1.0
HS32009004  515  0
HS32009100  -1  1  3.3252
HS32009101  3.5213  2
HS32009200  -1  * index for material
HS32009201  stainless-steel-304  1
HS32009300  0
HS32009400  1  152  'EXT'  0.9  0.9
HS32009500  8.284014146  0.01588  0.3965
HS32009600  1  162  'INT'  0.9  0.9
HS32009700  8.7725   0.340  0.3965
HS32009800  -1
HS32009801  764.0  1
HS32009802  764.0  2

*level 10
HS32010000  2  2  -1
HS32010001  cb_LVL_10
HS32010002  1.9825  1.0
HS32010004  516  0
HS32010100  -1  1  3.3252
HS32010101  3.5213  2
HS32010200  -1  * index for material
HS32010201  stainless-steel-304  1
HS32010300  0
```

HS32010400 1 152 'EXT' 0.9 0.9

HS32010500 8.284014146 0.01588 0.3965

HS32010600 1 162 'INT' 0.9 0.9

HS32010700 8.7725 0.340 0.3965

HS32010800 -1

HS32010801 764.0 1

HS32010802 764.0 2

*level 11

HS32011000 2 2 -1

HS32011001 cb_LVL_11

HS32011002 2.379 1.0

HS32011004 517 0

HS32011100 -1 1 3.3252

HS32011101 3.5213 2

HS32011200 -1 * index for material

HS32011201 stainless-steel-304 1

HS32011300 0

HS32011400 1 152 'EXT' 0.9 0.9

HS32011500 8.284014146 0.01588 0.3965

HS32011600 1 162 'INT' 0.9 0.9

HS32011700 8.7725 0.340 0.3965

HS32011800 -1

HS32011801 764.0 1

HS32011802 764.0 2

*level 12

HS32012000 2 2 -1

HS32012001 cb_LVL_12

```
HS32012002  2.7755  1.0
HS32012004  518  0
HS32012100  -1  1  3.3252
HS32012101  3.5213  2
HS32012200  -1  * index for material
HS32012201  stainless-steel-304  1
HS32012300  0
HS32012400  1  152  'EXT'  0.9  0.9
HS32012500  8.284014146  0.01588  0.3965
HS32012600  1  162  'INT'  0.9  0.9
HS32012700  8.7725   0.340  0.3965
HS32012800  -1
HS32012801  764.0  1
HS32012802  764.0  2

*level 13
HS32013000  2  2  -1
HS32013001  cb_LVL_13
HS32013002  3.172  1.0
HS32013004  519  0
HS32013100  -1  1  3.3252
HS32013101  3.5213  2
HS32013200  -1  * index for material
HS32013201  stainless-steel-304  1
HS32013300  0
HS32013400  1  153  'EXT'  0.9  0.9
HS32013500  8.284014146  0.01588  0.3965
HS32013600  1  163  'INT'  0.9  0.9
HS32013700  8.7725   0.340  0.3965
```

```
HS32013800  -1
HS32013801  764.0  1
HS32013802  764.0  2

*level 14
HS32014000  2  2  -1
HS32014001  cb_LVL_14
HS32014002  3.5685  1.0
HS32014004  520  0
HS32014100  -1  1  3.3252
HS32014101  3.5213  2
HS32014200  -1  * index for material
HS32014201  stainless-steel-304  1
HS32014300  0
HS32014400  1  153  'EXT'  0.9  0.9
HS32014500  8.284014146  0.01588  0.3965
HS32014600  1  163  'INT'  0.9  0.9
HS32014700  8.7725   0.340  0.3965
HS32014800  -1
HS32014801  764.0  1
HS32014802  764.0  2

*level 15
HS32015000  2  2  -1
HS32015001  cb_LVL_15
HS32015002  3.965  1.0
HS32015004  521  0
HS32015100  -1  1  3.3252
HS32015101  3.5213  2
```

HS32015200 -1 * index for material
HS32015201 stainless-steel-304 1
HS32015300 0
HS32015400 1 153 'EXT' 0.9 0.9
HS32015500 8.284014146 0.01588 0.3965
HS32015600 1 163 'INT' 0.9 0.9
HS32015700 8.7725 0.340 0.3965
HS32015800 -1
HS32015801 764.0 1
HS32015802 764.0 2

*level 16
HS32016000 2 2 -1
HS32016001 cb_LVL_16
HS32016002 4.3615 1.0
HS32016004 522 0
HS32016100 -1 1 3.3252
HS32016101 3.5213 2
HS32016200 -1 * index for material
HS32016201 stainless-steel-304 1
HS32016300 0
HS32016400 1 153 'EXT' 0.9 0.9
HS32016500 8.284014146 0.01588 0.3965
HS32016600 1 163 'INT' 0.9 0.9
HS32016700 8.7725 0.340 0.3965
HS32016800 -1
HS32016801 764.0 1
HS32016802 764.0 2

```
*level 17
HS32017000  2  2  -1
HS32017001  cb_LVL_17
HS32017002  4.758  1.0
HS32017004  523  0
HS32017100  -1  1  3.3252
HS32017101  3.5213  2
HS32017200  -1  * index for material
HS32017201  stainless-steel-304  1
HS32017300  0
HS32017400  1  154  'EXT'  0.9  0.9
HS32017500  8.284014146  0.01588  0.3965
HS32017600  1  164  'INT'  0.9  0.9
HS32017700  8.7725   0.340  0.3965
HS32017800  -1
HS32017801  764.0  1
HS32017802  764.0  2

*level 18
HS32018000  2  2  -1
HS32018001  cb_LVL_18
HS32018002  5.1545  1.0
HS32018004  524  0
HS32018100  -1  1  3.3252
HS32018101  3.5213  2
HS32018200  -1  * index for material
HS32018201  stainless-steel-304  1
HS32018300  0
HS32018400  1  154  'EXT'  0.9  0.9
```

```
HS32018500  8.284014146  0.01588  0.3965
HS32018600  1  164  'INT'  0.9  0.9
HS32018700  8.7725   0.340  0.3965
HS32018800  -1
HS32018801  764.0  1
HS32018802  764.0  2

*level 19
HS32019000  2  2  -1
HS32019001  cb_LVL_19
HS32019002  5.551  1.0
HS32019004  525  0
HS32019100  -1  1  3.3252
HS32019101  3.5213  2
HS32019200  -1  * index for material
HS32019201  stainless-steel-304  1
HS32019300  0
HS32019400  1  154  'EXT'  0.9  0.9
HS32019500  8.284014146  0.01588  0.3965
HS32019600  1  164  'INT'  0.9  0.9
HS32019700  8.7725   0.340  0.3965
HS32019800  -1
HS32019801  764.0  1
HS32019802  764.0  2

*level 20
HS32020000  2  2  -1
HS32020001  cb_LVL_20
HS32020002  5.9475  1.0
```

HS32020004 526 0
HS32020100 -1 1 3.3252
HS32020101 3.5213 2
HS32020200 -1 * index for material
HS32020201 stainless-steel-304 1
HS32020300 0
HS32020400 1 154 'EXT' 0.9 0.9
HS32020500 8.284014146 0.01588 0.3965
HS32020600 1 164 'INT' 0.9 0.9
HS32020700 8.7725 0.340 0.3965
HS32020800 -1
HS32020801 764.0 1
HS32020802 764.0 2

*level 21
HS32021000 2 2 -1
HS32021001 cb_LVL_21
HS32021002 6.344 1.0
HS32021004 527 0
HS32021100 -1 1 3.3252
HS32021101 3.5213 2
HS32021200 -1 * index for material
HS32021201 stainless-steel-304 1
HS32021300 0
HS32021400 1 155 'EXT' 0.9 0.9
HS32021500 8.284014146 0.01588 0.3965
HS32021600 1 165 'INT' 0.9 0.9
HS32021700 8.7725 0.340 0.3965
HS32021800 -1

```
HS32021801  764.0  1
HS32021802  764.0  2

*level 22
HS32022000  2  2  -1
HS32022001  cb_LVL_22
HS32022002  6.7405  1.0
HS32022004  528  0
HS32022100  -1  1  3.3252
HS32022101  3.5213  2
HS32022200  -1  * index for material
HS32022201  stainless-steel-304  1
HS32022300  0
HS32022400  1  155  'EXT'  0.9  0.9
HS32022500  8.284014146  0.01588  0.3965
HS32022600  1  165  'INT'  0.9  0.9
HS32022700  8.7725  0.340  0.3965
HS32022800  -1
HS32022801  764.0  1
HS32022802  764.0  2

*level 23
HS32023000  2  2  -1
HS32023001  cb_LVL_23
HS32023002  7.137  1.0
HS32023004  529  0
HS32023100  -1  1  3.3252
HS32023101  3.5213  2
HS32023200  -1  * index for material
```

HS32023201 stainless-steel-304 1
HS32023300 0
HS32023400 1 155 'EXT' 0.9 0.9
HS32023500 8.284014146 0.01588 0.3965
HS32023600 1 165 'INT' 0.9 0.9
HS32023700 8.7725 0.340 0.3965
HS32023800 -1
HS32023801 764.0 1
HS32023802 764.0 2

*level 24
HS32024000 2 2 -1
HS32024001 cb_LVL_24
HS32024002 7.5335 1.0
HS32024004 530 0
HS32024100 -1 1 3.3252
HS32024101 3.5213 2
HS32024200 -1 * index for material
HS32024201 stainless-steel-304 1
HS32024300 0
HS32024400 1 155 'EXT' 0.9 0.9
HS32024500 8.284014146 0.01588 0.3965
HS32024600 1 165 'INT' 0.9 0.9
HS32024700 8.7725 0.340 0.3965
HS32024800 -1
HS32024801 764.0 1
HS32024802 764.0 2

*level 25

```
HS32025000  2  2  -1
HS32025001  cb_LVL_25
HS32025002  7.93  1.0
HS32025004  531  0
HS32025100  -1  1  3.3252
HS32025101  3.5213  2
HS32025200  -1  * index for material
HS32025201  stainless-steel-304  1
HS32025300  0
HS32025400  1  156  'EXT'  0.9  0.9
HS32025500  8.279835577  0.01588  0.3963
HS32025600  1  166  'INT'  0.9  0.9
HS32025700  8.7681   0.340  0.3963
HS32025800  -1
HS32025801  764.0  1
HS32025802  764.0  2

*level 26
HS32026000  2  2  -1
HS32026001  cb_LVL_26
HS32026002  8.3263  1.0
HS32026004  532  0
HS32026100  -1  1  3.3252
HS32026101  3.5213  2
HS32026200  -1  * index for material
HS32026201  stainless-steel-304  1
HS32026300  0
HS32026400  1  156  'EXT'  0.9  0.9
HS32026500  8.279835577  0.01588  0.3963
```

HS32026600 1 166 'INT' 0.9 0.9

HS32026700 8.7681 0.340 0.3963

HS32026800 -1

HS32026801 764.0 1

HS32026802 764.0 2

*level 27

HS32027000 2 2 -1

HS32027001 cb_LVL_27

HS32027002 8.7226 1.0

HS32027004 533 0

HS32027100 -1 1 3.3252

HS32027101 3.5213 2

HS32027200 -1 * index for material

HS32027201 stainless-steel-304 1

HS32027300 0

HS32027400 1 156 'EXT' 0.9 0.9

HS32027500 8.281924861 0.01588 0.3964

HS32027600 1 166 'INT' 0.9 0.9

HS32027700 8.7703 0.340 0.3964

HS32027800 -1

HS32027801 764.0 1

HS32027802 764.0 2

****

* pressure vessel heat

* structures

****

```
*level 1
HS33001000  2  2  -1
HS33001001  pv_LVL_1
HS33001002  -1.585  1.0
HS33001100  -1  1  3.61315
HS33001101  3.82905  2
HS33001200  -1  * index for material
HS33001201  stainless-steel-304  1
HS33001300  0
HS33001400  1  160  'INT'  0.9  0.9
HS33001500  8.995703556  0.340  0.39625
HS33001600  0 -1 * symmetry boundary condition
HS33001800  -1
HS33001801  764.0  1
HS33001802  764.0  2

*level 2
HS33002000  2  2  -1
HS33002001  pv_LVL_2
HS33002002  -1.18875  1.0
HS33002100  -1  1  3.61315
HS33002101  3.82905  2
HS33002200  -1  * index for material
HS33002201  stainless-steel-304  1
HS33002300  0
HS33002400  1  160  'INT'  0.9  0.9
HS33002500  8.995703556  0.340  0.39625
HS33002600  0 -1 * symmetry boundary condition
HS33002800  -1
```

```
HS33002801  764.0  1
HS33002802  764.0  2

*level 3
HS33003000  2  2  -1
HS33003001  pv_LVL_3
HS33003002  -0.7925  1.0
HS33003100  -1  1  3.61315
HS33003101  3.82905  2
HS33003200  -1  * index for material
HS33003201  stainless-steel-304  1
HS33003300  0
HS33003400  1  160  'INT'  0.9  0.9
HS33003500  8.995703556  0.340  0.39625
HS33003600  0 -1 * symmetry boundary condition
HS33003800  -1
HS33003801  764.0  1
HS33003802  764.0  2

*level 4
HS33004000  2  2  -1
HS33004001  pv_LVL_4
HS33004002  -0.39625  1.0
HS33004100  -1  1  3.61315
HS33004101  3.82905  2
HS33004200  -1  * index for material
HS33004201  stainless-steel-304  1
HS33004300  0
HS33004400  1  160  'INT'  0.9  0.9
```

```
HS33004500  8.995703556  0.340  0.39625
HS33004600  0 -1 * symmetry boundary condition
HS33004800  -1
HS33004801  764.0  1
HS33004802  764.0  2

*level 5
HS33005000  2  2  -1
HS33005001  pv_LVL_5
HS33005002  0.0  1.0
HS33005100  -1  1  3.61315
HS33005101  3.82905  2
HS33005200  -1  * index for material
HS33005201  stainless-steel-304  1
HS33005300  0
HS33005400  1  161  'INT'  0.9  0.9
HS33005500  9.001379079  0.340  0.3965
HS33005600  0 -1 * symmetry boundary condition
HS33005800  -1
HS33005801  764.0  1
HS33005802  764.0  2

*level 6
HS33006000  2  2  -1
HS33006001  pv_LVL_6
HS33006002  0.3965  1.0
HS33006100  -1  1  3.61315
HS33006101  3.82905  2
HS33006200  -1  * index for material
```

```
HS33006201  stainless-steel-304  1
HS33006300  0
HS33006400  1  161  'INT'  0.9  0.9
HS33006500  9.001379079  0.340  0.3965
HS33006600  0 -1 * symmetry boundary condition
HS33006800  -1
HS33006801  764.0  1
HS33006802  764.0  2

*level 7
HS33007000  2  2  -1
HS33007001  pv_LVL_7
HS33007002  0.793  1.0
HS33007100  -1  1  3.61315
HS33007101  3.82905  2
HS33007200  -1  * index for material
HS33007201  stainless-steel-304  1
HS33007300  0
HS33007400  1  161  'INT'  0.9  0.9
HS33007500  9.001379079  0.340  0.3965
HS33007600  0 -1 * symmetry boundary condition
HS33007800  -1
HS33007801  764.0  1
HS33007802  764.0  2

*level 8
HS33008000  2  2  -1
HS33008001  pv_LVL_8
HS33008002  1.1895  1.0
```

```
HS33008100  -1  1  3.61315
HS33008101  3.82905  2
HS33008200  -1  * index for material
HS33008201  stainless-steel-304  1
HS33008300  0
HS33008400  1  161  'INT'  0.9  0.9
HS33008500  9.001379079  0.340  0.3965
HS33008600  0 -1 * symmetry boundary condition
HS33008800  -1
HS33008801  764.0  1
HS33008802  764.0  2

*level 9
HS33009000  2  2  -1
HS33009001  pv_LVL_9
HS33009002  1.586  1.0
HS33009100  -1  1  3.61315
HS33009101  3.82905  2
HS33009200  -1  * index for material
HS33009201  stainless-steel-304  1
HS33009300  0
HS33009400  1  162  'INT'  0.9  0.9
HS33009500  9.001379079  0.340  0.3965
HS33009600  0 -1 * symmetry boundary condition
HS33009800  -1
HS33009801  764.0  1
HS33009802  764.0  2

*level 10
```

```
HS33010000  2  2  -1
HS33010001  pv_LVL_10
HS33010002  1.9825  1.0
HS33010100  -1  1  3.61315
HS33010101  3.82905  2
HS33010200  -1  * index for material
HS33010201  stainless-steel-304  1
HS33010300  0
HS33010400  1  162  'INT'  0.9  0.9
HS33010500  9.001379079  0.340  0.3965
HS33010600  0 -1 * symmetry boundary condition
HS33010800  -1
HS33010801  764.0  1
HS33010802  764.0  2

*level 11
HS33011000  2  2  -1
HS33011001  pv_LVL_11
HS33011002  2.379  1.0
HS33011100  -1  1  3.61315
HS33011101  3.82905  2
HS33011200  -1  * index for material
HS33011201  stainless-steel-304  1
HS33011300  0
HS33011400  1  162  'INT'  0.9  0.9
HS33011500  9.001379079  0.340  0.3965
HS33011600  0 -1 * symmetry boundary condition
HS33011800  -1
HS33011801  764.0  1
```

```
HS33011802  764.0  2

*level 12
HS33012000  2  2  -1
HS33012001  pv_LVL_12
HS33012002  2.7755  1.0
HS33012100  -1  1  3.61315
HS33012101  3.82905  2
HS33012200  -1  * index for material
HS33012201  stainless-steel-304  1
HS33012300  0
HS33012400  1  162  'INT'  0.9  0.9
HS33012500  9.001379079  0.340  0.3965
HS33012600  0 -1 * symmetry boundary condition
HS33012800  -1
HS33012801  764.0  1
HS33012802  764.0  2

*level 13
HS33013000  2  2  -1
HS33013001  pv_LVL_13
HS33013002  3.172  1.0
HS33013100  -1  1  3.61315
HS33013101  3.82905  2
HS33013200  -1  * index for material
HS33013201  stainless-steel-304  1
HS33013300  0
HS33013400  1  163  'INT'  0.9  0.9
HS33013500  9.001379079  0.340  0.3965
```

```
HS33013600  0 -1 * symmetry boundary condition
HS33013800  -1
HS33013801  764.0  1
HS33013802  764.0  2

*level 14
HS33014000  2  2  -1
HS33014001  pv_LVL_14
HS33014002  3.5685  1.0
HS33014100  -1  1  3.61315
HS33014101  3.82905  2
HS33014200  -1  * index for material
HS33014201  stainless-steel-304  1
HS33014300  0
HS33014400  1  163  'INT'  0.9  0.9
HS33014500  9.001379079  0.340  0.3965
HS33014600  0 -1 * symmetry boundary condition
HS33014800  -1
HS33014801  764.0  1
HS33014802  764.0  2

*level 15
HS33015000  2  2  -1
HS33015001  pv_LVL_15
HS33015002  3.965  1.0
HS33015100  -1  1  3.61315
HS33015101  3.82905  2
HS33015200  -1  * index for material
HS33015201  stainless-steel-304  1
```

```
HS33015300  0
HS33015400  1  163  'INT'  0.9  0.9
HS33015500  9.001379079  0.340  0.3965
HS33015600  0 -1 * symmetry boundary condition
HS33015800  -1
HS33015801  764.0  1
HS33015802  764.0  2

*level 16
HS33016000  2  2  -1
HS33016001  pv_LVL_16
HS33016002  4.3615  1.0
HS33016100  -1  1  3.61315
HS33016101  3.82905  2
HS33016200  -1  * index for material
HS33016201  stainless-steel-304  1
HS33016300  0
HS33016400  1  163  'INT'  0.9  0.9
HS33016500  9.001379079  0.340  0.3965
HS33016600  0 -1 * symmetry boundary condition
HS33016800  -1
HS33016801  764.0  1
HS33016802  764.0  2

*level 17
HS33017000  2  2  -1
HS33017001  pv_LVL_17
HS33017002  4.758  1.0
HS33017100  -1  1  3.61315
```

```
HS33017101  3.82905  2
HS33017200  -1  * index for material
HS33017201  stainless-steel-304  1
HS33017300  0
HS33017400  1  164  'INT'  0.9  0.9
HS33017500  9.001379079  0.340  0.3965
HS33017600  0 -1 * symmetry boundary condition
HS33017800  -1
HS33017801  764.0  1
HS33017802  764.0  2

*level 18
HS33018000  2  2  -1
HS33018001  pv_LVL_18
HS33018002  5.1545  1.0
HS33018100  -1  1  3.61315
HS33018101  3.82905  2
HS33018200  -1  * index for material
HS33018201  stainless-steel-304  1
HS33018300  0
HS33018400  1  164  'INT'  0.9  0.9
HS33018500  9.001379079  0.340  0.3965
HS33018600  0 -1 * symmetry boundary condition
HS33018800  -1
HS33018801  764.0  1
HS33018802  764.0  2

*level 19
HS33019000  2  2  -1
```

```
HS33019001  pv_LVL_19
HS33019002  5.551  1.0
HS33019100  -1  1  3.61315
HS33019101  3.82905  2
HS33019200  -1  * index for material
HS33019201  stainless-steel-304  1
HS33019300  0
HS33019400  1  164  'INT'  0.9  0.9
HS33019500  9.001379079  0.340  0.3965
HS33019600  0 -1 * symmetry boundary condition
HS33019800  -1
HS33019801  764.0  1
HS33019802  764.0  2

*level 20
HS33020000  2  2  -1
HS33020001  pv_LVL_20
HS33020002  5.9475  1.0
HS33020100  -1  1  3.61315
HS33020101  3.82905  2
HS33020200  -1  * index for material
HS33020201  stainless-steel-304  1
HS33020300  0
HS33020400  1  164  'INT'  0.9  0.9
HS33020500  9.001379079  0.340  0.3965
HS33020600  0 -1 * symmetry boundary condition
HS33020800  -1
HS33020801  764.0  1
HS33020802  764.0  2
```

```
*level 21
HS33021000  2  2  -1
HS33021001  pv_LVL_21
HS33021002  6.344  1.0
HS33021100  -1  1  3.61315
HS33021101  3.82905  2
HS33021200  -1  * index for material
HS33021201  stainless-steel-304  1
HS33021300  0
HS33021400  1  165  'INT'  0.9  0.9
HS33021500  9.001379079  0.340  0.3965
HS33021600  0 -1 * symmetry boundary condition
HS33021800  -1
HS33021801  764.0  1
HS33021802  764.0  2

*level 22
HS33022000  2  2  -1
HS33022001  pv_LVL_22
HS33022002  6.7405  1.0
HS33022100  -1  1  3.61315
HS33022101  3.82905  2
HS33022200  -1  * index for material
HS33022201  stainless-steel-304  1
HS33022300  0
HS33022400  1  165  'INT'  0.9  0.9
HS33022500  9.001379079  0.340  0.3965
HS33022600  0 -1 * symmetry boundary condition
```

```
HS33022800  -1
HS33022801  764.0  1
HS33022802  764.0  2

*level 23
HS33023000  2  2  -1
HS33023001  pv_LVL_23
HS33023002  7.137  1.0
HS33023100  -1  1  3.61315
HS33023101  3.82905  2
HS33023200  -1  * index for material
HS33023201  stainless-steel-304  1
HS33023300  0
HS33023400  1  165  'INT'  0.9  0.9
HS33023500  9.001379079  0.340  0.3965
HS33023600  0 -1 * symmetry boundary condition
HS33023800  -1
HS33023801  764.0  1
HS33023802  764.0  2

*level 24
HS33024000  2  2  -1
HS33024001  pv_LVL_24
HS33024002  7.5335  1.0
HS33024100  -1  1  3.61315
HS33024101  3.82905  2
HS33024200  -1  * index for material
HS33024201  stainless-steel-304  1
HS33024300  0
```

HS33024400 1 165 'INT' 0.9 0.9
HS33024500 9.001379079 0.340 0.3965
HS33024600 0 -1 * symmetry boundary condition
HS33024800 -1
HS33024801 764.0 1
HS33024802 764.0 2

*level 25
HS33025000 2 2 -1
HS33025001 pv_LVL_25
HS33025002 7.93 1.0
HS33025100 -1 1 3.61315
HS33025101 3.82905 2
HS33025200 -1 * index for material
HS33025201 stainless-steel-304 1
HS33025300 0
HS33025400 1 166 'INT' 0.9 0.9
HS33025500 8.99683866 0.340 0.3963
HS33025600 0 -1 * symmetry boundary condition
HS33025800 -1
HS33025801 764.0 1
HS33025802 764.0 2

*level 26
HS33026000 2 2 -1
HS33026001 pv_LVL_26
HS33026002 8.3263 1.0
HS33026100 -1 1 3.61315
HS33026101 3.82905 2

HS33026200 -1 * index for material
HS33026201 stainless-steel-304 1
HS33026300 0
HS33026400 1 166 'INT' 0.9 0.9
HS33026500 8.99683866 0.340 0.3963
HS33026600 0 -1 * symmetry boundary condition
HS33026800 -1
HS33026801 764.0 1
HS33026802 764.0 2

*level 27
HS33027000 2 2 -1
HS33027001 pv_LVL_27
HS33027002 8.7226 1.0
HS33027100 -1 1 3.61315
HS33027101 3.82905 2
HS33027200 -1 * index for material
HS33027201 stainless-steel-304 1
HS33027300 0
HS33027400 1 166 'INT' 0.9 0.9
HS33027500 8.999108869 0.340 0.3964
HS33027600 0 -1 * symmetry boundary condition
HS33027800 -1
HS33027801 764.0 1
HS33027802 764.0 2

* System source to RPV
FL19000 SOURCEtoINLET 190 160 -2.9145 -0.7925
FL19001 2.05873074 2.122 1.0

FL19002 0 0 0 0

FL190S1 2.05873074 2.122 0.340

* RPV to system sink

FL20000 OUTLETToSINK 054 200 -2.9145 -2.9145

FL20001 3.660961536 3.3633 1.0

FL20002 3 0 0 0

FL200S1 3.660961536 3.3633 2.159

* Time-independent source

CV19000 SRC 2 0 4

CV19001 0 -1

CV190A0 3

CV190A1 MLFR.4 1.0 TATM 764.0 PVOL 7.12e6 PH2O 0.0

CV190B0 -3.994 0.0

CV190B1 -1.835 0.775208605

* Time-independent sink

CV20000 SNK 2 0 5

CV20001 0 -1

CV200A0 3

CV200A1 MLFR.4 1.0 TATM 1123.0 PVOL 7.014e6 PH2O 0.0

CV200B0 -3.994 0.0

CV200B1 -1.835 0.278965269

*Form loss coefficient

FL19003 1.2 1.2 1.0 1.0

FL20003 1.2 1.2 1.0 1.0

.

A.2.4 core-new-2.gen

```
*Core edit flags
* ITEMP IMASS IVOL IASUR IPMV IPOW
COREDV01 1 1 1 1 1 1

*General core and lower plenum input
COR00000 5 33 6 36 3 5 0
COR00001 0.006225 0.189013524 0.000125 0.0188 0.0 0.0

*Pitch value is taken from ORNL/TM-2002/156

*Vessel Parameters
COR00001A 3.3252 3.61315 3.3252 1 1 0.2159 0.2159
COR00001B -1.835 -1.835

COR00002 PWR B4C
COR00003 1.0 0.0 0.5 0.5 0.0
COR00004 0 -10 0

*Fission power control function no. is 10.

COR00012 100.0 2.0e7 6 1.0

COR00006 0 0 0 0 0
*There are no other structures in the reactor.

**********
```

```
* Steady-state core fission power
**********
CF01000 COREPOW EQUALS 1 0.0 600.0e6
CF01010 1.0 0.0 TIME

*Axial level input
CORZ0101 -3.994  0.4318 0.111 0.0
CORZ0201 -3.5622 0.4318 0.111 0.0
CORZ0301 -3.1304 0.4318 0.111 0.0
CORZ0401 -2.6986 0.4318 0.111 0.0
CORZ0501 -2.2668 0.4318 0.111 0.0
CORZ0601 -1.835 0.25 0.111 0.0
CORZ0701 -1.585  0.39625 0.111 0.0
CORZ0801 -1.18875 0.39625 0.111 0.0
CORZ0901 -0.7925 0.39625 0.111 0.0
CORZ1001 -0.39625 0.39625 0.111 0.0
CORZ1101 0.0 0.3965 0.111 0.0
CORZ1201 0.3965 0.3965 0.111 0.0
CORZ1301 0.793 0.3965 0.111 0.0
CORZ1401 1.1895 0.3965 0.111 0.0
CORZ1501 1.586 0.3965 0.111 0.0
CORZ1601 1.9825 0.3965 0.111 0.0
CORZ1701 2.379 0.3965 0.111 0.0
CORZ1801 2.7755 0.3965 0.111 0.0
CORZ1901 3.172 0.3965 0.111 0.0
CORZ2001 3.5685 0.3965 0.111 0.0
CORZ2101 3.965 0.3965 0.111 0.0
CORZ2201 4.3615 0.3965 0.111 0.0
CORZ2301 4.758 0.3965 0.111 0.0
```

CORZ2401 5.1545 0.3965 0.111 0.0
CORZ2501 5.551 0.3965 0.111 0.0
CORZ2601 5.9475 0.3965 0.111 0.0
CORZ2701 6.344 0.3965 0.111 0.0
CORZ2801 6.7405 0.3965 0.111 0.0
CORZ2901 7.137 0.3965 0.111 0.0
CORZ3001 7.5335 0.3965 0.111 0.0
CORZ3101 7.93 0.3963 0.111 0.0
CORZ3201 8.3263 0.3963 0.111 0.0
CORZ3301 8.7226 0.3964 0.111 0.0

*Core axial boundary heat structures
CORZ0102 0
CORZ0202 0
CORZ0302 0
CORZ0402 0
CORZ0502 0
CORZ0602 32000

CORZ0702 32001
CORZ0802 32002
CORZ0902 32003
CORZ1002 32004
CORZ1102 32005
CORZ1202 32006
CORZ1302 32007
CORZ1402 32008
CORZ1502 32009
CORZ1602 32010

CORZ1702 32011
CORZ1802 32012
CORZ1902 32013
CORZ2002 32014
CORZ2102 32015
CORZ2202 32016
CORZ2302 32017
CORZ2402 32018
CORZ2502 32019
CORZ2602 32020
CORZ2702 32021
CORZ2802 32022
CORZ2902 32023
CORZ3002 32024
CORZ3102 32025
CORZ3202 32026
CORZ3302 32027

****
* Axial power density profile
****
CORZ1103 1.1734
CORZ1203 1.2578
CORZ1303 1.3164
CORZ1403 1.3492
CORZ1503 1.3336
CORZ1603 1.2696
CORZ1703 1.1985
CORZ1803 1.1203

CORZ1903 1.0492

CORZ2003 0.9852

CORZ2103 0.9359

CORZ2203 0.9013

CORZ2303 0.86925

CORZ2403 0.83975

CORZ2503 0.8125

CORZ2603 0.7875

CORZ2703 0.75

CORZ2803 0.7

CORZ2903 0.63905

CORZ3003 0.56715

****

* radial power density profile

****

CORR0203 1.1

CORR0303 0.92

CORR0403 1.0

*Radial Ring Outer Radius

CORR0100 1.476242818

CORR0200 1.803074106

CORR0300 2.130074242

CORR0400 2.41965

CORR0500 3.3252

*Upper boundary heat structures

CORR0102 34001

CORR0202 34002
CORR0302 34003
CORR0402 34004
CORR0502 34005

*Upper Boundary Heat Structure
*and Lower Head Failure CF Specification

*COR cell-specific input
COR10101 -1 054 054
COR20101 -1 054 054
COR30101 -1 054 054
COR40101 -1 054 054
COR50101 -1 054 054

COR10201 101
COR20201 201
COR30201 301
COR40201 401
COR50201 501

COR10301 101
COR20301 201
COR30301 301
COR40301 401
COR50301 501

COR10401 101
COR20401 201

COR30401 301
COR40401 401
COR50401 501

COR10501 101
COR20501 201
COR30501 301
COR40501 401
COR50501 501

COR10601 -1 054 054
COR20601 -1 054 054
COR30601 -1 054 054
COR40601 -1 054 054
COR50601 -1 054 054

COR10701 -1 110 110
COR20701 -1 120 120
COR30701 -1 130 130
COR40701 -1 140 140
COR50701 -1 150 150

COR10801 107
COR20801 207
COR30801 307
COR40801 407
COR50801 507

COR10901 107

COR20901 207
COR30901 307
COR40901 407
COR50901 507

COR11001 107
COR21001 207
COR31001 307
COR41001 407
COR51001 507

COR11101 -1 111 111
COR21101 -1 121 121
COR31101 -1 131 131
COR41101 -1 141 141
COR51101 -1 151 151

COR11201 111
COR21201 211
COR31201 311
COR41201 411
COR51201 511

COR11301 111
COR21301 211
COR31301 311
COR41301 411
COR51301 511

COR11401 111
COR21401 211
COR31401 311
COR41401 411
COR51401 511

COR11501 -1 112 112
COR21501 -1 122 122
COR31501 -1 132 132
COR41501 -1 142 142
COR51501 -1 152 152

COR11601 115
COR21601 215
COR31601 315
COR41601 415
COR51601 515

COR11701 115
COR21701 215
COR31701 315
COR41701 415
COR51701 515

COR11801 115
COR21801 215
COR31801 315
COR41801 415
COR51801 515

COR11901 -1 113 113
COR21901 -1 123 123
COR31901 -1 133 133
COR41901 -1 143 143
COR51901 -1 153 153

COR12001 119
COR22001 219
COR32001 319
COR42001 419
COR52001 519

COR12101 -1 113 113
COR22101 -1 123 123
COR32101 -1 133 133
COR42101 -1 143 143
COR52101 -1 153 153

COR12201 121
COR22201 221
COR32201 321
COR42201 421
COR52201 521

COR12301 -1 114 114
COR22301 -1 124 124
COR32301 -1 134 134
COR42301 -1 144 144

COR52301 -1 154 154

COR12401 123
COR22401 223
COR32401 323
COR42401 423
COR52401 523

COR12501 123
COR22501 223
COR32501 323
COR42501 423
COR52501 523

COR12601 123
COR22601 223
COR32601 323
COR42601 423
COR52601 523

COR12701 -1 115 115
COR22701 -1 125 125
COR32701 -1 135 135
COR42701 -1 145 145
COR52701 -1 155 155

COR12801 127
COR22801 227
COR32801 327

COR42801 427
COR52801 527

COR12901 127
COR22901 227
COR32901 327
COR42901 427
COR52901 527

COR13001 127
COR23001 227
COR33001 327
COR43001 427
COR53001 527

COR13101 -1 116 116
COR23101 -1 126 126
COR33101 -1 136 136
COR43101 -1 146 146
COR53101 -1 156 156

COR13201 131
COR23201 231
COR33201 331
COR43201 431
COR53201 531

COR13301 -1 116 116
COR23301 -1 126 126

COR33301 -1 136 136

COR43301 -1 146 146

COR53301 -1 156 156

*Core support structure definitions

COR106SS PLATEG 0.25 0.2000 10e-20

COR206SS PLATEG 0.25 0.2000 10e-20

COR306SS PLATEG 0.25 0.2000 10e-20

COR406SS PLATEG 0.25 0.2000 10e-20

COR506SS PLATEG 0.25 0.2000 10e-20

COR106KSS 2978.205938 0.0 0.0 0.0

COR206KSS 1464.691445 0.0 0.0 0.0

COR306KSS 1757.629734 0.0 0.0 0.0

COR406KSS 1800.472141 0.0 0.0 0.0

COR506KSS 7109.355936 0.0 0.0 0.0

COR10606 0.0 0.0 0.0 0.0 2.318876796 0.0

COR20606 0.0 0.0 0.0 0.0 5.151138979 0.0

COR30606 0.0 0.0 0.0 0.0 6.178174978 0.0

COR40606 0.0 0.0 0.0 0.0 7.146690127 0.0

COR50606 0.0 0.0 0.0 0.0 9.023989278 0.0

****

* Core cell input

****

*Level 1

COR10103 764.0 764.0 764.0 764.0 764.0 0.0 764.0 764.0 0.0

COR10104 0.378027049 1.0 1.0 1.0 1.0 0.378027049 1.0 1.0

COR10106 0.0 0.0 0.0 0.0 4.005164002 0.0
COR101KSS 5143.957296 0.0 0.0 0.0
COR101KFU 0.0 0.0 0.0

COR20103 764.0 764.0 764.0 764.0 764.0 0.0 764.0 764.0 0.0
COR20104 0.378027049 1.0 1.0 1.0 1.0 0.378027049 1.0 1.0
COR20106 0.0 0.0 0.0 0.0 8.897047244 0.0
COR201KSS 2529.815064 0.0 0.0 0.0
COR201KFU 0.0 0.0 0.0

COR30103 764.0 764.0 764.0 764.0 764.0 0.0 764.0 764.0 0.0
COR30104 0.378027049 1.0 1.0 1.0 1.0 0.378027049 1.0 1.0
COR30106 0.0 0.0 0.0 0.0 10.67094382 0.0
COR301KSS 3035.778076 0.0 0.0 0.0
COR301KFU 0.0 0.0 0.0

COR40103 764.0 764.0 764.0 764.0 764.0 0.0 764.0 764.0 0.0
COR40104 0.378027049 1.0 1.0 1.0 1.0 0.378027049 1.0 1.0
COR40106 0.0 0.0 0.0 0.0 12.34376319 0.0
COR401KSS 3109.775483 0.0 0.0 0.0
COR401KFU 0.0 0.0 0.0

COR50103 764.0 764.0 764.0 764.0 764.0 0.0 764.0 764.0 0.0
COR50104 0.378027049 1.0 1.0 1.0 1.0 0.378027049 1.0 1.0
COR50106 0.0 0.0 0.0 0.0 15.58623428 0.0
COR501KSS 12279.27957 0.0 0.0 0.0
COR501KFU 0.0 0.0 0.0

*The default value of supporting structure is PLATEG with a default

*failure type of overtemperature at 1273.15 K.

*Level 6
COR10603 764.0 764.0 764.0 764.0 764.0 0.0 764.0 764.0 0.0
COR10604 0.378027049 1.0 1.0 1.0 1.0 2.952485636 1.0 1.0
COR106KFU 0.0 0.0 0.0

COR20603 764.0 764.0 764.0 764.0 764.0 0.0 764.0 764.0 0.0
COR20604 0.378027049 1.0 1.0 1.0 1.0 3.606148211 1.0 1.0
COR206KFU 0.0 0.0 0.0

COR30603 764.0 764.0 764.0 764.0 764.0 0.0 764.0 764.0 0.0
COR30604 0.378027049 1.0 1.0 1.0 1.0 4.260148485 1.0 1.0
COR306KFU 0.0 0.0 0.0

COR40603 764.0 764.0 764.0 764.0 764.0 0.0 764.0 764.0 0.0
COR40604 0.378027049 1.0 1.0 1.0 1.0 4.8393 1.0 1.0
COR406KFU 0.0 0.0 0.0

COR50603 764.0 764.0 764.0 764.0 764.0 0.0 764.0 764.0 0.0
COR50604 0.378027049 1.0 1.0 1.0 1.0 6.6504 1.0 1.0
COR506KFU 0.0 0.0 0.0

*Level 7
COR107SS PLATEG TSFAIL 1700.0
COR207SS PLATEG TSFAIL 1700.0
COR307SS PLATEG TSFAIL 1700.0
COR407SS PLATEG TSFAIL 1700.0
COR507SS PLATEG TSFAIL 1700.0

COR108SS PLATEG TSFAIL 1700.0
COR208SS PLATEG TSFAIL 1700.0
COR308SS PLATEG TSFAIL 1700.0
COR408SS PLATEG TSFAIL 1700.0
COR508SS PLATEG TSFAIL 1700.0

COR109SS PLATEG TSFAIL 1700.0
COR209SS PLATEG TSFAIL 1700.0
COR309SS PLATEG TSFAIL 1700.0
COR409SS PLATEG TSFAIL 1700.0
COR509SS PLATEG TSFAIL 1700.0

COR110SS PLATEG TSFAIL 1700.0
COR210SS PLATEG TSFAIL 1700.0
COR310SS PLATEG TSFAIL 1700.0
COR410SS PLATEG TSFAIL 1700.0
COR510SS PLATEG TSFAIL 1700.0

COR10703 764.0 764.0 764.0 764.0 764.0 0.0 764.0 764.0 0.0
COR10704 0.378027049 1.0 1.0 1.0 1.0 0.378027049 1.0 1.0
COR10706 0.0 0.0 0.0 0.0 10.52187015 0.0
COR107KSS 4720.456412 0.0 0.0 0.0
COR107KFU 0.0 0.0 0.0

COR20703 764.0 764.0 764.0 764.0 764.0 0.0 764.0 764.0 0.0
COR20704 0.378027049 1.0 1.0 1.0 1.0 0.378027049 1.0 1.0
COR20706 0.0 0.0 0.0 0.0 72.13636326 0.0
COR207KSS 1909.847866 0.0 0.0 0.0

COR207KFU 0.0 0.0 0.0

COR30703 764.0 764.0 764.0 764.0 764.0 0.0 764.0 764.0 0.0
COR30704 0.378027049 1.0 1.0 1.0 1.0 0.378027049 1.0 1.0
COR30706 0.0 0.0 0.0 0.0 88.03083404 0.0
COR307KSS 2276.492165 0.0 0.0 0.0
COR307KFU 0.0 0.0 0.0

COR40703 764.0 764.0 764.0 764.0 764.0 0.0 764.0 764.0 0.0
COR40704 0.378027049 1.0 1.0 1.0 1.0 0.378027049 1.0 1.0
COR40706 0.0 0.0 0.0 0.0 88.61280662 0.0
COR407KSS 2355.344005 0.0 0.0 0.0
COR407KFU 0.0 0.0 0.0

COR50703 764.0 764.0 764.0 764.0 764.0 0.0 764.0 764.0 0.0
COR50704 0.378027049 1.0 1.0 1.0 1.0 0.378027049 1.0 1.0
COR50706 0.0 0.0 0.0 0.0 30.64636999 0.0
COR507KSS 11268.32916 0.0 0.0 0.0
COR507KFU 0.0 0.0 0.0

*Level 11
COR111SS PLATEG TSFAIL 1700.0
COR211SS PLATEG TSFAIL 1700.0
COR311SS PLATEG TSFAIL 1700.0
COR411SS PLATEG TSFAIL 1700.0
COR511SS PLATEG TSFAIL 1700.0

COR112SS PLATEG TSFAIL 1700.0
COR212SS PLATEG TSFAIL 1700.0

COR312SS PLATEG TSFAIL 1700.0
COR412SS PLATEG TSFAIL 1700.0
COR512SS PLATEG TSFAIL 1700.0

COR113SS PLATEG TSFAIL 1700.0
COR213SS PLATEG TSFAIL 1700.0
COR313SS PLATEG TSFAIL 1700.0
COR413SS PLATEG TSFAIL 1700.0
COR513SS PLATEG TSFAIL 1700.0

COR114SS PLATEG TSFAIL 1700.0
COR214SS PLATEG TSFAIL 1700.0
COR314SS PLATEG TSFAIL 1700.0
COR414SS PLATEG TSFAIL 1700.0
COR514SS PLATEG TSFAIL 1700.0

COR11103 764.0 764.0 764.0 764.0 764.0 0.0 764.0 764.0 0.0
COR11104 0.378027049 1.0 1.0 1.0 1.0 0.378027049 1.0 1.0
COR11106 0.0 0.0 0.0 0.0 10.52418903 0.0
COR111KSS 4723.434617 0.0 0.0 0.0
COR111KFU 0.0 0.0 0.0

COR21103 764.0 764.0 764.0 764.0 764.0 0.0 764.0 764.0 0.0
COR21104 0.378027049 1.0 1.0 1.0 1.0 0.378027049 0.1016 1.0
COR21106 93.97991166 156.3481341 0.0 0.0 15.20864773 2.13565233
COR211KCL 1196.981901 0.0 0.0
COR211KSS 105.7972672 0.0 0.0 0.0
COR211KNS 0.0 15.37861886 0.0 0.0 0.0
COR211KFU 1.0e-6 0.0 585.1698736

COR31103 764.0 764.0 764.0 764.0 764.0 0.0 764.0 764.0 0.0

COR31104 0.378027049 1.0 1.0 1.0 1.0 0.378027049 0.09525 1.0

COR31106 115.3812776 192.3024287 0.0 0.0 17.1865404 2.562782796

COR311KCL 1518.005733 0.0 0.0

COR311KSS 63.42315792 0.0 0.0 0.0

COR311KNS 0.0 18.45434263 0.0 0.0 0.0

COR311KFU 1.0e-6 0.0 721.8263111

COR41103 764.0 764.0 764.0 764.0 764.0 0.0 764.0 764.0 0.0

COR41104 0.378027049 1.0 1.0 1.0 1.0 0.378027049 0.09525 1.0

COR41106 113.5202893 188.9562375 0.0 0.0 19.50610113 2.562782796

COR411KCL 1537.843012 0.0 0.0

COR411KSS 105.5764125 0.0 0.0 0.0

COR411KNS 0.0 18.45434263 0.0 0.0 0.0

COR411KFU 1.0e-6 0.0 707.8102663

COR51103 764.0 764.0 764.0 764.0 764.0 0.0 764.0 764.0 0.0

COR51104 0.378027049 1.0 1.0 1.0 1.0 0.378027049 0.1016 1.0

COR51106 0.0 0.0 0.0 0.0 34.91958841 0.0

COR511KSS 11074.07877 0.0 0.0 0.0

COR511KNS 0.0 0.0 0.0 0.0 0.0

COR511KFU 0.0 0.0 0.0

*Level 15

COR115SS PLATEG TSFAIL 1700.0

COR215SS PLATEG TSFAIL 1700.0

COR315SS PLATEG TSFAIL 1700.0

COR415SS PLATEG TSFAIL 1700.0

COR515SS PLATEG TSFAIL 1700.0

COR116SS PLATEG TSFAIL 1700.0
COR216SS PLATEG TSFAIL 1700.0
COR316SS PLATEG TSFAIL 1700.0
COR416SS PLATEG TSFAIL 1700.0
COR516SS PLATEG TSFAIL 1700.0

COR117SS PLATEG TSFAIL 1700.0
COR217SS PLATEG TSFAIL 1700.0
COR317SS PLATEG TSFAIL 1700.0
COR417SS PLATEG TSFAIL 1700.0
COR517SS PLATEG TSFAIL 1700.0

COR118SS PLATEG TSFAIL 1700.0
COR218SS PLATEG TSFAIL 1700.0
COR318SS PLATEG TSFAIL 1700.0
COR418SS PLATEG TSFAIL 1700.0
COR518SS PLATEG TSFAIL 1700.0

COR11503 764.0 764.0 764.0 764.0 764.0 0.0 764.0 764.0 0.0
COR11504 0.378027049 1.0 1.0 1.0 1.0 0.378027049 1.0 1.0
COR11506 0.0 0.0 0.0 0.0 10.52418903 0.0
COR115KSS 4723.434617 0.0 0.0 0.0
COR115KFU 0.0 0.0 0.0

COR21503 764.0 764.0 764.0 764.0 764.0 0.0 764.0 764.0 0.0
COR21504 0.378027049 1.0 1.0 1.0 1.0 0.378027049 0.1016 1.0
COR21506 93.97991166 156.3481341 0.0 0.0 15.20864773 2.13565233

COR215KCL 1196.981901 0.0 0.0

COR215KSS 105.7972672 0.0 0.0 0.0

COR215KNS 0.0 15.37861886 0.0 0.0 0.0

COR215KFU 1.0e-6 0.0 585.1698736

COR31503 764.0 764.0 764.0 764.0 764.0 0.0 764.0 764.0 0.0

COR31504 0.378027049 1.0 1.0 1.0 1.0 0.378027049 0.09525 1.0

COR31506 115.3812776 192.3024287 0.0 0.0 17.1865404 2.562782796

COR315KCL 1518.005733 0.0 0.0

COR315KSS 63.42315792 0.0 0.0 0.0

COR315KNS 0.0 18.45434263 0.0 0.0 0.0

COR315KFU 1.0e-6 0.0 721.8263111

COR41503 764.0 764.0 764.0 764.0 764.0 0.0 764.0 764.0 0.0

COR41504 0.378027049 1.0 1.0 1.0 1.0 0.378027049 0.09525 1.0

COR41506 113.5202893 188.9562375 0.0 0.0 19.50610113 2.562782796

COR415KCL 1537.843012 0.0 0.0

COR415KSS 105.5764125 0.0 0.0 0.0

COR415KNS 0.0 18.45434263 0.0 0.0 0.0

COR415KFU 1.0e-6 0.0 707.8102663

COR51503 764.0 764.0 764.0 764.0 764.0 0.0 764.0 764.0 0.0

COR51504 0.378027049 1.0 1.0 1.0 1.0 0.378027049 0.1016 1.0

COR51506 0.0 0.0 0.0 0.0 34.91958841 0.0

COR515KSS 11074.07877 0.0 0.0 0.0

COR515KNS 0.0 0.0 0.0 0.0 0.0

COR515KFU 0.0 0.0 0.0

*Level 19

COR119SS PLATEG TSFAIL 1700.0
COR219SS PLATEG TSFAIL 1700.0
COR319SS PLATEG TSFAIL 1700.0
COR419SS PLATEG TSFAIL 1700.0
COR519SS PLATEG TSFAIL 1700.0

COR120SS PLATEG TSFAIL 1700.0
COR220SS PLATEG TSFAIL 1700.0
COR320SS PLATEG TSFAIL 1700.0
COR420SS PLATEG TSFAIL 1700.0
COR520SS PLATEG TSFAIL 1700.0

COR121SS PLATEG TSFAIL 1700.0
COR221SS PLATEG TSFAIL 1700.0
COR321SS PLATEG TSFAIL 1700.0
COR421SS PLATEG TSFAIL 1700.0
COR521SS PLATEG TSFAIL 1700.0

COR122SS PLATEG TSFAIL 1700.0
COR222SS PLATEG TSFAIL 1700.0
COR322SS PLATEG TSFAIL 1700.0
COR422SS PLATEG TSFAIL 1700.0
COR522SS PLATEG TSFAIL 1700.0

COR11903 764.0 764.0 764.0 764.0 764.0 0.0 764.0 764.0 0.0
COR11904 0.378027049 1.0 1.0 1.0 1.0 0.378027049 1.0 1.0
COR11906 0.0 0.0 0.0 0.0 10.52418903 0.0
COR119KSS 4723.434617 0.0 0.0 0.0
COR119KFU 0.0 0.0 0.0

COR21903 764.0 764.0 764.0 764.0 764.0 0.0 764.0 764.0 0.0

COR21904 0.378027049 1.0 1.0 1.0 1.0 0.378027049 0.1016 1.0

COR21906 93.97991166 156.3481341 0.0 0.0 15.20864773 2.13565233

COR219KCL 1196.981901 0.0 0.0

COR219KSS 105.7972672 0.0 0.0 0.0

COR219KNS 0.0 15.37861886 0.0 0.0 0.0

COR219KFU 1.0e-6 0.0 585.1698736

COR31903 764.0 764.0 764.0 764.0 764.0 0.0 764.0 764.0 0.0

COR31904 0.378027049 1.0 1.0 1.0 1.0 0.378027049 0.09525 1.0

COR31906 115.3812776 192.3024287 0.0 0.0 17.1865404 2.562782796

COR319KCL 1518.005733 0.0 0.0

COR319KSS 63.42315792 0.0 0.0 0.0

COR319KNS 0.0 18.45434263 0.0 0.0 0.0

COR319KFU 1.0e-6 0.0 721.8263111

COR41903 764.0 764.0 764.0 764.0 764.0 0.0 764.0 764.0 0.0

COR41904 0.378027049 1.0 1.0 1.0 1.0 0.378027049 0.09525 1.0

COR41906 113.5202893 188.9562375 0.0 0.0 19.50610113 2.562782796

COR419KCL 1537.843012 0.0 0.0

COR419KSS 105.5764125 0.0 0.0 0.0

COR419KNS 0.0 18.45434263 0.0 0.0 0.0

COR419KFU 1.0e-6 0.0 707.8102663

COR51903 764.0 764.0 764.0 764.0 764.0 0.0 764.0 764.0 0.0

COR51904 0.378027049 1.0 1.0 1.0 1.0 0.378027049 0.1016 1.0

COR51906 0.0 0.0 0.0 0.0 34.91958841 0.0

COR519KSS 11074.07877 0.0 0.0 0.0

COR519KNS 0.0 0.0 0.0 0.0 0.0
COR519KFU 0.0 0.0 0.0

*level 21
COR12103 764.0 764.0 764.0 764.0 764.0 0.0 764.0 764.0 0.0
COR12104 0.378027049 1.0 1.0 1.0 1.0 0.378027049 1.0 1.0
COR12106 0.0 0.0 0.0 0.0 10.52418903 0.0
COR121KSS 4723.434617 0.0 0.0 0.0
COR121KFU 0.0 0.0 0.0

COR22103 764.0 764.0 764.0 764.0 764.0 0.0 764.0 764.0 0.0
COR22104 0.378027049 1.0 1.0 1.0 1.0 0.378027049 0.1016 1.0
COR22106 93.97991166 156.3481341 0.0 0.0 15.20864773 4.159570618
COR221KCL 1196.981901 0.0 0.0
COR221KSS 105.7972672 0.0 0.0 0.0
COR221KNS 0.0 53.37566081 0.0 0.0 0.0
COR221KFU 1.0e-6 0.0 585.1698736

COR32103 764.0 764.0 764.0 764.0 764.0 0.0 764.0 764.0 0.0
COR32104 0.378027049 1.0 1.0 1.0 1.0 0.378027049 0.09525 1.0
COR32106 115.3812776 192.3024287 0.0 0.0 17.1865404 2.562782796
COR321KCL 1518.005733 0.0 0.0
COR321KSS 63.42315792 0.0 0.0 0.0
COR321KNS 0.0 18.45434263 0.0 0.0 0.0
COR321KFU 1.0e-6 0.0 721.8263111

COR42103 764.0 764.0 764.0 764.0 764.0 0.0 764.0 764.0 0.0
COR42104 0.378027049 1.0 1.0 1.0 1.0 0.378027049 0.09525 1.0
COR42106 113.5202893 188.9562375 0.0 0.0 19.50610113 2.562782796

COR421KCL 1537.843012 0.0 0.0

COR421KSS 105.5764125 0.0 0.0 0.0

COR421KNS 0.0 18.45434263 0.0 0.0 0.0

COR421KFU 1.0e-6 0.0 707.8102663

COR52103 764.0 764.0 764.0 764.0 764.0 0.0 764.0 764.0 0.0

COR52104 0.378027049 1.0 1.0 1.0 1.0 0.378027049 0.1016 1.0

COR52106 0.0 0.0 0.0 0.0 34.91958841 6.071754865

COR521KSS 11074.07877 0.0 0.0 0.0

COR521KNS 0.0 113.9911258 0.0 0.0 0.0

COR521KFU 0.0 0.0 0.0

*Level 23

COR123SS PLATEG TSFAIL 1700.0

COR223SS PLATEG TSFAIL 1700.0

COR323SS PLATEG TSFAIL 1700.0

COR423SS PLATEG TSFAIL 1700.0

COR523SS PLATEG TSFAIL 1700.0

COR124SS PLATEG TSFAIL 1700.0

COR224SS PLATEG TSFAIL 1700.0

COR324SS PLATEG TSFAIL 1700.0

COR424SS PLATEG TSFAIL 1700.0

COR524SS PLATEG TSFAIL 1700.0

COR125SS PLATEG TSFAIL 1700.0

COR225SS PLATEG TSFAIL 1700.0

COR325SS PLATEG TSFAIL 1700.0

COR425SS PLATEG TSFAIL 1700.0

COR525SS PLATEG TSFAIL 1700.0

COR126SS PLATEG TSFAIL 1700.0
COR226SS PLATEG TSFAIL 1700.0
COR326SS PLATEG TSFAIL 1700.0
COR426SS PLATEG TSFAIL 1700.0
COR526SS PLATEG TSFAIL 1700.0

COR12303 764.0 764.0 764.0 764.0 764.0 0.0 764.0 764.0 0.0
COR12304 0.378027049 1.0 1.0 1.0 1.0 0.378027049 1.0 1.0
COR12306 0.0 0.0 0.0 0.0 10.52418903 0.0
COR123KSS 4723.434617 0.0 0.0 0.0
COR123KFU 0.0 0.0 0.0

COR22303 764.0 764.0 764.0 764.0 764.0 0.0 764.0 764.0 0.0
COR22304 0.378027049 1.0 1.0 1.0 1.0 0.378027049 0.1016 1.0
COR22306 93.97991166 156.3481341 0.0 0.0 15.20864773 4.159570618
COR223KCL 1196.981901 0.0 0.0
COR223KSS 105.7972672 0.0 0.0 0.0
COR223KNS 0.0 53.37566081 0.0 0.0 0.0
COR223KFU 1.0e-6 0.0 585.1698736

COR32303 764.0 764.0 764.0 764.0 764.0 0.0 764.0 764.0 0.0
COR32304 0.378027049 1.0 1.0 1.0 1.0 0.378027049 0.09525 1.0
COR32306 115.3812776 192.3024287 0.0 0.0 17.1865404 2.562782796
COR323KNS 0.0 18.45434263 0.0 0.0 0.0
COR323KCL 1518.005733 0.0 0.0
COR323KSS 63.42315792 0.0 0.0 0.0
COR323KFU 1.0e-6 0.0 721.8263111

COR42303 764.0 764.0 764.0 764.0 764.0 0.0 764.0 764.0 0.0

COR42304 0.378027049 1.0 1.0 1.0 1.0 0.378027049 0.09525 1.0

COR42306 113.5202893 188.9562375 0.0 0.0 19.50610113 2.562782796

COR423KCL 1537.843012 0.0 0.0

COR423KSS 105.5764125 0.0 0.0 0.0

COR423KNS 0.0 18.45434263 0.0 0.0 0.0

COR423KFU 1.0e-6 0.0 707.8102663

COR52303 764.0 764.0 764.0 764.0 764.0 0.0 764.0 764.0 0.0

COR52304 0.378027049 1.0 1.0 1.0 1.0 0.378027049 0.1016 1.0

COR52306 0.0 0.0 0.0 0.0 34.91958841 6.071754865

COR523KSS 11074.07877 0.0 0.0 0.0

COR523KNS 0.0 113.9911258 0.0 0.0 0.0

COR523KFU 0.0 0.0 0.0

*Level 27

COR127SS PLATEG TSFAIL 1700.0

COR227SS PLATEG TSFAIL 1700.0

COR327SS PLATEG TSFAIL 1700.0

COR427SS PLATEG TSFAIL 1700.0

COR527SS PLATEG TSFAIL 1700.0

COR128SS PLATEG TSFAIL 1700.0

COR228SS PLATEG TSFAIL 1700.0

COR328SS PLATEG TSFAIL 1700.0

COR428SS PLATEG TSFAIL 1700.0

COR528SS PLATEG TSFAIL 1700.0

COR129SS PLATEG TSFAIL 1700.0
COR229SS PLATEG TSFAIL 1700.0
COR329SS PLATEG TSFAIL 1700.0
COR429SS PLATEG TSFAIL 1700.0
COR529SS PLATEG TSFAIL 1700.0

COR130SS PLATEG TSFAIL 1700.0
COR230SS PLATEG TSFAIL 1700.0
COR330SS PLATEG TSFAIL 1700.0
COR430SS PLATEG TSFAIL 1700.0
COR530SS PLATEG TSFAIL 1700.0

COR12703 764.0 764.0 764.0 764.0 764.0 0.0 764.0 764.0 0.0
COR12704 0.378027049 1.0 1.0 1.0 1.0 0.378027049 1.0 1.0
COR12706 0.0 0.0 0.0 0.0 10.52418903 0.0
COR127KSS 4723.434617 0.0 0.0 0.0
COR127KFU 0.0 0.0 0.0

COR22703 764.0 764.0 764.0 764.0 764.0 0.0 764.0 764.0 0.0
COR22704 0.378027049 1.0 1.0 1.0 1.0 0.378027049 0.1016 1.0
COR22706 93.97991166 156.3481341 0.0 0.0 15.20864773 4.159570618
COR227KCL 1196.981901 0.0 0.0
COR227KSS 105.7972672 0.0 0.0 0.0
COR227KNS 0.0 53.37566081 0.0 0.0 0.0
COR227KFU 1.0e-6 0.0 585.1698736

COR32703 764.0 764.0 764.0 764.0 764.0 0.0 764.0 764.0 0.0
COR32704 0.378027049 1.0 1.0 1.0 1.0 0.378027049 0.09525 1.0
COR32706 115.3812776 192.3024287 0.0 0.0 17.1865404 2.562782796

COR327KCL 1518.005733 0.0 0.0

COR327KSS 63.42315792 0.0 0.0 0.0

COR327KNS 0.0 18.45434263 0.0 0.0 0.0

COR327KFU 1.0e-6 0.0 721.8263111

COR42703 764.0 764.0 764.0 764.0 764.0 0.0 764.0 764.0 0.0

COR42704 0.378027049 1.0 1.0 1.0 1.0 0.378027049 0.09525 1.0

COR42706 113.5202893 188.9562375 0.0 0.0 19.50610113 2.562782796

COR427KCL 1537.843012 0.0 0.0

COR427KSS 105.5764125 0.0 0.0

COR427KNS 0.0 18.45434263 0.0 0.0 0.0

COR427KFU 1.0e-6 0.0 707.8102663

COR52703 764.0 764.0 764.0 764.0 764.0 0.0 764.0 764.0 0.0

COR52704 0.378027049 1.0 1.0 1.0 1.0 0.378027049 0.1016 1.0

COR52706 0.0 0.0 0.0 0.0 34.91958841 6.071754865

COR527KSS 11074.07877 0.0 0.0 0.0

COR527KNS 0.0 113.9911258 0.0 0.0 0.0

COR527KFU 0.0 0.0 0.0

*Level 31

COR13103 764.0 764.0 764.0 764.0 764.0 0.0 764.0 764.0 0.0

COR13104 0.378027049 1.0 1.0 1.0 1.0 0.378027049 1.0 1.0

COR13106 0.0 0.0 0.0 0.0 10.52233393 0.0

COR131KSS 4721.052053 0.0 0.0 0.0

COR131KFU 0.0 0.0 0.0

COR23103 764.0 764.0 764.0 764.0 764.0 0.0 764.0 764.0 0.0

COR23104 0.378027049 1.0 1.0 1.0 1.0 0.378027049 1.0 1.0

COR23106 0.0 0.0 0.0 0.0 73.56574834 2.022897396
COR231KSS 1843.002861 0.0 0.0 0.0
COR231KNS 0.0 37.97787572 0.0 0.0 0.0
COR231KFU 0.0 0.0 0.0

COR33103 764.0 764.0 764.0 764.0 764.0 0.0 764.0 764.0 0.0
COR33104 0.378027049 1.0 1.0 1.0 1.0 0.378027049 1.0 1.0
COR33106 0.0 0.0 0.0 0.0 84.73974918 0.0
COR331KSS 2247.29827 0.0 0.0 0.0
COR331KNS 0.0 0.0 0.0 0.0 0.0
COR331KFU 0.0 0.0 0.0

COR43103 764.0 764.0 764.0 764.0 764.0 0.0 764.0 764.0 0.0
COR43104 0.378027049 1.0 1.0 1.0 1.0 0.378027049 1.0 1.0
COR43106 0.0 0.0 0.0 0.0 89.96110015 0.0
COR431KSS 2296.678909 0.0 0.0 0.0
COR431KNS 0.0 0.0 0.0 0.0 0.0
COR431KFU 0.0 0.0 0.0

COR53103 764.0 764.0 764.0 764.0 764.0 0.0 764.0 764.0 0.0
COR53104 0.378027049 1.0 1.0 1.0 1.0 0.378027049 1.0 1.0
COR53106 0.0 0.0 0.0 0.0 34.91007144 6.068692189
COR531KSS 11068.49305 0.0 0.0 0.0
COR531KNS 0.0 113.9336272 0.0 0.0 0.0
COR531KFU 0.0 0.0 0.0

*Level 33
COR13303 764.0 764.0 764.0 764.0 764.0 0.0 764.0 764.0 0.0
COR13304 0.378027049 1.0 1.0 1.0 1.0 0.378027049 1.0 1.0

COR13306 0.0 0.0 0.0 0.0 10.52326148 0.0

COR133KSS 4722.243335 0.0 0.0 0.0

COR133KNS 0.0 0.0 0.0 0.0 0.0

COR133KFU 0.0 0.0 0.0

COR23303 764.0 764.0 764.0 764.0 764.0 0.0 764.0 764.0 0.0

COR23304 0.378027049 1.0 1.0 1.0 1.0 0.378027049 1.0 1.0

COR23306 0.0 0.0 0.0 0.0 73.58363707 2.023407842

COR233KSS 1843.467914 0.0 0.0 0.0

COR233KNS 0.0 37.98745883 0.0 0.0 0.0

COR233KFU 0.0 0.0 0.0

COR33303 764.0 764.0 764.0 764.0 764.0 0.0 764.0 764.0 0.0

COR33304 0.378027049 1.0 1.0 1.0 1.0 0.378027049 1.0 1.0

COR33306 0.0 0.0 0.0 0.0 88.73167972 0.0

COR333KSS 2247.86534 0.0 0.0 0.0

COR333KNS 0.0 0.0 0.0 0.0 0.0

COR333KFU 0.0 0.0 0.0

COR43303 764.0 764.0 764.0 764.0 764.0 0.0 764.0 764.0 0.0

COR43304 0.378027049 1.0 1.0 1.0 1.0 0.378027049 1.0 1.0

COR43306 0.0 0.0 0.0 0.0 89.98260089 0.0

COR433KSS 2297.25844 0.0 0.0 0.0

COR433KNS 0.0 0.0 0.0 0.0 0.0

COR433KFU 0.0 0.0 0.0

COR53303 764.0 764.0 764.0 764.0 764.0 0.0 764.0 764.0 0.0

COR53304 0.378027049 1.0 1.0 1.0 1.0 0.378027049 1.0 1.0

COR53306 0.0 0.0 0.0 0.0 34.91483011 6.070223527

COR533KSS 11071.286 0.0 0.0 0.0
COR533KNS 0.0 113.9623765 0.0 0.0 0.0
COR533KFU 0.0 0.0 0.0

*Cell boundaries and flow areas
COR10105 4.005164002 0.123523844 0.0
COR20105 4.891883242 0.597103701 0.0
COR30105 5.77906058 0.738751896 0.0
COR40105 6.564702608 0.722875143 0.0
COR50105 9.021531673 0.288222304 0.0

COR10605 2.318876796 0.123523844 0.0
COR20605 2.832262183 0.597103701 0.0
COR30605 3.345912795 0.738751896 0.0
COR40605 3.800777332 0.722875143 0.0
COR50605 5.223211946 0.288222304 0.0

COR10705 3.675419722 0.123523844 0.0
COR20705 4.489135559 0.597103701 0.0
COR30705 5.30327178 0.738751896 0.0
COR40705 6.024232071 0.722875143 0.0
COR50705 8.278790934 0.288222304 0.0

COR11105 3.677738598 0.123523844 0.0
COR21105 4.491967822 0.597103701 0.0
COR31105 5.306617693 0.738751896 0.0
COR41105 6.028032849 0.722875143 0.0
COR51105 8.284014146 0.288222304 0.0

COR11505 3.677738598 0.123523844 0.0
COR21505 4.491967822 0.597103701 0.0
COR31505 5.306617693 0.738751896 0.0
COR41505 6.028032849 0.722875143 0.0
COR51505 8.284014146 0.288222304 0.0

COR11905 3.677738598 0.123523844 0.0
COR21905 4.491967822 0.597103701 0.0
COR31905 5.306617693 0.738751896 0.0
COR41905 6.028032849 0.722875143 0.0
COR51905 8.284014146 0.288222304 0.0

COR12105 3.677738598 0.123523844 0.0
COR22105 4.491967822 0.597103701 0.0
COR32105 5.306617693 0.738751896 0.0
COR42105 6.028032849 0.722875143 0.0
COR52105 8.284014146 0.288222304 0.0

COR12305 3.677738598 0.123523844 0.0
COR22305 4.491967822 0.597103701 0.0
COR32305 5.306617693 0.738751896 0.0
COR42305 6.028032849 0.722875143 0.0
COR52305 8.284014146 0.288222304 0.0

COR12705 3.677738598 0.123523844 0.0
COR22705 4.491967822 0.597103701 0.0
COR32705 5.306617693 0.738751896 0.0
COR42705 6.028032849 0.722875143 0.0
COR52705 8.284014146 0.288222304 0.0

COR13105 3.675883497 0.123523844 0.0
COR23105 4.489702012 0.597103701 0.0
COR33105 5.303940963 0.738751896 0.0
COR43105 6.024992227 0.722875143 0.0
COR53105 8.279835577 0.288222304 0.0

COR13305 3.676811048 0.123523844 0.0
COR23305 4.490834917 0.597103701 0.0
COR33305 5.305279328 0.738751896 0.0
COR43305 6.026512538 0.722875143 0.0
COR53305 8.281924861 0.288222304 0.0

*Lower head input
CORLHD01 1 764.0 1.476242818 050
CORLHD02 2 764.0 1.803074106 050
CORLHD03 3 764.0 2.130074242 050
CORLHD04 4 764.0 2.41965 050
CORLHD05 5 764.0 3.3252 050
CORLHD06 6 764.0 3.3252 050
CORLHD07 7 764.0 3.3252 050
CORLHD08 8 764.0 3.3252 050
CORLHD09 9 764.0 3.3252 050
CORLHD10 10 764.0 3.3252 050

*Extra fuel material record
CORXFUMAT INC

*Core material

CORMATa UO2 'URANIUM-DIOXIDE'
CORMATb SS 'STAINLESS-STEEL'
CORMATc ZR 'ZIRCALOY'

CORCLMAT ZR
.

A.2.5 ncg-mp-new.gen

* Definitions of noncondensible gases
NCG000 HE 4
NCG001 O2 5
NCG002 N2 6
NCG003 CO2 7
NCG004 CH4 8
NCG005 H2 9
NCG006 CO 10

****
* Helium properties
****
MPMAT00100 HELIUM

MPMAT00101 RHO 1
MPMAT00102 CPS 2
MPMAT00103 THC 3

*@ 7.0 MPa
TF00100 'RHO-HELIUM' 9 1.00 0.0

TF00112 700.0 4.757
TF00113 800.0 4.169
TF00114 900.0 3.711
TF00115 1000.0 3.343
TF00116 1100.0 3.042
TF00117 1200.0 2.79
TF00118 1300.0 2.577
TF00119 1400.0 2.394
TF00120 1500.0 2.235

*@ 7.0 MPa
TF00200 ’CPS-HELIUM’ 9 1.00 0.0
TF00212 700.0 5188.0
TF00213 800.0 5189.0
TF00214 900.0 5189.0
TF00215 1000.0 5190.0
TF00216 1100.0 5190.0
TF00217 1200.0 5190.0
TF00218 1300.0 5191.0
TF00219 1400.0 5191.0
TF00220 1500.0 5191.0

*@ 7.0 MPa
TF00300 ’THC-HELIUM’ 9 1.00 0.0
TF00312 700.0 0.2847
TF00313 800.0 0.3121
TF00314 900.0 0.3385
TF00315 1000.0 0.364
TF00316 1100.0 0.3888

TF00317 1200.0 0.413
TF00318 1300.0 0.4365
TF00319 1400.0 0.4596
TF00320 1500.0 0.4821

****
* Air properties
****
MPMAT00200 OXYGEN

MPMAT00201 RHO 4
MPMAT00202 CPS 5
MPMAT00203 THC 6

*@ 0.1MPA
TF00400 ’RHO-OXYGEN’ 5 1.00 0.0
TF00412 200.00 1.764995923
TF00413 400.00 0.882497961
TF00414 600.00 0.588331974
TF00415 800.00 0.441248981
TF00416 1000.00 0.352999185

*@ 0.1MPA
TF00500 ’CPS-OXYGEN’ 3 1.00 0.0
TF00512 300.00 1007.0
TF00513 1000.00 1141.0
TF00514 1500.00 1230.0

*@ 0.1MPA

TF00600 ’THC-OXYGEN’ 7 1.00 0.0

TF00612 255.370 0.0227081

TF00613 310.926 0.0270005

TF00614 366.482 0.0311544

TF00615 422.038 0.0360006

TF00616 477.594 0.0399815

TF00617 533.150 0.0425777

TF00618 588.706 0.0458662

****

* Fuel rod properties

* [replaces INC]

****

MPMAT00300 ’INC’

MPMAT00301 ENH 100

MPMAT00302 TMP 101

MPMAT00303 CPS 102

MPMAT00304 THC 103

MPMAT00305 RHO 104

MPMAT00350 DEN 1831.98

MPMAT00351 MLT 2900.0

MPMAT00352 LHF 1.0E3

*enthalphy(temp)

TF10000 ’FUEL-ENH’ 3 1.0 0.0

TF10001 1 1

TF10010 300.0 0.0

TF10011 500.0 345000.0

TF10012 900.0 1035000.0

*temp(enthalpy)
TF10100 ’FUEL-TMP’ 3 1.0 0.0
TF10101 1 1
TF10110 0.0 300.0
TF10111 345000.0 500.0
TF10112 1035000.0 900.0

*specific heat(temp)
TF10200 ’FUEL-SpcHt’ 3 1.0 0.0
TF10210 300.0 1725.0
TF10211 500.0 1725.0
TF10212 900.0 1725.0

*thermal conductivity(temp)
TF10300 ’FUEL-ThermCond’ 3 1.0 0.0
TF10310 300.0 20.0
TF10311 500.0 20.0
TF10312 900.0 20.0

*density(temp)
TF10400 ’FUEL-RHO’ 3 1.0 0.0
TF10410 300.0 1831.98
TF10411 500.0 1831.98
TF10412 900.0 1831.98

****
* Graphite block properties

```
* [replaces ZIRCALOY]
**********

MPMAT00400   'ZIRCALOY'

MPMAT00401   ENH         200
MPMAT00402   TMP         201
MPMAT00403   CPS         202
MPMAT00404   THC         203
MPMAT00405   RHO         204
MPMAT00450   DEN         1740.0
MPMAT00451   MLT         3866.0
MPMAT00452   LHF         1.0E3

*enthalphy(temp)
TF20000   'MOD-ENH' 12 1.0 0.0
TF20001   1 1
TF20010   750.0  719730.0
TF20011   800.0         822700.0
TF20012   850.0  925705.0
TF20013   900.0         1027440.0
TF20014   950.0         1129375.0
TF20015   1000.0  1233820.0
TF20016   1100.0  1446960.0
TF20017   1200.0  1669230.0
TF20018   1300.0  1892400.0
TF20019   1400.0  2118490.0
TF20020   1500.0  2351280.0
TF20021   1600.0  2579850.0
```

*temp(enthalpy)
TF20100 'MOD-TMP' 12 1.0 0.0
TF20101 1 1
TF20110 719730.0 750.0
TF20111 822700.0 800.0
TF20112 925705.0 850.0
TF20113 1027440.0 900.0
TF20114 1129375.0 950.0
TF20115 1233820.0 1000.0
TF20116 1446960.0 1100.0
TF20117 1669230.0 1200.0
TF20118 1892400.0 1300.0
TF20119 2118490.0 1400.0
TF20120 2351280.0 1500.0
TF20121 2579850.0 1600.0

*specific heat(temp)
TF20200 ’mod-SpcHt’ 12 1.0 0.0
TF20210 750.0 1599.4
TF20211 800.0 1645.4
TF20212 850.0 1683.1
TF20213 900.0 1712.4
TF20214 950.0 1737.5
TF20215 1000.0 1762.6
TF20216 1100.0 1808.7
TF20217 1200.0 1854.7
TF20218 1300.0 1892.4
TF20219 1400.0 1925.9

```
TF20220 1500.0 1959.4
TF20221 1600.0 1984.5

*thermal conductivity(temp)
TF20300   'MOD-ThermCond' 11 1.0 0.0
TF20310   673.0  75.6
TF20311   773.0  70.0
TF20312   800.0  69.6
TF20313   900.0  64.0
TF20314   1000.0  59.3
TF20315   1100.0  55.4
TF20316   1200.0  52.0
TF20317   1300.0  49.1
TF20318   1400.0  46.6
TF20319   1500.0  44.3
TF20320   1600.0  42.3

*density(temp)
TF20400   'MOD-RHO' 3 1.0 0.0
TF20410   300.0  1740.0
TF20411   500.0  1740.0
TF20412   900.0  1740.0

**********************************
* supporting structure properties
* [replaces STAINLESS-STEEL]
**********************************

MPMAT00500   'STAINLESS-STEEL'
```

```
MPMAT00501   ENH         200
MPMAT00502   TMP         201
MPMAT00503   CPS         202
MPMAT00504   THC         203
MPMAT00505   RHO         204
MPMAT00550   DEN         1740.0
MPMAT00551   MLT         3866.0
MPMAT00552   LHF         1.0E3

*enthalphy(temp)
TF30000   'MOD-ENH' 12 1.0 0.0
TF30001   1 1
TF30010   750.0  719730.0
TF30011   800.0         822700.0
TF30012   850.0  925705.0
TF30013   900.0         1027440.0
TF30014   950.0         1129375.0
TF30015   1000.0  1233820.0
TF30016   1100.0  1446960.0
TF30017   1200.0  1669230.0
TF30018   1300.0  1892400.0
TF30019   1400.0  2118490.0
TF30020   1500.0  2351280.0
TF30021   1600.0  2579850.0

*temp(enthalpy)
TF30100   'MOD-TMP' 12 1.0 0.0
TF30101   1 1
```

TF30110 719730.0 750.0
TF30111 822700.0 800.0
TF30112 925705.0 850.0
TF30113 1027440.0 900.0
TF30114 1129375.0 950.0
TF30115 1233820.0 1000.0
TF30116 1446960.0 1100.0
TF30117 1669230.0 1200.0
TF30118 1892400.0 1300.0
TF30119 2118490.0 1400.0
TF30120 2351280.0 1500.0
TF30121 2579850.0 1600.0

*specific heat(temp)
TF30200 ’mod-SpcHt’ 12 1.0 0.0
TF30210 750.0 1599.4
TF30211 800.0 1645.4
TF30212 850.0 1683.1
TF30213 900.0 1712.4
TF30214 950.0 1737.5
TF30215 1000.0 1762.6
TF30216 1100.0 1808.7
TF30217 1200.0 1854.7
TF30218 1300.0 1892.4
TF30219 1400.0 1925.9
TF30220 1500.0 1959.4
TF30221 1600.0 1984.5

*thermal conductivity(temp)

```
TF30300   'MOD-ThermCond' 11 1.0 0.0
TF30310   673.0  75.6
TF30311   773.0  70.0
TF30312   800.0  69.6
TF30313   900.0  64.0
TF30314   1000.0  59.3
TF30315   1100.0  55.4
TF30316   1200.0  52.0
TF30317   1300.0  49.1
TF30318   1400.0  46.6
TF30319   1500.0  44.3
TF30320   1600.0  42.3

*density(temp)
TF30400   'MOD-RHO' 3 1.0 0.0
TF30410   300.0  1740.0
TF30411   500.0  1740.0
TF30412   900.0  1740.0
.
```

APPENDIX B: SIMPLIFIED NGNP RPV MODEL

B Input Decks

B pointdesign.gen

```
* Definitions of noncondensible gases
NCG000 HE 4 CV0 5231.0

*CV type definitions
CVTYPE01 CORCVH
CVTYPE02 upv
CVTYPE03 uplenum
CVTYPE04 cehgp
CVTYPE05 SRC
CVTYPE06 SNK

*upper plenum volume
CV17100 upv 2 0 2
CV17101 0 0
CV171A0 3
CV171A1 MLFR.4 1.0 TATM 1200.0 PVOL 7.0448e6 PH2O 0.0
CV171B0 9.369 0.0
CV171B1 9.774 14.06826
CV171B2 10.179 28.13652
CV171B3 10.584 42.20478
CV171B4 10.989 56.27305
CV171B5 11.394 70.34131
CV171B6 11.799 84.40957
```

```
*upper plenum
CV17000 uplenum 2 0 3
CV17001 0 0
CV170A0 3
CV170A1 MLFR.4 1.0 TATM 1200.0 PVOL 7.0368e6 PH2O 0.0
CV170B0 9.119 0.0
CV170B1 9.369 8.684112033

*core exit hot gas plenum
CV05400   cehgp 2 0 4
CV05401   0 0
CV054A0   3
CV054A1   MLFR.4 1.0 TATM 1200.0 PVOL 6.9968e6 PH2O 0.0
CV054B0   -3.744   0.0
CV054B1   -3.3122  14.9992
CV054B2   -2.8804  29.9984
CV054B3   -2.4486  44.99759
CV054B4   -2.0168  59.99679
CV054B5   -1.585   74.99599

**********************************
* CVH cells for the core
**********************************

*Ring 1
CV11000   COR110  2  0  1
CV11001   0  0
CV110A0   3
```

```
CV110A1   MLFR.4  1.0  TATM  1200.0  PVOL  7.0018e6  PH2O  0.0
CV110B0   -1.585   0.0
CV110B1   -1.18875  0.93622
CV110B2   -0.7925  1.87243
CV110B3   -0.39625  2.80865
CV110B4   0.0  3.74487

CV11100   COR111  2  0  1
CV11101   0  0
CV111A0   3
CV111A1   MLFR.4  1.0  TATM  1200.0  PVOL  7.0068e6  PH2O  0.0
CV111B0   0.0   0.0
CV111B1   0.3965   0.936808
CV111B2   0.793    1.873615
CV111B3   1.1895   2.810423
CV111B4   1.586    3.74723

CV11200   COR112  2  0  1
CV11201   0  0
CV112A0   3
CV112A1   MLFR.4  1.0  TATM  1200.0  PVOL  7.0118e6  PH2O  0.0
CV112B0   1.586   0.0
CV112B1   1.9825  0.936808
CV112B2   2.379   1.873615
CV112B3   2.7755  2.810423
CV112B4   3.172   3.74723

CV11300   COR113  2  0  1
CV11301   0  0
```

```
CV113A0   3
CV113A1   MLFR.4  1.0  TATM  1200.0  PVOL  7.0168e6  PH2O  0.0
CV113B0   3.172    0.0
CV113B1   3.5685   0.936808
CV113B2   3.965    1.873615
CV113B3   4.3615   2.810423
CV113B4   4.758    3.74723

CV11400   COR114  2  0  1
CV11401   0  0
CV114A0   3
CV114A1   MLFR.4  1.0  TATM  1200.0  PVOL  7.0218e6  PH2O  0.0
CV114B0   4.758   0.0
CV114B1   5.1545  0.936808
CV114B2   5.551   1.873615
CV114B3   5.9475  2.810423
CV114B4   6.344   3.74723

CV11500   COR115  2  0  1
CV11501   0  0
CV115A0   3
CV115A1   MLFR.4  1.0  TATM  1200.0  PVOL  7.0268e6  PH2O  0.0
CV115B0   6.344   0.0
CV115B1   6.7405  0.936808
CV115B2   7.137   1.873615
CV115B3   7.5335  2.810423
CV115B4   7.93    3.74723

CV11600   COR116  2  0  1
```

```
CV11601   0  0
CV116A0   3
CV116A1   MLFR.4  1.0  TATM  1200.0  PVOL  7.0318e6  PH2O  0.0
CV116B0   7.93   0.0
CV116B1   8.326333  0.936414
CV116B2   8.722667  1.872828
CV116B3   9.119  2.809241

*Ring 2
CV12000   COR120  2  0  1
CV12001   0  0
CV120A0   3
CV120A1   MLFR.4  1.0  TATM  1200.0  PVOL  7.0018e6  PH2O  0.0
CV120B0   -1.585   0.0
CV120B1   -1.18875  2.28813
CV120B2   -0.7925  4.57625
CV120B3   -0.39625  6.86438
CV120B4   0.0  9.15251

CV12100   COR121  2  0  1
CV12101   0  0
CV121A0   3
CV121A1   MLFR.4  1.0  TATM  1200.0  PVOL  7.0068e6  PH2O  0.0
CV121B0   0.0   0.0
CV121B1   0.3965  2.28957
CV121B2   0.793   4.57914
CV121B3   1.1895  6.86871
CV121B4   1.586   9.15828
```

```
CV12200   COR122  2  0  1
CV12201   0  0
CV122A0   3
CV122A1   MLFR.4  1.0  TATM  1200.0  PVOL  7.0118e6  PH2O  0.0
CV122B0   1.586   0.0
CV122B1   1.9825  2.28957
CV122B2   2.379   4.57914
CV122B3   2.7755  6.86871
CV122B4   3.172   9.15828

CV12300   COR123  2  0  1
CV12301   0  0
CV123A0   3
CV123A1   MLFR.4  1.0  TATM  1200.0  PVOL  7.0168e6  PH2O  0.0
CV123B0   3.172   0.0
CV123B1   3.5685  2.28957
CV123B2   3.965   4.57914
CV123B3   4.3615  6.86871
CV123B4   4.758   9.15828

CV12400   COR124  2  0  1
CV12401   0  0
CV124A0   3
CV124A1   MLFR.4  1.0  TATM  1200.0  PVOL  7.0218e6  PH2O  0.0
CV124B0   4.758   0.0
CV124B1   5.1545  2.28957
CV124B2   5.551   4.57914
CV124B3   5.9475  6.86871
CV124B4   6.344   9.15828
```

```
CV12500   COR125  2  0  1
CV12501   0  0
CV125A0   3
CV125A1   MLFR.4  1.0  TATM  1200.0  PVOL  7.0268e6  PH2O  0.0
CV125B0   6.344   0.0
CV125B1   6.7405  2.28957
CV125B2   7.137   4.57914
CV125B3   7.5335  6.86871
CV125B4   7.93    9.15828

CV12600   COR126  2  0  1
CV12601   0  0
CV126A0   3
CV126A1   MLFR.4  1.0  TATM  1200.0  PVOL  7.0318e6  PH2O  0.0
CV126B0   7.93   0.0
CV126B1   8.326333  2.288608
CV126B2   8.722667  4.577215
CV126B3   9.119  6.865823

*Ring 3
CV13000   COR130  2  0  1
CV13001   0  0
CV130A0   3
CV130A1   MLFR.4  1.0  TATM  1200.0  PVOL  7.0018e6  PH2O  0.0
CV130B0   -1.585   0.0
CV130B1   -1.18875  1.35191
CV130B2   -0.7925  2.70382
CV130B3   -0.39625  4.05573
```

```
CV130B4   0.0  5.40764

CV13100   COR131  2  0  1
CV13101   0  0
CV131A0   3
CV131A1   MLFR.4  1.0  TATM  1200.0  PVOL  7.0068e6  PH2O  0.0
CV131B0   0.0   0.0
CV131B1   0.3965  1.352762
CV131B2   0.793   2.705525
CV131B3   1.1895  4.058287
CV131B4   1.586   5.41105

CV13200   COR132  2  0  1
CV13201   0  0
CV132A0   3
CV132A1   MLFR.4  1.0  TATM  1200.0  PVOL  7.0118e6  PH2O  0.0
CV132B0   1.586   0.0
CV132B1   1.9825  1.352762
CV132B2   2.379   2.705525
CV132B3   2.7755  4.058287
CV132B4   3.172   5.41105

CV13300   COR133  2  0  1
CV13301   0  0
CV133A0   3
CV133A1   MLFR.4  1.0  TATM  1200.0  PVOL  7.0168e6  PH2O  0.0
CV133B0   3.172   0.0
CV133B1   3.5685  1.352762
CV133B2   3.965   2.705525
```

```
CV133B3   4.3615  4.058287
CV133B4   4.758   5.41105

CV13400   COR134  2  0  1
CV13401   0  0
CV134A0   3
CV134A1   MLFR.4  1.0  TATM  1200.0  PVOL  7.0218e6  PH2O  0.0
CV134B0   4.758   0.0
CV134B1   5.1545  1.352762
CV134B2   5.551   2.705525
CV134B3   5.9475  4.058287
CV134B4   6.344   5.41105

CV13500   COR135  2  0  1
CV13501   0  0
CV135A0   3
CV135A1   MLFR.4  1.0  TATM  1200.0  PVOL  7.0268e6  PH2O  0.0
CV135B0   6.344   0.0
CV135B1   6.7405  1.352762
CV135B2   7.137   2.705525
CV135B3   7.5335  4.058287
CV135B4   7.93    5.41105

CV13600   COR136  2  0  1
CV13601   0  0
CV136A0   3
CV136A1   MLFR.4  1.0  TATM  1200.0  PVOL  7.0318e6  PH2O  0.0
CV136B0   7.93   0.0
CV136B1   8.326333  1.352194
```

```
CV136B2   8.722667  2.704388
CV136B3   9.119  4.056582

**********************************
* CVH cells for the helium inlet
**********************************
CV14000   inlet140  2  0  1
CV14001   0  0
CV140A0   3
CV140A1   MLFR.4  1.0  TATM  1200.0  PVOL  7.0672e6  PH2O  0.0
CV140B0   -1.585  0.0
CV140B1   -1.18875  1.849023261
CV140B2   -0.7925   3.698046523
CV140B3   -0.39625  5.547069784
CV140B4   0.0   7.39609

CV14100   inlet141  2  0  1
CV14101   0  0
CV141A0   3
CV141A1   MLFR.4  1.0  TATM  1200.0  PVOL  7.0644e6  PH2O  0.0
CV141B0   0.0   0.0
CV141B1   0.3965  1.850189837
CV141B2   0.793   3.700379675
CV141B3   1.1895  5.550569512
CV141B4   1.586   7.40075935

CV14200   inlet142  2  0  1
CV14201   0  0
CV142A0   3
```

CV142A1 MLFR.4 1.0 TATM 1200.0 PVOL 7.0616e6 PH2O 0.0
CV142B0 1.586 0.0
CV142B1 1.9825 1.850189837
CV142B2 2.379 3.700379675
CV142B3 2.7755 5.550569512
CV142B4 3.172 7.40075935

CV14300 inlet143 2 0 1
CV14301 0 0
CV143A0 3
CV143A1 MLFR.4 1.0 TATM 1200.0 PVOL 7.0588e6 PH2O 0.0
CV143B0 3.172 0.0
CV143B1 3.5685 1.850189837
CV143B2 3.965 3.700379675
CV143B3 4.3615 5.550569512
CV143B4 4.758 7.40075935

CV14400 inlet144 2 0 1
CV14401 0 0
CV144A0 3
CV144A1 MLFR.4 1.0 TATM 1200.0 PVOL 7.056e6 PH2O 0.0
CV144B0 4.758 0.0
CV144B1 5.1545 1.850189837
CV144B2 5.551 3.700379675
CV144B3 5.9475 5.550569512
CV144B4 6.344 7.40075935

CV14500 inlet145 2 0 1
CV14501 0 0

CV145A0 3

CV145A1 MLFR.4 1.0 TATM 1200.0 PVOL 7.0532e6 PH2O 0.0

CV145B0 6.344 0.0

CV145B1 6.7405 1.850189837

CV145B2 7.137 3.700379675

CV145B3 7.5335 5.550569512

CV145B4 7.93 7.40075935

CV14600 inlet146 2 0 1

CV14601 0 0

CV146A0 3

CV146A1 MLFR.4 1.0 TATM 1200.0 PVOL 7.0504e6 PH2O 0.0

CV146B0 7.93 0.0

CV146B1 8.326333 1.849412

CV146B2 8.722667 3.69882424

CV146B3 9.119 5.54823636

****

* Axial downward core flowpaths

****

*Upper plenum volume

FL17000 InletF71-T70 171 170 9.369 9.369

FL17001 2.058805709 1.34 1.0

FL17002 0 0 0 0

FL170S1 2.058805709 1.34 0.37455600

*Ring 1

FL11700 CoreRingF60-T16 170 116 9.119 9.119

FL11701 0.605531091 0.918 1.0

FL11702 0 0 0 0

FL117S1 0.605531091 0.918 0.01588

FL11600 CoreRingF16-T15 116 115 7.93 7.93

FL11601 0.605531091 1.3875 1.0

FL11602 0 0 0 0

FL116S1 0.605531091 1.3875 0.01588

FL11500 CoreRingF15-T14 115 114 6.344 6.344

FL11501 0.605531091 1.586 1.0

FL11502 0 0 0 0

FL115S1 0.605531091 1.586 0.01588

FL11400 CoreRingF14-T13 114 113 4.758 4.758

FL11401 0.605531091 1.586 1.0

FL11402 0 0 0 0

FL114S1 0.605531091 1.586 0.01588

FL11300 CoreRingF13-T12 113 112 3.172 3.172

FL11301 0.605531091 1.586 1.0

FL11302 0 0 0 0

FL113S1 0.605531091 1.586 0.01588

FL11200 CoreRingF12-T11 112 111 1.586 1.586

FL11201 0.605531091 1.586 1.0

FL11202 0 0 0 0

FL112S1 0.605531091 1.586 0.01588

FL11100 CoreRingF11-T10 111 110 0.0 0.0
FL11101 0.605531091 1.5855 1.0
FL11102 0 0 0 0
FL111S1 0.605531091 1.5855 0.01588

FL11000 CoreRingF10-T54 110 54 -1.585 -1.585
FL11001 0.605531091 1.8725 1.0
FL11002 0 0 0 0
FL110S1 0.605531091 1.8725 0.01588

*Ring 2
FL12700 CoreRingF60-T26 170 126 9.119 9.119
FL12701 0.726637309 0.918 1.0
FL12702 0 0 0 0
FL127S1 0.726637309 0.918 0.01588

FL12600 CoreRingF26-T25 126 125 7.93 7.93
FL12601 0.726637309 1.3875 1.0
FL12602 0 0 0 0
FL126S1 0.726637309 1.3875 0.01588

FL12500 CoreRingF25-T24 125 124 6.344 6.344
FL12501 0.726637309 1.586 1.0
FL12502 0 0 0 0
FL125S1 0.726637309 1.586 0.01588

FL12400 CoreRingF24-T23 124 123 4.758 4.758
FL12401 0.726637309 1.586 1.0
FL12402 0 0 0 0

FL124S1 0.726637309 1.586 0.01588

FL12300 CoreRingF23-T22 123 122 3.172 3.172
FL12301 0.726637309 1.586 1.0
FL12302 0 0 0 0
FL123S1 0.726637309 1.586 0.01588

FL12200 CoreRingF22-T21 122 121 1.586 1.586
FL12201 0.726637309 1.586 1.0
FL12202 0 0 0 0
FL122S1 0.726637309 1.586 0.01588

FL12100 CoreRingF21-T20 121 120 0.0 0.0
FL12101 0.726637309 1.5855 1.0
FL12102 0 0 0 0
FL121S1 0.726637309 1.5855 0.01588

FL12000 CoreRingF20-T54 120 54 -1.585 -1.585
FL12001 0.726637309 1.8725 1.0
FL12002 0 0 0 0
FL120S1 0.726637309 1.8725 0.01588

*Ring 3
FL13700 CoreRingF60-T36 170 136 9.119 9.119
FL13701 0.726637309 0.918 1.0
FL13702 0 0 0 0
FL137S1 0.726637309 0.918 0.01588

FL13600 CoreRingF36-T35 136 135 7.93 7.93

FL13601 0.726637309 1.3875 1.0

FL13602 0 0 0 0

FL136S1 0.726637309 1.3875 0.01588

FL13500 CoreRingF35-T34 135 134 6.344 6.344

FL13501 0.726637309 1.586 1.0

FL13502 0 0 0 0

FL135S1 0.726637309 1.586 0.01588

FL13400 CoreRingF34-T33 134 133 4.758 4.758

FL13401 0.726637309 1.586 1.0

FL13402 0 0 0 0

FL134S1 0.726637309 1.586 0.01588

FL13300 CoreRingF33-T32 133 132 3.172 3.172

FL13301 0.726637309 1.586 1.0

FL13302 0 0 0 0

FL133S1 0.726637309 1.586 0.01588

FL13200 CoreRingF32-T31 132 131 1.586 1.586

FL13201 0.726637309 1.586 1.0

FL13202 0 0 0 0

FL132S1 0.726637309 1.586 0.01588

FL13100 CoreRingF31-T30 131 130 0.0 0.0

FL13101 0.726637309 1.5855 1.0

FL13102 0 0 0 0

FL131S1 0.726637309 1.5855 0.01588

FL13000 CoreRingF30-T54 130 54 -1.585 -1.585

FL13001 0.726637309 1.8725 1.0

FL13002 0 0 0 0

FL130S1 0.726637309 1.8725 0.01588

****

* Axial upward core flowpaths

****

FL14100 InletF40-T41 140 141 0.0 0.0

FL14101 2.058805709 1.5855 1.0

FL14102 0 0 0 0

FL141S1 2.058805709 1.5855 0.374556001

FL14200 InletF41-T42 141 142 1.586 1.586

FL14201 2.058805709 1.586 1.0

FL14202 0 0 0 0

FL142S1 2.058805709 1.586 0.374556001

FL14300 InletF42-T43 142 143 3.172 3.172

FL14301 2.058805709 1.586 1.0

FL14302 0 0 0 0

FL143S1 2.058805709 1.586 0.374556001

FL14400 InletF43-T44 143 144 4.758 4.758

FL14401 2.058805709 1.586 1.0

FL14402 0 0 0 0

FL144S1 2.058805709 1.586 0.374556001

FL14500 InletF44-T45 144 145 6.344 6.344

FL14501 2.058805709 1.586 1.0

FL14502 0 0 0 0

FL145S1 2.058805709 1.586 0.374556001

FL14600 InletF45-T46 145 146 7.93 7.93

FL14601 2.058805709 1.3875 1.0

FL14602 0 0 0 0

FL146S1 2.058805709 1.3875 0.374556001

FL14700 InletF46-T71 146 171 9.119 9.369

FL14701 2.058805709 2.0595 1.0

FL14702 0 0 0 0

FL147S1 2.058805709 2.0595 0.374556001

****

* Center reflector heat

* structures

****

*level 1

HS32001000 7 2 -1

HS32001001 cntr_ref_LVL_1

HS32001002 -1.585 1.0

HS32001100 -1 2 0.0

HS32001101 0.246 1

HS32001102 0.492 1

HS32001103 0.738 1

HS32001104 0.984 1

```
HS32001105  1.23  1
HS32001106  1.476  1
HS32001200  -1  * index for material
HS32001201  graphite  6
HS32001300  0
HS32001400  0  -1  'INT'  0.9  0.9
HS32001600  1  110  'EXT'  0.9  0.9
HS32001700  7.349630224  1.476  0.7925
HS32001800  -1
HS32001801  764.0  1
HS32001802  764.0  2
HS32001803  764.0  3
HS32001804  764.0  4
HS32001805  764.0  5
HS32001806  764.0  6
HS32001807  764.0  7

*level 2
HS32002000  7  2  -1
HS32002001  cntr_ref_LVL_2
HS32002002  -0.7925  1.0
HS32002100  -1  2  0.0
HS32002101  0.246  1
HS32002102  0.492  1
HS32002103  0.738  1
HS32002104  0.984  1
HS32002105  1.23  1
HS32002106  1.476  1
HS32002200  -1  * index for material
```

```
HS32002201  graphite  6
HS32002300  0
HS32002400  0  -1  'INT'  0.9  0.9
HS32002600  1  110  'EXT'  0.9  0.9
HS32002700  7.349630224  1.476  0.7925
HS32002800  -1
HS32002801  764.0  1
HS32002802  764.0  2
HS32002803  764.0  3
HS32002804  764.0  4
HS32002805  764.0  5
HS32002806  764.0  6
HS32002807  764.0  7

*level 3
HS32003000  7  2  -1
HS32003001  cntr_ref_LVL_3
HS32003002  0.0  1.0
HS32003100  -1  2  0.0
HS32003101  0.246  1
HS32003102  0.492  1
HS32003103  0.738  1
HS32003104  0.984  1
HS32003105  1.23  1
HS32003106  1.476  1
HS32003200  -1  * index for material
HS32003201  graphite  6
HS32003300  0
HS32003400  0  -1  'INT'  0.9  0.9
```

```
HS32003600  1  111  'EXT'  0.9  0.9
HS32003700  7.35426734  1.476  0.793
HS32003800  -1
HS32003801  764.0  1
HS32003802  764.0  2
HS32003803  764.0  3
HS32003804  764.0  4
HS32003805  764.0  5
HS32003806  764.0  6
HS32003807  764.0  7

*level 4
HS32004000  7  2  -1
HS32004001  cntr_ref_LVL_4
HS32004002  0.793  1.0
HS32004100  -1  2  0.0
HS32004101  0.246  1
HS32004102  0.492  1
HS32004103  0.738  1
HS32004104  0.984  1
HS32004105  1.23  1
HS32004106  1.476  1
HS32004200  -1  * index for material
HS32004201  graphite  6
HS32004300  0
HS32004400  0  -1  'INT'  0.9  0.9
HS32004600  1  111  'EXT'  0.9  0.9
HS32004700  7.35426734  1.476  0.793
HS32004800  -1
```

HS32004801 764.0 1
HS32004802 764.0 2
HS32004803 764.0 3
HS32004804 764.0 4
HS32004805 764.0 5
HS32004806 764.0 6
HS32004807 764.0 7

*level 5
HS32005000 7 2 -1
HS32005001 cntr_ref_LVL_5
HS32005002 1.586 1.0
HS32005100 -1 2 0.0
HS32005101 0.246 1
HS32005102 0.492 1
HS32005103 0.738 1
HS32005104 0.984 1
HS32005105 1.23 1
HS32005106 1.476 1
HS32005200 -1 * index for material
HS32005201 graphite 6
HS32005300 0
HS32005400 0 -1 'INT' 0.9 0.9
HS32005600 1 112 'EXT' 0.9 0.9
HS32005700 7.35426734 1.476 0.793
HS32005800 -1
HS32005801 764.0 1
HS32005802 764.0 2
HS32005803 764.0 3

HS32005804 764.0 4
HS32005805 764.0 5
HS32005806 764.0 6
HS32005807 764.0 7

*level 6
HS32006000 7 2 -1
HS32006001 cntr_ref_LVL_6
HS32006002 2.379 1.0
HS32006100 -1 2 0.0
HS32006101 0.246 1
HS32006102 0.492 1
HS32006103 0.738 1
HS32006104 0.984 1
HS32006105 1.23 1
HS32006106 1.476 1
HS32006200 -1 * index for material
HS32006201 graphite 6
HS32006300 0
HS32006400 0 -1 'INT' 0.9 0.9
HS32006600 1 112 'EXT' 0.9 0.9
HS32006700 7.35426734 1.476 0.793
HS32006800 -1
HS32006801 764.0 1
HS32006802 764.0 2
HS32006803 764.0 3
HS32006804 764.0 4
HS32006805 764.0 5
HS32006806 764.0 6

```
HS32006807  764.0  7

*level 7
HS32007000  7  2  -1
HS32007001  cntr_ref_LVL_7
HS32007002  3.172  1.0
HS32007100  -1  2  0.0
HS32007101  0.246  1
HS32007102  0.492  1
HS32007103  0.738  1
HS32007104  0.984  1
HS32007105  1.23  1
HS32007106  1.476  1
HS32007200  -1  * index for material
HS32007201  graphite  6
HS32007300  0
HS32007400  0  -1  'INT'  0.9  0.9
HS32007600  1  113  'EXT'  0.9  0.9
HS32007700  7.35426734  1.476  0.793
HS32007800  -1
HS32007801  764.0  1
HS32007802  764.0  2
HS32007803  764.0  3
HS32007804  764.0  4
HS32007805  764.0  5
HS32007806  764.0  6
HS32007807  764.0  7

*level 8
```

```
HS32008000  7  2  -1
HS32008001  cntr_ref_LVL_8
HS32008002  3.965  1.0
HS32008100  -1  2  0.0
HS32008101  0.246  1
HS32008102  0.492  1
HS32008103  0.738  1
HS32008104  0.984  1
HS32008105  1.23  1
HS32008106  1.476  1
HS32008200  -1  * index for material
HS32008201  graphite  6
HS32008300  0
HS32008400  0  -1  'INT'  0.9  0.9
HS32008600  1  113  'EXT'  0.9  0.9
HS32008700  7.35426734  1.476  0.793
HS32008800  -1
HS32008801  764.0  1
HS32008802  764.0  2
HS32008803  764.0  3
HS32008804  764.0  4
HS32008805  764.0  5
HS32008806  764.0  6
HS32008807  764.0  7

*level 9
HS32009000  7  2  -1
HS32009001  cntr_ref_LVL_9
HS32009002  4.758  1.0
```

HS32009100 -1 2 0.0
HS32009101 0.246 1
HS32009102 0.492 1
HS32009103 0.738 1
HS32009104 0.984 1
HS32009105 1.23 1
HS32009106 1.476 1
HS32009200 -1 * index for material
HS32009201 graphite 6
HS32009300 0
HS32009400 0 -1 'INT' 0.9 0.9
HS32009600 1 114 'EXT' 0.9 0.9
HS32009700 7.35426734 1.476 0.793
HS32009800 -1
HS32009801 764.0 1
HS32009802 764.0 2
HS32009803 764.0 3
HS32009804 764.0 4
HS32009805 764.0 5
HS32009806 764.0 6
HS32009807 764.0 7

*level 10
HS32010000 7 2 -1
HS32010001 cntr_ref_LVL_10
HS32010002 5.551 1.0
HS32010100 -1 2 0.0
HS32010101 0.246 1
HS32010102 0.492 1

HS32010103 0.738 1

HS32010104 0.984 1

HS32010105 1.23 1

HS32010106 1.476 1

HS32010200 -1 * index for material

HS32010201 graphite 6

HS32010300 0

HS32010400 0 -1 'INT' 0.9 0.9

HS32010600 1 114 'EXT' 0.9 0.9

HS32010700 7.35426734 1.476 0.793

HS32010800 -1

HS32010801 764.0 1

HS32010802 764.0 2

HS32010803 764.0 3

HS32010804 764.0 4

HS32010805 764.0 5

HS32010806 764.0 6

HS32010807 764.0 7

*level 11

HS32011000 7 2 -1

HS32011001 cntr_ref_LVL_11

HS32011002 6.344 1.0

HS32011100 -1 2 0.0

HS32011101 0.246 1

HS32011102 0.492 1

HS32011103 0.738 1

HS32011104 0.984 1

HS32011105 1.23 1

HS32011106 1.476 1

HS32011200 -1 * index for material

HS32011201 graphite 6

HS32011300 0

HS32011400 0 -1 'INT' 0.9 0.9

HS32011600 1 115 'EXT' 0.9 0.9

HS32011700 7.35426734 1.476 0.793

HS32011800 -1

HS32011801 764.0 1

HS32011802 764.0 2

HS32011803 764.0 3

HS32011804 764.0 4

HS32011805 764.0 5

HS32011806 764.0 6

HS32011807 764.0 7

*level 12

HS32012000 7 2 -1

HS32012001 cntr_ref_LVL_12

HS32012002 7.137 1.0

HS32012100 -1 2 0.0

HS32012101 0.246 1

HS32012102 0.492 1

HS32012103 0.738 1

HS32012104 0.984 1

HS32012105 1.23 1

HS32012106 1.476 1

HS32012200 -1 * index for material

```
HS32012201  graphite  6
HS32012300  0
HS32012400  0  -1  'INT'  0.9  0.9
HS32012600  1  115  'EXT'  0.9  0.9
HS32012700  7.35426734  1.476  0.793
HS32012800  -1
HS32012801  764.0  1
HS32012802  764.0  2
HS32012803  764.0  3
HS32012804  764.0  4
HS32012805  764.0  5
HS32012806  764.0  6
HS32012807  764.0  7

*level 13
HS32013000  7  2  -1
HS32013001  cntr_ref_LVL_13
HS32013002  7.93  1.0
HS32013100  -1  2  0.0
HS32013101  0.246  1
HS32013102  0.492  1
HS32013103  0.738  1
HS32013104  0.984  1
HS32013105  1.23  1
HS32013106  1.476  1
HS32013200  -1  * index for material
HS32013201  graphite  6
HS32013300  0
HS32013400  0  -1  'INT'  0.9  0.9
```

```
HS32013600  1  116  'EXT'  0.9  0.9
HS32013700  5.513381916  1.476  0.5945
HS32013800  -1
HS32013801  764.0  1
HS32013802  764.0  2
HS32013803  764.0  3
HS32013804  764.0  4
HS32013805  764.0  5
HS32013806  764.0  6
HS32013807  764.0  7

*level 14
HS32014000  7  2  -1
HS32014001  cntr_ref_LVL_14
HS32014002  8.5245  1.0
HS32014100  -1  2  0.0
HS32014101  0.246  1
HS32014102  0.492  1
HS32014103  0.738  1
HS32014104  0.984  1
HS32014105  1.23  1
HS32014106  1.476  1
HS32014200  -1  * index for material
HS32014201  graphite  6
HS32014300  0
HS32014400  0  -1  'INT'  0.9  0.9
HS32014600  1  116  'EXT'  0.9  0.9
HS32014700  5.513381916  1.476  0.5945
HS32014800  -1
```

```
HS32014801  764.0  1
HS32014802  764.0  2
HS32014803  764.0  3
HS32014804  764.0  4
HS32014805  764.0  5
HS32014806  764.0  6
HS32014807  764.0  7

**********
* Side reflector heat
* structures
**********

*level 1
HS33001000  4  2  -1
HS33001001  sd_ref_LVL_1
HS33001002  -1.585  1.0
HS33001100  -1  2  2.41965
HS33001101  2.7215  1
HS33001102  3.02335  1
HS33001103  3.3252  1
HS33001200  -1  * index for material
HS33001201  graphite  3
HS33001300  0
HS33001400  1  130  'EXT'  0.9  0.9
HS33001500  12.04846394  2.41965  0.7925
HS33001600  1  140  'EXT'  0.9  0.9
HS33001700  16.55758159  3.3252  0.7925
HS33001800  -1
```

```
HS33001801  764.0  1
HS33001802  764.0  2
HS33001803  764.0  3
HS33001804  764.0  4

*level 2
HS33002000  4  2  -1
HS33002001  sd_ref_LVL_2
HS33002002  -0.7925  1.0
HS33002100  -1  2  2.41965
HS33002101  2.7215  1
HS33002102  3.02335  1
HS33002103  3.3252  1
HS33002200  -1  * index for material
HS33002201  graphite  3
HS33002300  0
HS33002400  1  130  'EXT'  0.9  0.9
HS33002500  12.04846394  2.41965  0.7925
HS33002600  1  140  'EXT'  0.9  0.9
HS33002700  16.55758159  3.3252  0.7925
HS33002800  -1
HS33002801  764.0  1
HS33002802  764.0  2
HS33002803  764.0  3
HS33002804  764.0  4

*level 3
HS33003000  4  2  -1
HS33003001  sd_ref_LVL_3
```

```
HS33003002  0.0  1.0
HS33003100  -1  2  2.41965
HS33003101  2.7215  1
HS33003102  3.02335  1
HS33003103  3.3252  1
HS33003200  -1  * index for material
HS33003201  graphite  3
HS33003300  0
HS33003400  1  131  'EXT'  0.9  0.9
HS33003500  12.05606549  2.41965  0.793
HS33003600  1  141  'EXT'  0.9  0.9
HS33003700  16.56802801  3.3252  0.793
HS33003800  -1
HS33003801  764.0  1
HS33003802  764.0  2
HS33003803  764.0  3
HS33003804  764.0  4

*level 4
HS33004000  4  2  -1
HS33004001  sd_ref_LVL_4
HS33004002  0.793  1.0
HS33004100  -1  2  2.41965
HS33004101  2.7215  1
HS33004102  3.02335  1
HS33004103  3.3252  1
HS33004200  -1  * index for material
HS33004201  graphite  3
HS33004300  0
```

HS33004400 1 131 'EXT' 0.9 0.9

HS33004500 12.05606549 2.41965 0.793

HS33004600 1 141 'EXT' 0.9 0.9

HS33004700 16.56802801 3.3252 0.793

HS33004800 -1

HS33004801 764.0 1

HS33004802 764.0 2

HS33004803 764.0 3

HS33004804 764.0 4

*level 5

HS33005000 4 2 -1

HS33005001 sd_ref_LVL_5

HS33005002 1.586 1.0

HS33005100 -1 2 2.41965

HS33005101 2.7215 1

HS33005102 3.02335 1

HS33005103 3.3252 1

HS33005200 -1 * index for material

HS33005201 graphite 3

HS33005300 0

HS33005400 1 132 'EXT' 0.9 0.9

HS33005500 12.05606549 2.41965 0.793

HS33005600 1 142 'EXT' 0.9 0.9

HS33005700 16.56802801 3.3252 0.793

HS33005800 -1

HS33005801 764.0 1

HS33005802 764.0 2

HS33005803 764.0 3

```
HS33005804  764.0  4

*level 6
HS33006000  4  2  -1
HS33006001  sd_ref_LVL_6
HS33006002  2.379  1.0
HS33006100  -1  2  2.41965
HS33006101  2.7215  1
HS33006102  3.02335  1
HS33006103  3.3252  1
HS33006200  -1  * index for material
HS33006201  graphite  3
HS33006300  0
HS33006400  1  132  'EXT'  0.9  0.9
HS33006500  12.05606549  2.41965  0.793
HS33006600  1  142  'EXT'  0.9  0.9
HS33006700  16.56802801  3.3252  0.793
HS33006800  -1
HS33006801  764.0  1
HS33006802  764.0  2
HS33006803  764.0  3
HS33006804  764.0  4

*level 7
HS33007000  4  2  -1
HS33007001  sd_ref_LVL_7
HS33007002  3.172  1.0
HS33007100  -1  2  2.41965
HS33007101  2.7215  1
```

```
HS33007102  3.02335  1
HS33007103  3.3252  1
HS33007200  -1  * index for material
HS33007201  graphite  3
HS33007300  0
HS33007400  1  133  'EXT'  0.9  0.9
HS33007500  12.05606549  2.41965  0.793
HS33007600  1  143  'EXT'  0.9  0.9
HS33007700  16.56802801  3.3252  0.793
HS33007800  -1
HS33007801  764.0  1
HS33007802  764.0  2
HS33007803  764.0  3
HS33007804  764.0  4

*level 8
HS33008000  4  2  -1
HS33008001  sd_ref_LVL_8
HS33008002  3.965  1.0
HS33008100  -1  2  2.41965
HS33008101  2.7215  1
HS33008102  3.02335  1
HS33008103  3.3252  1
HS33008200  -1  * index for material
HS33008201  graphite  3
HS33008300  0
HS33008400  1  133  'EXT'  0.9  0.9
HS33008500  12.05606549  2.41965  0.793
HS33008600  1  143  'EXT'  0.9  0.9
```

HS33008700 16.56802801 3.3252 0.793

HS33008800 -1

HS33008801 764.0 1

HS33008802 764.0 2

HS33008803 764.0 3

HS33008804 764.0 4

*level 9

HS33009000 4 2 -1

HS33009001 sd_ref_LVL_9

HS33009002 4.758 1.0

HS33009100 -1 2 2.41965

HS33009101 2.7215 1

HS33009102 3.02335 1

HS33009103 3.3252 1

HS33009200 -1 * index for material

HS33009201 graphite 3

HS33009300 0

HS33009400 1 134 'EXT' 0.9 0.9

HS33009500 12.05606549 2.41965 0.793

HS33009600 1 144 'EXT' 0.9 0.9

HS33009700 16.56802801 3.3252 0.793

HS33009800 -1

HS33009801 764.0 1

HS33009802 764.0 2

HS33009803 764.0 3

HS33009804 764.0 4

*level 10

```
HS33010000  4  2  -1
HS33010001  sd_ref_LVL_10
HS33010002  5.551  1.0
HS33010100  -1  2  2.41965
HS33010101  2.7215  1
HS33010102  3.02335  1
HS33010103  3.3252  1
HS33010200  -1  * index for material
HS33010201  graphite  3
HS33010300  0
HS33010400  1  134  'EXT'  0.9  0.9
HS33010500  12.05606549  2.41965  0.793
HS33010600  1  144  'EXT'  0.9  0.9
HS33010700  16.56802801  3.3252  0.793
HS33010800  -1
HS33010801  764.0  1
HS33010802  764.0  2
HS33010803  764.0  3
HS33010804  764.0  4

*level 11
HS33011000  4  2  -1
HS33011001  sd_ref_LVL_11
HS33011002  6.344  1.0
HS33011100  -1  2  2.41965
HS33011101  2.7215  1
HS33011102  3.02335  1
HS33011103  3.3252  1
HS33011200  -1  * index for material
```

```
HS33011201  graphite  3
HS33011300  0
HS33011400  1  135  'EXT'  0.9  0.9
HS33011500  12.05606549  2.41965  0.793
HS33011600  1  145  'EXT'  0.9  0.9
HS33011700  16.56802801  3.3252  0.793
HS33011800  -1
HS33011801  764.0  1
HS33011802  764.0  2
HS33011803  764.0  3
HS33011804  764.0  4

*level 12
HS33012000  4  2  -1
HS33012001  sd_ref_LVL_12
HS33012002  7.137  1.0
HS33012100  -1  2  2.41965
HS33012101  2.7215  1
HS33012102  3.02335  1
HS33012103  3.3252  1
HS33012200  -1  * index for material
HS33012201  graphite  3
HS33012300  0
HS33012400  1  135  'EXT'  0.9  0.9
HS33012500  12.05606549  2.41965  0.793
HS33012600  1  145  'EXT'  0.9  0.9
HS33012700  16.56802801  3.3252  0.793
HS33012800  -1
HS33012801  764.0  1
```

HS33012802 764.0 2
HS33012803 764.0 3
HS33012804 764.0 4

*level 13
HS33013000 4 2 -1
HS33013001 sd_ref_LVL_13
HS33013002 7.93 1.0
HS33013100 -1 2 2.41965
HS33013101 2.7215 1
HS33013102 3.02335 1
HS33013103 3.3252 1
HS33013200 -1 * index for material
HS33013201 graphite 3
HS33013300 0
HS33013400 1 136 'EXT' 0.9 0.9
HS33013500 9.038248342 2.41965 0.5945
HS33013600 1 146 'EXT' 0.9 0.9
HS33013700 12.4207978 3.3252 0.5945
HS33013800 -1
HS33013801 764.0 1
HS33013802 764.0 2
HS33013803 764.0 3
HS33013804 764.0 4

*level 14
HS33014000 4 2 -1
HS33014001 sd_ref_LVL_14
HS33014002 8.5245 1.0

```
HS33014100  -1  2  2.41965
HS33014101  2.7215  1
HS33014102  3.02335  1
HS33014103  3.3252  1
HS33014200  -1  * index for material
HS33014201  graphite  3
HS33014300  0
HS33014400  1  136  'EXT'  0.9  0.9
HS33014500  9.038248342  2.41965  0.5945
HS33014600  1  146  'EXT'  0.9  0.9
HS33014700  12.4207978  3.3252  0.5945
HS33014800  -1
HS33014801  764.0  1
HS33014802  764.0  2
HS33014803  764.0  3
HS33014804  764.0  4

* System source to RPV
FL14000 SOURCEtoINLET 160 140 -2.6645 -0.7925
FL14001 2.058805709 6.15 1.0
FL14002 0 0 0 0
FL140S1 2.058805709 6.15 0.374556001
FL140T1 2 200

* RPV to system sink
FL20000 OUTLETToSINK 054 200 -2.6645 -2.6645
FL20001 2.058805709 1.872 1.0
FL20002 3 0 0 0
FL200S1 2.058805709 1.872 0.374556001
```

```
* Time-independent source
CV16000 SOURCE 2 0 5
CV16001 0 -1
CV160A0 3
CV160A1 MLFR.4 1.0 TATM 1200.0 PVOL 7.07e6 PH2O 0.0
CV160B0 -2.9145 0.0
CV160B1 -2.4145 0.015625

* Time-independent sink
CV20000 SINK 2 0 6
CV20001 0 -1
CV200A0 3
CV200A1 MLFR.4 1.0 TATM 1273.0 PVOL 6.9968e6 PH2O 0.0
CV200B0 -2.9145 0.0
CV200B1 -2.4145 1.25

**********
* Steady-state source
**********

CF20000 VSOURCE DIVIDE 2 1.0 0.0
CF20010 1.0 0.0 CFVALU.199
CF20011 0.0 226.0 TIME
CF19900 VSOURCE MULTIPLY 2 1.0 0.0
CF19910 1.0 0.0 CVH-RHO.160
CF19911 0.0 2.058805709 TIME

* FLOW AREA=2.058805709
```

```
* DENSITY= CVH-RHO.4.160
* MASS FLOW RATE= 226 kg/s

**********************************
* DLL Test
**********************************

*CF20000 VSOURCE FUN1 5 1.0 0.0
*CF20010 1.0 0.0 CVH-RHO.160
*CF20011 0.0 2.058805709 TIME
*CF20012 0.0 226.0 TIME
*CF20013 0.0 0.0 TIME
*CF20014 0.0 0.0 TIME
.
```

APPENDIX C: DETAILED NGNP RPV MODEL

C Documentation

C. NGNP

FLnnn03	FRICFO	2.8	Forward loss coefficient
	FRICRO	2.8	Reverse loss coefficient

The same values for FRICFO and FRICRO are used for all the flow paths in order to achieve a total mass flow rate of around 226 kg/s.

CDCHKF	1.0	default value; Choked flow forward discharge coefficient
CDCHKR	1.0	default value; Choked flow reverse discharge coefficient

Table C.1

NGNP Flow Areas

Ring	flow path area (m2)
01	0.061761922
02	0.597103701
03	0.738751896
04	0.722875143
05	0.144111152

Table C.2

NGNP Initial Control Volume Pressure

Control volme	Pressure (MPa)
190	7.12
160	7.115
161	7.11
162	7.105
163	7.1
164	7.095
165	7.09
166	7.085
280	7.07
1n6	7.06425
1n5	7.0585
1n4	7.05275
1n3	7.047
1n2	7.04125
1n1	7.0355
1n0	7.02975
054	7.024
200	7.019

APPENDIX D: RCCS MODEL

D.1 Documentation

FLnnn03	FRICFO	0.0	Forward loss coefficient
	FRICRO	0.0	Reverse loss coefficient

The same values for FRICFO and FRICRO are used for all the flow paths in the RCCS risers. The riser are straight ducts, so there is no form loss due change in the shape or angle of the flow area.

	CDCHKF	1.0	default value; Choked flow forward discharge coefficient
	CDCHKR	1.0	default value; Choked flow reverse discharge coefficient

HSRDCCCCC0	IHSRD1		Heat structure number for the first surface of the pair.
	IHSRD2		Heat structure number for the second surface of the pair.
	VIEW	1.0	View factor between surface 1 and surface 2
	ICFRD1	501	Optional real-valued control function index whose value is the emissivity of surface 1
	ICFRD2	502	Optional real-valued control function index whose value is the emissivity of surface 2

Table D.1

RCCS CVH Elevation Data

Elevation (m)	CVs
from -1.585m to -1.18875m	CV301, 401, 501
from -1.18875m to -0.7925m	CV302, 402, 502
from -0.7925m to -0.39625m	CV303, 403, 503
from -0.39625m to 0m	CV304, 404, 504
from 0m to 0.3965m	CV305, 405, 505
from 0.3965m to 0.793m	CV306, 406, 506
from 0.793m to 1.1895m	CV307, 407, 507
from 1.1895m to 1.586m	CV308, 408, 508
from 1.586m to 1.9825m	CV309, 409, 509
from 1.9825m to 2.379m	CV310, 410, 510
from 2.379m to 2.7755m	CV311, 411, 511
from 2.7755m to 3.172m	CV312, 412, 512
from 3.172m to 3.5685m	CV313, 413, 513
from 3.5685m to 3.965m	CV314, 414, 514
from 3.965m to 4.3615m	CV315, 415, 515
from 4.3615m to 4.758m	CV316, 416, 516
from 4.758m to 5.1545m	CV317, 417, 517
from 5.1545m to 5.551m	CV318, 418, 518
from 5.551m to 5.9475m	CV319, 419, 519
from 5.9475m to 6.344m	CV320, 420, 520
from 6.344m to 6.7405m	CV321, 421, 521
from 6.7405m to 7.137m	CV322, 422, 522
from 7.137m to 7.5335m	CV323, 423, 523
from 7.5335m to 7.93m	CV324, 424, 524
from 7.93m to 8.3263m	CV325, 425, 525
from 8.3263m to 8.7226m	CV326, 426, 526
from 8.7226m to 9.119m	CV327, 427, 527

Table D.2

CUA Volume

CV	cross sectional area (m2)	volume (m3)
3mm	27.87092818	11.043855
3nn	27.87092818	11.050823
3pp	27.87092818	11.045249
327	27.87092818	11.048036

mm: 01 to 04

nn: 05 to 24

pp: 25 and 26

Table D.3

CUA Hydraulic Diameter

Flow Area (m2)	27.8709
Wetted Perimeter (m)	184.4469
Hydraulic Diameter (m)	0.6044

Table D.4

Heat Structure 33 Data

HS	IBVL (outer)	ASURFL (outer)
330mm	3mm	9.5332
330nn	3nn	9.5392
330pp	3pp	9.5344
33027	327	9.5368

Table D.5

Heat Structure 30 Data

HS	IBVL (inner)	ASURFL (inner)	IBVL (outer)	ASURFL (outer)
300mm	3mm	63.5539	4mm	61.3497
300nn	3nn	63.5940	4nn	61.3884
300pp	3pp	63.5619	4pp	61.3574
30027	327	63.5779	427	61.3729

Table D.6

Heat Structure 30 Radii

Cross sectional area (m2)	0.750603337
Inner radius (m)	4.8511
Outer radius (m)	4.8757

Table D.7

Riser Air Volume

CV	cross-sectional area (m2)	volume (m3)
4mm	2.946486043	1.1675451
4nn	2.946486043	1.1682817
4pp	2.946486043	1.1676924
427	2.946486043	1.1679871

Table D.8

Riser Duct Hydraulic Diameter

Flow Area (m2)	2.94649
Wetted Perimeter (m)	0.5715
Hydraulic Diameter (m)	0.070626111

Table D.9

Riser Hot Plenum and Top and Bottom Time Independent CVs

CV	elevation (m)	cross sectional area (m2)	volume (m3)
400	-3.994	2.946486	0
	-3.5622	2.946486	1.272
	-3.1304	2.946486	2.545
	-2.6986	2.946486	3.817
	-2.2668	2.946486	5.089
	-1.835	2.946486	6.361
	-1.585	2.946486	7.098
428	9.119	2.946486	0
	9.219	2.946486	0.295
	9.624	2.946486	1.488
	10.029	2.946486	2.681
	10.434	2.946486	3.875
	10.839	2.946486	5.068
	11.244	2.946486	6.261
	11.649	2.946486	7.455
429	11.649	2.946486	0
	12.149	2.946486	1.473

Table D.10

Heat Structure 31 Data

HS	IBVL (inner)	ASURFL (inner)	IBVL (outer)	ASURFL (outer)
310mm	4mm	4.7757	5mm	5.3268
310nn	4nn	4.7787	5nn	5.3301
310pp	4pp	4.7763	5pp	5.3274
31027	427	4.7775	527	5.3288

Table D.11

Heat Structure 31 Radii

Cross sectional area (m2)	0.3532251
Inner radius (m)	4.971
Outer radius (m)	4.982

Table D.12

CDA Volume

CV	cross sectional area (m2)	volume (m3)
5mm	341.7444685	135.41625
5nn	341.7444685	135.50168
5pp	341.7444685	135.43333
527	341.7444685	135.46751

Table D.13

CDA Hydraulic Diameter

Flow Area (m2)	341.7445
Wetted Perimeter (m)	4005.9746
Hydraulic Diameter (m)	0.3412

Table D.14

Heat Structure 35 Data

HS	IBVL (inner)	ASURFL (inner)
350mm	5mm	1552.9447
350nn	5nn	1553.9245
350pp	5pp	1553.1407
35027	527	1553.5326

Table D.15

Heat Structure 35 Radii

Cross sectional area (m2)	9.3324
Inner radius (m)	11.5587
Outer radius (m)	11.6865

Table D.16

RCCS Initial Pressure Data

	pressure (Pa)	h (m)	density (kg/m3)
CV400	1.01325E+05	1.402625	1.11709
CVn01	1.01310E+05	0.39625	1.11692
CVn02	1.01305E+05	0.39625	1.11687
CVn03	1.01301E+05	0.39625	1.11682
CVn04	1.01297E+05	0.396375	1.11677
CVn05	1.01292E+05	0.3965	1.11673
CVn06	1.01288E+05	0.3965	1.11668
CVn07	1.01284E+05	0.3965	1.11663
CVn08	1.01279E+05	0.3965	1.11658
CVn09	1.01275E+05	0.3965	1.11653
CVn10	1.01271E+05	0.3965	1.11649
CVn11	1.01266E+05	0.3965	1.11644
CVn12	1.01262E+05	0.3965	1.11639
CVn13	1.01258E+05	0.3965	1.11634
CVn14	1.01253E+05	0.3965	1.11629
CVn15	1.01249E+05	0.3965	1.11625
CVn16	1.01245E+05	0.3965	1.11620
CVn17	1.01240E+05	0.3965	1.11615
CVn18	1.01236E+05	0.3965	1.11610
CVn19	1.01232E+05	0.3965	1.11606
CVn20	1.01227E+05	0.3965	1.11601
CVn21	1.01223E+05	0.3965	1.11596
CVn22	1.01219E+05	0.3965	1.11591
CVn23	1.01214E+05	0.3965	1.11586
CVn24	1.01210E+05	0.3964	1.11582
CVn25	1.01206E+05	0.3963	1.11577
CVn26	1.01201E+05	0.39635	1.11572
CVn27	1.01197E+05	1.4632	1.11567
CV428	1.01181E+05	1.515	1.11550
CV429	1.01164E+05		

n = 3, 4 and 5

Table D.17:

CUA Flow Path Data

Flow path	Name	From	To	Elev. (m)	Length (m)
326	upairF26-T27	326	327	8.7226	0.39635
325	upairF25-T26	325	326	8.3263	0.3963
324	upairF24-T25	324	325	7.93	0.3964
323	upairF23-T24	323	324	7.5335	0.3965
304	upairF04-T05	304	305	0.0	0.396375
303	upairF03-T04	303	304	-0.39625	0.39625

For FLn22 to FLn05 and FLn03 to FLn01, each flow path has the same elevation as the top elevation of the CV with the same number and the same height as that CV. For instance, FL322 has the same elevation as the top elevation of CV322 and a height of 0.3965 which is the height of CV322.

n = 3 and 4

Table D.18:

Riser Air Flow Path Data

Flow path	Name	From	To	Elev. (m)	Length (m)
428	hptoSINK	428	429	11.649	1.515
427	riserF27-T28	427	428	9.119	1.4632
426	riserF26-T27	426	427	8.7226	0.39635
425	riserF25-T26	425	426	8.3263	0.3963
424	riserF24-T25	424	425	7.93	0.3964
423	riserF23-T24	423	424	7.5335	0.3965
404	riserF04-T05	404	405	0.0	0.396375
403	riserF03-T04	403	404	-0.39625	0.39625
400	riserF00-T01	400	401	-1.585	1.402625

Table D.19:

CDA Flow Path Data

Flow path	Name	From	To	Elev. (m)	Length (m)
527	downairF27-T26	527	526	8.7226	0.39635
526	downairF26-T25	526	525	8.3263	0.3963
525	downairF25-T24	525	524	7.93	0.3964
524	downairF24-T23	524	523	7.5335	0.3965
505	downairF05-T04	505	504	0.0	0.396375
504	downairF04-T03	504	503	-0.39625	0.39625

For FL523 to FL506 and FL504 to FL502, each flow path has the same elevation as the top elevation of the CV with the same number and the same height as that CV.

Table D.20:

Horizontal Flow Path Data

	Elev. (m)	Length (m)
from CV 501 to CV301	-1.386875	3.930371096
from CV 327 to CV527	8.9208	3.930371096

D.2 Input Decks

D.2 cavity-cooling.gen

*CV type definitions
CVTYPE07 upair
CVTYPE08 hp
CVTYPE09 tv
CVTYPE10 riserbv

CVTYPE11 risertv

CVTYPE12 bv

CVTYPE13 hd

CVTYPE14 downair

*hot plenum

CV42800 hp 2 0 8

CV42801 0 0

CV428A0 3

CV428A1 MLFR.5 1.0 TATM 316.0 PVOL 1.01181e5 PH2O 0.0

CV428B0 9.119 0.0

CV428B1 9.219 0.294648604

CV428B2 9.624 1.487975451

CV428B3 10.029 2.681302299

CV428B4 10.434 3.874629146

CV428B5 10.839 5.067955993

CV428B6 11.244 6.26128284

CV428B7 11.649 7.454609688

****

* Cavity up air volume

****

CV30100 upair301 2 2 7

CV30101 0 0

CV301A0 3

CV301A1 MLFR.5 1.0 TATM 316.0 PVOL 1.01310e5 PH2O 0.0

CV301B0 -1.585 0.0

CV301B1 -1.18875 11.04385529

```
CV30200   upair302  2  2  7
CV30201   0  0
CV302A0   3
CV302A1   MLFR.5  1.0  TATM  316.0  PVOL  1.01305e5  PH2O  0.0
CV302B0   -1.18875  0.0
CV302B1   -0.7925  11.04385529

CV30300   upair303  2  2  7
CV30301   0  0
CV303A0   3
CV303A1   MLFR.5  1.0  TATM  316.0  PVOL  1.01301e5  PH2O  0.0
CV303B0   -0.7925  0.0
CV303B1   -0.39625  11.04385529

CV30400   upair304  2  2  7
CV30401   0  0
CV304A0   3
CV304A1   MLFR.5  1.0  TATM  316.0  PVOL  1.01297e5  PH2O  0.0
CV304B0   -0.39625  0.0
CV304B1   0.0  11.04385529

CV30500   upair305  2  2  7
CV30501   0  0
CV305A0   3
CV305A1   MLFR.5  1.0  TATM  316.0  PVOL  1.01292e5  PH2O  0.0
CV305B0   0.0  0.0
CV305B1   0.3965  11.05082302

CV30600   upair306  2  2  7
```

```
CV30601   0  0
CV306A0   3
CV306A1   MLFR.5  1.0  TATM  316.0  PVOL  1.01288e5  PH2O  0.0
CV306B0   0.3965  0.0
CV306B1   0.793  11.05082302

CV30700   upair307  2  2  7
CV30701   0  0
CV307A0   3
CV307A1   MLFR.5  1.0  TATM  316.0  PVOL  1.01284e5  PH2O  0.0
CV307B0   0.793  0.0
CV307B1   1.1895  11.05082302

CV30800   upair308  2  2  7
CV30801   0  0
CV308A0   3
CV308A1   MLFR.5  1.0  TATM  316.0  PVOL  1.01279e5  PH2O  0.0
CV308B0   1.1895  0.0
CV308B1   1.586  11.05082302

CV30900   upair309  2  2  7
CV30901   0  0
CV309A0   3
CV309A1   MLFR.5  1.0  TATM  316.0  PVOL  1.01275e5  PH2O  0.0
CV309B0   1.586  0.0
CV309B1   1.9825  11.05082302

CV31000   upair310  2  2  7
CV31001   0  0
```

```
CV310A0   3
CV310A1   MLFR.5  1.0  TATM  316.0  PVOL  1.01271e5  PH2O  0.0
CV310B0   1.9825  0.0
CV310B1   2.379  11.05082302

CV31100   upair311  2  2  7
CV31101   0  0
CV311A0   3
CV311A1   MLFR.5  1.0  TATM  316.0  PVOL  1.01266e5  PH2O  0.0
CV311B0   2.379  0.0
CV311B1   2.7755  11.05082302

CV31200   upair312  2  2  7
CV31201   0  0
CV312A0   3
CV312A1   MLFR.5  1.0  TATM  316.0  PVOL  1.01262e5  PH2O  0.0
CV312B0   2.7755  0.0
CV312B1   3.172  11.05082302

CV31300   upair313  2  2  7
CV31301   0  0
CV313A0   3
CV313A1   MLFR.5  1.0  TATM  316.0  PVOL  1.01258e5  PH2O  0.0
CV313B0   3.172  0.0
CV313B1   3.5685  11.05082302

CV31400   upair314  2  2  7
CV31401   0  0
CV314A0   3
```

CV314A1 MLFR.5 1.0 TATM 316.0 PVOL 1.01253e5 PH2O 0.0
CV314B0 3.5685 0.0
CV314B1 3.965 11.05082302

CV31500 upair315 2 2 7
CV31501 0 0
CV315A0 3
CV315A1 MLFR.5 1.0 TATM 316.0 PVOL 1.01249e5 PH2O 0.0
CV315B0 3.965 0.0
CV315B1 4.3615 11.05082302

CV31600 upair316 2 2 7
CV31601 0 0
CV316A0 3
CV316A1 MLFR.5 1.0 TATM 316.0 PVOL 1.01245e5 PH2O 0.0
CV316B0 4.3615 0.0
CV316B1 4.758 11.05082302

CV31700 upair317 2 2 7
CV31701 0 0
CV317A0 3
CV317A1 MLFR.5 1.0 TATM 316.0 PVOL 1.01240e5 PH2O 0.0
CV317B0 4.758 0.0
CV317B1 5.1545 11.05082302

CV31800 upair318 2 2 7
CV31801 0 0
CV318A0 3
CV318A1 MLFR.5 1.0 TATM 316.0 PVOL 1.01236e5 PH2O 0.0

CV318B0 5.1545 0.0
CV318B1 5.551 11.05082302

CV31900 upair319 2 2 7
CV31901 0 0
CV319A0 3
CV319A1 MLFR.5 1.0 TATM 316.0 PVOL 1.01232e5 PH2O 0.0
CV319B0 5.551 0.0
CV319B1 5.9475 11.05082302

CV32000 upair320 2 2 7
CV32001 0 0
CV320A0 3
CV320A1 MLFR.5 1.0 TATM 316.0 PVOL 1.01227e5 PH2O 0.0
CV320B0 5.9475 0.0
CV320B1 6.344 11.05082302

CV32100 upair321 2 2 7
CV32101 0 0
CV321A0 3
CV321A1 MLFR.5 1.0 TATM 316.0 PVOL 1.01223e5 PH2O 0.0
CV321B0 6.344 0.0
CV321B1 6.7405 11.05082302

CV32200 upair322 2 2 7
CV32201 0 0
CV322A0 3
CV322A1 MLFR.5 1.0 TATM 316.0 PVOL 1.01219e5 PH2O 0.0
CV322B0 6.7405 0.0

```
CV322B1   7.137  11.05082302

CV32300   upair323  2  2  7
CV32301   0  0
CV323A0   3
CV323A1   MLFR.5  1.0  TATM  316.0  PVOL  1.01214e5  PH2O  0.0
CV323B0   7.137  0.0
CV323B1   7.5335  11.05082302

CV32400   upair324  2  2  7
CV32401   0  0
CV324A0   3
CV324A1   MLFR.5  1.0  TATM  316.0  PVOL  1.01210e5  PH2O  0.0
CV324B0   7.5335  0.0
CV324B1   7.93  11.05082302

CV32500   upair325  2  2  7
CV32501   0  0
CV325A0   3
CV325A1   MLFR.5  1.0  TATM  316.0  PVOL  1.01206e5  PH2O  0.0
CV325B0   7.93  0.0
CV325B1   8.3263  11.04524884

CV32600   upair326  2  2  7
CV32601   0  0
CV326A0   3
CV326A1   MLFR.5  1.0  TATM  316.0  PVOL  1.01201e5  PH2O  0.0
CV326B0   8.3263  0.0
CV326B1   8.7226  11.04524884
```

```
CV32700   upair327  2  2  7
CV32701   0  0
CV327A0   3
CV327A1   MLFR.5  1.0  TATM  316.0  PVOL  1.01197e5  PH2O  0.0
CV327B0   8.7226  0.0
CV327B1   9.119  11.04803593

*******************************
* RCCS riser air
*******************************
CV40100   hd401  2  2  13
CV40101   0  0
CV401A0   3
CV401A1   MLFR.5  1.0  TATM  316.0  PVOL  1.01310e5  PH2O  0.0
CV401B0   -1.585  0.0
CV401B1   -1.18875  1.167545094

CV40200   hd402  2  2  13
CV40201   0  0
CV402A0   3
CV402A1   MLFR.5  1.0  TATM  316.0  PVOL  1.01305e5  PH2O  0.0
CV402B0   -1.18875  0.0
CV402B1   -0.7925  1.167545094

CV40300   hd403  2  2  13
CV40301   0  0
CV403A0   3
CV403A1   MLFR.5  1.0  TATM  316.0  PVOL  1.01301e5  PH2O  0.0
```

```
CV403B0   -0.7925  0.0
CV403B1   -0.39625  1.167545094

CV40400   hd404  2  2  13
CV40401   0  0
CV404A0   3
CV404A1   MLFR.5  1.0  TATM  316.0  PVOL  1.01297e5  PH2O  0.0
CV404B0   -0.39625  0.0
CV404B1   0.0  1.167545094

CV40500   hd405  2  2  13
CV40501   0  0
CV405A0   3
CV405A1   MLFR.5  1.0  TATM  316.0  PVOL  1.01292e5  PH2O  0.0
CV405B0   0.0  0.0
CV405B1   0.3965  1.168281716

CV40600   hd406  2  2  13
CV40601   0  0
CV406A0   3
CV406A1   MLFR.5  1.0  TATM  316.0  PVOL  1.01288e5  PH2O  0.0
CV406B0   0.3965  0.0
CV406B1   0.793  1.168281716

CV40700   hd407  2  2  13
CV40701   0  0
CV407A0   3
CV407A1   MLFR.5  1.0  TATM  316.0  PVOL  1.01284e5  PH2O  0.0
CV407B0   0.793  0.0
```

```
CV407B1   1.1895  1.168281716

CV40800   hd408  2  2  13
CV40801   0  0
CV408A0   3
CV408A1   MLFR.5  1.0  TATM  316.0  PVOL  1.01279e5  PH2O  0.0
CV408B0   1.1895  0.0
CV408B1   1.586  1.168281716

CV40900   hd409  2  2  13
CV40901   0  0
CV409A0   3
CV409A1   MLFR.5  1.0  TATM  316.0  PVOL  1.01275e5  PH2O  0.0
CV409B0   1.586  0.0
CV409B1   1.9825  1.168281716

CV41000   hd410  2  2  13
CV41001   0  0
CV410A0   3
CV410A1   MLFR.5  1.0  TATM  316.0  PVOL  1.01271e5  PH2O  0.0
CV410B0   1.9825  0.0
CV410B1   2.379  1.168281716

CV41100   hd411  2  2  13
CV41101   0  0
CV411A0   3
CV411A1   MLFR.5  1.0  TATM  316.0  PVOL  1.01266e5  PH2O  0.0
CV411B0   2.379  0.0
CV411B1   2.7755  1.168281716
```

```
CV41200   hd412  2  2  13
CV41201   0  0
CV412A0   3
CV412A1   MLFR.5  1.0  TATM  316.0  PVOL  1.01262e5  PH2O  0.0
CV412B0   2.7755  0.0
CV412B1   3.172  1.168281716

CV41300   hd413  2  2  13
CV41301   0  0
CV413A0   3
CV413A1   MLFR.5  1.0  TATM  316.0  PVOL  1.01258e5  PH2O  0.0
CV413B0   3.172  0.0
CV413B1   3.5685  1.168281716

CV41400   hd414  2  2  13
CV41401   0  0
CV414A0   3
CV414A1   MLFR.5  1.0  TATM  316.0  PVOL  1.01253e5  PH2O  0.0
CV414B0   3.5685  0.0
CV414B1   3.965  1.168281716

CV41500   hd415  2  2  13
CV41501   0  0
CV415A0   3
CV415A1   MLFR.5  1.0  TATM  316.0  PVOL  1.01249e5  PH2O  0.0
CV415B0   3.965  0.0
CV415B1   4.3615  1.168281716
```

```
CV41600   hd416  2  2  13
CV41601   0  0
CV416A0   3
CV416A1   MLFR.5  1.0  TATM  316.0  PVOL  1.01245e5  PH2O  0.0
CV416B0   4.3615  0.0
CV416B1   4.758  1.168281716

CV41700   hd417  2  2  13
CV41701   0  0
CV417A0   3
CV417A1   MLFR.5  1.0  TATM  316.0  PVOL  1.01240e5  PH2O  0.0
CV417B0   4.758  0.0
CV417B1   5.1545  1.168281716

CV41800   hd418  2  2  13
CV41801   0  0
CV418A0   3
CV418A1   MLFR.5  1.0  TATM  316.0  PVOL  1.01236e5  PH2O  0.0
CV418B0   5.1545  0.0
CV418B1   5.551  1.168281716

CV41900   hd419  2  2  13
CV41901   0  0
CV419A0   3
CV419A1   MLFR.5  1.0  TATM  316.0  PVOL  1.01232e5  PH2O  0.0
CV419B0   5.551  0.0
CV419B1   5.9475  1.168281716

CV42000   hd420  2  2  13
```

```
CV42001   0  0
CV420A0   3
CV420A1   MLFR.5  1.0  TATM  316.0  PVOL  1.01227e5  PH2O  0.0
CV420B0   5.9475  0.0
CV420B1   6.344  1.168281716

CV42100   hd421  2  2  13
CV42101   0  0
CV421A0   3
CV421A1   MLFR.5  1.0  TATM  316.0  PVOL  1.01223e5  PH2O  0.0
CV421B0   6.344  0.0
CV421B1   6.7405  1.168281716

CV42200   hd422  2  2  13
CV42201   0  0
CV422A0   3
CV422A1   MLFR.5  1.0  TATM  316.0  PVOL  1.01219e5  PH2O  0.0
CV422B0   6.7405  0.0
CV422B1   7.137  1.168281716

CV42300   hd423  2  2  13
CV42301   0  0
CV423A0   3
CV423A1   MLFR.5  1.0  TATM  316.0  PVOL  1.01214e5  PH2O  0.0
CV423B0   7.137  0.0
CV423B1   7.5335  1.168281716

CV42400   hd424  2  2  13
CV42401   0  0
```

```
CV424A0   3
CV424A1   MLFR.5  1.0  TATM  316.0  PVOL  1.01210e5  PH2O  0.0
CV424B0   7.5335  0.0
CV424B1   7.93  1.168281716

CV42500   hd425  2  2  13
CV42501   0  0
CV425A0   3
CV425A1   MLFR.5  1.0  TATM  316.0  PVOL  1.01206e5  PH2O  0.0
CV425B0   7.93  0.0
CV425B1   8.3263  1.167692419

CV42600   hd426  2  2  13
CV42601   0  0
CV426A0   3
CV426A1   MLFR.5  1.0  TATM  316.0  PVOL  1.01201e5  PH2O  0.0
CV426B0   8.3263  0.0
CV426B1   8.7226  1.167692419

CV42700   hd427  2  2  13
CV42701   0  0
CV427A0   3
CV427A1   MLFR.5  1.0  TATM  316.0  PVOL  1.01197e5  PH2O  0.0
CV427B0   8.7226  0.0
CV427B1   9.119  1.167987067

*******************************
* Cavity down air
*******************************
```

```
CV50100   downair501  2  2  14
CV50101   0  0
CV501A0   3
CV501A1   MLFR.5  1.0  TATM  316.0  PVOL  1.01310e5  PH2O  0.0
CV501B0   -1.585  0.0
CV501B1   -1.18875  135.4162457

CV50200   downair502  2  2  14
CV50201   0  0
CV502A0   3
CV502A1   MLFR.5  1.0  TATM  316.0  PVOL  1.01305e5  PH2O  0.0
CV502B0   -1.18875  0.0
CV502B1   -0.7925  135.4162457

CV50300   downair503  2  2  14
CV50301   0  0
CV503A0   3
CV503A1   MLFR.5  1.0  TATM  316.0  PVOL  1.01301e5  PH2O  0.0
CV503B0   -0.7925  0.0
CV503B1   -0.39625  135.4162457

CV50400   downair504  2  2  14
CV50401   0  0
CV504A0   3
CV504A1   MLFR.5  1.0  TATM  316.0  PVOL  1.01297e5  PH2O  0.0
CV504B0   -0.39625  0.0
CV504B1   0.0  135.4162457

CV50500   downair505  2  2  14
```

```
CV50501   0  0
CV505A0   3
CV505A1   MLFR.5  1.0  TATM  316.0  PVOL  1.01292e5  PH2O  0.0
CV505B0   0.0  0.0
CV505B1   0.3965  135.5016818

CV50600   downair506  2  2  14
CV50601   0  0
CV506A0   3
CV506A1   MLFR.5  1.0  TATM  316.0  PVOL  1.01288e5  PH2O  0.0
CV506B0   0.3965  0.0
CV506B1   0.793  135.5016818

CV50700   downair507  2  2  14
CV50701   0  0
CV507A0   3
CV507A1   MLFR.5  1.0  TATM  316.0  PVOL  1.01284e5  PH2O  0.0
CV507B0   0.793  0.0
CV507B1   1.1895  135.5016818

CV50800   downair508  2  2  14
CV50801   0  0
CV508A0   3
CV508A1   MLFR.5  1.0  TATM  316.0  PVOL  1.01279e5  PH2O  0.0
CV508B0   1.1895  0.0
CV508B1   1.586  135.5016818

CV50900   downair509  2  2  14
CV50901   0  0
```

CV509A0 3
CV509A1 MLFR.5 1.0 TATM 316.0 PVOL 1.01275e5 PH2O 0.0
CV509B0 1.586 0.0
CV509B1 1.9825 135.5016818

CV51000 downair510 2 2 14
CV51001 0 0
CV510A0 3
CV510A1 MLFR.5 1.0 TATM 316.0 PVOL 1.01271e5 PH2O 0.0
CV510B0 1.9825 0.0
CV510B1 2.379 135.5016818

CV51100 downair511 2 2 14
CV51101 0 0
CV511A0 3
CV511A1 MLFR.5 1.0 TATM 316.0 PVOL 1.01266e5 PH2O 0.0
CV511B0 2.379 0.0
CV511B1 2.7755 135.5016818

CV51200 downair512 2 2 14
CV51201 0 0
CV512A0 3
CV512A1 MLFR.5 1.0 TATM 316.0 PVOL 1.01262e5 PH2O 0.0
CV512B0 2.7755 0.0
CV512B1 3.172 135.5016818

CV51300 downair513 2 2 14
CV51301 0 0
CV513A0 3

CV513A1 MLFR.5 1.0 TATM 316.0 PVOL 1.01258e5 PH2O 0.0
CV513B0 3.172 0.0
CV513B1 3.5685 135.5016818

CV51400 downair514 2 2 14
CV51401 0 0
CV514A0 3
CV514A1 MLFR.5 1.0 TATM 316.0 PVOL 1.01253e5 PH2O 0.0
CV514B0 3.5685 0.0
CV514B1 3.965 135.5016818

CV51500 downair515 2 2 14
CV51501 0 0
CV515A0 3
CV515A1 MLFR.5 1.0 TATM 316.0 PVOL 1.01249e5 PH2O 0.0
CV515B0 3.965 0.0
CV515B1 4.3615 135.5016818

CV51600 downair516 2 2 14
CV51601 0 0
CV516A0 3
CV516A1 MLFR.5 1.0 TATM 316.0 PVOL 1.01245e5 PH2O 0.0
CV516B0 4.3615 0.0
CV516B1 4.758 135.5016818

CV51700 downair517 2 2 14
CV51701 0 0
CV517A0 3
CV517A1 MLFR.5 1.0 TATM 316.0 PVOL 1.01240e5 PH2O 0.0

```
CV517B0   4.758  0.0
CV517B1   5.1545  135.5016818

CV51800   downair518  2  2  14
CV51801   0  0
CV518A0   3
CV518A1   MLFR.5  1.0  TATM  316.0  PVOL  1.01236e5  PH2O  0.0
CV518B0   5.1545  0.0
CV518B1   5.551  135.5016818

CV51900   downair519  2  2  14
CV51901   0  0
CV519A0   3
CV519A1   MLFR.5  1.0  TATM  316.0  PVOL  1.01232e5  PH2O  0.0
CV519B0   5.551  0.0
CV519B1   5.9475  135.5016818

CV52000   downair520  2  2  14
CV52001   0  0
CV520A0   3
CV520A1   MLFR.5  1.0  TATM  316.0  PVOL  1.01227e5  PH2O  0.0
CV520B0   5.9475  0.0
CV520B1   6.344  135.5016818

CV52100   downair521  2  2  14
CV52101   0  0
CV521A0   3
CV521A1   MLFR.5  1.0  TATM  316.0  PVOL  1.01223e5  PH2O  0.0
CV521B0   6.344  0.0
```

```
CV521B1   6.7405  135.5016818

CV52200   downair522  2  2  14
CV52201   0  0
CV522A0   3
CV522A1   MLFR.5  1.0  TATM  316.0  PVOL  1.01219e5  PH2O  0.0
CV522B0   6.7405  0.0
CV522B1   7.137  135.5016818

CV52300   downair523  2  2  14
CV52301   0  0
CV523A0   3
CV523A1   MLFR.5  1.0  TATM  316.0  PVOL  1.01214e5  PH2O  0.0
CV523B0   7.137  0.0
CV523B1   7.5335  135.5016818

CV52400   downair524  2  2  14
CV52401   0  0
CV524A0   3
CV524A1   MLFR.5  1.0  TATM  316.0  PVOL  1.01210e5  PH2O  0.0
CV524B0   7.5335  0.0
CV524B1   7.93  135.5016818

CV52500   downair525  2  2  14
CV52501   0  0
CV525A0   3
CV525A1   MLFR.5  1.0  TATM  316.0  PVOL  1.01206e5  PH2O  0.0
CV525B0   7.93  0.0
CV525B1   8.3263  135.4333329
```

CV52600 downair526 2 2 14

CV52601 0 0

CV526A0 3

CV526A1 MLFR.5 1.0 TATM 316.0 PVOL 1.01201e5 PH2O 0.0

CV526B0 8.3263 0.0

CV526B1 8.7226 135.4333329

CV52700 downair527 2 2 14

CV52701 0 0

CV527A0 3

CV527A1 MLFR.5 1.0 TATM 316.0 PVOL 1.01197e5 PH2O 0.0

CV527B0 8.7226 0.0

CV527B1 9.119 135.4675073

****

* Axial upward RCCS flowpaths

****

*cavity up air flow paths

FL32700 upairF27-T27 327 527 8.9208 8.9208

FL32701 27.87092818 3.930371096 1.0

FL32702 3 0 0 0

FL327S1 27.87092818 3.930371096 0.60442162

FL32600 upairF26-T27 326 327 8.7226 8.7226

FL32601 27.87092818 0.39635 1.0

FL32602 0 0 0 0

FL326S1 27.87092818 0.39635 0.60442162

FL32500 upairF25-T26 325 326 8.3263 8.3263

FL32501 27.87092818 0.3963 1.0

FL32502 0 0 0 0

FL325S1 27.87092818 0.3963 0.60442162

FL32400 upairF24-T25 324 325 7.93 7.93

FL32401 27.87092818 0.3964 1.0

FL32402 0 0 0 0

FL324S1 27.87092818 0.3964 0.60442162

FL32300 upairF23-T24 323 324 7.5335 7.5335

FL32301 27.87092818 0.3965 1.0

FL32302 0 0 0 0

FL323S1 27.87092818 0.3965 0.60442162

FL32200 upairF22-T23 322 323 7.137 7.137

FL32201 27.87092818 0.3965 1.0

FL32202 0 0 0 0

FL322S1 27.87092818 0.3965 0.60442162

FL32100 upairF21-T22 321 322 6.7405 6.7405

FL32101 27.87092818 0.3965 1.0

FL32102 0 0 0 0

FL321S1 27.87092818 0.3965 0.60442162

FL32000 upairF20-T21 320 321 6.344 6.344

FL32001 27.87092818 0.3965 1.0

FL32002 0 0 0 0

FL320S1 27.87092818 0.3965 0.60442162

FL31900 upairF19-T20 319 320 5.9475 5.9475
FL31901 27.87092818 0.3965 1.0
FL31902 0 0 0 0
FL319S1 27.87092818 0.3965 0.60442162

FL31800 upairF18-T19 318 319 5.551 5.551
FL31801 27.87092818 0.3965 1.0
FL31802 0 0 0 0
FL318S1 27.87092818 0.3965 0.60442162

FL31700 upairF17-T18 317 318 5.1545 5.1545
FL31701 27.87092818 0.3965 1.0
FL31702 0 0 0 0
FL317S1 27.87092818 0.3965 0.60442162

FL31600 upairF16-T17 316 317 4.758 4.758
FL31601 27.87092818 0.3965 1.0
FL31602 0 0 0 0
FL316S1 27.87092818 0.3965 0.60442162

FL31500 upairF15-T16 315 316 4.3615 4.3615
FL31501 27.87092818 0.3965 1.0
FL31502 0 0 0 0
FL315S1 27.87092818 0.3965 0.60442162

FL31400 upairF14-T15 314 315 3.965 3.965
FL31401 27.87092818 0.3965 1.0

FL31402 0 0 0 0

FL314S1 27.87092818 0.3965 0.60442162

FL31300 upairF13-T14 313 314 3.5685 3.5685

FL31301 27.87092818 0.3965 1.0

FL31302 0 0 0 0

FL313S1 27.87092818 0.3965 0.60442162

FL31200 upairF12-T13 312 313 3.172 3.172

FL31201 27.87092818 0.3965 1.0

FL31202 0 0 0 0

FL312S1 27.87092818 0.3965 0.60442162

FL31100 upairF11-T12 311 312 2.7755 2.7755

FL31101 27.87092818 0.3965 1.0

FL31102 0 0 0 0

FL311S1 27.87092818 0.3965 0.60442162

FL31000 upairF10-T11 310 311 2.379 2.379

FL31001 27.87092818 0.3965 1.0

FL31002 0 0 0 0

FL310S1 27.87092818 0.3965 0.60442162

FL30900 upairF09-T10 309 310 1.9825 1.9825

FL30901 27.87092818 0.3965 1.0

FL30902 0 0 0 0

FL309S1 27.87092818 0.3965 0.60442162

FL30800 upairF08-T09 308 309 1.586 1.586

FL30801 27.87092818 0.3965 1.0

FL30802 0 0 0 0

FL308S1 27.87092818 0.3965 0.60442162

FL30700 upairF07-T08 307 308 1.1895 1.1895

FL30701 27.87092818 0.3965 1.0

FL30702 0 0 0 0

FL307S1 27.87092818 0.3965 0.60442162

FL30600 upairF06-T07 306 307 0.793 0.793

FL30601 27.87092818 0.3965 1.0

FL30602 0 0 0 0

FL306S1 27.87092818 0.3965 0.60442162

FL30500 upairF05-T06 305 306 0.3965 0.3965

FL30501 27.87092818 0.3965 1.0

FL30502 0 0 0 0

FL305S1 27.87092818 0.3965 0.60442162

FL30400 upairF04-T05 304 305 0.0 0.0

FL30401 27.87092818 0.396375 1.0

FL30402 0 0 0 0

FL304S1 27.87092818 0.396375 0.60442162

FL30300 upairF03-T04 303 304 -0.39625 -0.39625

FL30301 27.87092818 0.39625 1.0

FL30302 0 0 0 0

FL303S1 27.87092818 0.39625 0.60442162

FL30200 upairF02-T03 302 303 -0.7925 -0.7925

FL30201 27.87092818 0.39625 1.0

FL30202 0 0 0 0

FL302S1 27.87092818 0.39625 0.60442162

FL30100 upairF01-T02 301 302 -1.18875 -1.18875

FL30101 27.87092818 0.39625 1.0

FL30102 0 0 0 0

FL301S1 27.87092818 0.39625 0.60442162

*RCCS riser

FL42700 riserF27-T28 427 428 9.119 9.119

FL42701 2.946486043 1.4632 1.0

FL42702 0 0 0 0

FL427S1 2.946486043 1.4632 0.070626111

FL42600 riserF26-T27 426 427 8.7226 8.7226

FL42601 2.946486043 0.39635 1.0

FL42602 0 0 0 0

FL426S1 2.946486043 0.39635 0.070626111

FL42500 riserF25-T26 425 426 8.3263 8.3263

FL42501 2.946486043 0.3963 1.0

FL42502 0 0 0 0

FL425S1 2.946486043 0.3963 0.070626111

FL42400 riserF24-T25 424 425 7.93 7.93

FL42401 2.946486043 0.3964 1.0

FL42402 0 0 0 0

FL424S1 2.946486043 0.3964 0.070626111

FL42300 riserF23-T24 423 424 7.5335 7.5335

FL42301 2.946486043 0.3965 1.0

FL42302 0 0 0 0

FL423S1 2.946486043 0.3965 0.070626111

FL42200 riserF22-T23 422 423 7.137 7.137

FL42201 2.946486043 0.3965 1.0

FL42202 0 0 0 0

FL422S1 2.946486043 0.3965 0.070626111

FL42100 riserF21-T22 421 422 6.7405 6.7405

FL42101 2.946486043 0.3965 1.0

FL42102 0 0 0 0

FL421S1 2.946486043 0.3965 0.070626111

FL42000 riserF20-T21 420 421 6.344 6.344

FL42001 2.946486043 0.3965 1.0

FL42002 0 0 0 0

FL420S1 2.946486043 0.3965 0.070626111

FL41900 riserF19-T20 419 420 5.9475 5.9475

FL41901 2.946486043 0.3965 1.0

FL41902 0 0 0 0

FL419S1 2.946486043 0.3965 0.070626111

FL41800 riserF18-T19 418 419 5.551 5.551

FL41801 2.946486043 0.3965 1.0

FL41802 0 0 0 0

FL418S1 2.946486043 0.3965 0.070626111

FL41700 riserF17-T18 417 418 5.1545 5.1545

FL41701 2.946486043 0.3965 1.0

FL41702 0 0 0 0

FL417S1 2.946486043 0.3965 0.070626111

FL41600 riserF16-T17 416 417 4.758 4.758

FL41601 2.946486043 0.3965 1.0

FL41602 0 0 0 0

FL416S1 2.946486043 0.3965 0.070626111

FL41500 riserF15-T16 415 416 4.3615 4.3615

FL41501 2.946486043 0.3965 1.0

FL41502 0 0 0 0

FL415S1 2.946486043 0.3965 0.070626111

FL41400 riserF14-T15 414 415 3.965 3.965

FL41401 2.946486043 0.3965 1.0

FL41402 0 0 0 0

FL414S1 2.946486043 0.3965 0.070626111

FL41300 riserF13-T14 413 414 3.5685 3.5685

FL41301 2.946486043 0.3965 1.0

FL41302 0 0 0 0

FL413S1 2.946486043 0.3965 0.070626111

FL41200 riserF12-T13 412 413 3.172 3.172

FL41201 2.946486043 0.3965 1.0

FL41202 0 0 0 0

FL412S1 2.946486043 0.3965 0.070626111

FL41100 riserF11-T12 411 412 2.7755 2.7755

FL41101 2.946486043 0.3965 1.0

FL41102 0 0 0 0

FL411S1 2.946486043 0.3965 0.070626111

FL41000 riserF10-T11 410 411 2.379 2.379

FL41001 2.946486043 0.3965 1.0

FL41002 0 0 0 0

FL410S1 2.946486043 0.3965 0.070626111

FL40900 riserF09-T10 409 410 1.9825 1.9825

FL40901 2.946486043 0.3965 1.0

FL40902 0 0 0 0

FL409S1 2.946486043 0.3965 0.070626111

FL40800 riserF08-T09 408 409 1.586 1.586

FL40801 2.946486043 0.3965 1.0

FL40802 0 0 0 0

FL408S1 2.946486043 0.3965 0.070626111

FL40700 riserF07-T08 407 408 1.1895 1.1895

FL40701 2.946486043 0.3965 1.0

FL40702 0 0 0 0

FL407S1 2.946486043 0.3965 0.070626111

FL40600 riserF06-T07 406 407 0.793 0.793

FL40601 2.946486043 0.3965 1.0

FL40602 0 0 0 0

FL406S1 2.946486043 0.3965 0.070626111

FL40500 riserF05-T06 405 406 0.3965 0.3965

FL40501 2.946486043 0.3965 1.0

FL40502 0 0 0 0

FL405S1 2.946486043 0.3965 0.070626111

FL40400 riserF04-T05 404 405 0.0 0.0

FL40401 2.946486043 0.396375 1.0

FL40402 0 0 0 0

FL404S1 2.946486043 0.396375 0.070626111

FL40300 riserF03-T04 403 404 -0.39625 -0.39625

FL40301 2.946486043 0.39625 1.0

FL40302 0 0 0 0

FL403S1 2.946486043 0.39625 0.070626111

FL40200 riserF02-T03 402 403 -0.7925 -0.7925

FL40201 2.946486043 0.39625 1.0

FL40202 0 0 0 0

FL402S1 2.946486043 0.39625 0.070626111

FL40100 riserF01-T02 401 402 -1.18875 -1.18875

FL40101 2.946486043 0.39625 1.0

FL40102 0 0 0 0

FL401S1 2.946486043 0.39625 0.070626111

*Form loss coefficient for the RCCS riser duct

FL40103 0.0 0.0 1.0 1.0

FL40203 0.0 0.0 1.0 1.0

FL40303 0.0 0.0 1.0 1.0

FL40403 0.0 0.0 1.0 1.0

FL40503 0.0 0.0 1.0 1.0

FL40603 0.0 0.0 1.0 1.0

FL40703 0.0 0.0 1.0 1.0

FL40803 0.0 0.0 1.0 1.0

FL40903 0.0 0.0 1.0 1.0

FL41003 0.0 0.0 1.0 1.0

FL41103 0.0 0.0 1.0 1.0

FL41203 0.0 0.0 1.0 1.0

FL41303 0.0 0.0 1.0 1.0

FL41403 0.0 0.0 1.0 1.0

FL41503 0.0 0.0 1.0 1.0

FL41603 0.0 0.0 1.0 1.0

FL41703 0.0 0.0 1.0 1.0

FL41803 0.0 0.0 1.0 1.0

FL41903 0.0 0.0 1.0 1.0

FL42003 0.0 0.0 1.0 1.0

FL42103 0.0 0.0 1.0 1.0

FL42203 0.0 0.0 1.0 1.0

FL42303 0.0 0.0 1.0 1.0

FL42403 0.0 0.0 1.0 1.0

FL42503 0.0 0.0 1.0 1.0

FL42603 0.0 0.0 1.0 1.0

*cavity down air flow paths

FL52700 downairF27-T26 527 526 8.7226 8.7226
FL52701 341.7444685 0.39635 1.0
FL52702 0 0 0 0
FL527S1 341.7444685 0.39635 0.341234781

FL52600 downairF26-T25 526 525 8.3263 8.3263
FL52601 341.7444685 0.3963 1.0
FL52602 0 0 0 0
FL526S1 341.7444685 0.3963 0.341234781

FL52500 downairF25-T24 525 524 7.93 7.93
FL52501 341.7444685 0.3964 1.0
FL52502 0 0 0 0
FL525S1 341.7444685 0.3964 0.341234781

FL52400 downairF24-T23 524 523 7.5335 7.5335
FL52401 341.7444685 0.3965 1.0
FL52402 0 0 0 0
FL524S1 341.7444685 0.3965 0.341234781

FL52300 downairF23-T22 523 522 7.137 7.137
FL52301 341.7444685 0.3965 1.0
FL52302 0 0 0 0
FL523S1 341.7444685 0.3965 0.341234781

FL52200 downairF22-T21 522 521 6.7405 6.7405

FL52201 341.7444685 0.3965 1.0

FL52202 0 0 0 0

FL522S1 341.7444685 0.3965 0.341234781

FL52100 downairF21-T20 521 520 6.344 6.344

FL52101 341.7444685 0.3965 1.0

FL52102 0 0 0 0

FL521S1 341.7444685 0.3965 0.341234781

FL52000 downairF20-T19 520 519 5.9475 5.9475

FL52001 341.7444685 0.3965 1.0

FL52002 0 0 0 0

FL520S1 341.7444685 0.3965 0.341234781

FL51900 downairF19-T18 519 518 5.551 5.551

FL51901 341.7444685 0.3965 1.0

FL51902 0 0 0 0

FL519S1 341.7444685 0.3965 0.341234781

FL51800 downairF18-T17 518 517 5.1545 5.1545

FL51801 341.7444685 0.3965 1.0

FL51802 0 0 0 0

FL518S1 341.7444685 0.3965 0.341234781

FL51700 downairF17-T16 517 516 4.758 4.758

FL51701 341.7444685 0.3965 1.0

FL51702 0 0 0 0

FL517S1 341.7444685 0.3965 0.341234781

FL51600 downairF16-T15 516 515 4.3615 4.3615

FL51601 341.7444685 0.3965 1.0

FL51602 0 0 0 0

FL516S1 341.7444685 0.3965 0.341234781

FL51500 downairF15-T14 515 514 3.965 3.965

FL51501 341.7444685 0.3965 1.0

FL51502 0 0 0 0

FL515S1 341.7444685 0.3965 0.341234781

FL51400 downairF14-T13 514 513 3.5685 3.5685

FL51401 341.7444685 0.3965 1.0

FL51402 0 0 0 0

FL514S1 341.7444685 0.3965 0.341234781

FL51300 downairF13-T12 513 512 3.172 3.172

FL51301 341.7444685 0.3965 1.0

FL51302 0 0 0 0

FL513S1 341.7444685 0.3965 0.341234781

FL51200 downairF12-T11 512 511 2.7755 2.7755

FL51201 341.7444685 0.3965 1.0

FL51202 0 0 0 0

FL512S1 341.7444685 0.3965 0.341234781

FL51100 downairF11-T10 511 510 2.379 2.379

FL51101 341.7444685 0.3965 1.0

FL51102 0 0 0 0

FL511S1 341.7444685 0.3965 0.341234781

FL51000 downairF10-T09 510 509 1.9825 1.9825

FL51001 341.7444685 0.3965 1.0

FL51002 0 0 0 0

FL510S1 341.7444685 0.3965 0.341234781

FL50900 downairF09-T08 509 508 1.586 1.586

FL50901 341.7444685 0.3965 1.0

FL50902 0 0 0 0

FL509S1 341.7444685 0.3965 0.341234781

FL50800 downairF08-T07 508 507 1.1895 1.1895

FL50801 341.7444685 0.3965 1.0

FL50802 0 0 0 0

FL508S1 341.7444685 0.3965 0.341234781

FL50700 downairF07-T06 507 506 0.793 0.793

FL50701 341.7444685 0.3965 1.0

FL50702 0 0 0 0

FL507S1 341.7444685 0.3965 0.341234781

FL50600 downairF06-T05 506 505 0.3965 0.3965

FL50601 341.7444685 0.3965 1.0

FL50602 0 0 0 0

FL506S1 341.7444685 0.3965 0.341234781

FL50500 downairF05-T04 505 504 0.0 0.0

FL50501 341.7444685 0.396375 1.0

FL50502 0 0 0 0

FL505S1 341.7444685 0.396375 0.341234781

FL50400 downairF04-T03 504 503 -0.39625 -0.39625
FL50401 341.7444685 0.39625 1.0
FL50402 0 0 0 0
FL504S1 341.7444685 0.39625 0.341234781

FL50300 downairF03-T02 503 502 -0.7925 -0.7925
FL50301 341.7444685 0.39625 1.0
FL50302 0 0 0 0
FL503S1 341.7444685 0.39625 0.341234781

FL50200 downairF02-T01 502 501 -1.18875 -1.18875
FL50201 341.7444685 0.39625 1.0
FL50202 0 0 0 0
FL502S1 341.7444685 0.39625 0.341234781

FL50100 downairF01-T01 501 301 -1.386875 -1.386875
FL50101 27.87092818 3.930371096 1.0
FL50102 3 0 0 0
FL501S1 27.87092818 3.930371096 0.60442162

****
* Three hot sides of the hot ducts
****
*level 1
HS30001000 2 2 -1
HS30001001 hsides_LVL_1
HS30001002 -1.585 1.0

HS30001100 -1 1 4.8511

HS30001101 4.8757 2

HS30001200 -1 * index for material

HS30001201 stainless-steel-304 1

HS30001300 0

HS30001400 1 301 'EXT' 0.9 0.9

HS30001500 63.55386388 0.60442162 0.39625

HS30001600 1 401 'INT' 0.9 0.9

HS30001700 61.34968363 0.070626111 0.39625

HS30001800 -1

HS30001801 316.0 1

HS30001802 316.0 2

*level 2

HS30002000 2 2 -1

HS30002001 hsides_LVL_2

HS30002002 -1.18875 1.0

HS30002100 -1 1 4.8511

HS30002101 4.8757 2

HS30002200 -1 * index for material

HS30002201 stainless-steel-304 1

HS30002300 0

HS30002400 1 302 'EXT' 0.9 0.9

HS30002500 63.55386388 0.60442162 0.39625

HS30002600 1 402 'INT' 0.9 0.9

HS30002700 61.34968363 0.070626111 0.39625

HS30002800 -1

HS30002801 316.0 1

HS30002802 316.0 2

```
*level 3
HS30003000  2  2  -1
HS30003001  hsides_LVL_3
HS30003002  -0.7925  1.0
HS30003100  -1  1  4.8511
HS30003101  4.8757  2
HS30003200  -1  * index for material
HS30003201  stainless-steel-304  1
HS30003300  0
HS30003400  1  303  'EXT'  0.9  0.9
HS30003500  63.55386388   0.60442162  0.39625
HS30003600  1  403  'INT'  0.9  0.9
HS30003700  61.34968363   0.070626111  0.39625
HS30003800  -1
HS30003801  316.0  1
HS30003802  316.0  2

*level 4
HS30004000  2  2  -1
HS30004001  hsides_LVL_4
HS30004002  -0.39625  1.0
HS30004100  -1  1  4.8511
HS30004101  4.8757  2
HS30004200  -1  * index for material
HS30004201  stainless-steel-304  1
HS30004300  0
HS30004400  1  304  'EXT'  0.9  0.9
HS30004500  63.55386388   0.60442162  0.39625
```

HS30004600 1 404 'INT' 0.9 0.9

HS30004700 61.34968363 0.070626111 0.39625

HS30004800 -1

HS30004801 316.0 1

HS30004802 316.0 2

*level 5

HS30005000 2 2 -1

HS30005001 hsides_LVL_5

HS30005002 0.0 1.0

HS30005100 -1 1 4.8511

HS30005101 4.8757 2

HS30005200 -1 * index for material

HS30005201 stainless-steel-304 1

HS30005300 0

HS30005400 1 305 'EXT' 0.9 0.9

HS30005500 63.59396095 0.60442162 0.3965

HS30005600 1 405 'INT' 0.9 0.9

HS30005700 61.38839005 0.070626111 0.3965

HS30005800 -1

HS30005801 316.0 1

HS30005802 316.0 2

*level 6

HS30006000 2 2 -1

HS30006001 hsides_LVL_6

HS30006002 0.3965 1.0

HS30006100 -1 1 4.8511

HS30006101 4.8757 2

HS30006200 -1 * index for material
HS30006201 stainless-steel-304 1
HS30006300 0
HS30006400 1 306 'EXT' 0.9 0.9
HS30006500 63.59396095 0.60442162 0.3965
HS30006600 1 406 'INT' 0.9 0.9
HS30006700 61.38839005 0.070626111 0.3965
HS30006800 -1
HS30006801 316.0 1
HS30006802 316.0 2

*level 7
HS30007000 2 2 -1
HS30007001 hsides_LVL_7
HS30007002 0.793 1.0
HS30007100 -1 1 4.8511
HS30007101 4.8757 2
HS30007200 -1 * index for material
HS30007201 stainless-steel-304 1
HS30007300 0
HS30007400 1 307 'EXT' 0.9 0.9
HS30007500 63.59396095 0.60442162 0.3965
HS30007600 1 407 'INT' 0.9 0.9
HS30007700 61.38839005 0.070626111 0.3965
HS30007800 -1
HS30007801 316.0 1
HS30007802 316.0 2

*level 8

```
HS30008000  2  2  -1
HS30008001  hsides_LVL_8
HS30008002  1.1895  1.0
HS30008100  -1  1  4.8511
HS30008101  4.8757  2
HS30008200  -1  * index for material
HS30008201  stainless-steel-304  1
HS30008300  0
HS30008400  1  308  'EXT'  0.9  0.9
HS30008500  63.59396095   0.60442162  0.3965
HS30008600  1  408  'INT'  0.9  0.9
HS30008700  61.38839005   0.070626111  0.3965
HS30008800  -1
HS30008801  316.0  1
HS30008802  316.0  2

*level 9
HS30009000  2  2  -1
HS30009001  hsides_LVL_9
HS30009002  1.586  1.0
HS30009100  -1  1  4.8511
HS30009101  4.8757  2
HS30009200  -1  * index for material
HS30009201  stainless-steel-304  1
HS30009300  0
HS30009400  1  309  'EXT'  0.9  0.9
HS30009500  63.59396095   0.60442162  0.3965
HS30009600  1  409  'INT'  0.9  0.9
HS30009700  61.38839005   0.070626111  0.3965
```

```
HS30009800  -1
HS30009801  316.0  1
HS30009802  316.0  2

*level 10
HS30010000  2  2  -1
HS30010001  hsides_LVL_10
HS30010002  1.9825  1.0
HS30010100  -1  1  4.8511
HS30010101  4.8757  2
HS30010200  -1  * index for material
HS30010201  stainless-steel-304  1
HS30010300  0
HS30010400  1  310  'EXT'  0.9  0.9
HS30010500  63.59396095   0.60442162  0.3965
HS30010600  1  410  'INT'  0.9  0.9
HS30010700  61.38839005   0.070626111  0.3965
HS30010800  -1
HS30010801  316.0  1
HS30010802  316.0  2

*level 11
HS30011000  2  2  -1
HS30011001  hsides_LVL_11
HS30011002  2.379  1.0
HS30011100  -1  1  4.8511
HS30011101  4.8757  2
HS30011200  -1  * index for material
HS30011201  stainless-steel-304  1
```

```
HS30011300  0
HS30011400  1  311  'EXT'  0.9  0.9
HS30011500  63.59396095   0.60442162  0.3965
HS30011600  1  411  'INT'  0.9  0.9
HS30011700  61.38839005   0.070626111  0.3965
HS30011800  -1
HS30011801  316.0  1
HS30011802  316.0  2

*level 12
HS30012000  2  2  -1
HS30012001  hsides_LVL_12
HS30012002  2.7755  1.0
HS30012100  -1  1  4.8511
HS30012101  4.8757  2
HS30012200  -1  * index for material
HS30012201  stainless-steel-304  1
HS30012300  0
HS30012400  1  312  'EXT'  0.9  0.9
HS30012500  63.59396095   0.60442162  0.3965
HS30012600  1  412  'INT'  0.9  0.9
HS30012700  61.38839005   0.070626111  0.3965
HS30012800  -1
HS30012801  316.0  1
HS30012802  316.0  2

*level 13
HS30013000  2  2  -1
HS30013001  hsides_LVL_13
```

HS30013002 3.172 1.0
HS30013100 -1 1 4.8511
HS30013101 4.8757 2
HS30013200 -1 * index for material
HS30013201 stainless-steel-304 1
HS30013300 0
HS30013400 1 313 'EXT' 0.9 0.9
HS30013500 63.59396095 0.60442162 0.3965
HS30013600 1 413 'INT' 0.9 0.9
HS30013700 61.38839005 0.070626111 0.3965
HS30013800 -1
HS30013801 316.0 1
HS30013802 316.0 2

*level 14
HS30014000 2 2 -1
HS30014001 hsides_LVL_14
HS30014002 3.5685 1.0
HS30014100 -1 1 4.8511
HS30014101 4.8757 2
HS30014200 -1 * index for material
HS30014201 stainless-steel-304 1
HS30014300 0
HS30014400 1 314 'EXT' 0.9 0.9
HS30014500 63.59396095 0.60442162 0.3965
HS30014600 1 414 'INT' 0.9 0.9
HS30014700 61.38839005 0.070626111 0.3965
HS30014800 -1
HS30014801 316.0 1

```
HS30014802  316.0  2

*level 15
HS30015000  2  2  -1
HS30015001  hsides_LVL_15
HS30015002  3.965  1.0
HS30015100  -1  1  4.8511
HS30015101  4.8757  2
HS30015200  -1  * index for material
HS30015201  stainless-steel-304  1
HS30015300  0
HS30015400  1  315  'EXT'  0.9  0.9
HS30015500  63.59396095   0.60442162  0.3965
HS30015600  1  415  'INT'  0.9  0.9
HS30015700  61.38839005   0.070626111  0.3965
HS30015800  -1
HS30015801  316.0  1
HS30015802  316.0  2

*level 16
HS30016000  2  2  -1
HS30016001  hsides_LVL_16
HS30016002  4.3615  1.0
HS30016100  -1  1  4.8511
HS30016101  4.8757  2
HS30016200  -1  * index for material
HS30016201  stainless-steel-304  1
HS30016300  0
HS30016400  1  316  'EXT'  0.9  0.9
```

HS30016500 63.59396095 0.60442162 0.3965
HS30016600 1 416 'INT' 0.9 0.9
HS30016700 61.38839005 0.070626111 0.3965
HS30016800 -1
HS30016801 316.0 1
HS30016802 316.0 2

*level 17
HS30017000 2 2 -1
HS30017001 hsides_LVL_17
HS30017002 4.758 1.0
HS30017100 -1 1 4.8511
HS30017101 4.8757 2
HS30017200 -1 * index for material
HS30017201 stainless-steel-304 1
HS30017300 0
HS30017400 1 317 'EXT' 0.9 0.9
HS30017500 63.59396095 0.60442162 0.3965
HS30017600 1 417 'INT' 0.9 0.9
HS30017700 61.38839005 0.070626111 0.3965
HS30017800 -1
HS30017801 316.0 1
HS30017802 316.0 2

*level 18
HS30018000 2 2 -1
HS30018001 hsides_LVL_18
HS30018002 5.1545 1.0
HS30018100 -1 1 4.8511

HS30018101 4.8757 2
HS30018200 -1 * index for material
HS30018201 stainless-steel-304 1
HS30018300 0
HS30018400 1 318 'EXT' 0.9 0.9
HS30018500 63.59396095 0.60442162 0.3965
HS30018600 1 418 'INT' 0.9 0.9
HS30018700 61.38839005 0.070626111 0.3965
HS30018800 -1
HS30018801 316.0 1
HS30018802 316.0 2

*level 19
HS30019000 2 2 -1
HS30019001 hsides_LVL_19
HS30019002 5.551 1.0
HS30019100 -1 1 4.8511
HS30019101 4.8757 2
HS30019200 -1 * index for material
HS30019201 stainless-steel-304 1
HS30019300 0
HS30019400 1 319 'EXT' 0.9 0.9
HS30019500 63.59396095 0.60442162 0.3965
HS30019600 1 419 'INT' 0.9 0.9
HS30019700 61.38839005 0.070626111 0.3965
HS30019800 -1
HS30019801 316.0 1
HS30019802 316.0 2

```
*level 20
HS30020000  2  2  -1
HS30020001  hsides_LVL_20
HS30020002  5.9475  1.0
HS30020100  -1  1  4.8511
HS30020101  4.8757  2
HS30020200  -1  * index for material
HS30020201  stainless-steel-304  1
HS30020300  0
HS30020400  1  320  'EXT'  0.9  0.9
HS30020500  63.59396095   0.60442162  0.3965
HS30020600  1  420  'INT'  0.9  0.9
HS30020700  61.38839005   0.070626111  0.3965
HS30020800  -1
HS30020801  316.0  1
HS30020802  316.0  2

*level 21
HS30021000  2  2  -1
HS30021001  hsides_LVL_21
HS30021002  6.344  1.0
HS30021100  -1  1  4.8511
HS30021101  4.8757  2
HS30021200  -1  * index for material
HS30021201  stainless-steel-304  1
HS30021300  0
HS30021400  1  321  'EXT'  0.9  0.9
HS30021500  63.59396095   0.60442162  0.3965
HS30021600  1  421  'INT'  0.9  0.9
```

HS30021700 61.38839005 0.070626111 0.3965
HS30021800 -1
HS30021801 316.0 1
HS30021802 316.0 2

*level 22
HS30022000 2 2 -1
HS30022001 hsides_LVL_22
HS30022002 6.7405 1.0
HS30022100 -1 1 4.8511
HS30022101 4.8757 2
HS30022200 -1 * index for material
HS30022201 stainless-steel-304 1
HS30022300 0
HS30022400 1 322 'EXT' 0.9 0.9
HS30022500 63.59396095 0.60442162 0.3965
HS30022600 1 422 'INT' 0.9 0.9
HS30022700 61.38839005 0.070626111 0.3965
HS30022800 -1
HS30022801 316.0 1
HS30022802 316.0 2

*level 23
HS30023000 2 2 -1
HS30023001 hsides_LVL_23
HS30023002 7.137 1.0
HS30023100 -1 1 4.8511
HS30023101 4.8757 2
HS30023200 -1 * index for material

HS30023201 stainless-steel-304 1
HS30023300 0
HS30023400 1 323 'EXT' 0.9 0.9
HS30023500 63.59396095 0.60442162 0.3965
HS30023600 1 423 'INT' 0.9 0.9
HS30023700 61.38839005 0.070626111 0.3965
HS30023800 -1
HS30023801 316.0 1
HS30023802 316.0 2

*level 24
HS30024000 2 2 -1
HS30024001 hsides_LVL_24
HS30024002 7.5335 1.0
HS30024100 -1 1 4.8511
HS30024101 4.8757 2
HS30024200 -1 * index for material
HS30024201 stainless-steel-304 1
HS30024300 0
HS30024400 1 324 'EXT' 0.9 0.9
HS30024500 63.59396095 0.60442162 0.3965
HS30024600 1 424 'INT' 0.9 0.9
HS30024700 61.38839005 0.070626111 0.3965
HS30024800 -1
HS30024801 316.0 1
HS30024802 316.0 2

*level 25
HS30025000 2 2 -1

```
HS30025001  hsides_LVL_25
HS30025002  7.93  1.0
HS30025100  -1  1  4.8511
HS30025101  4.8757  2
HS30025200  -1  * index for material
HS30025201  stainless-steel-304  1
HS30025300  0
HS30025400  1  325  'EXT'  0.9  0.9
HS30025500  63.56188329   0.60442162  0.3963
HS30025600  1  425  'INT'  0.9  0.9
HS30025700  61.35742491   0.070626111  0.3963
HS30025800  -1
HS30025801  316.0  1
HS30025802  316.0  2

*level 26
HS30026000  2  2  -1
HS30026001  hsides_LVL_26
HS30026002  8.3263  1.0
HS30026100  -1  1  4.8511
HS30026101  4.8757  2
HS30026200  -1  * index for material
HS30026201  stainless-steel-304  1
HS30026300  0
HS30026400  1  326  'EXT'  0.9  0.9
HS30026500  63.56188329   0.60442162  0.3963
HS30026600  1  426  'INT'  0.9  0.9
HS30026700  61.35742491   0.070626111  0.3963
HS30026800  -1
```

HS30026801 316.0 1
HS30026802 316.0 2

*level 27
HS30027000 2 2 -1
HS30027001 hsides_LVL_27
HS30027002 8.7226 1.0
HS30027100 -1 1 4.8511
HS30027101 4.8757 2
HS30027200 -1 * index for material
HS30027201 stainless-steel-304 1
HS30027300 0
HS30027400 1 327 'EXT' 0.9 0.9
HS30027500 63.57792212 0.60442162 0.3964
HS30027600 1 427 'INT' 0.9 0.9
HS30027700 61.37290748 0.070626111 0.3964
HS30027800 -1
HS30027801 316.0 1
HS30027802 316.0 2

****
* Back sides of the hot ducts
****
*level 1
HS31001000 2 2 -1
HS31001001 bsides_LVL_1
HS31001002 -1.585 1.0
HS31001100 -1 1 4.971
HS31001101 4.982 2

HS31001200 -1 * index for material
HS31001201 stainless-steel-304 1
HS31001300 0
HS31001400 1 401 'INT' 0.9 0.9
HS31001500 4.775723875 0.070626111 0.39625
HS31001600 1 501 'EXT' 0.9 0.9
HS31001700 5.326768938 0.341234781 0.39625
HS31001800 -1
HS31001801 316.0 1
HS31001802 316.0 2

*level 2
HS31002000 2 2 -1
HS31002001 bsides_LVL_2
HS31002002 -1.18875 1.0
HS31002100 -1 1 4.971
HS31002101 4.982 2
HS31002200 -1 * index for material
HS31002201 stainless-steel-304 1
HS31002300 0
HS31002400 1 402 'INT' 0.9 0.9
HS31002500 4.775723875 0.070626111 0.39625
HS31002600 1 502 'EXT' 0.9 0.9
HS31002700 5.326768938 0.341234781 0.39625
HS31002800 -1
HS31002801 316.0 1
HS31002802 316.0 2

*level 3

HS31003000 2 2 -1
HS31003001 bsides_LVL_3
HS31003002 -0.7925 1.0
HS31003100 -1 1 4.971
HS31003101 4.982 2
HS31003200 -1 * index for material
HS31003201 stainless-steel-304 1
HS31003300 0
HS31003400 1 403 'INT' 0.9 0.9
HS31003500 4.775723875 0.070626111 0.39625
HS31003600 1 503 'EXT' 0.9 0.9
HS31003700 5.326768938 0.341234781 0.39625
HS31003800 -1
HS31003801 316.0 1
HS31003802 316.0 2

*level 4
HS31004000 2 2 -1
HS31004001 bsides_LVL_4
HS31004002 -0.39625 1.0
HS31004100 -1 1 4.971
HS31004101 4.982 2
HS31004200 -1 * index for material
HS31004201 stainless-steel-304 1
HS31004300 0
HS31004400 1 404 'INT' 0.9 0.9
HS31004500 4.775723875 0.070626111 0.39625
HS31004600 1 504 'EXT' 0.9 0.9
HS31004700 5.326768938 0.341234781 0.39625

```
HS31004800  -1
HS31004801  316.0  1
HS31004802  316.0  2

*level 5
HS31005000  2  2  -1
HS31005001  bsides_LVL_5
HS31005002  0.0  1.0
HS31005100  -1  1  4.971
HS31005101  4.982  2
HS31005200  -1  * index for material
HS31005201  stainless-steel-304  1
HS31005300  0
HS31005400  1  405  'INT'  0.9  0.9
HS31005500  4.77873695   0.070626111  0.3965
HS31005600  1  505  'EXT'  0.9  0.9
HS31005700  5.330129675   0.341234781  0.3965
HS31005800  -1
HS31005801  316.0  1
HS31005802  316.0  2

*level 6
HS31006000  2  2  -1
HS31006001  bsides_LVL_6
HS31006002  0.3965  1.0
HS31006100  -1  1  4.971
HS31006101  4.982  2
HS31006200  -1  * index for material
HS31006201  stainless-steel-304  1
```

```
HS31006300  0
HS31006400  1  406  'INT'  0.9  0.9
HS31006500  4.77873695   0.070626111  0.3965
HS31006600  1  506  'EXT'  0.9  0.9
HS31006700  5.330129675   0.341234781  0.3965
HS31006800  -1
HS31006801  316.0  1
HS31006802  316.0  2

*level 7
HS31007000  2  2  -1
HS31007001  bsides_LVL_7
HS31007002  0.793  1.0
HS31007100  -1  1  4.971
HS31007101  4.982  2
HS31007200  -1  * index for material
HS31007201  stainless-steel-304  1
HS31007300  0
HS31007400  1  407  'INT'  0.9  0.9
HS31007500  4.77873695   0.070626111  0.3965
HS31007600  1  507  'EXT'  0.9  0.9
HS31007700  5.330129675   0.341234781  0.3965
HS31007800  -1
HS31007801  316.0  1
HS31007802  316.0  2

*level 8
HS31008000  2  2  -1
HS31008001  bsides_LVL_8
```

```
HS31008002  1.1895  1.0
HS31008100  -1  1  4.971
HS31008101  4.982  2
HS31008200  -1  * index for material
HS31008201  stainless-steel-304  1
HS31008300  0
HS31008400  1  408  'INT'  0.9  0.9
HS31008500  4.77873695   0.070626111  0.3965
HS31008600  1  508  'EXT'  0.9  0.9
HS31008700  5.330129675   0.341234781  0.3965
HS31008800  -1
HS31008801  316.0  1
HS31008802  316.0  2

*level 9
HS31009000  2  2  -1
HS31009001  bsides_LVL_9
HS31009002  1.586  1.0
HS31009100  -1  1  4.971
HS31009101  4.982  2
HS31009200  -1  * index for material
HS31009201  stainless-steel-304  1
HS31009300  0
HS31009400  1  409  'INT'  0.9  0.9
HS31009500  4.77873695   0.070626111  0.3965
HS31009600  1  509  'EXT'  0.9  0.9
HS31009700  5.330129675   0.341234781  0.3965
HS31009800  -1
HS31009801  316.0  1
```

```
HS31009802  316.0  2

*level 10
HS31010000  2  2  -1
HS31010001  bsides_LVL_10
HS31010002  1.9825  1.0
HS31010100  -1  1  4.971
HS31010101  4.982  2
HS31010200  -1  * index for material
HS31010201  stainless-steel-304  1
HS31010300  0
HS31010400  1  410  'INT'  0.9  0.9
HS31010500  4.77873695   0.070626111  0.3965
HS31010600  1  510  'EXT'  0.9  0.9
HS31010700  5.330129675   0.341234781  0.3965
HS31010800  -1
HS31010801  316.0  1
HS31010802  316.0  2

*level 11
HS31011000  2  2  -1
HS31011001  bsides_LVL_11
HS31011002  2.379  1.0
HS31011100  -1  1  4.971
HS31011101  4.982  2
HS31011200  -1  * index for material
HS31011201  stainless-steel-304  1
HS31011300  0
HS31011400  1  411  'INT'  0.9  0.9
```

```
HS31011500  4.77873695   0.070626111  0.3965
HS31011600  1  511  'EXT'  0.9  0.9
HS31011700  5.330129675   0.341234781  0.3965
HS31011800  -1
HS31011801  316.0  1
HS31011802  316.0  2

*level 12
HS31012000  2  2  -1
HS31012001  bsides_LVL_12
HS31012002  2.7755  1.0
HS31012100  -1  1  4.971
HS31012101  4.982  2
HS31012200  -1  * index for material
HS31012201  stainless-steel-304  1
HS31012300  0
HS31012400  1  412  'INT'  0.9  0.9
HS31012500  4.77873695   0.070626111  0.3965
HS31012600  1  512  'EXT'  0.9  0.9
HS31012700  5.330129675   0.341234781  0.3965
HS31012800  -1
HS31012801  316.0  1
HS31012802  316.0  2

*level 13
HS31013000  2  2  -1
HS31013001  bsides_LVL_13
HS31013002  3.172  1.0
HS31013100  -1  1  4.971
```

HS31013101 4.982 2
HS31013200 -1 * index for material
HS31013201 stainless-steel-304 1
HS31013300 0
HS31013400 1 413 'INT' 0.9 0.9
HS31013500 4.77873695 0.070626111 0.3965
HS31013600 1 513 'EXT' 0.9 0.9
HS31013700 5.330129675 0.341234781 0.3965
HS31013800 -1
HS31013801 316.0 1
HS31013802 316.0 2

*level 14
HS31014000 2 2 -1
HS31014001 bsides_LVL_14
HS31014002 3.5685 1.0
HS31014100 -1 1 4.971
HS31014101 4.982 2
HS31014200 -1 * index for material
HS31014201 stainless-steel-304 1
HS31014300 0
HS31014400 1 414 'INT' 0.9 0.9
HS31014500 4.77873695 0.070626111 0.3965
HS31014600 1 514 'EXT' 0.9 0.9
HS31014700 5.330129675 0.341234781 0.3965
HS31014800 -1
HS31014801 316.0 1
HS31014802 316.0 2

```
*level 15
HS31015000  2  2  -1
HS31015001  bsides_LVL_15
HS31015002  3.965  1.0
HS31015100  -1  1  4.971
HS31015101  4.982  2
HS31015200  -1  * index for material
HS31015201  stainless-steel-304  1
HS31015300  0
HS31015400  1  415  'INT'  0.9  0.9
HS31015500  4.77873695   0.070626111  0.3965
HS31015600  1  515  'EXT'  0.9  0.9
HS31015700  5.330129675   0.341234781  0.3965
HS31015800  -1
HS31015801  316.0  1
HS31015802  316.0  2

*level 16
HS31016000  2  2  -1
HS31016001  bsides_LVL_16
HS31016002  4.3615  1.0
HS31016100  -1  1  4.971
HS31016101  4.982  2
HS31016200  -1  * index for material
HS31016201  stainless-steel-304  1
HS31016300  0
HS31016400  1  416  'INT'  0.9  0.9
HS31016500  4.77873695   0.070626111  0.3965
HS31016600  1  516  'EXT'  0.9  0.9
```

```
HS31016700  5.330129675   0.341234781  0.3965
HS31016800  -1
HS31016801  316.0  1
HS31016802  316.0  2

*level 17
HS31017000  2  2  -1
HS31017001  bsides_LVL_17
HS31017002  4.758  1.0
HS31017100  -1  1  4.971
HS31017101  4.982  2
HS31017200  -1  * index for material
HS31017201  stainless-steel-304  1
HS31017300  0
HS31017400  1  417  'INT'  0.9  0.9
HS31017500  4.77873695   0.070626111  0.3965
HS31017600  1  517  'EXT'  0.9  0.9
HS31017700  5.330129675   0.341234781  0.3965
HS31017800  -1
HS31017801  316.0  1
HS31017802  316.0  2

*level 18
HS31018000  2  2  -1
HS31018001  bsides_LVL_18
HS31018002  5.1545  1.0
HS31018100  -1  1  4.971
HS31018101  4.982  2
HS31018200  -1  * index for material
```

HS31018201 stainless-steel-304 1
HS31018300 0
HS31018400 1 418 'INT' 0.9 0.9
HS31018500 4.77873695 0.070626111 0.3965
HS31018600 1 518 'EXT' 0.9 0.9
HS31018700 5.330129675 0.341234781 0.3965
HS31018800 -1
HS31018801 316.0 1
HS31018802 316.0 2

*level 19
HS31019000 2 2 -1
HS31019001 bsides_LVL_19
HS31019002 5.551 1.0
HS31019100 -1 1 4.971
HS31019101 4.982 2
HS31019200 -1 * index for material
HS31019201 stainless-steel-304 1
HS31019300 0
HS31019400 1 419 'INT' 0.9 0.9
HS31019500 4.77873695 0.070626111 0.3965
HS31019600 1 519 'EXT' 0.9 0.9
HS31019700 5.330129675 0.341234781 0.3965
HS31019800 -1
HS31019801 316.0 1
HS31019802 316.0 2

*level 20
HS31020000 2 2 -1

```
HS31020001  bsides_LVL_20
HS31020002  5.9475  1.0
HS31020100  -1  1  4.971
HS31020101  4.982  2
HS31020200  -1  * index for material
HS31020201  stainless-steel-304  1
HS31020300  0
HS31020400  1  420  'INT'  0.9  0.9
HS31020500  4.77873695   0.070626111  0.3965
HS31020600  1  520  'EXT'  0.9  0.9
HS31020700  5.330129675   0.341234781  0.3965
HS31020800  -1
HS31020801  316.0  1
HS31020802  316.0  2

*level 21
HS31021000  2  2  -1
HS31021001  bsides_LVL_21
HS31021002  6.344  1.0
HS31021100  -1  1  4.971
HS31021101  4.982  2
HS31021200  -1  * index for material
HS31021201  stainless-steel-304  1
HS31021300  0
HS31021400  1  421  'INT'  0.9  0.9
HS31021500  4.77873695   0.070626111  0.3965
HS31021600  1  521  'EXT'  0.9  0.9
HS31021700  5.330129675   0.341234781  0.3965
HS31021800  -1
```

```
HS31021801  316.0  1
HS31021802  316.0  2

*level 22
HS31022000  2  2  -1
HS31022001  bsides_LVL_22
HS31022002  6.7405  1.0
HS31022100  -1  1  4.971
HS31022101  4.982  2
HS31022200  -1  * index for material
HS31022201  stainless-steel-304  1
HS31022300  0
HS31022400  1  422  'INT'  0.9  0.9
HS31022500  4.77873695   0.070626111  0.3965
HS31022600  1  522  'EXT'  0.9  0.9
HS31022700  5.330129675   0.341234781  0.3965
HS31022800  -1
HS31022801  316.0  1
HS31022802  316.0  2

*level 23
HS31023000  2  2  -1
HS31023001  bsides_LVL_23
HS31023002  7.137  1.0
HS31023100  -1  1  4.971
HS31023101  4.982  2
HS31023200  -1  * index for material
HS31023201  stainless-steel-304  1
HS31023300  0
```

HS31023400 1 423 'INT' 0.9 0.9
HS31023500 4.77873695 0.070626111 0.3965
HS31023600 1 523 'EXT' 0.9 0.9
HS31023700 5.330129675 0.341234781 0.3965
HS31023800 -1
HS31023801 316.0 1
HS31023802 316.0 2

*level 24
HS31024000 2 2 -1
HS31024001 bsides_LVL_24
HS31024002 7.5335 1.0
HS31024100 -1 1 4.971
HS31024101 4.982 2
HS31024200 -1 * index for material
HS31024201 stainless-steel-304 1
HS31024300 0
HS31024400 1 424 'INT' 0.9 0.9
HS31024500 4.77873695 0.070626111 0.3965
HS31024600 1 524 'EXT' 0.9 0.9
HS31024700 5.330129675 0.341234781 0.3965
HS31024800 -1
HS31024801 316.0 1
HS31024802 316.0 2

*level 25
HS31025000 2 2 -1
HS31025001 bsides_LVL_25
HS31025002 7.93 1.0

```
HS31025100  -1  1  4.971
HS31025101  4.982  2
HS31025200  -1  * index for material
HS31025201  stainless-steel-304  1
HS31025300  0
HS31025400  1  425  'INT'  0.9  0.9
HS31025500  4.77632649   0.070626111  0.3963
HS31025600  1  525  'EXT'  0.9  0.9
HS31025700  5.327441085   0.341234781  0.3963
HS31025800  -1
HS31025801  316.0  1
HS31025802  316.0  2

*level 26
HS31026000  2  2  -1
HS31026001  bsides_LVL_26
HS31026002  8.3263  1.0
HS31026100  -1  1  4.971
HS31026101  4.982  2
HS31026200  -1  * index for material
HS31026201  stainless-steel-304  1
HS31026300  0
HS31026400  1  426  'INT'  0.9  0.9
HS31026500  4.77632649   0.070626111  0.3963
HS31026600  1  526  'EXT'  0.9  0.9
HS31026700  5.327441085   0.341234781  0.3963
HS31026800  -1
HS31026801  316.0  1
HS31026802  316.0  2
```

```
*level 27
HS31027000  2  2  -1
HS31027001  bsides_LVL_27
HS31027002  8.7226  1.0
HS31027100  -1  1  4.971
HS31027101  4.982  2
HS31027200  -1  * index for material
HS31027201  stainless-steel-304  1
HS31027300  0
HS31027400  1  427  'INT'  0.9  0.9
HS31027500  4.77753172   0.070626111  0.3964
HS31027600  1  527  'EXT'  0.9  0.9
HS31027700  5.32878538   0.341234781  0.3964
HS31027800  -1
HS31027801  316.0  1
HS31027802  316.0  2

**********
* Plates HS
**********
*level 1
HS35001000  2  2  -1
HS35001001  plate_LVL_1
HS35001002  -1.585  1.0
HS35001100  -1  1  11.55868
HS35001101  11.68648  2
HS35001200  -1  * index for material
HS35001201  stainless-steel-304  1
```

HS35001300 0

HS35001400 1 501 'EXT' 0.9 0.9

HS35001500 1552.944717 0.341234781 0.39625

HS35001600 0 -1 * symmetry boundary condition

HS35001800 -1

HS35001801 316.0 1

HS35001802 316.0 2

*level 2

HS35002000 2 2 -1

HS35002001 plate_LVL_2

HS35002002 -1.18875 1.0

HS35002100 -1 1 11.55868

HS35002101 11.68648 2

HS35002200 -1 * index for material

HS35002201 stainless-steel-304 1

HS35002300 0

HS35002400 1 502 'EXT' 0.9 0.9

HS35002500 1552.944717 0.341234781 0.39625

HS35002600 0 -1 * symmetry boundary condition

HS35002800 -1

HS35002801 316.0 1

HS35002802 316.0 2

*level 3

HS35003000 2 2 -1

HS35003001 plate_LVL_3

HS35003002 -0.7925 1.0

HS35003100 -1 1 11.55868

```
HS35003101  11.68648  2
HS35003200  -1  * index for material
HS35003201  stainless-steel-304  1
HS35003300  0
HS35003400  1  503  'EXT'  0.9  0.9
HS35003500  1552.944717  0.341234781  0.39625
HS35003600  0 -1 * symmetry boundary condition
HS35003800  -1
HS35003801  316.0  1
HS35003802  316.0  2

*level 4
HS35004000  2  2  -1
HS35004001  plate_LVL_4
HS35004002  -0.39625  1.0
HS35004100  -1  1  11.55868
HS35004101  11.68648  2
HS35004200  -1  * index for material
HS35004201  stainless-steel-304  1
HS35004300  0
HS35004400  1  504  'EXT'  0.9  0.9
HS35004500  1552.944717  0.341234781  0.39625
HS35004600  0 -1 * symmetry boundary condition
HS35004800  -1
HS35004801  316.0  1
HS35004802  316.0  2

*level 5
HS35005000  2  2  -1
```

```
HS35005001  plate_LVL_5
HS35005002  0.0  1.0
HS35005100  -1  1  11.55868
HS35005101  11.68648  2
HS35005200  -1  * index for material
HS35005201  stainless-steel-304  1
HS35005300  0
HS35005400  1  505  'EXT'  0.9  0.9
HS35005500  1553.924493  0.341234781  0.3965
HS35005600  0 -1 * symmetry boundary condition
HS35005800  -1
HS35005801  316.0  1
HS35005802  316.0  2

*level 6
HS35006000  2  2  -1
HS35006001  plate_LVL_6
HS35006002  0.3965  1.0
HS35006100  -1  1  11.55868
HS35006101  11.68648  2
HS35006200  -1  * index for material
HS35006201  stainless-steel-304  1
HS35006300  0
HS35006400  1  506  'EXT'  0.9  0.9
HS35006500  1553.924493  0.341234781  0.3965
HS35006600  0 -1 * symmetry boundary condition
HS35006800  -1
HS35006801  316.0  1
HS35006802  316.0  2
```

```
*level 7
HS35007000  2  2  -1
HS35007001  plate_LVL_7
HS35007002  0.793  1.0
HS35007100  -1  1  11.55868
HS35007101  11.68648  2
HS35007200  -1  * index for material
HS35007201  stainless-steel-304  1
HS35007300  0
HS35007400  1  507  'EXT'  0.9  0.9
HS35007500  1553.924493  0.341234781  0.3965
HS35007600  0 -1 * symmetry boundary condition
HS35007800  -1
HS35007801  316.0  1
HS35007802  316.0  2

*level 8
HS35008000  2  2  -1
HS35008001  plate_LVL_8
HS35008002  1.1895  1.0
HS35008100  -1  1  11.55868
HS35008101  11.68648  2
HS35008200  -1  * index for material
HS35008201  stainless-steel-304  1
HS35008300  0
HS35008400  1  508  'EXT'  0.9  0.9
HS35008500  1553.924493  0.341234781  0.3965
HS35008600  0 -1 * symmetry boundary condition
```

```
HS35008800  -1
HS35008801  316.0  1
HS35008802  316.0  2

*level 9
HS35009000  2  2  -1
HS35009001  plate_LVL_9
HS35009002  1.586  1.0
HS35009100  -1  1  11.55868
HS35009101  11.68648  2
HS35009200  -1  * index for material
HS35009201  stainless-steel-304  1
HS35009300  0
HS35009400  1  509  'EXT'  0.9  0.9
HS35009500  1553.924493  0.341234781  0.3965
HS35009600  0 -1 * symmetry boundary condition
HS35009800  -1
HS35009801  316.0  1
HS35009802  316.0  2

*level 10
HS35010000  2  2  -1
HS35010001  plate_LVL_10
HS35010002  1.9825  1.0
HS35010100  -1  1  11.55868
HS35010101  11.68648  2
HS35010200  -1  * index for material
HS35010201  stainless-steel-304  1
HS35010300  0
```

```
HS35010400  1  510  'EXT'  0.9  0.9
HS35010500  1553.924493  0.341234781  0.3965
HS35010600  0 -1 * symmetry boundary condition
HS35010800  -1
HS35010801  316.0  1
HS35010802  316.0  2

*level 11
HS35011000  2  2  -1
HS35011001  plate_LVL_11
HS35011002  2.379  1.0
HS35011100  -1  1  11.55868
HS35011101  11.68648  2
HS35011200  -1  * index for material
HS35011201  stainless-steel-304  1
HS35011300  0
HS35011400  1  511  'EXT'  0.9  0.9
HS35011500  1553.924493  0.341234781  0.3965
HS35011600  0 -1 * symmetry boundary condition
HS35011800  -1
HS35011801  316.0  1
HS35011802  316.0  2

*level 12
HS35012000  2  2  -1
HS35012001  plate_LVL_12
HS35012002  2.7755  1.0
HS35012100  -1  1  11.55868
HS35012101  11.68648  2
```

HS35012200 -1 * index for material
HS35012201 stainless-steel-304 1
HS35012300 0
HS35012400 1 512 'EXT' 0.9 0.9
HS35012500 1553.924493 0.341234781 0.3965
HS35012600 0 -1 * symmetry boundary condition
HS35012800 -1
HS35012801 316.0 1
HS35012802 316.0 2

*level 13
HS35013000 2 2 -1
HS35013001 plate_LVL_13
HS35013002 3.172 1.0
HS35013100 -1 1 11.55868
HS35013101 11.68648 2
HS35013200 -1 * index for material
HS35013201 stainless-steel-304 1
HS35013300 0
HS35013400 1 513 'EXT' 0.9 0.9
HS35013500 1553.924493 0.341234781 0.3965
HS35013600 0 -1 * symmetry boundary condition
HS35013800 -1
HS35013801 316.0 1
HS35013802 316.0 2

*level 14
HS35014000 2 2 -1
HS35014001 plate_LVL_14

HS35014002 3.5685 1.0
HS35014100 -1 1 11.55868
HS35014101 11.68648 2
HS35014200 -1 * index for material
HS35014201 stainless-steel-304 1
HS35014300 0
HS35014400 1 514 'EXT' 0.9 0.9
HS35014500 1553.924493 0.341234781 0.3965
HS35014600 0 -1 * symmetry boundary condition
HS35014800 -1
HS35014801 316.0 1
HS35014802 316.0 2

*level 15
HS35015000 2 2 -1
HS35015001 plate_LVL_15
HS35015002 3.965 1.0
HS35015100 -1 1 11.55868
HS35015101 11.68648 2
HS35015200 -1 * index for material
HS35015201 stainless-steel-304 1
HS35015300 0
HS35015400 1 515 'EXT' 0.9 0.9
HS35015500 1553.924493 0.341234781 0.3965
HS35015600 0 -1 * symmetry boundary condition
HS35015800 -1
HS35015801 316.0 1
HS35015802 316.0 2

```
*level 16
HS35016000  2  2  -1
HS35016001  plate_LVL_16
HS35016002  4.3615  1.0
HS35016100  -1  1  11.55868
HS35016101  11.68648  2
HS35016200  -1  * index for material
HS35016201  stainless-steel-304  1
HS35016300  0
HS35016400  1  516  'EXT'  0.9  0.9
HS35016500  1553.924493  0.341234781  0.3965
HS35016600  0 -1 * symmetry boundary condition
HS35016800  -1
HS35016801  316.0  1
HS35016802  316.0  2

*level 17
HS35017000  2  2  -1
HS35017001  plate_LVL_17
HS35017002  4.758  1.0
HS35017100  -1  1  11.55868
HS35017101  11.68648  2
HS35017200  -1  * index for material
HS35017201  stainless-steel-304  1
HS35017300  0
HS35017400  1  517  'EXT'  0.9  0.9
HS35017500  1553.924493  0.341234781  0.3965
HS35017600  0 -1 * symmetry boundary condition
HS35017800  -1
```

```
HS35017801  316.0  1
HS35017802  316.0  2

*level 18
HS35018000  2  2  -1
HS35018001  plate_LVL_18
HS35018002  5.1545  1.0
HS35018100  -1  1  11.55868
HS35018101  11.68648  2
HS35018200  -1  * index for material
HS35018201  stainless-steel-304  1
HS35018300  0
HS35018400  1  518  'EXT'  0.9  0.9
HS35018500  1553.924493  0.341234781  0.3965
HS35018600  0 -1 * symmetry boundary condition
HS35018800  -1
HS35018801  316.0  1
HS35018802  316.0  2

*level 19
HS35019000  2  2  -1
HS35019001  plate_LVL_19
HS35019002  5.551  1.0
HS35019100  -1  1  11.55868
HS35019101  11.68648  2
HS35019200  -1  * index for material
HS35019201  stainless-steel-304  1
HS35019300  0
HS35019400  1  519  'EXT'  0.9  0.9
```

```
HS35019500  1553.924493  0.341234781  0.3965
HS35019600  0 -1 * symmetry boundary condition
HS35019800  -1
HS35019801  316.0  1
HS35019802  316.0  2

*level 20
HS35020000  2  2  -1
HS35020001  plate_LVL_20
HS35020002  5.9475  1.0
HS35020100  -1  1  11.55868
HS35020101  11.68648  2
HS35020200  -1  * index for material
HS35020201  stainless-steel-304  1
HS35020300  0
HS35020400  1  520  'EXT'  0.9  0.9
HS35020500  1553.924493  0.341234781  0.3965
HS35020600  0 -1 * symmetry boundary condition
HS35020800  -1
HS35020801  316.0  1
HS35020802  316.0  2

*level 21
HS35021000  2  2  -1
HS35021001  plate_LVL_21
HS35021002  6.344  1.0
HS35021100  -1  1  11.55868
HS35021101  11.68648  2
HS35021200  -1  * index for material
```

```
HS35021201  stainless-steel-304  1
HS35021300  0
HS35021400  1  521  'EXT'  0.9  0.9
HS35021500  1553.924493  0.341234781  0.3965
HS35021600  0 -1 * symmetry boundary condition
HS35021800  -1
HS35021801  316.0  1
HS35021802  316.0  2

*level 22
HS35022000  2  2  -1
HS35022001  plate_LVL_22
HS35022002  6.7405  1.0
HS35022100  -1  1  11.55868
HS35022101  11.68648  2
HS35022200  -1  * index for material
HS35022201  stainless-steel-304  1
HS35022300  0
HS35022400  1  522  'EXT'  0.9  0.9
HS35022500  1553.924493  0.341234781  0.3965
HS35022600  0 -1 * symmetry boundary condition
HS35022800  -1
HS35022801  316.0  1
HS35022802  316.0  2

*level 23
HS35023000  2  2  -1
HS35023001  plate_LVL_23
HS35023002  7.137  1.0
```

HS35023100 -1 1 11.55868

HS35023101 11.68648 2

HS35023200 -1 * index for material

HS35023201 stainless-steel-304 1

HS35023300 0

HS35023400 1 523 'EXT' 0.9 0.9

HS35023500 1553.924493 0.341234781 0.3965

HS35023600 0 -1 * symmetry boundary condition

HS35023800 -1

HS35023801 316.0 1

HS35023802 316.0 2

*level 24

HS35024000 2 2 -1

HS35024001 plate_LVL_24

HS35024002 7.5335 1.0

HS35024100 -1 1 11.55868

HS35024101 11.68648 2

HS35024200 -1 * index for material

HS35024201 stainless-steel-304 1

HS35024300 0

HS35024400 1 524 'EXT' 0.9 0.9

HS35024500 1553.924493 0.341234781 0.3965

HS35024600 0 -1 * symmetry boundary condition

HS35024800 -1

HS35024801 316.0 1

HS35024802 316.0 2

*level 25

HS35025000 2 2 -1
HS35025001 plate_LVL_25
HS35025002 7.93 1.0
HS35025100 -1 1 11.55868
HS35025101 11.68648 2
HS35025200 -1 * index for material
HS35025201 stainless-steel-304 1
HS35025300 0
HS35025400 1 525 'EXT' 0.9 0.9
HS35025500 1553.140673 0.341234781 0.3963
HS35025600 0 -1 * symmetry boundary condition
HS35025800 -1
HS35025801 316.0 1
HS35025802 316.0 2

*level 26
HS35026000 2 2 -1
HS35026001 plate_LVL_26
HS35026002 8.3263 1.0
HS35026100 -1 1 11.55868
HS35026101 11.68648 2
HS35026200 -1 * index for material
HS35026201 stainless-steel-304 1
HS35026300 0
HS35026400 1 526 'EXT' 0.9 0.9
HS35026500 1553.140673 0.341234781 0.3963
HS35026600 0 -1 * symmetry boundary condition
HS35026800 -1
HS35026801 316.0 1

```
HS35026802  316.0  2

*level 27
HS35027000  2  2  -1
HS35027001  plate_LVL_27
HS35027002  8.7226  1.0
HS35027100  -1  1  11.55868
HS35027101  11.68648  2
HS35027200  -1  * index for material
HS35027201  stainless-steel-304  1
HS35027300  0
HS35027400  1  527  'EXT'  0.9  0.9
HS35027500  1553.532583  0.341234781  0.3964
HS35027600  0 -1 * symmetry boundary condition
HS35027800  -1
HS35027801  316.0  1
HS35027802  316.0  2

* Structure to structure radiation
HSRD100010  -32001  33001  1.0  501  502
HSRD100020  -32002  33002  1.0  501  502
HSRD100030  -32003  33003  1.0  501  502
HSRD100040  -32004  33004  1.0  501  502
HSRD100050  -32005  33005  1.0  501  502
HSRD100060  -32006  33006  1.0  501  502
HSRD100070  -32007  33007  1.0  501  502
HSRD100080  -32008  33008  1.0  501  502
HSRD100090  -32009  33009  1.0  501  502
HSRD100100  -32010  33010  1.0  501  502
```

```
HSRD100110  -32011  33011  1.0  501  502
HSRD100120  -32012  33012  1.0  501  502
HSRD100130  -32013  33013  1.0  501  502
HSRD100140  -32014  33014  1.0  501  502
HSRD100150  -32015  33015  1.0  501  502
HSRD100160  -32016  33016  1.0  501  502
HSRD100170  -32017  33017  1.0  501  502
HSRD100180  -32018  33018  1.0  501  502
HSRD100190  -32019  33019  1.0  501  502
HSRD100200  -32020  33020  1.0  501  502
HSRD100210  -32021  33021  1.0  501  502
HSRD100220  -32022  33022  1.0  501  502
HSRD100230  -32023  33023  1.0  501  502
HSRD100240  -32024  33024  1.0  501  502
HSRD100250  -32025  33025  1.0  501  502
HSRD100260  -32026  33026  1.0  501  502
HSRD100270  -32027  33027  1.0  501  502

* Structure to structure radiation
HSRD200010  -33001  30001  1.0  501  502
HSRD200020  -33002  30002  1.0  501  502
HSRD200030  -33003  30003  1.0  501  502
HSRD200040  -33004  30004  1.0  501  502
HSRD200050  -33005  30005  1.0  501  502
HSRD200060  -33006  30006  1.0  501  502
HSRD200070  -33007  30007  1.0  501  502
HSRD200080  -33008  30008  1.0  501  502
HSRD200090  -33009  30009  1.0  501  502
HSRD200100  -33010  30010  1.0  501  502
```

HSRD200110 -33011 30011 1.0 501 502
HSRD200120 -33012 30012 1.0 501 502
HSRD200130 -33013 30013 1.0 501 502
HSRD200140 -33014 30014 1.0 501 502
HSRD200150 -33015 30015 1.0 501 502
HSRD200160 -33016 30016 1.0 501 502
HSRD200170 -33017 30017 1.0 501 502
HSRD200180 -33018 30018 1.0 501 502
HSRD200190 -33019 30019 1.0 501 502
HSRD200200 -33020 30020 1.0 501 502
HSRD200210 -33021 30021 1.0 501 502
HSRD200220 -33022 30022 1.0 501 502
HSRD200230 -33023 30023 1.0 501 502
HSRD200240 -33024 30024 1.0 501 502
HSRD200250 -33025 30025 1.0 501 502
HSRD200260 -33026 30026 1.0 501 502
HSRD200270 -33027 30027 1.0 501 502

* Structure to structure radiation
HSRD300010 -33001 31001 1.0 501 502
HSRD300020 -33002 31002 1.0 501 502
HSRD300030 -33003 31003 1.0 501 502
HSRD300040 -33004 31004 1.0 501 502
HSRD300050 -33005 31005 1.0 501 502
HSRD300060 -33006 31006 1.0 501 502
HSRD300070 -33007 31007 1.0 501 502
HSRD300080 -33008 31008 1.0 501 502
HSRD300090 -33009 31009 1.0 501 502
HSRD300100 -33010 31010 1.0 501 502

HSRD300110 -33011 31011 1.0 501 502
HSRD300120 -33012 31012 1.0 501 502
HSRD300130 -33013 31013 1.0 501 502
HSRD300140 -33014 31014 1.0 501 502
HSRD300150 -33015 31015 1.0 501 502
HSRD300160 -33016 31016 1.0 501 502
HSRD300170 -33017 31017 1.0 501 502
HSRD300180 -33018 31018 1.0 501 502
HSRD300190 -33019 31019 1.0 501 502
HSRD300200 -33020 31020 1.0 501 502
HSRD300210 -33021 31021 1.0 501 502
HSRD300220 -33022 31022 1.0 501 502
HSRD300230 -33023 31023 1.0 501 502
HSRD300240 -33024 31024 1.0 501 502
HSRD300250 -33025 31025 1.0 501 502
HSRD300260 -33026 31026 1.0 501 502
HSRD300270 -33027 31027 1.0 501 502

* Control functions for the emissivities
CF50100 EMSV1 EQUALS 1 0.0 0.8
CF50110 1.0 0.0 TIME

CF50200 EMSV2 EQUALS 1 0.0 0.8
CF50210 1.0 0.0 TIME

* Bottom time-independent volume to hot duct
FL40000 riserF00-T01 400 401 -1.585 -1.585
FL40001 2.946486043 1.402625 1.0
FL40002 0 0 0 0

FL400S1 2.946486043 1.402625 0.070626111

* Riser to top time-independent volume
FL42800 hptoSINK 428 429 11.649 11.649
FL42801 2.946486043 1.515 1.0
FL42802 0 0 0 0
FL428S1 2.946486043 1.515 0.070626111

* Bottom time-independent volume for the riser
CV40000 riserbv 2 0 10
CV40001 0 -1
CV400A0 3
CV400A1 MLFR.5 1.0 TATM 316.0 PVOL 1.01325e5 PH2O 0.0
CV400B0 -3.994 0.0
CV400B1 -3.5622 1.272292673
CV400B2 -3.1304 2.544585346
CV400B3 -2.6986 3.816878019
CV400B4 -2.2668 5.089170693
CV400B5 -1.835 6.361463366
CV400B6 -1.585 7.098084876

* Top time-independent volume for the riser
CV42900 risertv 2 0 11
CV42901 0 -1
CV429A0 3
CV429A1 MLFR.5 1.0 TATM 547.0 PVOL 1.01e5 PH2O 0.0
CV429B0 11.649 0.0
CV429B1 12.149 1.473243021
.

APPENDIX E: PCC MODEL

E.1 Documentation

FLnnnVk	NVTRIP	-1	If negative then a trip is not used and the fraction open is defined by the "on forward" control function.
	NVFONF		Control function used to defined the fraction open of the flow path for an "on-forward" state of the trip.
	NVFONR		Control function used to define the fraction open of the flow path for an "on-reverse" state of the trip.

E.2 Input Decks

E.2 test.gen

```
*CV type definitions
CVTYPE15 inlet
CVTYPE16 outlet

**********************
* PCC inlet and outlet
**********************
*Valves
FL190V1 -1 30 30
FL200V1 -1 30 30
CF03000 VAL TAB-FUN 1 1.0 0.0
```

CF03003 666

CF03010 1.0 0.0 TIME

TF66600 VALOPEN 4 1.0

TF66610 1.0 1.0

TF66611 36000.0 1.0

TF66612 36000.10 0.0

TF66613 56000.0 0.0

*inlet

CV69000 inlet 2 0 15

CV69001 0 -1

CV690A0 3

CV690A1 MLFR.4 1.0 TATM 764.0 PVOL 5.03e6 PH2O 0.0

CV690B0 -3.994 0.0

CV690B1 -1.835 0.775208605

*outlet

CV70000 outlet 2 0 16

CV70001 0 -1

CV700A0 3

CV700A1 MLFR.4 1.0 TATM 764.0 PVOL 5.03e6 PH2O 0.0

CV700B0 -3.994 0.0

CV700B1 -1.835 0.278965269

* inlet to RPV

FL66600 PCCINLET 690 160 -2.9145 -0.7925

FL66601 2.05873074 2.122 1.0

FL66602 0 0 0 0

FL666S1 2.05873074 2.122 0.344

```
*RPV to outlet
FL66500 PCCOUTLET 054 700 -2.9145 -2.9145
FL66501 3.660961536 3.3633 1.0
FL66502 3 0 0 0
FL665S1 3.660961536 3.3633 2.159

*Valves
FL666V1 -1 31 31
FL665V1 -1 31 31
CF03100 VAL TAB-FUN 1 1.0 0.0
CF03103 667
CF03110 1.0 0.0 TIME
TF66700 VALOPEN 4 1.0
TF66710 1.0 0.0
TF66711 36000.0 0.0
TF66712 36000.10 1.0
TF66713 56000.0 1.0
.

**********************************
* core power
**********************************
CF01000 COREPOW TAB-FUN 1 600.0e6 0.0
CF01003 500
CF01010 1.0 0.0 TIME

TF50000 decayht  27  1.0
TF50010 1.0  1.0
```

TF50011 36000.0 1.0
TF50012 36000.1 0.079232537
TF50013 36100.0 0.074559195
TF50014 36210.0 0.069739124
TF50015 36320.0 0.065230659
TF50016 36450.0 0.060276749
TF50017 36600.0 0.055026344
TF50018 36760.0 0.049929001
TF50019 36930.0 0.045029434
TF50020 37110.0 0.040364678
TF50021 37300.0 0.035963991
TF50022 37500.0 0.031848989
TF50023 37740.0 0.027527641
TF50024 38000.0 0.023505946
TF50025 39000.0 0.020235813
TF50026 40000.0 0.017419703
TF50027 43000.0 0.01402378
TF50028 46000.0 0.011289757
TF50029 52000.0 0.009935445
TF50030 56000.0 0.009124705
TF50031 58000.0 0.008871528
TF50032 61000.0 0.008512983
TF50033 64000.0 0.008168929
TF50034 66000.0 0.00795481
TF50035 71000.0 0.007575179
TF50036 72000.0 0.0075
.

VITA

Name: Ni Zhen

Address: Department of Nuclear Engineering; c/o Dr. Karen Vierow, Texas A&M University, 3133 TAMU, College Station, TX 77843-3133

Email Address: janie513@tamu.edu

Education:

B.En., Mechanical Engineering, Beijing Polytechnic University, People's Republic of China, 2004

M.S., Energy and Environment, Ecole Polytechnique Feminine, France, 2006

M.S., Nuclear Engineering, Texas A&M University, USA, 2008